2-2014

A dichotomous key for the identification of nine salmonids of the Inland Northwest using six diagnostic skull bones : and associated equations to estimate total length and weight from bones ingested by piscivores or found in archeological sites

Aaron G. Stroud
Eastern Washington University

Allan T. Scholz
Eastern Washington University

Fisheries Research Center (Cheney, Wash.)

Eastern Washington University Fisheries Research Center
Contributions to Fisheries Management in Eastern Washington State
Number 27 • February 2014

A dichotomous key for the identification of nine salmonids of the Inland Northwest using six diagnostic skull bones; and associated equations to estimate total length and weight from bones ingested by piscivores or found in archeological sites

By
Aaron G. Stroud and Allan T. Scholz

Eastern Washington University
Department of Biology
Fisheries Research Center
258 Science Hall
Cheney, Washington 99004

Photography
by
Larry Conboy

Eastern Washington University
University Graphics
Cheney Washington 99004

Abstract

The fish skull is a complex anatomical structure, comprised of numerous bones that are often unique to the fish's genera or species. These unique qualities allow researchers to use bone to identify and quantify fish in piscivore and archeological investigations. Due to the high degree of similarity among skull bones of salmonids, adequate descriptions for keying out most salmoinds is limited in the available literature. To address this, eight different bones from a sample of 273 fish, representing nine salmonid species, were observed and measured. Observations and measurements were used to construct dichotomous keys and regression models for identifying and quantifying each of the nine salmonids when a single bone is present. Of the eight bones, the premaxillary, maxillary, dentary, cleithra, preopercle and opercle displayed species specific qualities for all nine species. These unique qualities have been used to construct a dichotomous key. The remaining two bones, the pharyngeal arch and vertebra, were not different enough to key out these bones from each species. All eight bones provided a precise single or multilinear regression model for all nine fish usable to back calculate fish total length from the length of a single bone. Total length to weight regressions are also presented for each species.

Table of Contents

List of Figures

List of Tables

Acknowledgments

The production of this document would not have been possible without the generous help and support of Larry Conboy, University Graphics Department, who took and helped process all of the photographs. We also thank the following individuals for providing bull trout samples: Wade Fredenberg, United States Fish and Wildlife Service, Creston National Fish Hatchery, Kalispel, Montana, and Jason Connor, Jason Olson, and Joe Maroney, Kalispel Tribe Department of Natural Resources, Usk, Washington.

Introduction

The identification of salmonids in the Inland Northwest using external taxonomy is abundant and comprehensive (Simpson and Wallace 1982; Wydoski and Whitney 2003; Parrish et al. 2006; Scholz and McLellan 2009, 2010). Once an intact fish loses some or all of its soft external structures, due to digestion or decay, identification can only be made based on DNA extraction or observed hard boney structures. However, since it is not possible to extrapolate fish body size and weight from DNA, fish identification based on boney structures has a few advantages. It is well documented that bone growth is highly correlated to an intact fish's total weight and length. This allows for the back calculation and estimation of how large and potentially how old a once living organism was. For these reasons, anthropologists, archeologists and biologists have relied on well documented descriptions of boney structures to identify and quantify fish species for a number of purposes.

The adaptive variation of fish has created minute differences in the bone structure and skull anatomy that can be used to visually identify fish (Gregory 1933, Cailliet et al. 1986, Colley 1990). The premaxillary, maxillary, dentary, cleithra, preopercle, opercle, pharyngeal arch, vertebra, and otoliths have all been used to identify fish with a great deal of accuracy (Curtis and Smith 1994, Scharf et al. 1998, Granadeiro and Silvia 2000, Radke et al. 2000, Prenda et al. 2002, Britton et al. 2005, Beyer et al. 2006, Parrish et al. 2006, Tarken et al. 2007 and Novais et al. 2010). As previously mentioned, these eight skull bones grow in a manner that correlates to a fish's total length, allowing them to provide information regarding the original intact fish. These two pieces of information allow for an accurate identification of species and a quantification of biomass as generated from calculating fish total length and weight from bone length.

In fisheries science the information provided from estimating total length and weight is invaluable, and the use of boney structures has become a commonly employed method for the identification and quantification of piscivory. Once a fish has been consumed and exposed to the gastrointestinal tract of a piscivore soft tissue identifiers quickly deteriorate, leaving only macerated tissue and disarticulated boney structures (Scharf et al. 1997; Frost 2000). Previous work, however, suggests the large boney structures of the head are able to maintain a high frequency of occurrence (Hajkova et al. 2003) and retain diagnostic qualities long into the digestive process (Hansel et al. 1988, Tarken et al. 2007). Properly using retained diagnostic qualities on boney structions to identify fish from, however, requires a considerable amount of familiarity with skull bones and/or a highly detailed description of each aforementioned bone laid out in a diagnostic key.

Earlier diagnostic bone keys provided by Frost (2000) and Parrish et al. (2006) describe and identify these boney structures for a few salmonid species inhabiting the Pacific Northwest. True discrimination between the bones of these species, however, is not available in this literature. Despite this lack of knowledge the identification of consumed prey fish is a necessity, especially when trying to better understand the bioenergetics of predatory species, species-species interactions, and predatory limitations on sensitive or threatened species (Mann and Beaumont 1980, Carss and Elston 1996, Jacobsen and Hansen 1996, Anderson and Neumann 1997, Miranda and Escala 2005).

Presented in this document is a detailed description and regression equations for estimating total length and weight from the premaxillary, maxillary, dentary, cleithra, preopercle and opercle from nine salmonid species common to eastern Washington, northern Idaho and western Montana.

Methods

Osteological Descriptions and Anatomy

The salmonid skull is a complex anatomical structure that contains many different bones held together by connective tissues (Figure 1). Over the evolutionary history of each fish, the bones present in the fish skull have had the chance to develop an appearance unique to each species. These unique appearances generally coincide with functionality and the fish's body structure, and often share common resemblances with other members of the fish's order, family and genus. This unique appearance can initially be viewed by comparing the complete skulls of different fish (Figure 2). Complete skulls can vary greatly among fish families, as displayed by the drastically different appearance of fish from the family Salmonidae, mountain whitefish (*Prosopium williamsoni*) from the subfamily Coregoninae, and the rainbow trout (*Oncorhynchus mykiss*), cutthroat trout (*Oncorhynchus clarkii*) and the lake trout (*Salvelinus namaycush*) from the subfamily Salmoninae.

When differences are viewed on a single bone, the premaxillary for example, it is clear that differences are much greater inter-subfamilies than intra-subfamily (Figure 3). When the premaxillary is viewed among members of the same subfamily, but different genus, differences can still be readily identified. Inter-generic differences of a single bone are more difficult to quickly identify, but the premaxillary of the rainbow trout and cutthroat trout, both members of the genus *Oncorhynchus*, have a slightly different appearance that can be observed on close examination. To address these differences and familiarize readers with each bone, the six identifying bones; premaxillary, maxillary, dentary, preopercle, opercle and cleithra, are briefly described in the following section. Figures matched to each bones description are also provided, with examples of some of the differences present between the nine species observed in this study. Following the initial descriptions of each bone is a dichotomous key which can be used to differentiate the nine species from each other.

Anatomical descriptions of each bone were done using structures and names provided in part by the previous work of Cailliet et al. (1986), Hansel et al. (1988) Frost (2000), and Parrish et al. (2006), though, when needed additional anatomical structures have been named to adequately convey information. In an attempt to pin point anatomical structures easily and give relevant reference to them, the description of each bone has been paired with a large figure presenting the lateral and medial side of each bone. In text descriptions of each anatomical structure are marked with a letter that directly corresponds to marked structures in the figure and figure caption. Information regarding what species each presented bone came from, as well as, the side of the head bones originated from is presented in figure captions. To help orient readers a description of where each of these bones roughly fits into the skull is provided in text, though frequent references to Figure 1

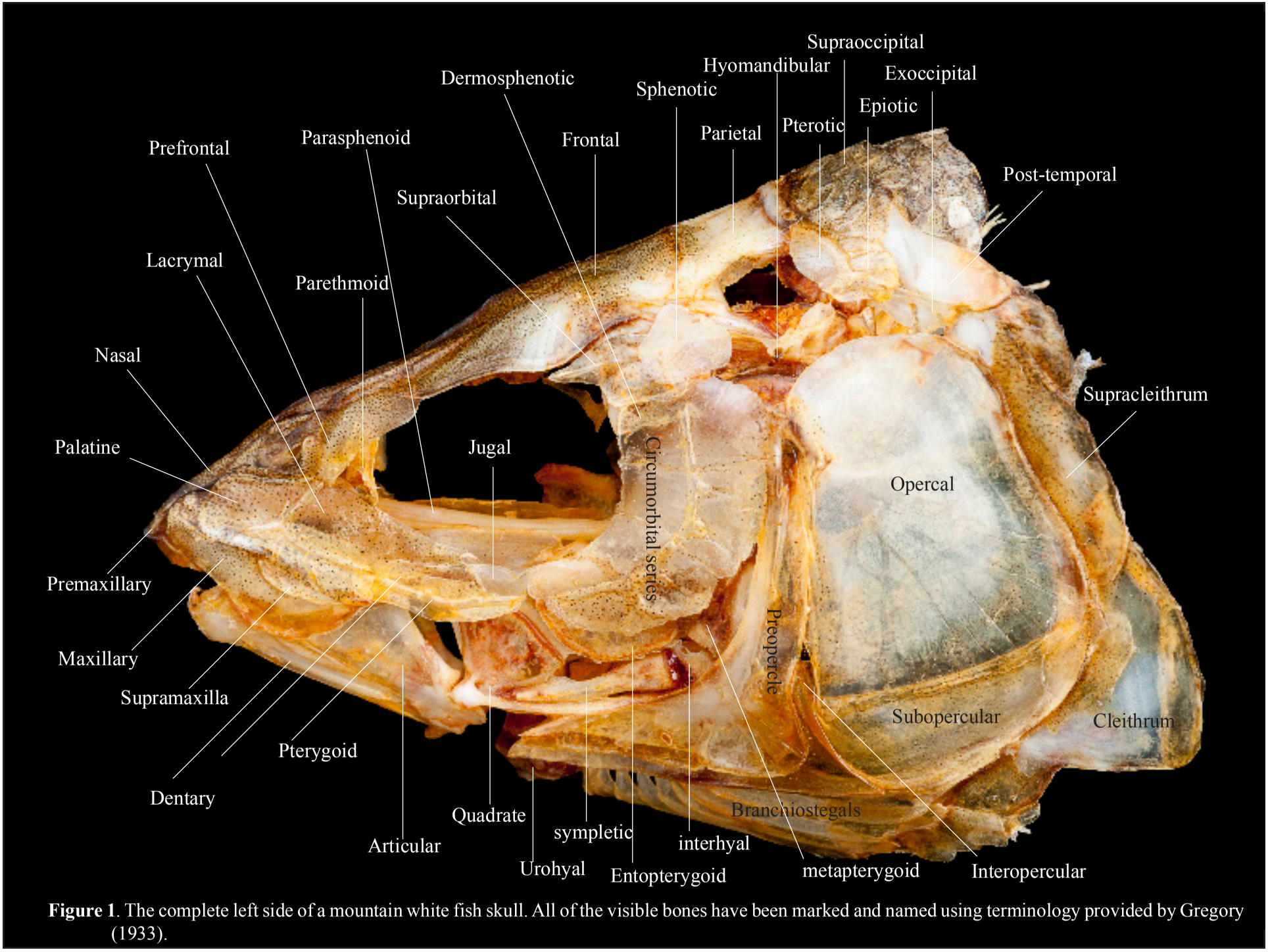

Figure 1. The complete left side of a mountain white fish skull. All of the visible bones have been marked and named using terminology provided by Gregory (1933).

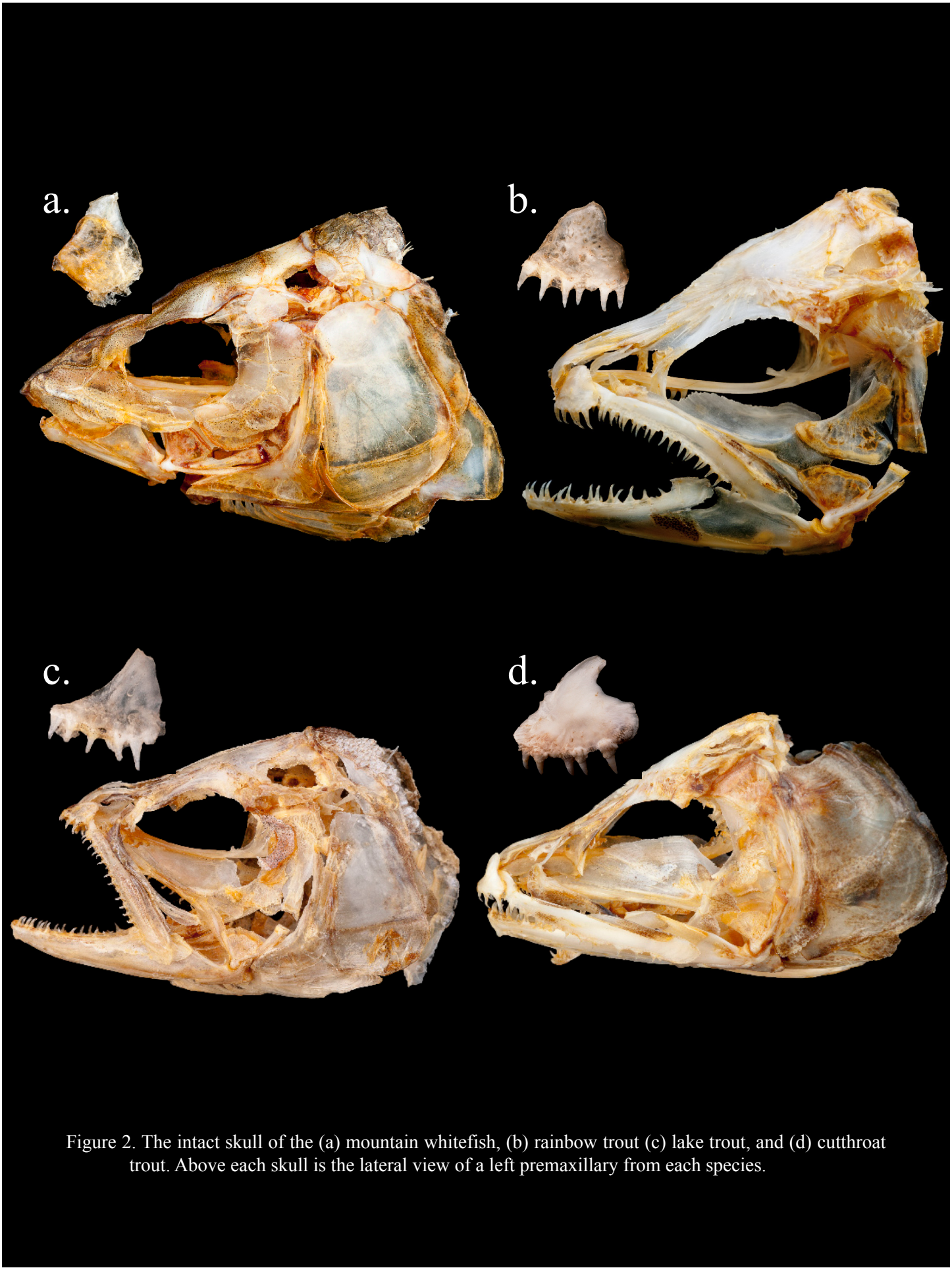

Figure 2. The intact skull of the (a) mountain whitefish, (b) rainbow trout (c) lake trout, and (d) cutthroat trout. Above each skull is the lateral view of a left premaxillary from each species.

should be made. It is important to note that Figure 1 is based on the mountain whitefish skull, and subtle differences in skull formation are present in the other eight fish.

Table 1. The sample population (n) of fish used for this study, with total length (TL, mm) and weight (Wt, g) ranges. Species denoted with ˇ came from newly collected samples, whereas species denoted with * came from samples collected by Scott (2002). A denotation of × represents missing data that was back calculated using a standard condition factor of 1.0 and Fulton-type condition factor equations.

Species Name	Common Name	n	Total Length Range (mm)	Total Weight Range (g)
**Onchorynchus clarkii lewisi*	cutthroat trout	14	28-285	1.0 - 228.0
**Oncorhynchus mykiss*	rainbow trout	12	89-263	8.0 - 194.0
ˇ Oncorhynchus nerka*	kokanee	11	54-360	1.0 - 560.0
ˇ Oncorhynchus tshawytscha	Chinook	63	71-182	3.0 - 68.0
*ˇ*Prosopium williamsoni*	mountain whitefish	24	95-303	6.0 - 249.0
**Salmo trutta*	brown trout	4	95-133	10.0 - 23.0
ˇ Salvelinus confluentus	bull trout	73	31.5-544	0.394 - 1426.5
ˇ Salvelinus frontinalis	brook trout	36	108.1-235.2	10.0 - 161.5
**Salvelinus namaycush*	lake trout	14	85-791	21.97-4949×

Sample Processing and Dissecting

Bones for this study were obtained from a sample population of 263 fish, representing nine salmonid species (Table 1). This population consisted of salmonids collected or donated specifically for this study and fish skeletons collected by Scott (2002) and housed in the Eastern Washington University's Fisheries Research Lab. Salmonid bones from previous studies were all re-measured according to the methods described in this study.

Fish collected specifically for this study arrived fully intact, frozen or bathed in formalin. Each desired skull bone was manually dissected from intact specimens using the following methods. Prior to dissection, soft tissue was loosened from bones using one of three methods. The most effective method was boiling fish in water for 10-60 seconds, depending on fish size (Hansel et al. 1988, Radke et al. 2000, Prenda et al. 2002, Hajkova et al. 2003, Britton & Shepherd 2005, Beyer et al. 2006, Tarken et al 2007). This method was relatively poor for loosening the flesh of formalin preserved fish and attempts to better break down formalin-preserved samples included two experimental methods: (1) microwaving whole fish for 30–90 seconds (Granadeiro and Silvia 2000), and (2) boiling whole fish for >1 hour. Neither of these methods produced better results, and often damaged bony structures. Subsequently, formalin preserved samples were manually dissected under a dissecting microscope (Nikon, SMZ-1B) without loosening soft tissue.

To minimize damage to bones during dissection the majority of soft connective and muscle tissue was first removed using tweezers and a scalpel. Bones were then gently teased out from their position in the skull and carefully scraped/wiped clean before being placed on paper towels to dry. Bones visibly damaged by the dissection process were discarded. Bone measurements (n=26) for constructing biometric estimation equations were taken from the premaxillary, maxillary, dentary, cleithra, preopercle, opercle, pharyngeal arch, and vertebra of each fish as shown (Figure 3). Bones

were measured using a basic design described by Radke et al. (2000) and Tarken et al. (2007) and were taken in an attempt to generate a multivariate linear regression for the estimation of total length using each bone. All measurements were taken to the nearest 0.5 mm using hand calipers.

The identification and description of common characteristics for each of the nine species came from a subset (n=5) of our sample population of skull bones. Each bone was viewed under a light microscope. Definable characteristics were recorded and compared between species. If a particular characteristic could not be defined with the five randomly chosen samples, more fish were added. To adequately portray information presented in each figure, and due to concerns over slight damage caused over time to bones collected by Scott (2002), at least one fish from each of the nine species presented here was collected intact and dissected using the aforementioned methods. This allowed us to photograph and present bones that were relatively equivalent in age, and provided the best opportunity to adequately present subtle details.

The identification of classifying meristic counts were made using a randomly chosen subsample of undamaged bones from each species. All measurements that were taken from each bone are depicted in Figure 3.

Statistical Analysis

To address the concern that a difference may be present between the right and left side of a fishes skull, a subset (n=20) of paired right and left bones were measured and compared using a simple two-way analysis of variance (ANOVA, α=0.05; Tarken et al. 2007). If no significant difference was present between the right and left side, then no discrimination between head side was made during the construction of total length regressions. Unfortunately, statistical analysis of right and left head bones was unobtainable from previously collected specimens due to a lack of available paired and undamaged head bones. Right and left head bones from previously collected samples were therefore clumped during analysis.

The construction of biometric predictor models from bone measurements were carried out with a two step process. First, multiple linear regression equations were constructed in program Systat 12 (Systat Software Inc., Chicago, Illinois) using backward stepwise regression models to determine if multivariate equations could be used to create accurate bone length to fish total length regressions. An ANOVA (α=0.05) was used to determine if each regression provided a residual between predicted and dependent variable significantly small enough to reject the null hypothesis that no relationship between total length and bone length was present. Models that provided the largest r^2 value and tolerance less than 0.9 were adopted as the best estimator of total length. To better meet the assumptions of normality and homoscedasticity all data points for bone length were transformed (ln[X+1]) prior to analysis. Second, a total weight to total length regression was constructed using a simple linear regression of fish weight and total length. These two regression equations can be used in tandem to estimate first, fish total length, and then, fish weight, from each skull bone. Due to concerns over small sample sizes not producing accurate, or biologically significant, regression equations, we only constructed equations for fish with sample sizes greater then five. It should additionally be noted, however, that regressions created with these low sample

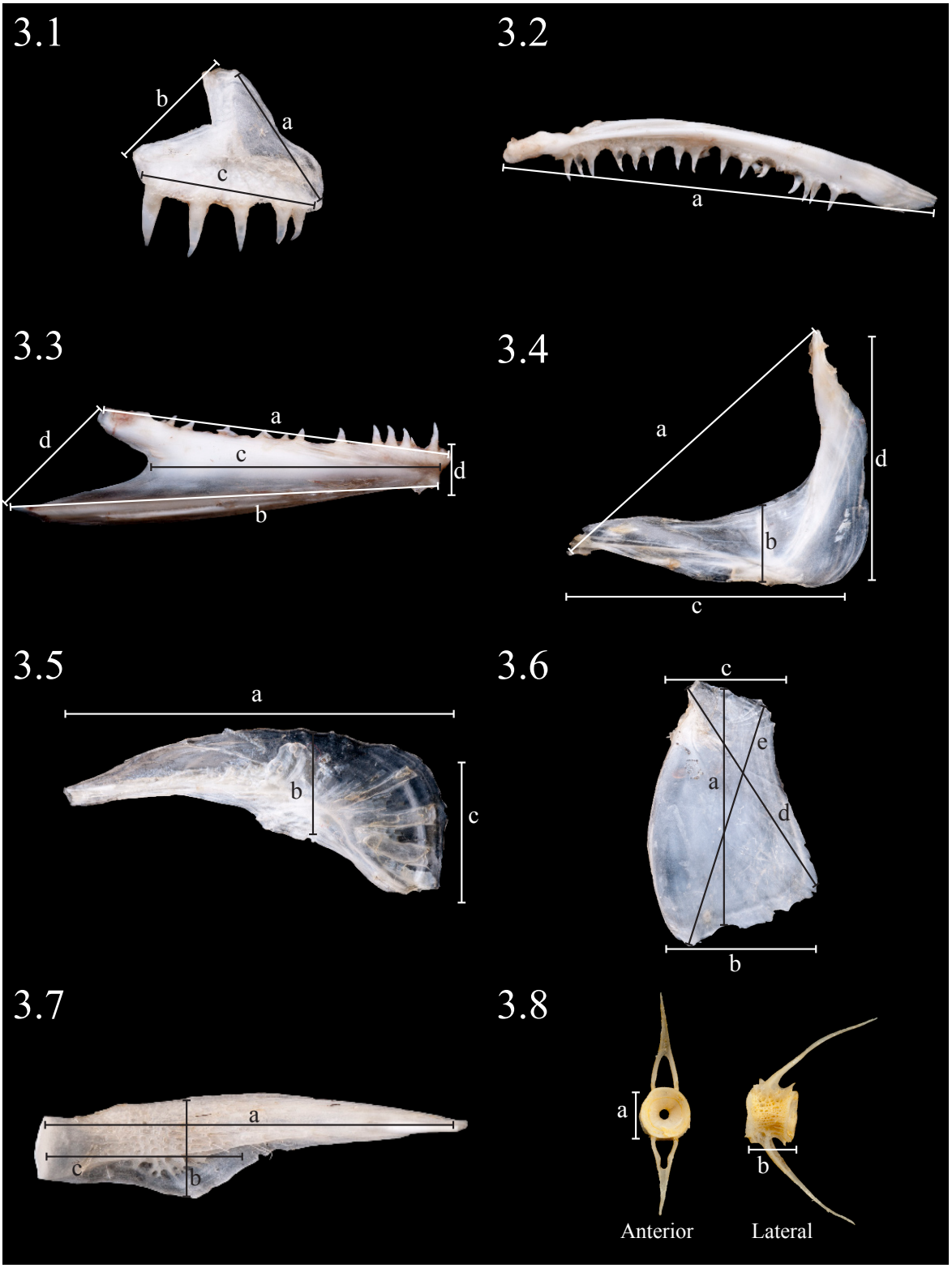

Figure 3. The lateral views and measurements taken from (3.1) the premaxillary (a) anterior margin, (b) posterior margin, and (c) dental palate. (3.2) the maxillary (a) body length. (3.3) the dentary (a) dental palate, (b) ventral margin, (c) body length, (d) mandibular symphysis, and (d) the posterior margin. (3.4) the cleithra (a) dorsal tip to anterior tip, (b) width of the horizontal limb, (c) ventral margin, and (d) posterior margin. (3.5) the preopercle (a) posterior margin, (b) width of preopercle body, and (c) posterior margin. (3.6) the opercle (a) body height, (b) ventral margin, (c) dorsal margin, (d) anterior dorsal tip to the posterior ventral tip, and (e) posterior dorsal tip to the anterior ventral tip. (3.7) the pharyngeal arch (a) length, (b) body width, and (c) pharyngeal arch shelf length and (3.8) the anterior and lateral view of the vertebra (a) height and (b) width.

sizes likely represent the actual population poorly. These equations, and equations provided by this study, will be presented for each bone together in each bones respective dichotomous key found in the appendix.

Results

Osteological Descriptions and Analysis

Upon visual analysis of the eight salmonid bones (the premaxillary, maxillary, dentary, cleithra, peropercle, opercle, pharyngeal arch and vertebra) studied in this document, it was found that all but the pharyngeal arch and vertebra could be used to differentiate the nine species listed in Table 1. The following results section has been setup to present a brief visual description of the premaxilary, maxillary, dentary, cleithra, preopercle and opercle. Additionally, a brief review of the differences present between genera and species are given. After the visual description of each bone the most significant regression models for estimating fish total length from bone length are given. For a more detailed description, and comparisons of each bone for the nine species presented in this document, please refer to the dichotomous keys located in the appendices.

The Premaxillary

The premaxillae are a paired set of bones located at the anterior most tip of the fish's snout (Figure 4). These two bones connect to each other along their premaxillary symphysis and cup the ethmoid bone in the bowl shaped ethmoid fossa. The posterior angle of these bones connects to the nasal bone and helps maintain the medial opening to the nasal canal.

In primitive teleost fish the premaxillae and maxillae are involved in maintaining the upper gape of the mouth. This is true for many salmonids and especially for those of the subfamily Salmoninae, which maintain a dental palate that houses a single row of homodont caniform teeth. Unfortunately, these teeth are only lightly anchored to the bones of the premaxillae, maxillae, and dentary (Vladykov 1962). For this reason it is important to view the dental palate for the presence of not only teeth but also alveolus where a tooth was present. When connected to the maxillae this creates a continuous row of teeth along the upper jaw (Figure 4). In contrast to this members of the subfamily Coregoninae have a dental palate that is smooth and has no teeth.

The major anatomical structures of the premaxillae are centered around two to three ridges that are visible on the medial side of this bone (Figure 4). The osseous membrane of the anterior lobe bridges the anterior ridge and ascending ridge. Along the posterior section of the premaxillae, the osseous membrane of the posterior lobe bridges the posterior ridge and ascending ridge. The posterior ridge often appears notched, creating a Y or square shaped angle in the posterior margin of the premaxillary. This notch is referred to as the posterior angle. In some instances, all three ridges may not be present, as seen in Figure 4. Further, the shape and angle of these three ridges can be variable, as seen in Figure 4. When these ridges are all present, though, they meet at the medial prominence.

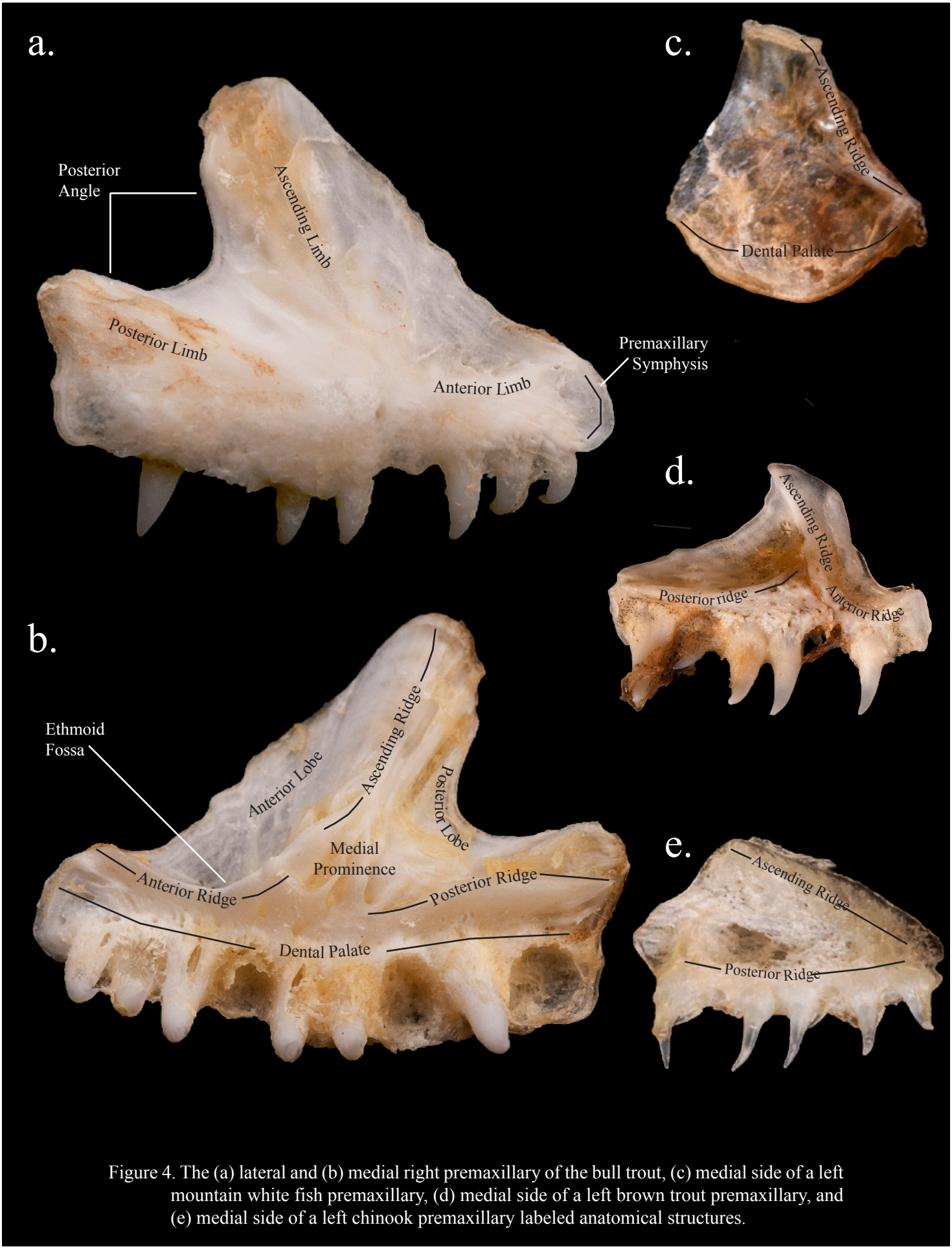

Figure 4. The (a) lateral and (b) medial right premaxillary of the bull trout, (c) medial side of a left mountain white fish premaxillary, (d) medial side of a left brown trout premaxillary, and (e) medial side of a left chinook premaxillary labeled anatomical structures.

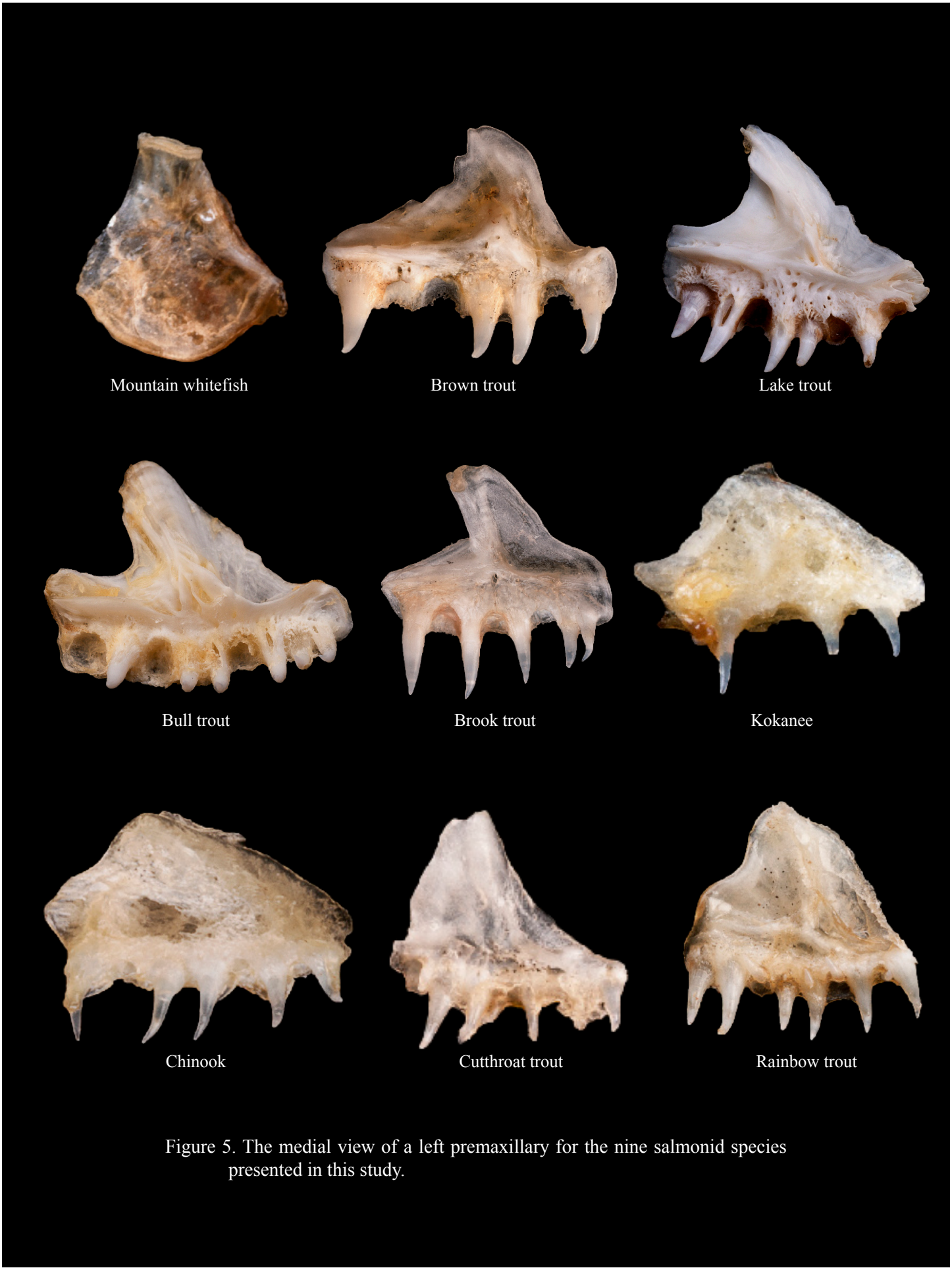

Figure 5. The medial view of a left premaxillary for the nine salmonid species presented in this study.

For the premaxillary, the first differentiation between the nine species presented in this study was made based on the presence or absence of the single row of teeth along the dental palate (Figure 5). This is one of the major identifying characters present between the subfamilies Salmoninae and Coregoninae. Members of the subfamily Coregoninae, in this case the mountain whitefish, have a dental palate that is smooth with no teeth or alveoli and is ventrally rounded. In contrast, members of the subfamily Salmoninae, which includes the remaining eight species, all have teeth along their dental palates.

Differentiating the three genera (*Salvelinus*, *Salmo*, and *Oncorhynchus*) of the subfamily Salmoninae takes closer inspection. The main differences that exist, however, can be pin pointed once familiarity with the premaxillary has been gained. The premaxillary of the genus *Salvelinus* (Figure 5) has a deeply notched posterior margin, and three, well defined, ridges on their medial aspect. These three medial ridges meet each other at a heavily ossified medial prominence, that is located near midway along the length of the dental palate. The premaxillaries from the one member of the genus *Salmo*, the brown trout, were similar to those from the genus *Salvelinus*. The brown trout premaxillary also presented with a notched posterior margin, and three prominent ridges on the medial aspect. The brown trout, however, had a premaxillary that was only shallowly or moderately notched in its posterior margin, and maintained an anterior and ascending ridge that were highly falcate in appearance (Figure 4). It is worth noting, that the medial prominence of the brown trout premaxillary is also positioned almost near the premaxillary symphysis and the posterior ridge is greatly extended. This difference is important, as occasionally the lake trout premaxillary will presented with an ascending ridge that is mildly curved or falcate.

Unlike the lake trout, the bull trout and brook trout presented with an ascending ridge that extended dorsally as a straight, often boxy osseous structure. The boxy appearance of the ascending ridge is much more prominent in brook trout specimens, which maintained an ascending ridge that projected near straight up from the medial prominence with flat anterior and posterior margins. In addition to this the brook trout anterior and posterior ridges meet the boxy ascending ridge at near square angles, which created an upside down T shape on the medial aspect. The ascending limb of the bull trout is more rounded in appearance then that of the brook trout. The ascending limb from the bull trout premaxillary, also tended to project away from the medial prominence at a gentle posterior angle, which made the posterior notch appear more acute and rounded then seen in the brook trout.

The premaxillary of the genus *Oncorhynchus*, were dissimilar from those presented by members of the *Salvelinus* and *Salmo* genera. The premaxillary's from the four species of the genus *Oncorhynchus* presented in this study all displayed a non-notched posterior margin (Figure 5). In addition to this, the ridging present on the medial aspect of the premaxillary body was diminutive, and met at an equally diminutive medial prominence. Within the genus *Oncorhynchus*, the Pacific salmon generally maintained a short, and highly posteriorly angled ascending ridge and limb. Between the Pacific salmon, the kokanee presented with a shallow ethmoid fossa and a small posteriorly projecting point. The Chinook kept a deeply bowled out ethmoid fossa and lacked the small posterior projecting point.

In contrast to the short ascending ridge and limb of the Pacific salmon, the Pacific trout presented with an ascending limb and ridge that extended dorsally giving the premaxillary body the appearance of having a large dorsal lobe. Between the Pacific trout, the cutthroat trout's premaxillary symphysis extended far anteriorly, with the anterior lobe being thin and deeply curved inward. The rainbow trout, on the other hand, had a premaxillary symphysis that did not project far anteriorly and a relatively wide anterior lobe.

Analysis of the Premaxillae

The analysis of measurements generated from the premaxillary's of the Chinook, brook trout, bull trout and mountain whitefish, showed there was no statistical difference between paired right and left premaxillaries. For this reason the side of the head each premaxillary originated from was not taken into account during the construction of total length regression equations.

At least one of the three measurement taken from the nine salmonid premaxillaries were able to generate a significant regression equation for the back calculation of total fish length (Table 3). In only two occasions, the premaxillary of the mountain whitefish and the lake trout, did the use of a multi-linear regression equation provide a suitable, and statistically significant model for estimating total fish length. In the remaining fish a simple linear regression, with only a single variable, was the only statistically significant model produced.

Table 2. Linear regression equations for the premaxillary of each species using the measurements displayed in Figure 3. Total length range (TL mm) of each species, sample sizes (n) and respective p-values, r^2, and r^2 adjusted values for each equation presented are shown.

Species	Length Range TL (mm)	Regression Equation	Regression p-vlaue	r^2	r^2 Adjusted	n
Cutthroat trout	28-285	2.51*(Premaxillary A)+4.35	<0.001	0.985	0.971	7
Rainbow trout	89-263	2.61*(Premaxillary C)+4.47	<0.001	0.941	0.929	7
Chinook	71-182	2.19*(Premaxillary A)+4.28	<0.001	0.803	0.799	54
Mountain whitefish	95-303	2.07*(Premaxillary B)+2.59*(Premaxillary C)+4.54	<0.001	0.840	0.814	15
Brook trout	108.1-235.2	2.67*(Premaxillary B)+4.23	<0.001	0.555	0.527	18
Lake trout	85-791	4.45*(Premaxillary A)+ -0.74*(Premaxillary C)+3.96	<0.001	0.951	0.94	12

The Maxillary

The maxillae are also a paired set of bones that help make the upper gape of the fish (Figure 6). These two bones run the length of the mouth from where they articulate with the premaxillae in the snout to the posterior margin of the mouth and can be clearly seen over hanging the lower jaw of a fully intact fish. Members of the sub-family Salmoninae maintain a single row of homodont caniform teeth on the dental palate of this bone. As seen in the premaxillae, bones from members of the sub-family Coegoninae are vastly different. This holds true for the maxillary, which as seen in the mountain whitefish, has a broader and shorter maxillary body, with no teeth and a deeply curved dental palate (Figure 6). For the remainder of the salmonids displayed here the maxillary body maintains a relatively elongate and slender shape with a broadly curved dorsal margin.

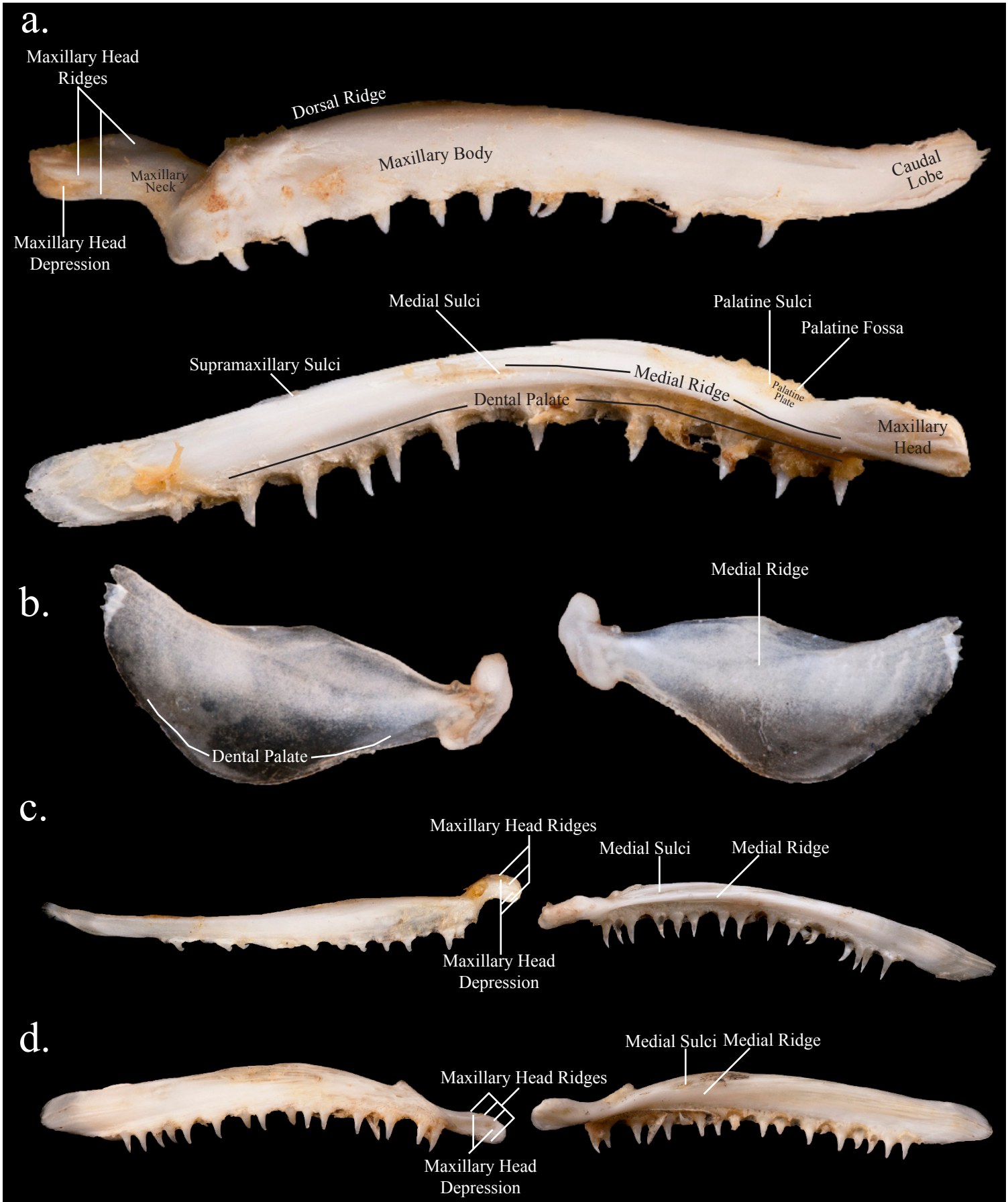

Figure 6.a. The lateral (top) and medial (bottom) left maxillary of the bull trout; b. the lateral (left) and medial (right) left maxillary of a mountain white fish; c. the lateral (left) and medial (right) right maxillary of a brook trout; and d. the lateral (left) and medial (right) right maxillary of a brown trout marked with anatomical structures.

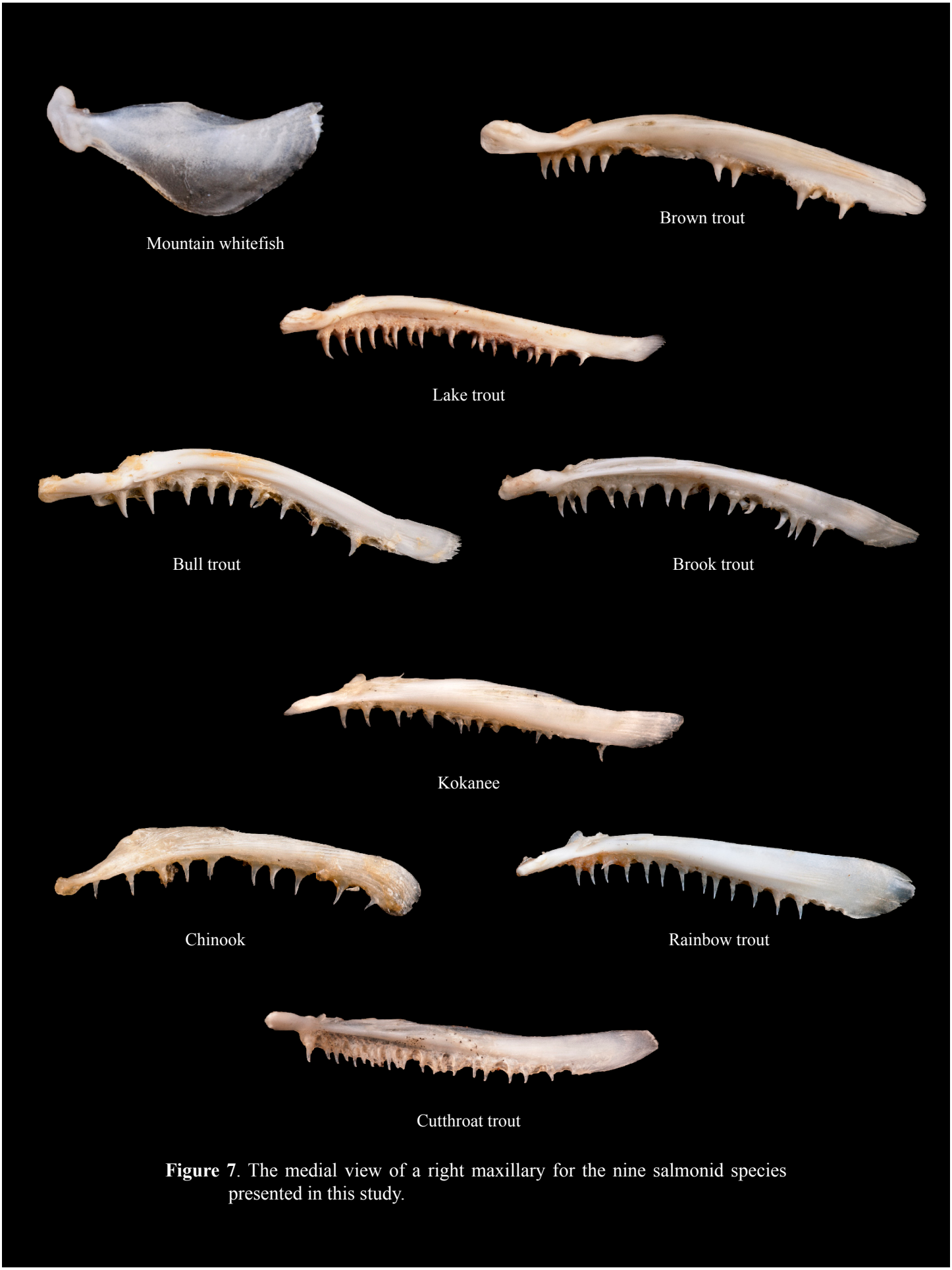

Figure 7. The medial view of a right maxillary for the nine salmonid species presented in this study.

The anterior portion of the maxillae has a head that extends away from the anterior part of the maxillae to articulate with the premaxillae at the maxillary fossa (Figure 6). There are a number of ridges and depressions present on the maxillary head. These ridges and depressions vary in number and position between species. Posterior to the head is the maxillary neck, palatine plate and palatine sulcus. The palatine plate and sulcus are an articulation point with the palatine bone. The remainder of the bone, the maxillary body, is elongated along the outer margin of the mouth. The medial side of the maxillary body may have a set of ridges and sulci. The number and orientation of these ridges and sulci differ slightly among the species observed in this study. The dorsal edge of this bone has a ridge and sulcus that associate with the supramaxilla bones. The maxillary body widens at its posterior margins into the smooth flat osseous membrane of the caudal lobe. In all species observed in this study, this portion of the maxillae maintains no teeth and is generally rounded along its posterior margin, though as presented in Figure 6 the posterior margin may present with a more pointed posterior margin.

The lack of teeth and the presence of a dental palate that maintains a broad ventral curvature is a key identifying feature of the mountain whitefish and a major difference present between species from the Coregoninae and Salmoninae subfamilies. As displayed in Figure 7, the maxillary of the mountain whitefish appears much shorter and stouter than the other eight species from the subfamily Salmoniae. These other eight species maintain a maxillary that is long and slender and has a dental palate that is full of teeth and is either flat or curved dorsally.

The maxillaries of the eight species of Salmoninae can be divided into two distinct groups based on the general appearance of the maxillary head and neck. The first group, which is composed of the sole member from the genus *Salmo*, the brown trout, and the three members of the genus *Salvelinus*, display a maxillary head and neck that extend away from the maxillary body in a widened club shaped structure. The lateral face of this club shaped maxillary head is additionally covered by a number of alternating ridges and depressions. Conversely, the second grouping, made up of our members of the *Oncorhynchus* genus, displays a maxillary head and neck complex that extends away from the maxillary body as a thin and more cylindrical shaped structure. Though, in the kokanee and cutthroat trout, this maxillary head neck structure is flattened on the lateral face.

Among the salmonids present in the first group, the brown trout presents with one single dominate ridge on the lateral surface of the maxillary head. Members of the genus *Salvelinus* did not display this dominate medial ridge on the maxillary head. Rather, they displayed three to four maxillary head ridges that were relatively equivalent in size. Differences present among the three members of the genus *Salvelinus* can initially be made on the appearance of the lateral fusion point between the maxillary neck and body. On the bull trout this area extends anteriorly away from the maxillary neck into a large rounded prominence. Medial to this rounded prominence is a deep crease that runs up towards the palatine plate. The maxillary of the lake and brook trout do not present with this large rounded prominence and deep crease. Rather, these two fish present with either a very shallow crease and a ventrally pointed prominence, as seen in the lake trout, or no crease and prominence, as seen in the brook trout.

Among the salmonids present in the second group a quick distinction between the two members of the Pacific salmon and the two members of the Pacific trout can be made based on the presence of a heavily striated and pockmarked lateral surface, which is present in the Pacific salmon, or a smooth lateral surface, which is present in the Pacific trout. From this initial distinction the differences between Chinook and kokanee are stark, with the maxillae of the Chinook being greatly dorso-ventrally curved and having a highly cylindrical maxillary head-neck complex. Conversely, the maxillae of the kokanee is generally straight and maintains a maxillary head with a flattened lateral face. The maxillae of the cutthroat and rainbow trout are much closer in appearance to the kokanee than the Chinook. Between these two species, the rainbow trout has a slightly dorso-ventrally curved maxillae with a thin cylindrical maxillary head-neck complex. Additionally, the rainbow trout maxillary widens considerably as the maxillary body transitions into the caudal lobe. The maxillary of the cutthroat trout displays a maxillary head that, like the kokanee, is flattened along its lateral surface. Additionally, the maxillary body of the cutthroat is straight with a slight dorsal curvature of the caudal lobe, and the maxillary body of the cutthroat does not greatly increase its width as it transitions into the caudal lobe.

Analysis of the Maxillary

The analysis of the measurements generated from the maxillaries of the Chinook, brook trout, bull trout, and mountain whitefish, showed there was no statistical difference between right and left paired maxillaries. For this reason the side of the head each maxillary originated from was not taken into account during the construction of total length regression equations.

With the exception of the brook trout, a highly significant regression equation could be generated using the single measurement taken from the maxillary (Table 4).

Table 3. Linear regression equations for the maxillary of each species using the measurements displayed in Figure 3. Total length range (TL mm) of each species, sample sizes (n) and respective p-values, r^2, and r^2 adjusted values for each equation presented are shown.

Species	Length Range TL (mm)	Regression Equation	Regression p-vlaue	r^2	r^2 Adjusted	n
Cutthroat trout	28-285	1.38*(Maxillary A)+3.88	<0.001	0.880	0.867	11
Rainbow trout	89-263	2.61*(Maxillary A)+4.47	<0.001	0.941	0.929	7
Chinook	71-182	1.48*(Maxillary A)+3.67	<0.001	0.908	0.906	58
Mountain whitefish	95-303	2.26*(Maxillary A)+4.11	<0.001	0.842	0.834	20
Brook trout	108.1-235.2	0.42*(Maxillary A)+4.65	<0.001	0.396	0.372	27
Lake trout	85-791	2.03*(Maxillary A)+3.29	<0.001	0.709	0.689	17

The Dentary

The dentaries are a paired set of bones that are the major component of the lower jaw (Figure 8). These two bones articulate with each other at the mandibular symphysis, the anterior most portion of the lower jaw. From this point, these bones extend back to create the lower gape. Like the premaxillary and maxillary, primitive fish (i.e. members of the subfamily Salmoninae) generally have teeth along the dental plate. More advanced fish, (members of the subfamily Core-

goninae) do not have teeth on the dental palate (Figure 8). In an intact fish, the medial side of each dentary is broadly connected to the angular bone (Figure 8). Where the angular bone connects to the posterior of the dentary, a wide Y shaped gap, the meckelian notch, is present. The angle and appearance of the meckelian notch can vary greatly between species (Figure 8 and 8). Jutting away from the meckelian notch and wrapping around the angular bone are the coronoid and ventral processes. Like the meckelian notch these two structures can also differ greatly among species.

The dentary body is composed of two osseous membranes that form a medial and lateral wall of the dentary body. These two sheets of bone are more or less fused together into a single solid structure, however, the medial wall can sometimes be seen jutting slightly posterior of the lateral wall at the meckelian notch. On the medial side of the dentary the medial wall is bordered by a prominent dorsal and ventral ridge. The inferior to the ventral ridge is a small osseous shelf, the ventral shelf. The dorsal and ventral ridges often meet and fuse at their anterior most portions, leaving a round hollowed fossa, the sublingual fossa under the lingual palate. Along the ventral margin a large sensory canal runs from the mandibular symphysis to the ventral tip. This sensory canal can be seen on both the medial (the ventral ridge) and lateral aspects of the dentary. Along the later aspect in most species a number of well defined sensory pores open into this large sensory canal. Variations in the number of pores (Figure 8) and the presence of one or two rows of pores helps differentiate a number of the species observed in this study. Further, differentiation of the dentaries can be made by viewing the wide variation in dentary shape and structure amongst different species. A few of these differences and a number of the different styles of dentaries observed in this study can be viewed in Figure 8.

Like the premaxillary and maxillary, ancestral fish (i.e. members of the subfamily Salmoninae) present with teeth along the dental plate. Conversely, members of the subfamily Coregoninae do not have teeth on the dental palate (Figure 9). Like the maxillary and premaxillary the presence or absence of teeth is the first diagnostic characteristic seen between the nine salmonids presented in this study. This diagnostic characteristic is the main feature that separates the mountain whitefish from the remaining eight species.

From this point, the eight species of the subfamily Salmoninae can be divided into two groups. These two groups are separated based on the size and shape of the coronoid process and the ventral limb. Like the maxillary, group one represents the members of the genus *Salmo* and *Salvelinus*. This group displays a coronoid process and ventral limb that are relatively even in size and are separated by a wide mekelian notch. In group two are the members of the genus *Oncorhychus* (Figure 9). These fish from group two display a ventral limb that is much larger then the diminutive appearing coronoid process. Additionally, members of this group have a small mekelian notch that sits just inferior to the coronoid process.

Among the four members of group one, the brown trout is the only species that presents with a forward projection of the dental palate (Figure 9). This forward projection creates a small overhanging shelf along the lateral side of the dentary body right next to the mandibular symphysis. Of the remaining three fish in this group, the brook trout presents with a curved ventral margin that has five to six major sensory pores located directly on its ventral most margin. The bull trout and lake trout present with a strait ventral margin with sensory pores that are superior to the ventral

margin. Between the lake trout and the bull trout there are some variations present in the number of sensory pores, with lake trout displaying between six to seven major sensory pores and the bull trout displaying between four to six. The major difference between these two fish, however, is the presence of a small ventral jutting of the mandibular symphysis, which is seen in the lake trout.

Among the four members of group two, an initial separation can be made between the Pacific salmon, which have a heavily striated and pockmarked lateral dentary body, and the Pacific trout, which have a mostly smooth lateral dentary body (Figure 9). Between the Chinook and kokanee, there is a drastic difference in the size of the ventral process, which is large in the kokanee. The Chinook can also be identified by the noticeable curvature present across the entire dentary. Between the rainbow trout and the cutthroat trout the main identifying difference is also present in the ventral process, with the rainbow trout having a ventral limb that projects away from the mandibular symphysis in a ventral angle. This ventrally angled ventral process is also wide. Conversely, the ventral limb of the cutthroat trout extends nearly straight back from the mandibular symphysis.

Analysis of the Dentary

Meristic counts of the major and minor sensory pores were taken from the dentaries of the cutthroat trout, rainbow trout, kokanee, Chinook, bull trout, brook trout and lake trout. Major sensory pore counts varied between four to six in most species, except the lake trout which varied between six and seven (Table 5). The Chinook was the only species that presented with no minor sensory pores. For the other six species the cutthroat trout, rainbow trout and bull trout minor sensory pores varied between two and four. The minor sensory pores of the brook trout varied between zero and four and the lake trout and kokanee varied between three and six.

The analysis of the measurements generated from paired dentaries of the Chinook, brook trout, bull trout, and mountain whitefish, showed there was no statistical difference between right and left side of the head. For this reason the side of the head each dentary originated from was not taken into account during the construction of total length regression equations.

Table 4. The range of meristic counts taken from the dentaries major and minor sensory pores.

Species	n	Range of Major Sensory Pores	Range of Minor Sensory Pores
Cutthroat trout	6	5-6	3-4
Rainbow trout	8	4-5	2-4
Kokanee	8	4	3-5
Chinook	10	5-6	0
Bull trout	13	4-6	2-4
Brook trout	15	5-6	0-4
Lake trout	10	6-7	3-6

At least one of the five measurement taken from the nine salmonid dentaries were able to generate a significant regression equation for the back calculation of total fish length (Table 6).

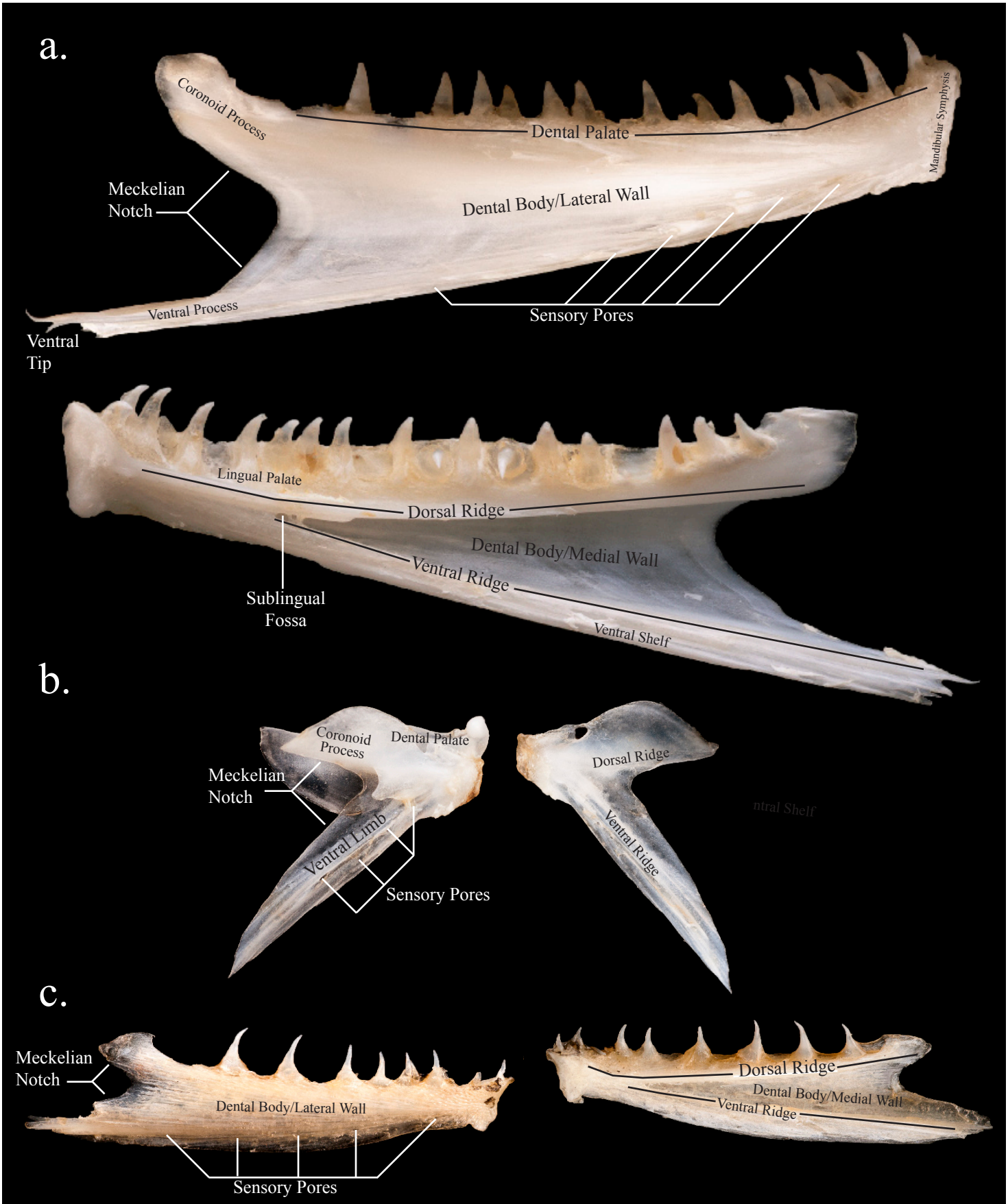

Figure 8.a. The lateral (top) and medial (bottom) left dentarty of the bull trout; b. The lateral (left) and medial (right) right dentary of a mountain white fish; and c. The lateral (left) and medial (right) right dentary of a chinook labeled with anatomical structures.

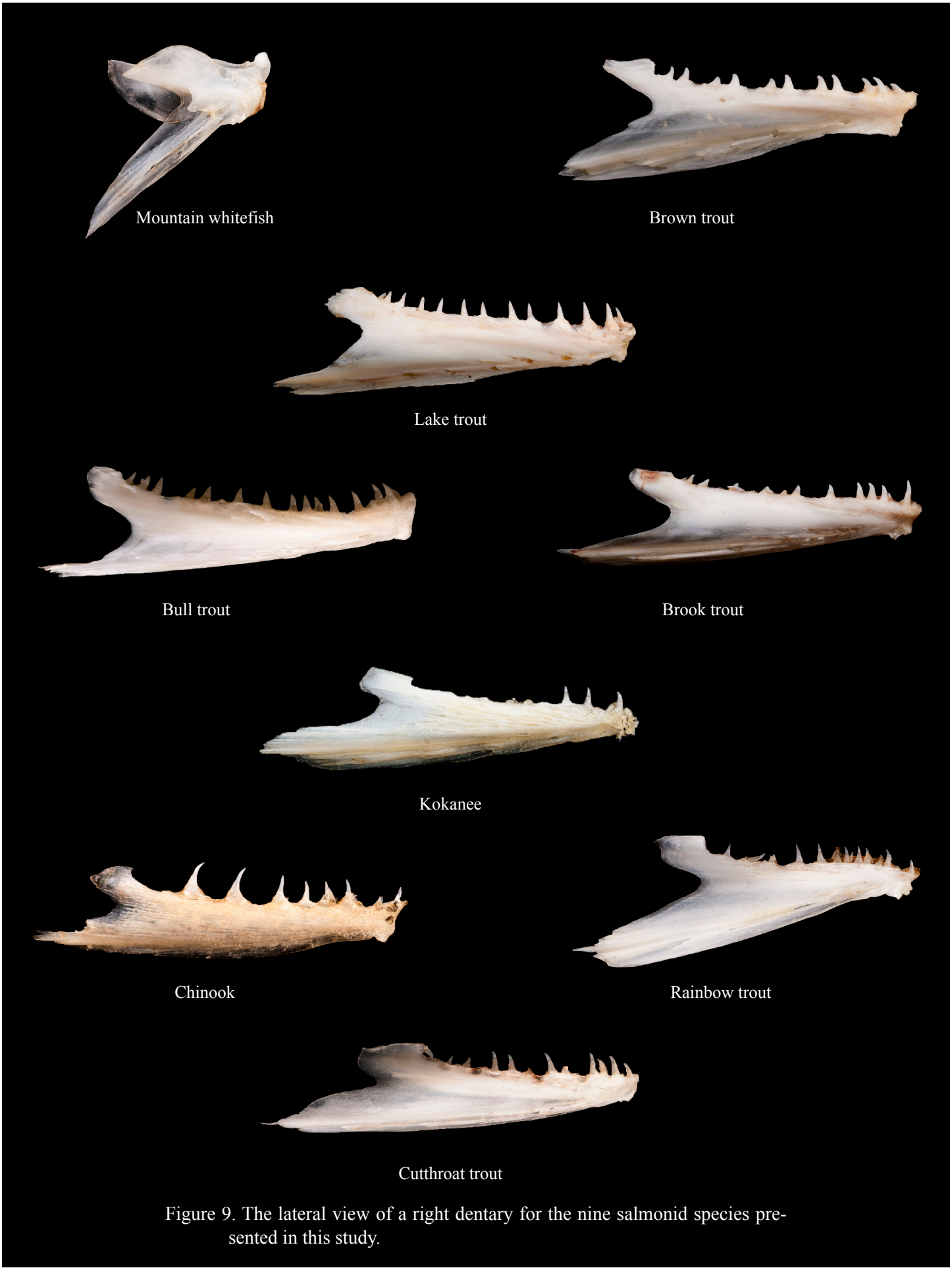

Figure 9. The lateral view of a right dentary for the nine salmonid species presented in this study.

It was found that in three species, the mountain whitefish, brook trout, and the lake trout, did the use of a multi-linear regression equation provide a suitable, and statistically significant model for estimating total fish length. In the remaining fish a simple linear regression, with only a single variable, was the only statistically significant model produced.

Table 5. Linear regression equations for the dentary of each species using the measurements displayed in Figure 3. Total length range (TL mm) of each species, sample sizes (n) and respective p-values, r^2, and r^2 adjusted values for each equation presented are shown.

Species	Length Range TL (mm)	Regression Equation	Regression p-vlaue	r^2	r^2 Adjusted	n
Cutthroat trout	28-285	1.71*(Dentary A)+3.78	<0.001	0.867	0.850	10
Rainbow trout	89-263	2.02*(Dentary C)+3.75	<0.001	0.977	0.974	9
Kokanee	54-360	2.02*(Dentary E)+4.15	<0.001	0.902	0.886	8
Chinook	71-182	1.35*(Dentary B)+3.65	<0.001	0.925	0.924	62
Mountain whitefish	95-303	2.39*(Dentary A)+2.96*(Dentary D)+3.67	<0.001	0.880	0.862	16
Bull trout	31.5-544	1.995*(Dentary B)+3.03	<0.001	0.877	0.875	66
Brook trout	108.1-235.2	1.08*(Dentary C)+0.71*(Dentary E)+3.89	<0.001	0.964	0.961	35
Lake trout	85-791	2.34*(Dentary B)+ -2.92*(Dentary D)+3.38	<0.001	0.987	0.985	14

The Cleithra

The cleithra is located posterior to the opercular complex and is a major component of the pectoral girdle. In salmonids this large L shaped bone can be broken up into two major sections, the vertical and horizontal limbs (Figure 10). These two limbs meet at a heavily ossified laterally protruding point, the lateral prominence. The vertical limb projects dorsally from the lateral prominence in a thick osseous ridge, the vertical line, that connects with the supracleithrum in an intact fish. Located along the posterior edge of the vertical line can often be found a number of long sensory canals that open up towards the dorsal margins of the vertical limb. In some species observed in this study, mainly those from the genus *Oncorhynchus* and in particular members classified as pacific salmon, maintain numerous sensory canals and pores that project back away from the vertical line towards the posterior margin of the cleithra. This area, the dorso-posterior lobe, were these sensory canals and pores can be found is a large flat sheet of osseous material that fans out along the posterior margin of vertical limb. The dorso-posterior lobe generally maintains a flat or gently rounded posterior margin and can vary greatly in size between genera and species.

The horizontal limb projects anteriorly away from the lateral prominence and under the ventral margins of the opercular complex. The horizontal limb fans out into two, often wide, osseous membranes of the dorsal and ventral lobes. These two lobes are separated by a thickened osseous ridge, the horizontal line, and thin crease, the horizontal sulcus. The horizontal line and sulcus are two of the most prominent structures on the body of the horizontal limb, and are clearly visible from both the lateral and medial aspects of the cleithra. These two structures usually protrude anteriorly from the lateral prominence towards the ventral tip, often remaining relatively near each other. Along the medial side of the horizontal line, right in front of the lateral prominence, a thin osseous structure, the medial process, is often seen projecting inward. This structure fans out away from the medial side of the horizontal limb and progresses anteriorly, often along the same tract

as the horizontal line. Variations present in how much lateral bow the horizontal limb presents with, as displayed in Figure 10, the width of the horizontal limbs dorsal and ventral lobes, and the position/angle of the horizontal line and sulcus are able to define all of the species observed in this study.

Glancing over the cleithra from the nine salmonids displayed in Figure 11 shows the drastic difference in the width of the dorso-posterior, dorsal, and ventral lobes present between the mountain whitefish and the remaining eight members of the subfamily Salmoninae. Additional diagnostic characteristics that set the mountain whitefish apart are the presence of a prominent ventral notch below the lateral prominence, and a dorsal lobe and dorso-posterior lobe that meet each other at about the same location up the vertical limb.

The next separation among the cleithra of the nine salmonids is displayed in the brown trout. The horizontal limb of the brown trout cleithra is strongly curved laterally and maintains a ventral tip that curves down to an over hung point. The horizontal limb of the remaining seven species do not display the high degree of lateral curvature that is seen in the brown trout, nor does the ventral tip curve down to an over hung point.

Separating the cleithra of the genera *Salvelinus* and *Oncorhynchus* takes close inspection of the medial side of the horizontal limb and the curvature of the vertical line. The three members of genus *Salvelinus* present with a vertical line that curves forward as it transitions into the dorsal spine. This is not seen on the four members of genus *Oncorhynchus*, which have a more straightened vertical line and dorsal spine. In addition to the difference seen in the vertical line between these two groups, there is a drastic difference in the length of the medial process, a small osseous sheet that projects medially away from the horizontal limb. The medial process is small and short among the members of *Salvelinus*. Conversely, the medial process is elongated in the genus *Oncorhynchus* and occasionally even progresses all the way out to the dorso-anterior margins of the dorsal lobe.

Differentiating among the three members of the genus *Salvelinus*, can be made based on variations in the osseous lobes of the vertical and horizontal limbs. In the bull trout all three of these lobes are relatively wide. Additionally, the dorso-posterior lobe of the bull trout is quite rounded along its posterior margin and more squared along its dorsal margin. In the lake trout and brook trout all three lobes are relatively thin, when compared to the bull trout. The main difference between these two species, however, is that the lake trout presents with a vertical lobe that is noticeably wider than the dorsal lobe. Conversely, the ventral lobe of the brook trout is very thin and the dorsal lobe is wider.

Similar to the premaxillary and dentary, the cleithra of the Pacific salmon and trout differ in the amount of striation present. The difference, however, seen in the cleithra is restricted to the medial side of the dorso-posterior lobe. In the Pacific salmon the dorso-posterior lobe is covered in numerous striations that progress back from the medial side of the lateral prominence towards the posterior margins. This is not seen in the Pacific trout, which have a more or less smooth dorso-posterior lobe. Between the Pacific salmon the main differing characteristic is seen in the variation of the horizontal limb, with the horizontal limb of the Chinook appearing to curve downward

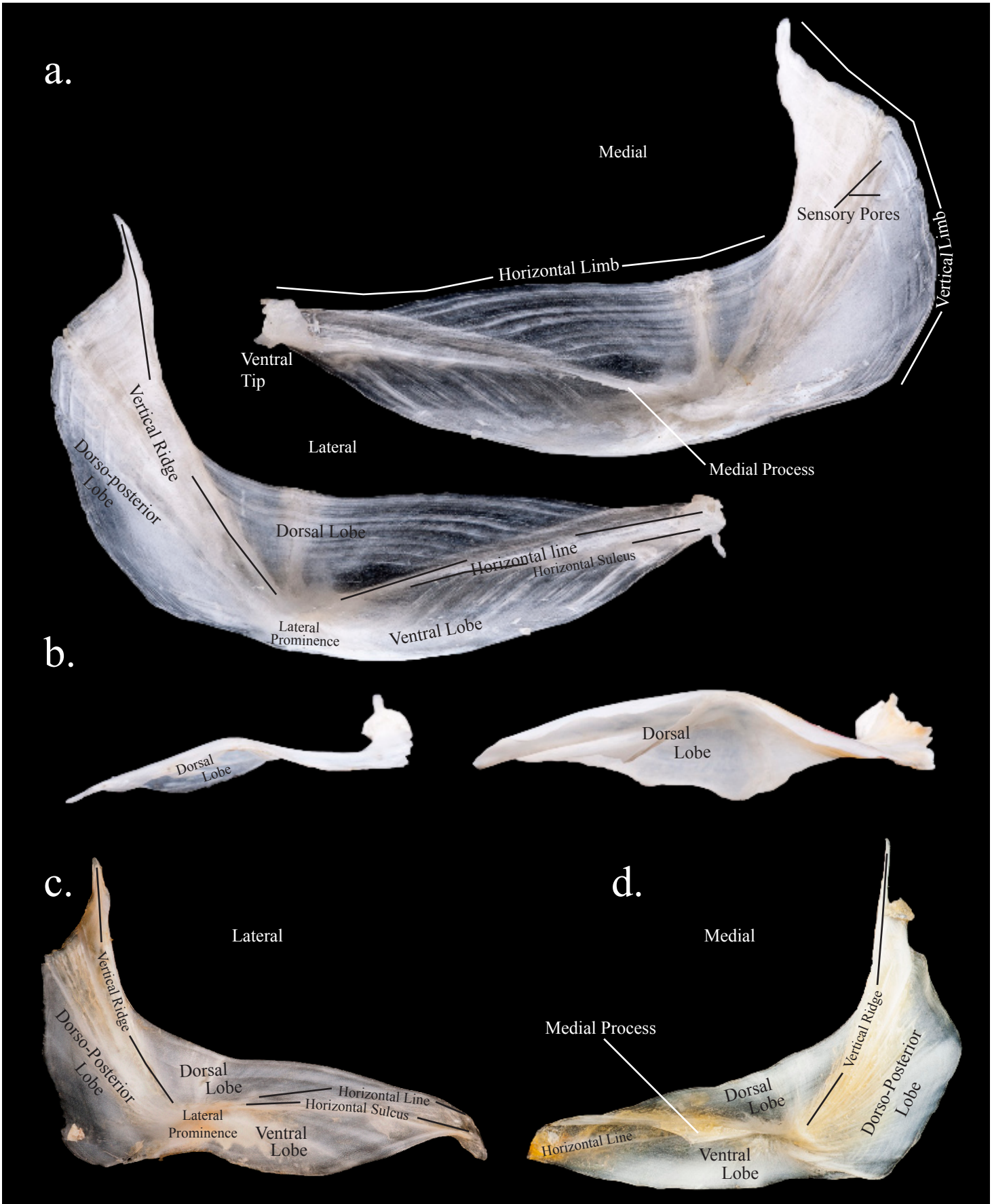

Figure 10.a. The right cleithra of a bull trout; b. ventral view of a bull trout (left) and cutthroat trout (right) cleithra; c. a right brown trout cleithra; and d. a right kokanee cleithra marked with anatomical structures.

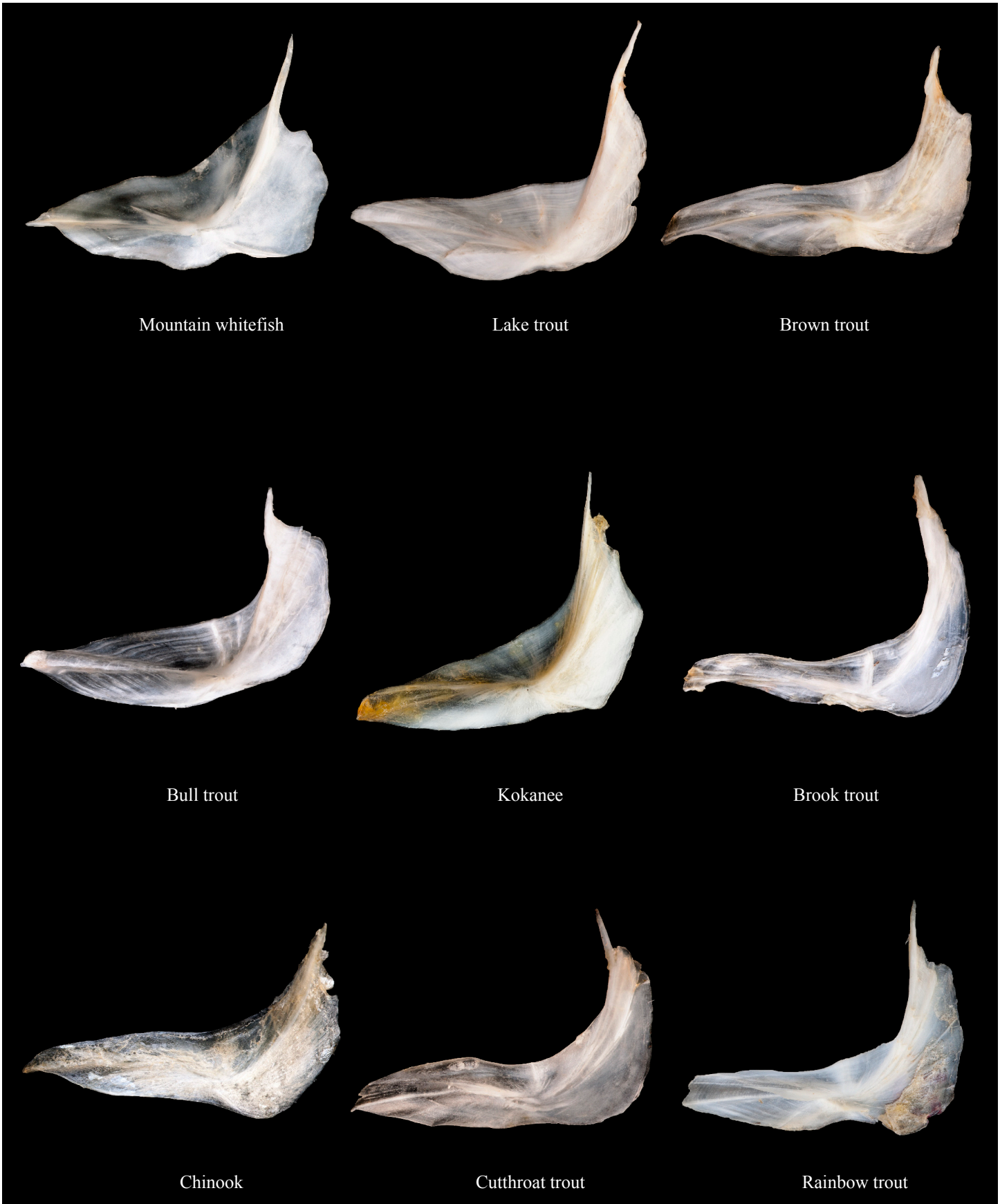

Figure 11. The lateral view of a left cleithra for the nine salmonid species presented in this study.

away from the rest of the cleithra. The horizontal limb of the kokanee, however, appears to project straight out of the lateral prominence.

Like the Pacific salmon, the Pacific trout also differ in the appearance of their horizontal limb. The difference between these two species, however, is mainly based on the appearance of the horizontal limbs length, with the horizontal limb of the cutthroat trout appearing much longer and more slender then the rainbow trout.

Analysis of the Cleithra

The analysis of the measurements generated from cleithra of the Chinook, brook trout, bull trout, and mountain whitefish, showed there was no statistical difference between paired right and left cleithra. For this reason the side of the body that each cleithra originated from was not taken into account during the construction of total length regression equations.

Total bone length to total length regressions for each fish provided at least one highly significant regression (Table 7). Three of the nine species, the Chinook, bull trout, and lake trout, were able to generate a significant model using multi-linear regression equation. For the remaining fish a simple linear regression, with only a single variable, was the only statistically significant model produced.

Table 6. Linear regression equations for the cleithra of each species using the measurements displayed in Figure 3. Total length range (TL mm) of each species, sample sizes (n) and respective p-values, r^2, and r^2 adjusted values for each equation presented are shown.

Species	Length Range TL (mm)	Regression Equation	Regression p-vlaue	r^2	r^2 Adjusted	n
Cutthroat trout	28-285	1.31*(Cleithra A)+3.84	<0.001	0.633	0.581	9
Rainbow trout	89-263	1.48*(Cleithra A)+3.63	<0.001	0.886	0.870	9
Kokanee	54-360	1.16*(Cleithra A)+4.02	<0.001	0.934	0.925	9
Chinook	71-182	1.02*(Cleithra A)+0.42*(Cleithra C)+3.68	<0.001	0.928	0.926	57
Mountain whitefish	95-303	1.64*(Cleithra A)+3.62	<0.001	0.979	0.978	19
Bull trout	31.5-544	2.51*(Cleithra A)+ -1.19*(Cleithra B)+2.98	<0.001	0.948	0.946	62
Brook trout	108.1-235.2	1.46*(Cleithra A)+3.64	<0.001	0.913	0.911	35
Lake trout	85-791	3.17*(Cleithra A)+ -1.73*(Cleithra C)+3.13	<0.001	0.970	0.964	13

The Preopercle

The preopercle is a small crescent shaped bone that helps create the anterior margin of the opercular complex (Figure 12). Like the Cleithra, the preopercle is divided into the two sections, the horizontal and vertical limbs. The major component of the preopercular body is a large and flat osseous membrane that fans out and back. This membrane, the posterior wing, remains relatively thin across the majority of its surface, though it does thicken as it nears the anterior margins of the preoperle. At first glance this thickened area appears to have a simple construction, with a single ridge that runs down the anterior margin. Along this ridge the preopercle connects to the hypomandibular, metapterygoid, symphletic, and quadrate bones. To help define, and classify par

ticular portions of the preopercle this anterior ridge has been divided into two different sections, each named for a major bone the section connects to. These sections, the hypomandibular ridge, and quadrate ridge can be viewed in Figure 12.

On the medial side of the preopercle there is a small depressed area between the dividing point of the hypomandibular and quadrate ridges. A small osseous shelf projects anterior of this depressed area and overhangs the inferior portions of the hypomandibular ridge's anterior margin. This shelf, the symphletic shelf, is a relatively minor portion of the preopercle, but will be used to help describe a few of the species in the following dichotomous key. At the anterior most point of the preopercle, the posterior wings osseous membrane projects past the end of the quadrate ridge, leaving a thin osseous shelf. This section of the bone is referred to here as the retroarticular joint.

When the preopercle is inspected closely, a single large sensory canal and many smaller sensory canals are present on the posterior wing and anterior (hypomandibular) ridge. These canals are a portion of the acoustico-lateralis system, a major branch of the nervous system that gathers information about displacement and sound. The major sensory canal of the preopercle that is associated with this system runs down the length of the anterior ridges, ending at the anterio-ventral tip. Numerous smaller sensory canals branch off this major canal and cover most of the posterior wings body. In most of the species observed in this study it was common to have these minor sensory canals project dorsally, posteriorly, and ventrally. In a few cases, the rainbow trout and brown trout for example, clusters of small pores were found jutting dorsally right behind the hypomandibular ridge. The number and orientation of these minor sensory branches can be used to differentiate the species observed here.

The first identifiable difference among the nine salmonids in this study can be seen in the length of the horizontal limb, which is much longer in the mountain whitefish (Figure 13). This lengthening of the horizontal limb gives the mountain whitefish's preopercle a more L shaped appearance then the crescent shape of the other salmonids.

Like the premaxillary, maxillary, and dentary, the preopercle of the eight species from the subfamily Salmoninae can be divided into two groups. This division is based mainly on the hypomandibular ridge, which has a slight medial bow and the presence of four ventrally descending sensory pores and canals in fish from the genus *Salvelinus* and *Salmo* (Figure 13). In contrast to this, fish from the genus *Oncorhynchus* have a hypomandibular ridge that is either bowed slightly laterally or not at all, and presents with more then four ventrally descending sensory pores and canals.

Between the four fish of group one, the preopercle of the brown trout is most dissimilar and is characterized by a very short and blunted horizontal limb (Figure 13). Among the remaining three species, the lake trout present with a very slender posterior wing that narrows considerably as it progresses up the vertical limb. The brook trout has a peropercluar body that is more club like in appearance, with a wide ventral portion of the posterior wing and blunted anterior-ventral tip. Conversely, the preopercle of the bull trout has a posterior wing that has a gently curved posterior margin and is relatively even in size across the entire preopercular body.

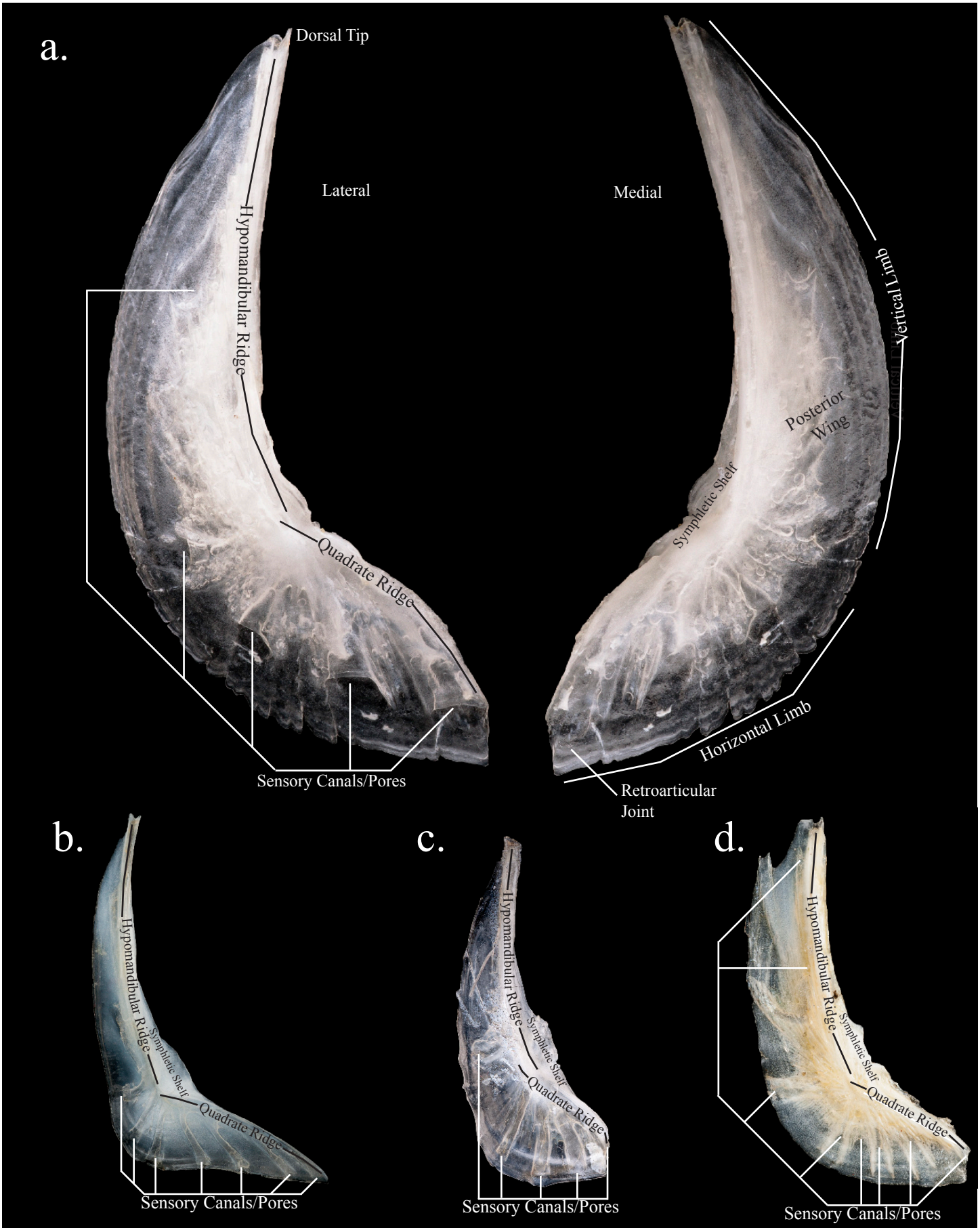

Figure 12.a. The left preopercle of a bull trout; and the left medial view of b. a mountain whitefish; c. brook trout; and d. kokanee preopercle marked with anatomical structures.

Figure 13. The medial view of a right preopercle for the nine salmonid species presented in this study.

Among the four fish of group two, a separation can be made between the Pacific salmon and trout based on the width of the posterior wing and the length of the horizontal limb (Figure 13). The Chinook and kokanee both have a posterior wing that remains wide as it progresses up the vertical limb, and have a short and blunted horizontal limb. Conversely, the cutthroat trout and rainbow trout have a posterior wing that thins as it progresses up the vertical limb and a longer more rounded horizontal limb.

The main difference between the Chinook and kokanee is the presence of one or two long dorsally protruding spines that extend upward from the hypomandibular ridge past the dorso-posterior margins of the posterior wing (Figure 13). These spines are only present in the preopercle of the kokanee. In contrast to this the preopercle of the Chinook is smoothly curved along its posterior margins and there are no dorsally ascending spines.

Differentiating the rainbow trout and the cutthroat trout takes close inspection of the small sensory pores and canals that branch off the major sensory canal in the hypomandibular ridge (Figure 13). In the rainbow trout these small sensory pores are grouped in numerous clusters on both the vertical and horizontal limbs. In the cutthroat trout these sensory pores are not clustered. Rather, the sensory pores located on the posterior wing of the cutthroat trout each progress away from the hypomandibular and quadrate ridge as long slender canals.

Analysis of the Preopercle

The analysis of the measurements generated from the preopercle of the Chinook, brook trout, bull trout, and mountain whitefish, showed there was no statistical difference between paired right and left preopercles. For this reason the side of the body that each preopercle originated from was not taken into account during the construction of the following total length regression equations.

Total bone length to total length regressions for each fish provided at least one highly significant regression (Table 8). Three of the nine species, the Chinook, bull trout, and lake trout, were able to generate a significant model using multi-linear regression equation. For the remaining fish a simple linear regression, with only a single variable, was the only statistically significant model produced.

Table 7. Linear regression equations for the preopercle of each species using the measurements displayed in Figure 3. Total length range (TL mm) of each species, sample sizes (n) and respective p-values, r^2, and r^2 adjusted values for each equation presented are shown.

Species	Length Range TL (mm)	Regression Equation	Regression p-vlaue	r^2	r^2 Adjusted	n
Cutthroat trout	28-285	1.87*(Preopercle A)+3.64	<0.001	0.937	0.928	9
Rainbow trout	89-263	1.68*(Preopercle C)+4.32	<0.001	0.943	0.936	10
Chinook	71-182	1.55*(Preopercle A)+3.71	<0.001	0.933	0.931	60
Mountain whitefish	95-303	1.57*(Preopercle A)+3.80	<0.001	0.960	0.958	22
Bull trout	31.5-544	2.22*(Preopercle A)+3.17	<0.001	0.921	0.920	68
Brook trout	108.1-235.2	1.03*(Preopercle A)+1.06*(Preopercle B)+3.93	<0.001	0.870	0.862	35
Lake trout	85-791	2.13*(Preopercle A)+ -0.79*(Preopercle C)+3.73	<0.001	0.981	0.978	14

The Opercle

The salmonid opercle is a large flat, four sided bone with margins clearly visible even on an intact fish. The opercle is broadly connected to the preopercle along its anterior margins and the subopercle along its ventral margins. Along the posterior margins, however, the opercle is not connected to any other bone. Instead a flap of tissue, the opercular valve, forms a seal over posterior edge of the opercular chamber. Inside the operclular chamber is where a fishes gills are located. Innervation of the operculum and the branchiostegal rays allows a fish to expand and contract the volume of the opercular chamber. This action changes the volume of the opercular chamber to, allowing the fish to create a water pressure gradient between the mouth/buccal chamber and the opercular chamber. This helps pull water from the fishes mouth, an area of high pressure during opercular expansion, into the opercular chamber and past the gill filaments. Water is then expelled out of the rear of the opercular chamber when the opercular valve is released.

The fact that the opercle is more or less one flat sheet of bony material makes classifying this bone challenging. Classification and differentiation between salmonid species is, therefore, made off the basis of variations in bone shape, curvature or lack of curvature in the anterior, dorsal, posterior and ventral margins, and the presence and absence of the few minor structures present (Figure 14). To do this the large bony sheet that is the body of the opercle has been divided into a dorsal and ventral lobe. A thin ridge, the dorsal ridge, separates these two lobes. The remaining defining features of the opercle exist around the articular fossa, a large and defining feature in the anterior dorsal region of the opercle. Three ridges; the anterior, dorsal, and vertical ridges, are visible on the medial side of the opercle. These three ridges all originate from the articular fossa. One should note that in larger specimens, the area around the articular fossa can become quite porous in appearance. This may obscure details, and may present issues in the identification of fish based on these three ridges. On the lateral side of the articular fossa a number of small pores or large striations may be present. These pores and striations also appear to become more abundant and deeper in larger specimens.

As aforementioned, differentiating the opercle between the nine salmonid species is based mainly on slight variations in the shape of the opercular margins, and the size and appearance of the dorsal and ventral lobes. It is this second difference, the size of the lobes, which initially differentiates the mountain whitefish from the other eight species. The mountain whitefish has a greatly enlarged dorsal lobe that has a broadly curved dorsal margin that sweeps back to a shallow posterior notch (Figure 15). The other eight species have a more reduced dorsal lobe, that extends upward only slightly superior to the articular fossa.

Among the three genera of the subfamily Salmoninae, the brown trout is the most dissimilar, presenting with an anterior margin the scoops out from the articular fossa to a far anterior position (Figure 15). Though the anterior margin of the remaining two genera, *Salvelinus* and *Oncorhynchus*, did allow for differentiation of these two groups, no other species displayed the same degree of forward scooping that the brown trout did.

Differentiation between the genus *Salvelinus* and *Oncorhynchus* was mainly made based on the appearance of the anterior margin. The anterior margin of the genus *Salvelinus* presented

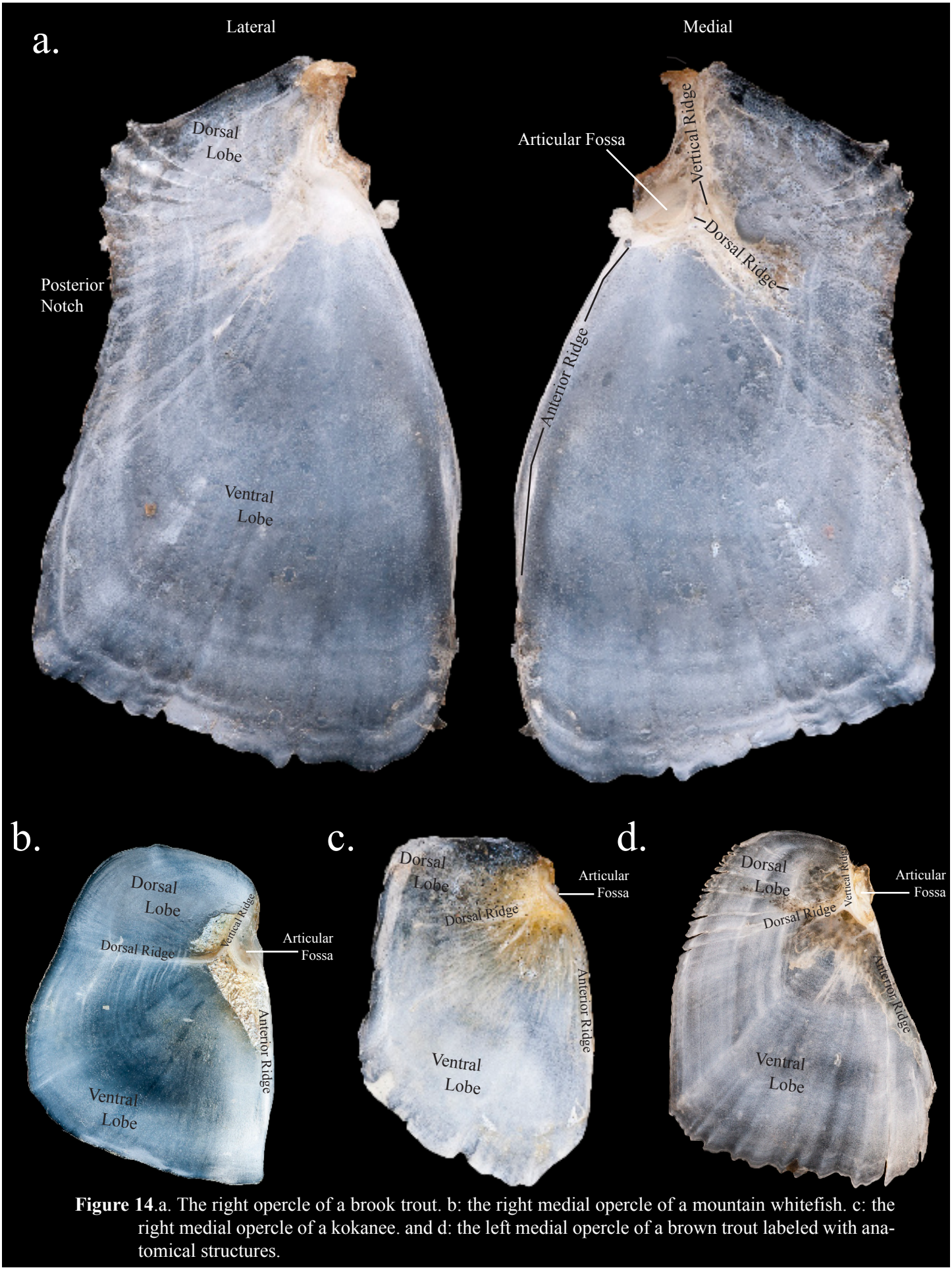

Figure 14.a. The right opercle of a brook trout. b: the right medial opercle of a mountain whitefish. c: the right medial opercle of a kokanee. and d: the left medial opercle of a brown trout labeled with anatomical structures.

Figure 15. The medial view of a right opercle for the nine salmonid species presented in this study.

with a noticeable forward curvature that progressed from the articular fossa to the ventral tip (Figure 15). This was not seen in the genus *Oncorhynchus*, which presented with an anterior margin that generally appeared as flat or only slightly curved just inferior to the articular fossa.

Among the three species of the genus *Salvelinus* the lake trout presented with a large notch along its dorsal margin (Figure 15). This notch is located just posterior to the upward projecting vertical ridge. Conversely, the brook trout and bull trout did not present with this same dorsal lobe notching. Instead dorsal lobe was either flat with a ventrally descending angle, as seen in the brook trout, or was gently curved, as seen in the bull trout. Further differentiations between the brook trout and bull trout can be made based on the presence of a unique pattern of dorso-posteriorlly fanning striations present on the dorsal lobe of the brook trout.

Among the four members of the genus *Oncorhynchus*, the kokanee and Chinook present with a medial opercular surface that is heavily striated (Figure 15). These numerous striations originate from the articular fossa and progress back towards the posterior ventral margins of the opercle. The rainbow trout and cutthroat trout did not present with these striations and instead maintained a medial opercular surface that was smooth.

Between the kokanee and the Chinook there was slight variation present between the anterior margin and the anterior ridge (Figure 15). In the kokanee the anterior margin has an abrupt curve as it leaves the articular fossa. Additionally, the anterior ridge of the kokanee is clearly visible. In the Chinook the anterior margin dose not have an abrupt curve as it leaves the articular fossa, and the anterior ridge is reduced and obscured by the numerous striations that are present along the opercular body.

Similar to the kokanee and Chinook, the anterior margin of the rainbow trout and cutthroat trout are a major differentiating characteristic. The anterior margin of the cutthroat trout maintains a flat face that extends almost all the way from the top of the dorsal lobe to the ventral tip (Figure 15). Conversely, the anterior margin of the rainbow trout, though it is mostly flat, tappers back considerably as it nears the ventral tip.

Analysis of the Opercle

The analysis of the measurements generated from the opercles of the Chinook, brook trout, bull trout, and mountain whitefish, showed there was no statistical difference between paired right and left opercles. For this reason the side of the body that each opercle originated from was not taken into account during the construction of the following total length regression equations.

Total bone length to total length regressions for each fish provided at least one highly significant regression (Table 9). Five of the nine species, the Chinook, mountain whitefish, bull trout, brook trout, and lake trout, were able to generate a significant model using multi-linear regression equation. For the remaining fish a simple linear regression, with only a single variable, was the only statistically significant model produced.

Table 8. Linear regression equations for the opercle of each species using the measurements displayed in Figure 3. Total length range (TL mm) of each species, sample sizes (n) and respective p-values, r^2, and r^2 adjusted values for each equation presented are shown.

Species	Length Range TL (mm)	Regression Equation	Regression p-vlaue	r^2	r^2 Adjusted	n
Cutthroat trout	28-285	2.40*(Opercle D)+3.50	<0.001	0.779	0.735	7
Rainbow trout	89-263	1.70*(Opercle B)+4.11	<0.001	0.953	0.945	8
Kokanee	54-360	1.22*(Opercle A)+4.34	0.002	0.935	0.919	6
Chinook	71-182	0.81*(Opercle B)+0.89*(Opercle D)+3.90	<0.001	0.929	0.927	57
Mountain whitefish	95-303	1.33*(Opercle D)+ -0.79*(Opercle E)+3.68	<0.001	0.880	0.862	16
Bull trout	31.5-544	2.10*(Opercle B)+ -2.91*(Opercle C)+2.52 *(Opercle D)+3.18	<0.001	0.943	0.940	68
Brook trout	108.1-235.2	0.90*(Opercle D)+0.95*(Opercle E)+3.81	<0.001	0.930	0.925	27
Lake trout	85-791	-4.88*(Opercle A)+5.05*(Opercle D)+1.72 *(Opercle E)+3.69	<0.001	0.987	0.983	13

The Pharyngeal Arch and Vertebra

Visual analysis of both the pharyngeal arch and the vertebra of the nine salmoid species from this study revealed no discernible characteristics. Therefore this document will only present the results from the total bone length to total fish length regression analysis in Tables 10 and 11.

For the pharyngeal arch samples from only the Chinook, mountain whitefish, bull trout, and brook trout were available for analysis. Of these four species the total length of the mountain whitefish and brook trout could only be estimated through the use of s simple linear regressing with the measurement "pharyngeal A". The most significant models for the Chinook and bull trout, however, were created by using multiple linear regression (Table 10).

Vertebra samples were available for eight of the nine species in this study. For the rainbow trout, kokanee, mountain whitefish, bull trout and brook trout a simple linear regression produced the most significant regression for the estimation of total fish length (Table 11). For the cutthroat trout, Chinook, and lake trout it was found that the use of both vertebral measurements can be used to estimate total fish length.

Table 9. Linear regression equations for the pharyngeal arch of each species using the measurements displayed in Figure 3. Total length range (TL mm) of each species, sample sizes (n) and respective p-values, r^2, and r^2 adjusted values for each equation presented are shown.

Species	Length Range TL (mm)	Regression Equation	Regression p-vlaue	r^2	r^2 Adjusted	n
Chinook	71-182	1.60*(Pharyngeal Arch A)+0.43*(Pharyngeal C)+4.10	<0.001	0.778	0.768	48
Mountain whitefish	95-303	1.91*(Pharyngeal Arch A)+4.43	<0.001	0.601	0.557	11
Bull trout	31.5-544	3.27*(Pharyngeal Arch A)+ -1.23 *(Pharyngeal Arch B)+3.22	<0.001	0.868	0.864	61
Brook trout	108.1-235.2	1.93*(Pharyngeal Arch A)+3.94	<0.001	0.888	0.884	32

Table 10. Linear regression equations for the vertebra of each species using the measurements displayed in Figure 3. Total length range (TL mm) of each species, sample sizes (n) and respective p-values, r^2, and r^2 adjusted values for each equation presented are shown.

Species	Length Range TL (mm)	Regression Equation	Regression p-vlaue	r^2	r^2 Adjusted	n
Cutthroat trout	28-285	3.09*(Vertebra A)+2.16*(Vertebra B)+4.21	<0.001	0.956	0.948	14
Rainbow trout	89-263	4.91*(vertebra B)+4.31	<0.001	0.893	0.880	10
Kokanee	54-360	7.20*(Vertebra A)+3.74	0.001	0.844	0.817	8
Chinook	71-182	2.24*(Vertebra A)+4.03*(Vertebra B)+4.05	<0.001	0.690	0.679	59
Mountain whitefish	95-303	5.44*(Vertebra A)+4.16	<0.001	0.889	0.883	22
Bull trout	31.5-544	5.66*(Vertebra B)+3.47	<0.001	0.661	0.654	50
Brook trout	108.1-235.2	3.84*(Vertebra A)+4.32	<0.001	0.638	0.623	26
Lake trout	85-791	10.29*(Vertebra A)+ -5.26*(Vertebra B)+3.92	<0.001	0.959	0.951	13

Total Weight to Length Regressions

Regression models for fish total length to fish total weight were highly significant for eight salmonids present in this study (Table 2). A total length to weight regression for the brown trout was unattainable with the limited sample size we had present in this study. Unfortunately, in this study the only the sample populations of the Chinook, mountain whitefish, bull trout, and brook trout are large enough to be recommended for use. For the remaining five species we suggest using equations generated from the previous works of Parrish et al. (2006), Prenda et al. (2002), or Mettler (2014). All of these equations are presented in Table 11. Equations that were generated from data outside of this study are marked with the study they originated from.

Table 11. Linear regression equations for the calculation of fish weight from total length. Total length range (TL mm) of each species, sample sizes (n) and respective p-values, r^2 values for each equation presented are shown. If the equation was not generated from this study the citation where it came from is presented. Table cells denoted with an * represent data not provided in previous works.

Species	Length Range TL (mm)	Regression Equation	Regression p-vlaue	r^2	n
Cutthroat trout	28-285	-82.846+(0.857*TL)	<0.001	0.757	13
	81-188	0.000008*TL^3.16 (Parrish et al. 2006)	*	0.990	32
Rainbow trout	89-263	-105.696+(1.01*TL)	<0.001	0.888	7
	137-245	0.00002*TL^2.95 (Parrish et al. 2006)	*	0.920	31
Kokanee	54-360	-156.445+(1.741*TL)	<0.001	0.883	9
	48-50	0.000005*TL^3.32 (Parrish et al. 2006)	*	0.880	19
Chinook	71-182	-51.924+(0.591*TL)	<0.001	0.877	62
Mountain whitefish	95-303	-140.684+(1.158*TL)	<0.001	0.888	24
Brown trout	95-133	-25.522+(0.363 * TL)	0.094	0.978	3
	58-555	115.5475+(-1.9177*TL)+(0.0081*TL^2) (Mettler 2014)	<0.001	0.969	317
	*	-11.2537*TL^3.00203 (Prenda et al. 2002)	<0.001	0.994	31
Bull trout	31.5-226	-14.588+(0.286 * TL)	<0.001	0.747	68
Brook trout	108.1-235.2	-102.801+(0.925*TL)	<0.001	0.830	32
Lake trout	85-791	-78.92+(0.864*TL)	<0.001	0.951	16

Discussion

As expected, total length to weight regressions were strongly correlated for most of the nine species present in this study. One surprising finding, however, was the poor relationship between the weight and length of the brown trout. Other studies have shown that there is a clear and strong relationship between the weight and length of brown trout (Prenda et al. 2002, Mettler 2014). However, due to the low sample size (n=3) used in this study we highly suggest not using the total weight to length equations provided in this study for brown trout.

From the nine species that were viewed in this study, the premaxillary, maxillary, dentary, cleithra, preopercle and opercle were all visually different enough to provide species-specific taxonomy and accurate bone length to total length regressions. Pharyngeal arches and vertebra, though they could be used to construct bone length to total length regressions, were only visually distinguishable to the family Salmonidae. Further, it is worth noting that variations between individual vertebrae associated with progression down vertebral column generally make vertebra poor indicators of total length, especially when it is unclear exactly where the vertebra originated from in the vertebral column, which is likely if the fish specimen is partially or completely disarticulated (Novais et al. 2010).

The identification of a fish using boney structures takes a considerable amount of time and practice. Novice researchers should take into consideration that many described structures and identifiers are minutely different between species. We suggest using more than one bone during identification to aid in verifying identification. However, when present a single bone can be viewed under a microscope to adequately identify a salmonid. We also suggest that if available, the bones from other salmonids should be at hand and viewed in tandem with unknown bones to compare structures during identification. This is invaluable as it helps to discern subtle differences between structures.

Among fish species, meristic counts of anatomical structures often vary greatly among individuals of the same species. Additionally, overlap between meristic counts is common between species (Scholz and McLellan 2010). This makes the use of meristic counts as taxonomically diagnostic structures tricky. Data provided for the meristic counts of pores on the dentary indicate that though there may be subtle differences between the counts of each species, variations in the number of pores present in each individual make these not an accurate diagnostic characteristics. Larger sample sizes of each of the species observed here may help to shed more light on if the sensory pores of the dentary are actually statisitcally different between varied groups of salmonids (i.e. sub- families, genera, or species). However, at this time we are not confident that counts of these structures are taxinomically significant.

Studies assessing the statistical difference between right and left sided bones in length estimation show a significant difference for the pharyngeal arch in many non-salmonid species and the operculum in silver bream, *Blicca bjoerkna* (Radke et al. 2000, Prenda et al. 2002, Beyer et al. 2006, and Tarken et al. 2007). Data acquired by Tarken et al. (2007), however, suggests that more often than not no statistical difference between right and left sided large bones are present (tested in Cyprinidea). We confirmed this finding in salmonids and subsequently clumped right and left

skull bones during statistical comparisons and regression formations for this study.

With the exception of the brook trout maxillary, total bone length to total fish length regressions were highly significant for all of the fish and bones used in this study. It should be noted, however, that some of our sample sizes are small, which may provide less precise total length estimations then found in previous studies. For this reason we suggest using data published by Hansel et al. (1988), for the total length estimation of kokanee, and Prenda et al. (2002), for the total length estimation of brown trout and rainbow trout. Regressions equations produced by Hansel et al. (1988) for estimating sockeye (an anadromus variety of O. nerka species) total length using the cleithra, dentary, and opercle were constructed using a sample of 53 sockeye salmon. Regression equations produced by Prenda et al. (2002) for the brown trout premaxillae, maxillae, dentary, and vertebrae, and for the rainbow trout cleithra, dentary and opercle were constructed using a sample population of 26-36 brown trout, and 45 rainbow trout. These equations are likely more precise then the equations provided in this study which used a sample size of 11 kokanee, 4 brown trout, and 12 rainbow trout.

For bull trout samples, variations in preservation methods created difficulties in the efficacy of bone removal. In frozen specimens, the skin and muscle tissue were easy to remove from structural bones. In formalin preserved specimens, bones (especially the vertebra and pharyngeal arch) were often quite difficult to remove undamaged. This suggests that the relationships between bull trout total length in vertebral and pharyngeal structures may have been skewed and additional research to provide more accurate bone length to total length regressions for these structures may be worthwhile.

Otolith measurements are commonly used to identify salmonids and estimate total length of many prey species. In past studies they have provided a smaller amount of error when estimating total length and have shown species distinguishable features among many salmonids (Parrish et al. 2006, Tarkan et al. 2007). However, previous studies also suggest otoliths have a lower resistance to the digestive environment than larger bony structures (Tarken et al. 2007), perhaps making finding undamaged otoliths in an actual diet study more difficult. Otoliths were not used in this study due to difficulties in obtaining otoliths from formalin preserved bull trout and the lack of otoliths present from previously gathered samples to use in visual comparisons. The addition of taxonomically useful otilith characteristics and the total length regressions analysis into the diagnostic potentials of bull trout otoliths, however, may be worth comparing due their potential to increase the precision of bull trout identification.

Though there have been numerous studies exploring the use of diagnostic head bones for identifying fish, the outputs of this study provide some valuable and unique information. First, this study provides a true differentiation between the diagnostic head bones from members of the Salmoniae subfamily have previously been poor. Additionally, any true description, and differentiation of the diagnostic head bones from the bull trout, an Endangered Species Act listed species, have been basically absent from available literature. This makes this in depth analysis of the biometric relationships of the large identifiable skull bones in bull trout a unique tool to identify bull trout when only diagnostic bones are present. This data should prove useful for the identification of bull trout and the precise estimation of fish total length and weight when diagnostic bones are

present in diet samples. This information should improve bull trout identification in piscivore assessments, help to identify and quantify predation of bull trout, and improve the identification of bull trout bones found in archeological sites.

Literature Cited

Anderson, R.O., and R.M. Neumann. 1996. Length, weight, and associated structural indices. Pages 447-482 (Chapter 15) in: B.R. Murphy and D.W. Willis. Fisheries Techniques, second edition. American Fisheries Society, Bethesda, Maryland.

Beyer, K., R. Miranda, G.H. Copp and R.R. Gozlan. 2006. Biometric data and bone identification of topmouth gudgeon, Pseudorasbora parva and sunbleak, Leucaspius delineatus. Folia Zoology 55(3):287-292.

Britton, J.R. and J.S. Shepherd 2005. Biometric data to facilitate the diet reconstruction of piscivorous fauna. Folia Zoololgy 54(1-2):193–200.

Broughton, J. 2000. Terminal Plestocene fish remains from Homestead Cave, Utah, and implications for fish biogeography in the Bonneville Basin. Copeia 2000(3):645-656.

Cailliet, G. M., M. S. Love and A.W. Ebeling. 1986. Fishes: a field and laboratory manual on their structure, identification, and natural history. Wadsworth Publishing Company. Belmont, California. 194 pp.

Carss, D.N. and D.A. Elston. 1996. Estimating prey size distributions from bone recovery in spraints. Journal of Zoology (London) 238: 319-332.

Colley, S.M. 1990. The analysis and interpretation of archaeological fish remains. Archaeological Method and Theory 2:207-253.

Curtis, M.K. and G.R. Smith. 1994. Osteological evidence of genetic divergence of lake trout (Salvelinus namaycush) in lake superior. Copeia 1994:843-850.

Frost, C. 2000. A key for identifying prey fish in the Columbia river based on diagnostic bones. U.S. Geological Survey. Western fisheries Research Center. Columbia River Research Laboratory, Cook, Washington. 50 pp.

Granadeiro, J.P. and M.A. Silva. 2000. The use of otoliths and vertebrae in the identification and size-estimation of fish in predatory-prey studies. Cybium 24(4):383-393.

Gregory, W.K. 1933. Fish skulls: A study of the evolution of natural mechanisms. Transactions of the American Philosophical Society 23(2):i-vii,75-481.

Hajkova, P., K. Roche and L. Kocian. 2003. On the use of diagnostic bones of brown trout, Salmo trutta m. fario, grayling, Thymallus thymallus and Carpathian sculpin, Cottus poecilopus in Eurasian otter, Lutra lutra diet analysis. Folia. Zoology 52(4):389-398.

Hansel, H.C.S., S.D. Duke, P.T. Lofy and G.A. Gray. 1988. Use of diagnostic bones to identify and estimate original lengths of ingested prey fishes. Transactions of the American Fisheries Society 117:55-62.

Hyatt, M.H., and W.A. Hubert. 2000. Proposed standard-weight (W) equations for kokanee, golden trout and bull trout. Journal of Freshwater Ecology 15(4):559-563.

Jacobsen, L. and H.M. Hansen. 1996. Estimation of the size of prey fish. Journal of Zoology: (London), 238: 167-180.

Mann, R.H.K. and W.R.C. Beaumont. 1980. The collection, identification and reconstruction of lengths of fish prey from their remains in pike stomachs. Fisheries Management: 11: 169–172.

Mettler, A. 2014. Abundance, distribution and life histories of fishes occupying the Colville River watershed, Stevens County, Washington.M.S. thesis. Eastern Washington University, Cheney, Washington.

Miranda, R. and M.C. Escala. 2005. Morphometrical comparison of cleithra, opercular and pharyngeal bones of autochthonous Leuciscinae (cyprinidae) of spain. Folia Zoology: 54 (1-2): 173-188.

Novais, A., A. Sedlmayr, M. Moreira-Santos, R. Goncalves and R. Ribeiro. 2010. Diet of the otter, Lutra lutra in an almost pristine Portuguese river: seasonality and analysis of fish prey through scale and vertebrae keys and length relationships: Mammalia 74:71-81.

Parrish, J.K., K. Haapa-aho, W. Walker, M. Stratton, J. Walsh and H. Ziel. 2006. A guide to small- bodied and juvenile fishes of the mid-columbia region. University of Washington, Seattle, WA 137pp.

Prenda, J., M.P. Arenas, D. Freitas, M. Santos-Reis, and M.J. Collares-Pereira. 2002. Bone length of Iberian freshwater fish, as a predictor of length and biomass of prey consumed by piscivores. Limnetica 21(1-2):15-24.

Radke, R.J., T. Petzoldt and C. Wolter. 2000. Suitability of pharyngeal bone measures commonly used for reconstruction of pry fish length. Journal of Fish Biology 57:961-967.

Scharf. F.S., R.M. Yetter, A.P. Summers and F. Juanes. 1998. Enhancing diet analysis of piscivorous fishes in the Northwest Atlantic through identification and reconstruction of original prey sizes from ingested remains. Fishery Bulletin 96:575-588.

Scholz, A.T. and H.J. McLellan. 2009. Feild guide to the fish of Eastern Washington. Eagles Printing, Cheney, Washington. 310pp.

Scholz, A.T. and H.J. McLellan. 2010. Fishes of the Columbia and Snake River Basin in Eastern Washington. Eagle Printing. Cheney, Washington. 771pp.

Simpson, J.C., and R.L. Wallace. 1982. Fishes of Idaho, 2nd edition. University of Idaho Press, Moscow, Idaho. 238pp.

Scott, J.L. 2002. Investigations into the feeding habits of piscivorous fishes in Coeur D'Alene Lake, Idaho. MS thesis. Eastern Washington University, Cheney, Washington. 226 pp.

Tarkan, A.S., C. Gursoy Gaygusuz, O. Gaygusuz and H. Acipinar. 2007. Use of bone and otolith measures for size-estimation of fish in predatory-prey studies. Folia Zoology 56(3):328-336.

Vladykov, V. 1962. Osteological studies on Pacific salmon of the genus Oncorhynchus. Fisheries Research Board of Canada Bulletin. 136:1-172.

Wydoski, R.S., and R.R. Whitney. 2003. Inland fishes of Washington, 2nd edition, revised amd expanded. University of Washington Press, Seattle, Washington. 384pp.

Appendices

The appendices A & B presented here provide the dichotomous keys required for the visual identification of premaxillaries, maxillaries, dentary, cleithra, preopercle, and the opercle for the nine salmonid species presented in Table 1, and a graphical depiction of each regression with regression line and equation that were presented throughout the results section of this document.

Appendix A: Dichotomous Bone Keys

Appendix A contains the following dichotomous keys for the six different bones observed in this study:

Use of the Diagnostic key

Detailed observation of the premaxillary, maxillary, dentary, cleithra, preopercle and opercle demonstrated that all of these bones are visually different enough to provide species-specific taxonomy for the nine species presented in Table 1. Pharyngeal arches and vertebra, though they can be used to construct bone length to total length regressions, are only visually distinguishable to the salmonid genera, which provides little taxonomic value. Therefore, this guide is presented to allow users to identify the premaxillary, maxillary, dentary, cleithra, preopercle, and opercle of the nine species in Table 1.

The dichotomous keys presented here contain numbered couplets that describe one or a few morphological character(s) present on each bone with two alternatives (a or b). The bone being examined will be described correctly by only one of the alternatives presented. Following each alternative is given either a "Go to" statement that directs the user to the next couplet or provides the user with the species name that identifies the bone being viewed. Below each couplet are detailed photographs to help determine if your diagnosis of each bone is correct. Appendix A contains the dichotomous keys for the six different bones observed in this study.

The identification of a fish using boney structures takes a considerable amount of time and practice. Novice researchers should, therefore, take into consideration that many described structures and identifiers are minutely different between species. With this said, this key has been setup in a dichotomous fashion to provide researchers with one of two choices at each step. When presented with an intact undamaged bone the user should start at step one and progress through the key in a sequential manner. Users should match as many descriptions presented in each step to the bone in hand before progressing forward. Users should also examine the figures and descriptions

presented in the two following steps to assure they have made the right choice prior to progressing on.

Due to the damage that may be present in partially digested bones, we suggest that prior to moving from one step to another the user should not only attempt to match up as many described features as possible in the current step and in each of the following steps but a single undamaged bone from each of the nine species should be on hand.

Since many stomachs can become jumbled mess of disarticulated bones, presumably from more than one fish, difficulties in deciding which bone belongs to which fish can arise. Assuming the right and left sides of a fish skull will remain in the digestive track for a relatively equivalent time; researchers should first make an attempt to pair right and left sided bones of the same size. This should help determine how many fish are present in a single stomach. Researchers should follow this with matching as many skull bones from each fish present as possible, making matches based on comparable bone size. Total length back calculations should then be made from all matched bones to assure bones originated from a single fish. Assuming paired bones represent one fish, back calculated lengths should be relatively similar between paired bones. All bones determined to originate from a single fish should be used during identification.

In an attempt to setup the following dichotomous key in a uniform and easy to use way all bone specimens and figures for each step of the key are displayed in a uniform fashion. Each step of the following keys is presented on a single page set up with a large figure for each choice available. Figures are all setup with the lateral side of the bone positioned on the left hand side and the medial side of the bone positioned on the right hand side of each figure. In text descriptions of each bone are marked with a letter that directly corresponds to adjacent figures, and figure captions are presented with information regarding the species, the side of the head each bone originated from, and all of the anatomical structures marked. Markings for anatomical structures are a continuous string of letters that is unique to each structure per page.

Appendix A I: The dichotomous key for the premaxillary

1.a The ascending limb of the premaxillary has a squared dorsal margin, and gently sloping anterior and posterior margins (a). The anterior margin sweeps into a distinct point at the premaxillary symphysis (b). The ventral margin is broadly curved with no teeth present on the dental palate (c)… **mountain whitefish**

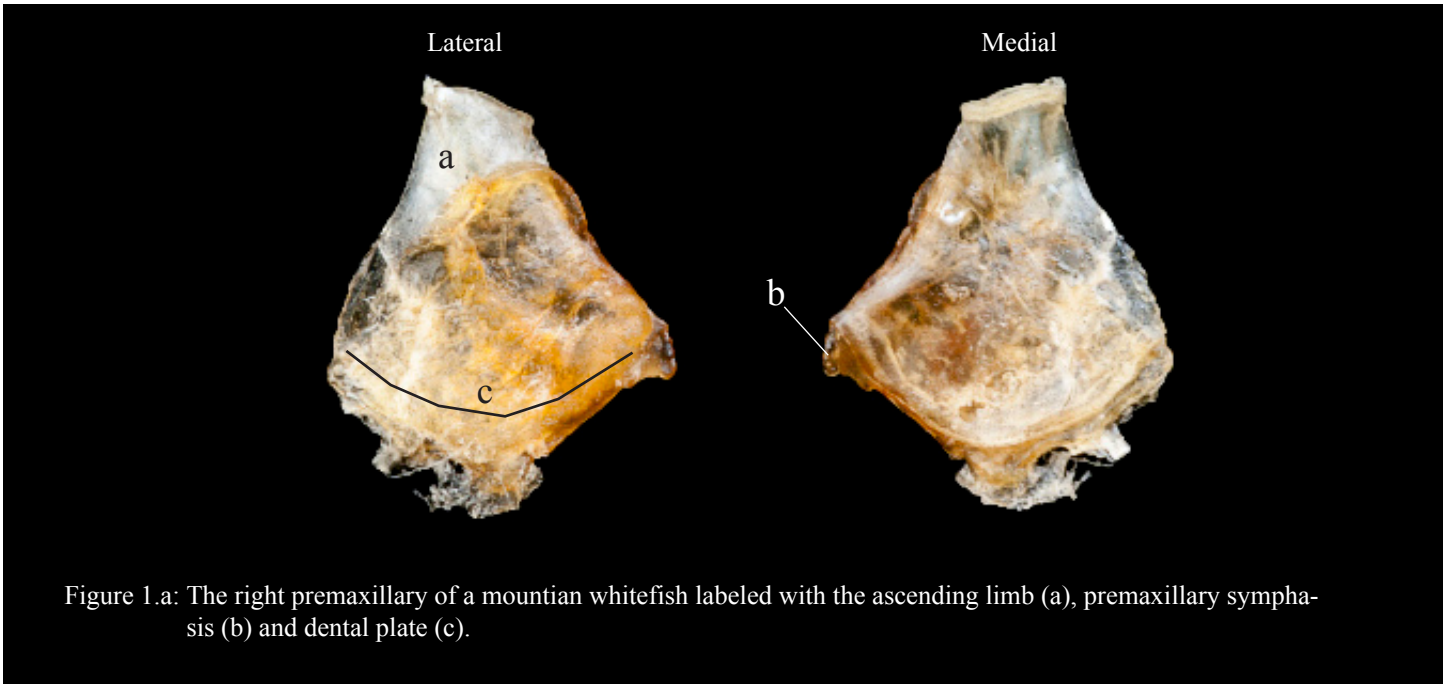

Figure 1.a: The right premaxillary of a mountian whitefish labeled with the ascending limb (a), premaxillary symphasis (b) and dental plate (c).

1.b The ascending limb (a) has a rounded or pointed dorsal margin. The dental palate (c) houses a single row of homodont caniform teeth… **go to 2**

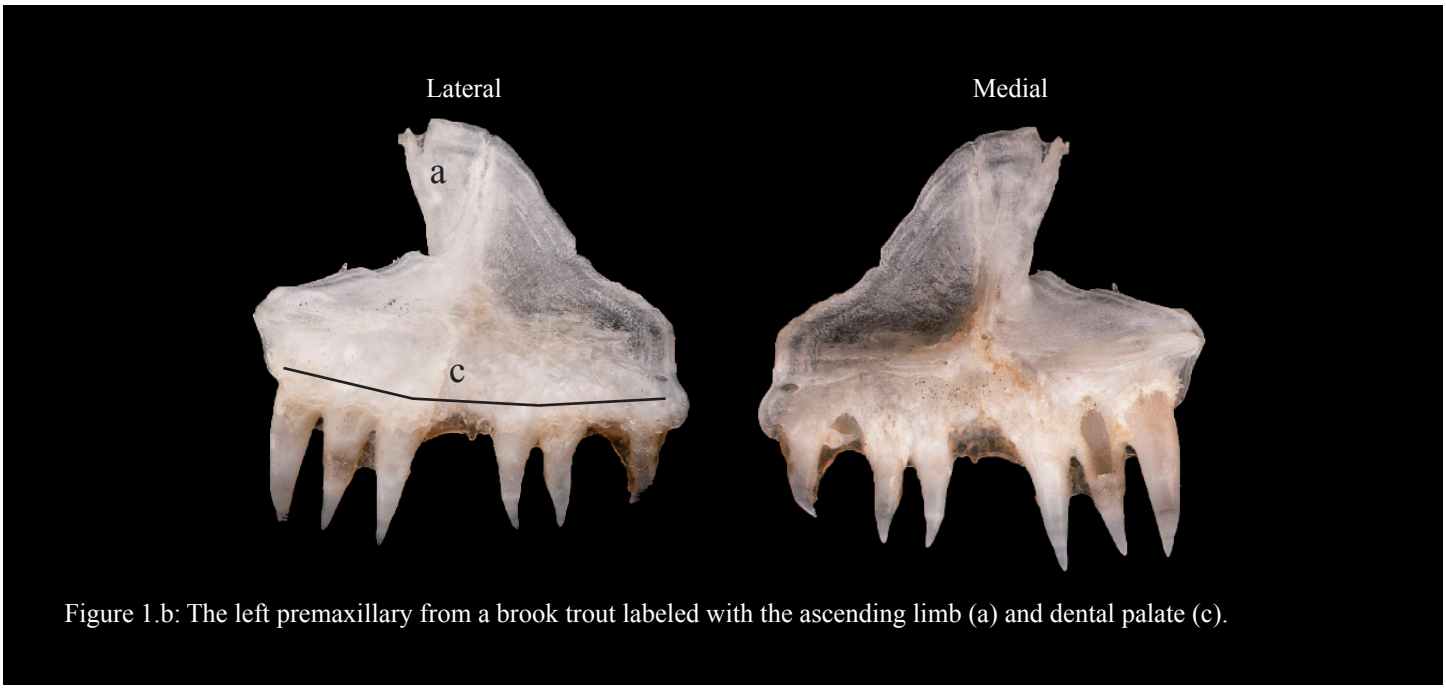

Figure 1.b: The left premaxillary from a brook trout labeled with the ascending limb (a) and dental palate (c).

2.a Three prominent ridges, the ascending (a), anterior (b) and posterior (c) are present on the medial aspect. These ridges meet at a robust medial prominence (d)... **go to 3**

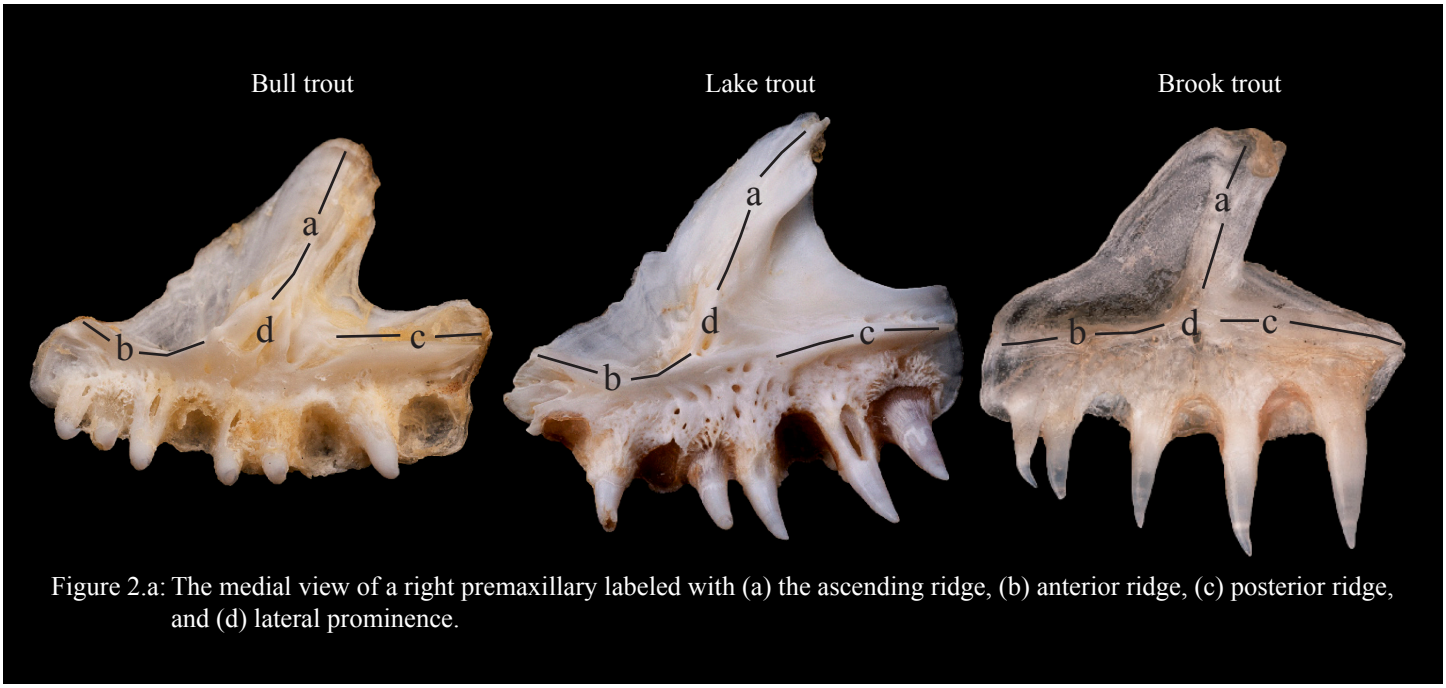

Figure 2.a: The medial view of a right premaxillary labeled with (a) the ascending ridge, (b) anterior ridge, (c) posterior ridge, and (d) lateral prominence.

2.b A diminutive ascending (a), anterior (b) and posterior (c) ridges or only two ridges, the ascending and posterior, may be present on the medial aspect. These ridges meet at an equally diminutive or non-existent medial prominence... **go to 6**

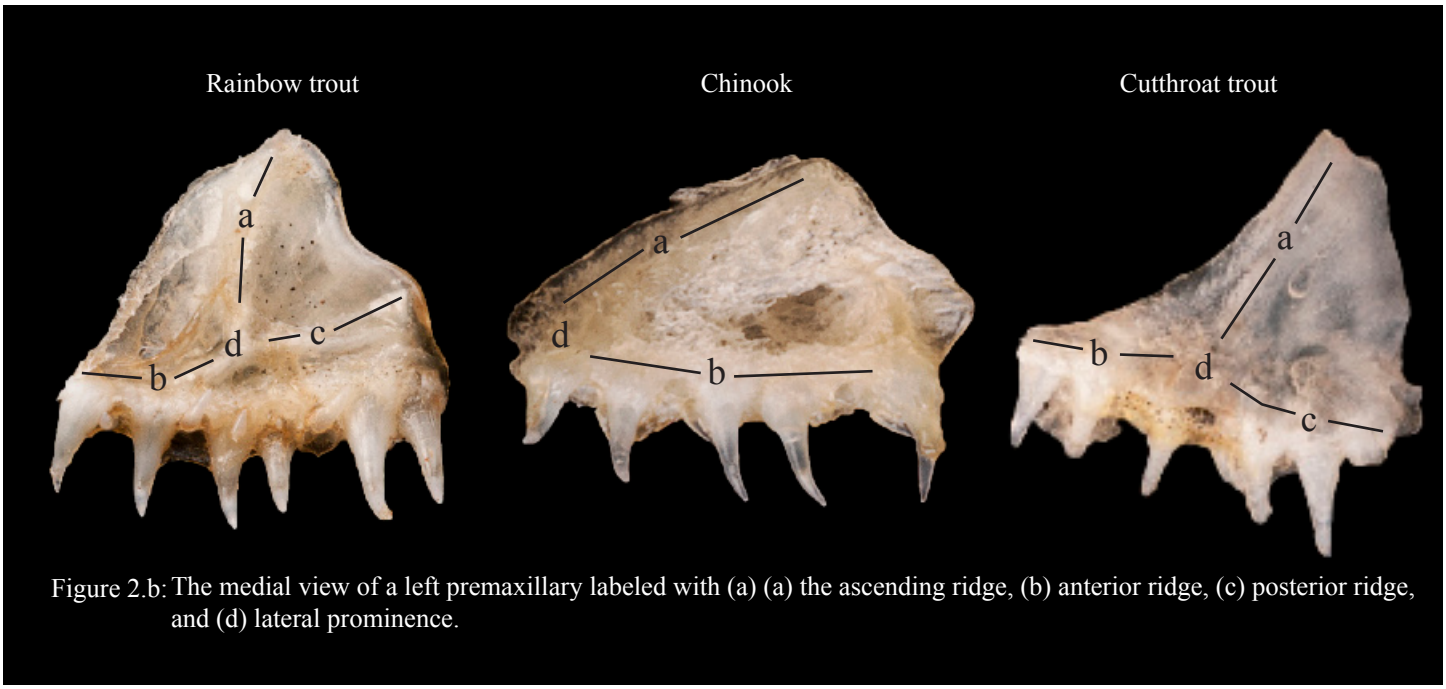

Figure 2.b: The medial view of a left premaxillary labeled with (a) (a) the ascending ridge, (b) anterior ridge, (c) posterior ridge, and (d) lateral prominence.

3.a The ascending (a) ridge projects upward from the medial prominence in a heavily curved or falcate appearing structure. The posterior ridge (b) is greatly extended and much longer then the anterior ridge (c). The premaxillary symphysis (d) ends at a squared anterior margin. The medial prominence (e) is located near the premaxillary symphysis... **brown trout**

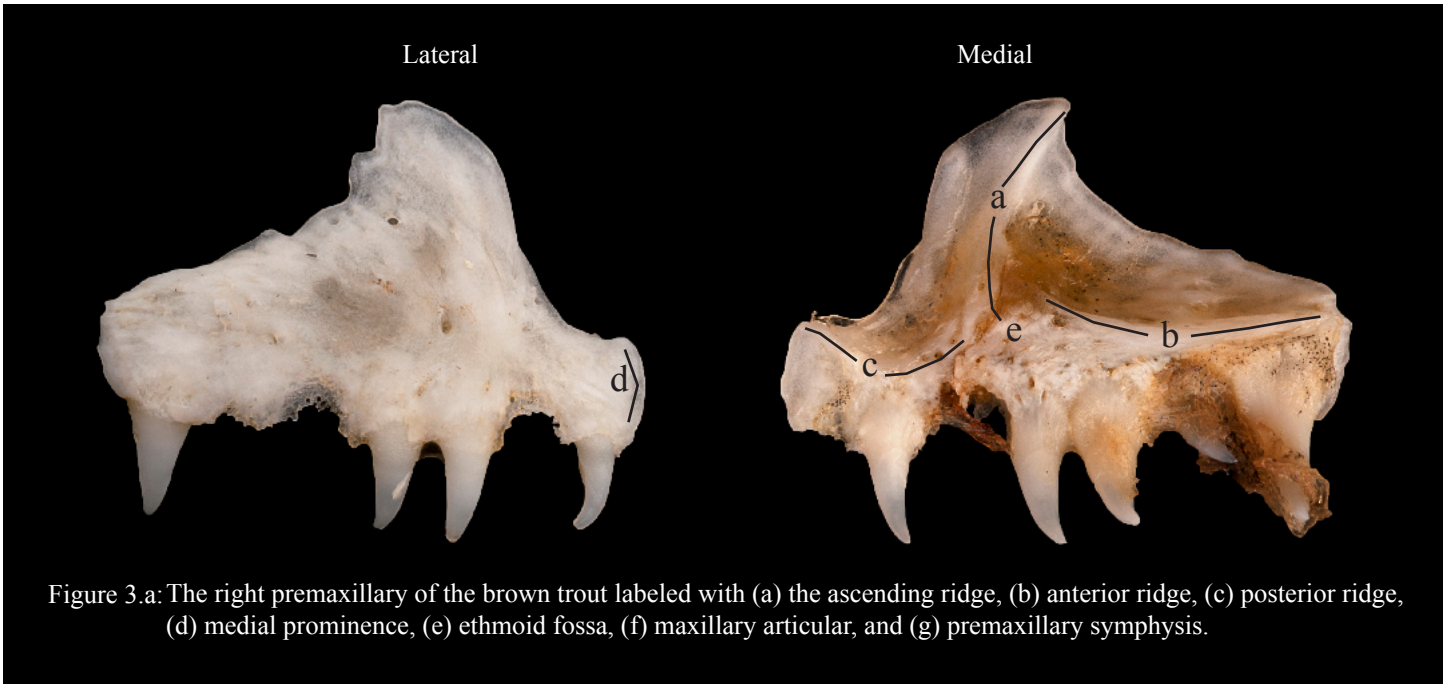

Figure 3.a: The right premaxillary of the brown trout labeled with (a) the ascending ridge, (b) anterior ridge, (c) posterior ridge, (d) medial prominence, (e) ethmoid fossa, (f) maxillary articular, and (g) premaxillary symphysis.

3.b The ascending ridge (a) projects up away from the lateral prominence in a straight or minimally curved structure. The posterior ridge (b) has a relatively equicalent length to the anterior ridge (c). The premaxillary symphysis (d) if gently rounded. The medial prominence (e) is located near the middle of the dental palate... **go to 4**

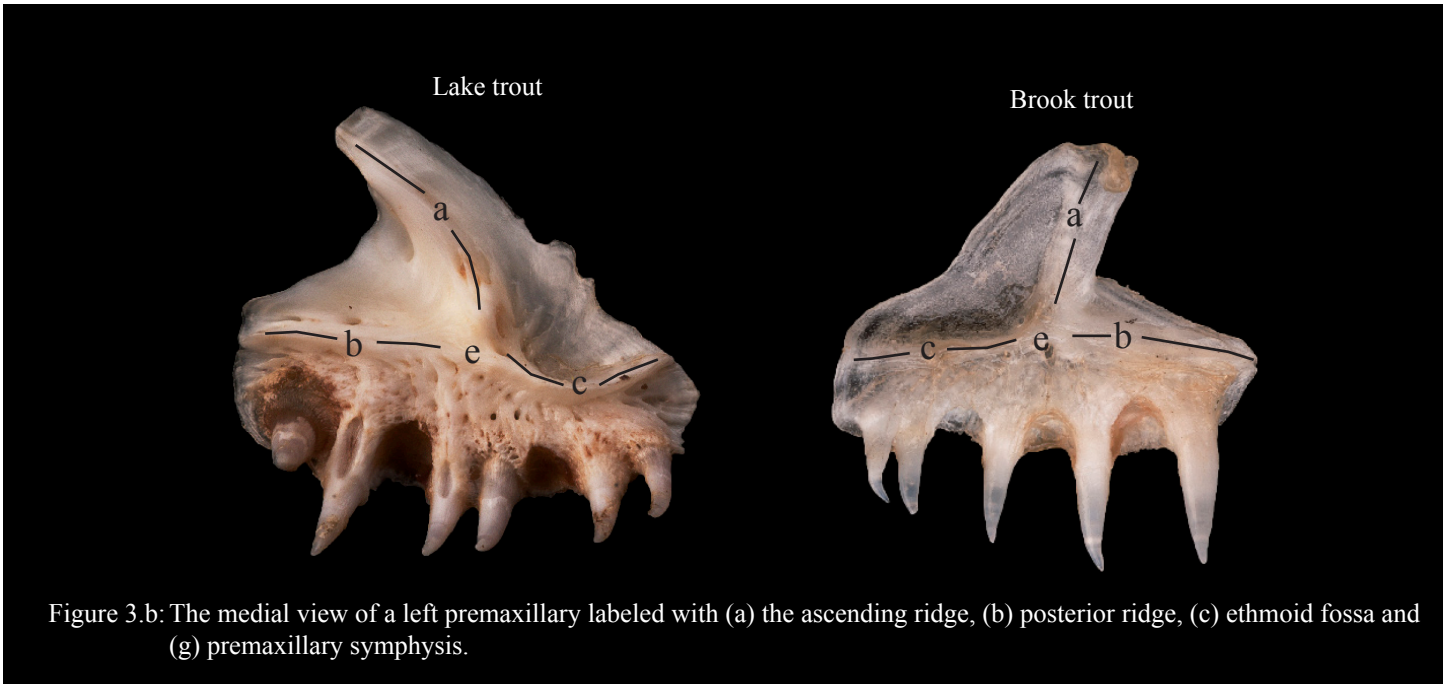

Figure 3.b: The medial view of a left premaxillary labeled with (a) the ascending ridge, (b) posterior ridge, (c) ethmoid fossa and (g) premaxillary symphysis.

4.a The ascending limb (a) juts far dorsally from the remainder of the premaxillary body giving it the appearance of a prominent spine that may be curved or straight. The dorsal tip (b) of the ascending limb is pointed… **lake trout**

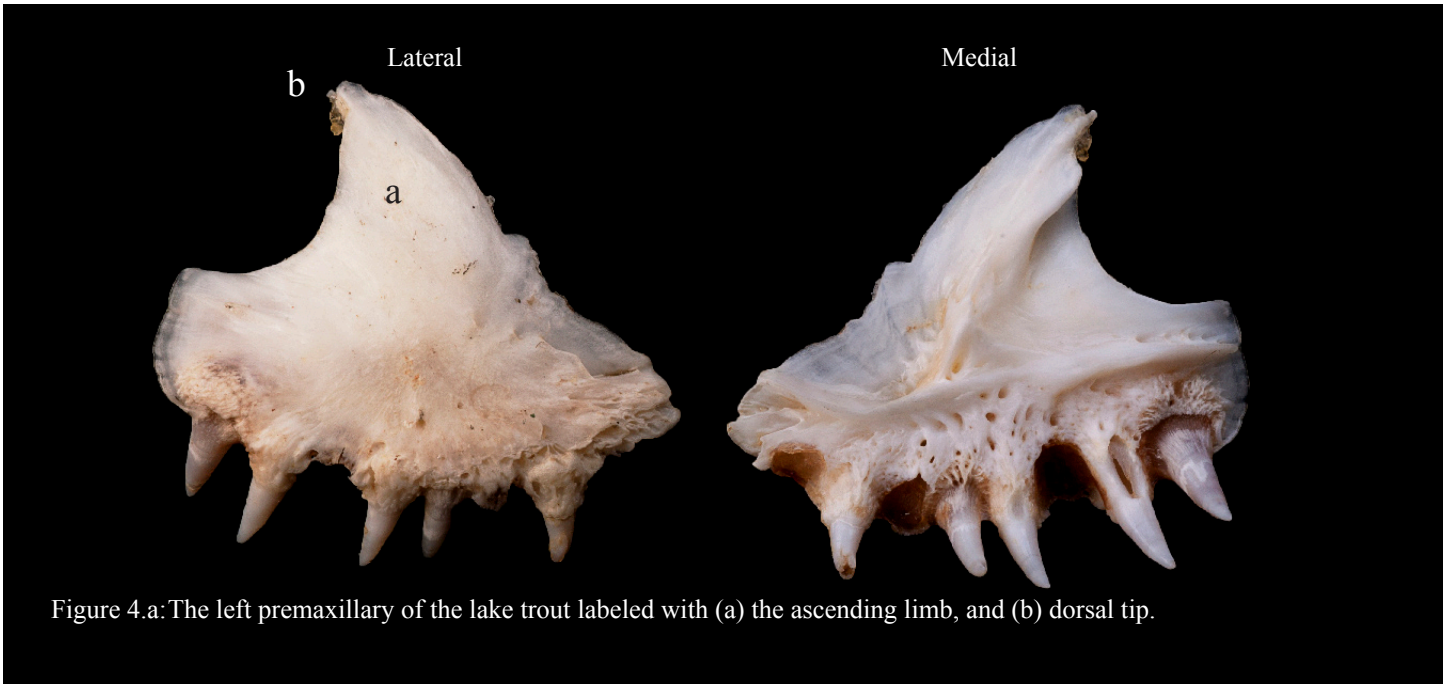

Figure 4.a:The left premaxillary of the lake trout labeled with (a) the ascending limb, and (b) dorsal tip.

4.b The ascending limb (a) juts out of the remainder of the premaxillary at a slightly posterior angle. The dorsal tip (b) of the ascending limb is round or square… **go to 5**

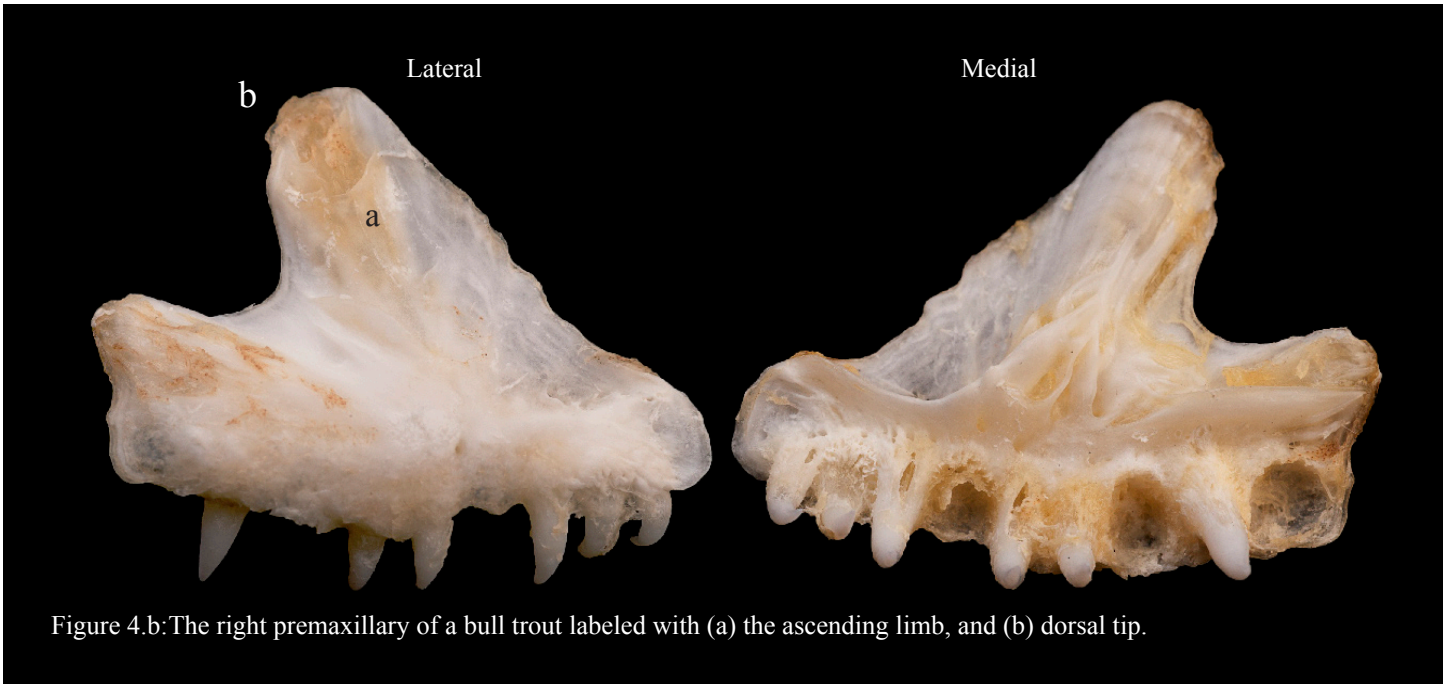

Figure 4.b:The right premaxillary of a bull trout labeled with (a) the ascending limb, and (b) dorsal tip.

5.a The ascending ridge (a) leaves the medial prominence (b) as a heavily ossified, wide, and boxy structure. All three medial ridges project out from the medial prominence in straight lines. This causes the ascending ridge, anterior ridge (c), and posterior ridge (d) to create an upside down T shape across the medial body of the premaxillary. The posterior angle (e) is squared… **brook trout**

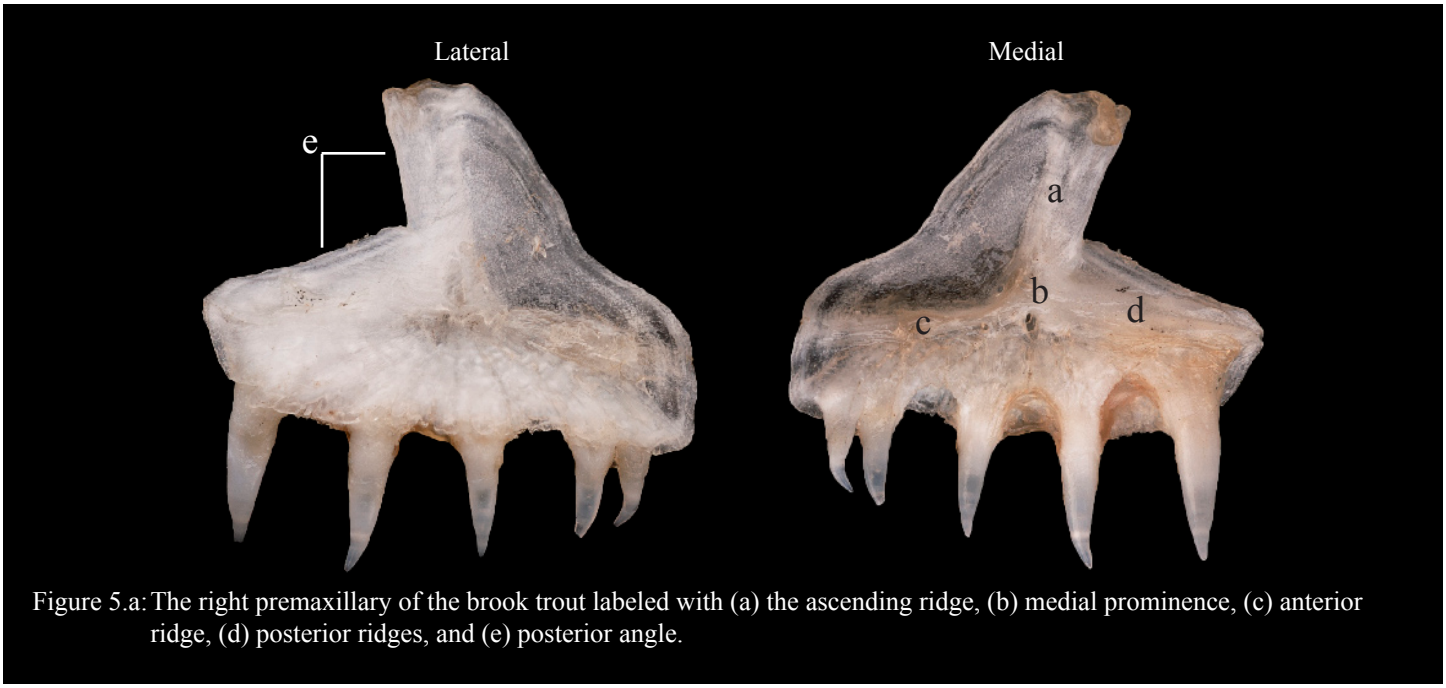

Figure 5.a: The right premaxillary of the brook trout labeled with (a) the ascending ridge, (b) medial prominence, (c) anterior ridge, (d) posterior ridges, and (e) posterior angle.

5.b The ascending limb (a) leaves the medial prominence (b) in a gently rounded structure at a noticeably dorso-posterior angle. All three medial ridges are not straight, and the anterior ridge can be quite curved. The anterior, and posterior (d) ridges curve dorsally as they leave the medial prominence and do not create an upside down T shape across the medial body of the premaxillary. the posterior angle is acute and rounded… **bull trout**

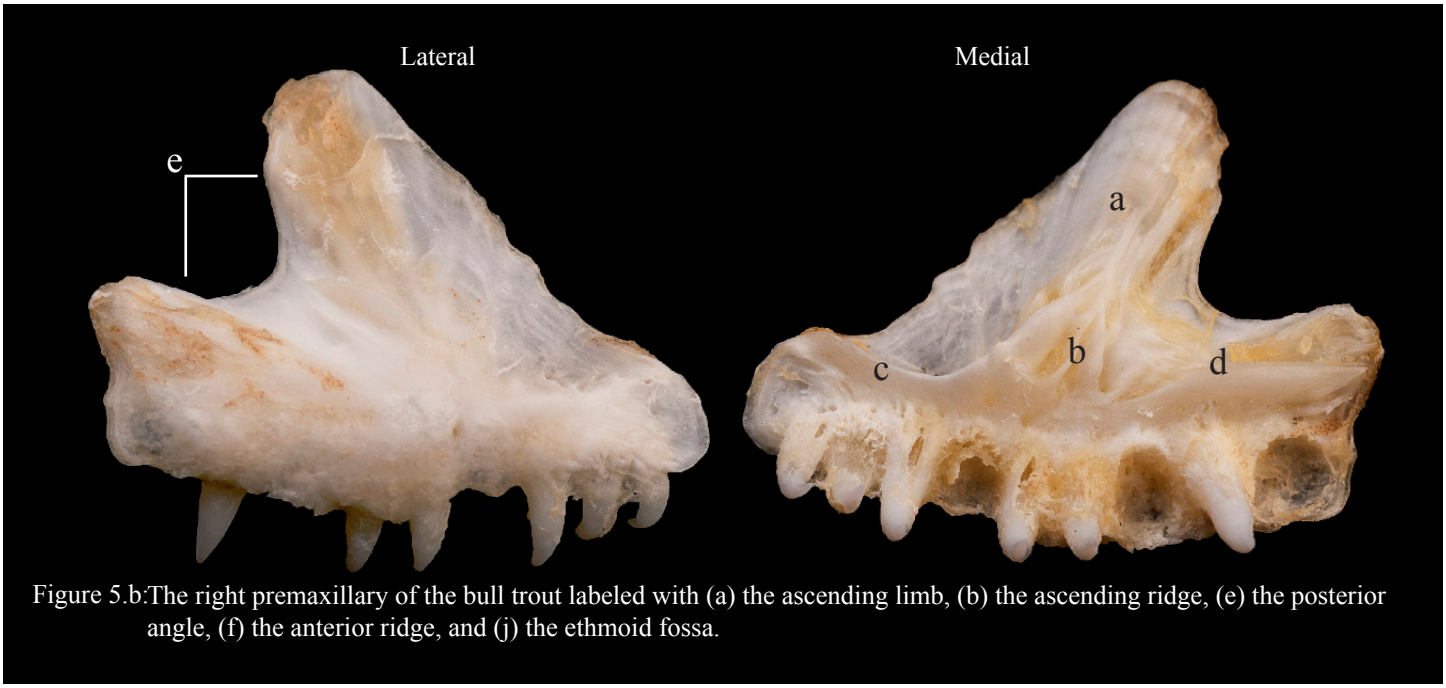

Figure 5.b:The right premaxillary of the bull trout labeled with (a) the ascending limb, (b) the ascending ridge, (e) the posterior angle, (f) the anterior ridge, and (j) the ethmoid fossa.

6.a The ascending limb (a) sweeps back causing the anterior margin to maintain a broad curvature. This creates a very obtuse angle at the junction of the ascending (b) and anterior (c) ridges and causes the ethmoid fossa (d) to be very open. The anterior ridge extends far forward from the medial prominence (e)… **cutthroat trout**

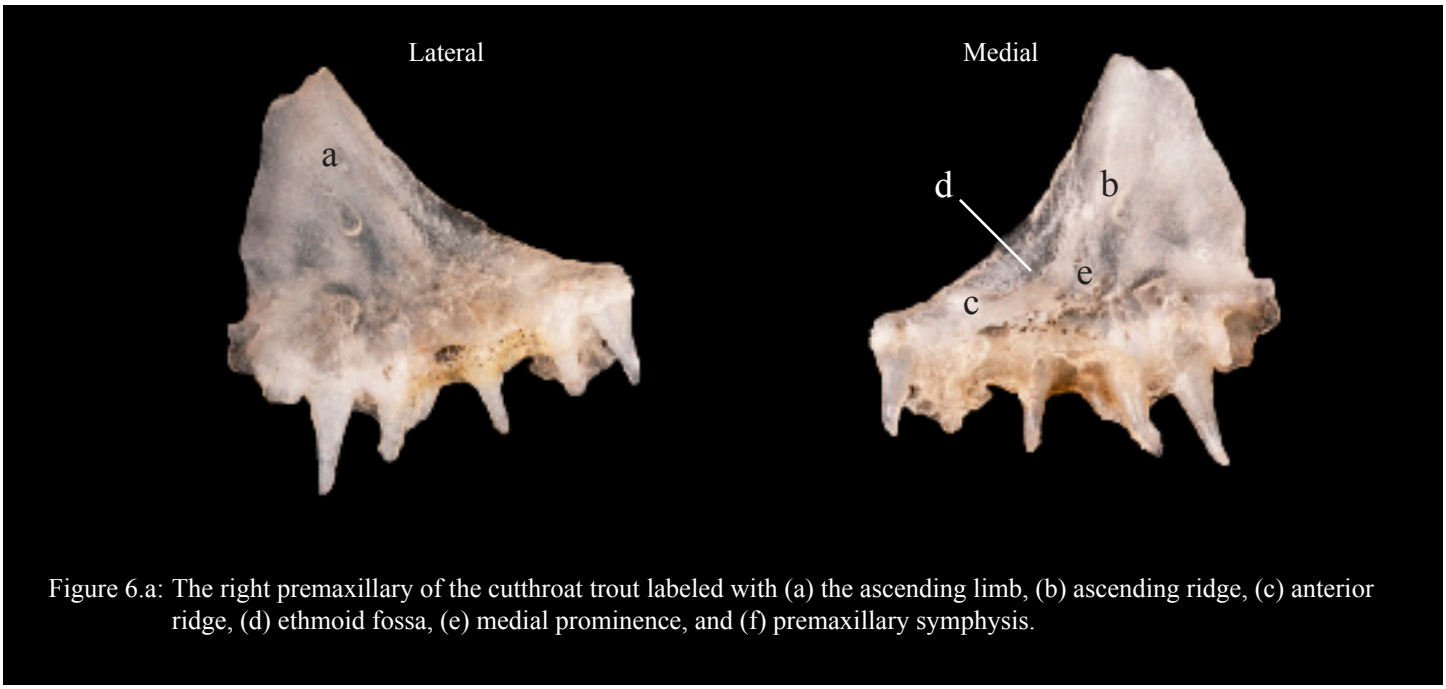

Figure 6.a: The right premaxillary of the cutthroat trout labeled with (a) the ascending limb, (b) ascending ridge, (c) anterior ridge, (d) ethmoid fossa, (e) medial prominence, and (f) premaxillary symphysis.

6.b The ascending limb (a) does not sweep back in an inward curved anterior margin. All ridging on the medial side of the premaxillary is diminutive. The ascending ridge (b) and limb are not curved posteriorly. The anterior ridge does not extend far forward from the medial prominence (e)... **go to 7**

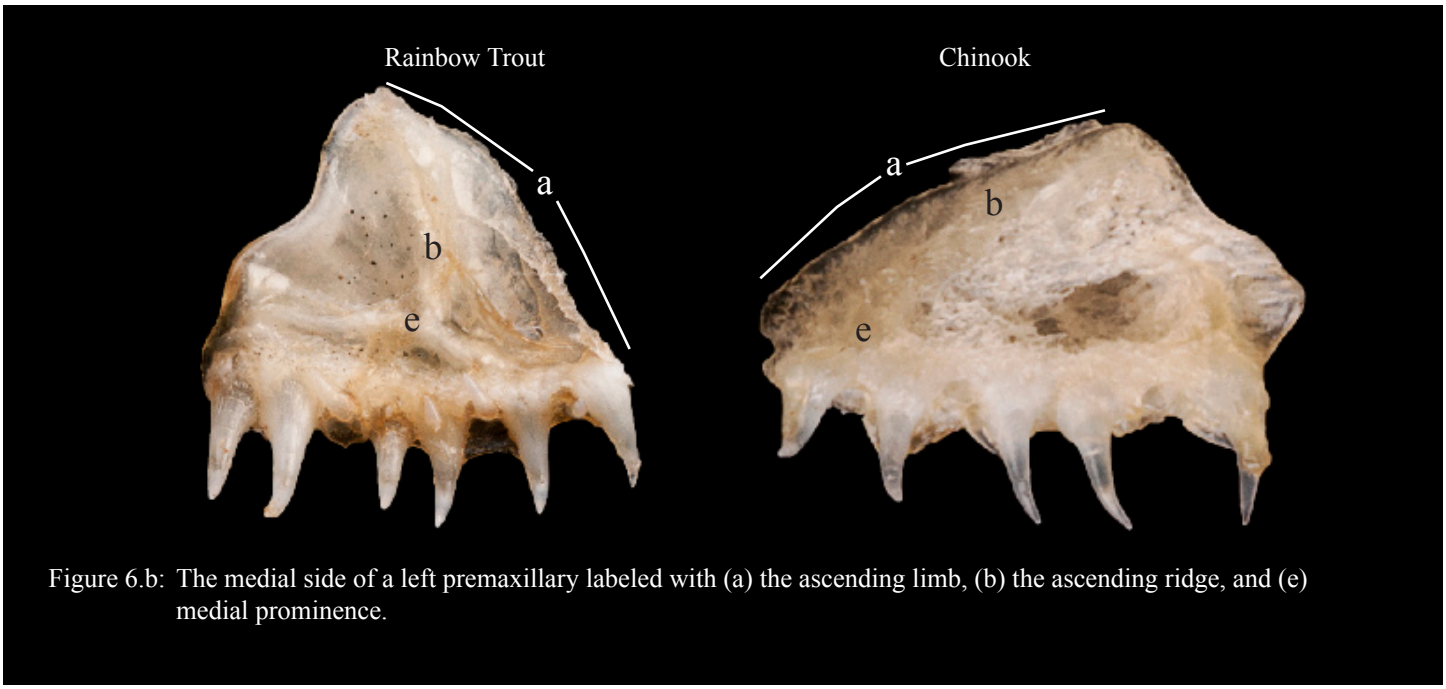

Figure 6.b: The medial side of a left premaxillary labeled with (a) the ascending limb, (b) the ascending ridge, and (e) medial prominence.

7.a The ascending limb (a) appears as a large dome bifurcated by a small crease or diminutive ascending ridge (b). The anterior (c) ridge cuts around the ventral margin of a deeply bowled out ethmoid fossa (d). None of the three medial ridges progress to the outer most margins of the premaxillary… **rainbow trout**

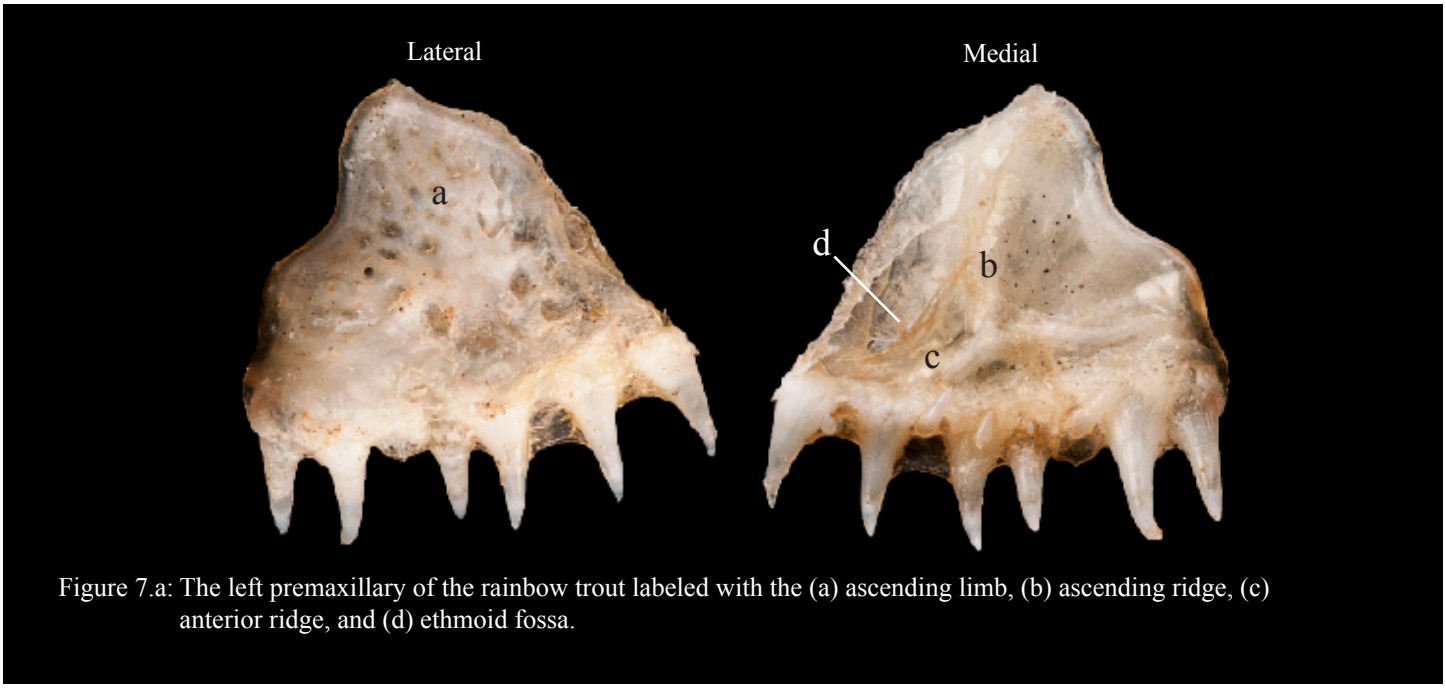

Figure 7.a: The left premaxillary of the rainbow trout labeled with the (a) ascending limb, (b) ascending ridge, (c) anterior ridge, and (d) ethmoid fossa.

7.b The ascending limb (a) is not large and dome shaped. The ascending ridge (b) is diminutive but runs directly along the anterior margin of the ascending limb. The lateral aspect of the posterior lobe is pockmarked with multiple pores or striations… **go to 8**

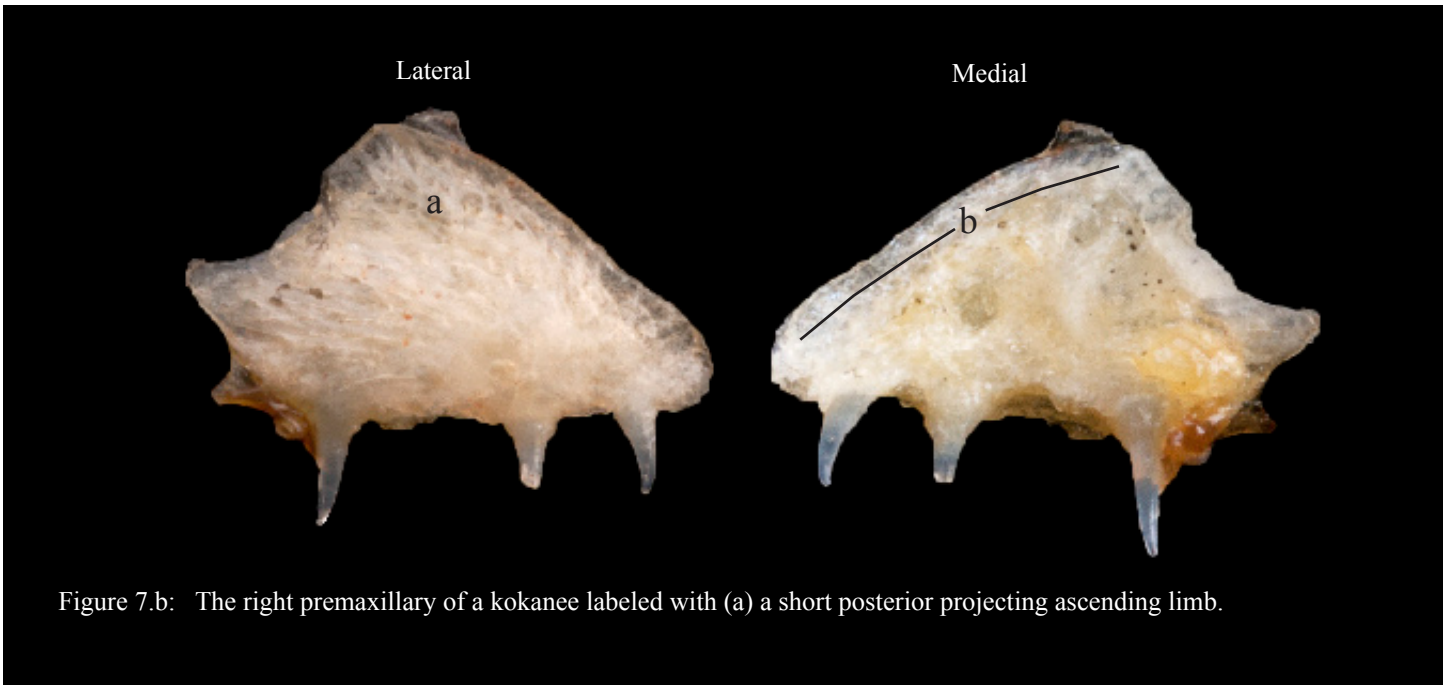

Figure 7.b: The right premaxillary of a kokanee labeled with (a) a short posterior projecting ascending limb.

8.a The anterior margin of the ascending lobe gently slopes down to the premaxillary symphysis (a). Though there is a slight increase in the ossification along the anterior (b) and ventral (c) margins, these two areas are relatively muted against the remaining medial side of the premaxillary. Between these two ossified ridges, on the posterior margin, a slight bowled out depression is visible at the ethmoid fossa (d). The posterior margin has a prominent spur… **kokanee**

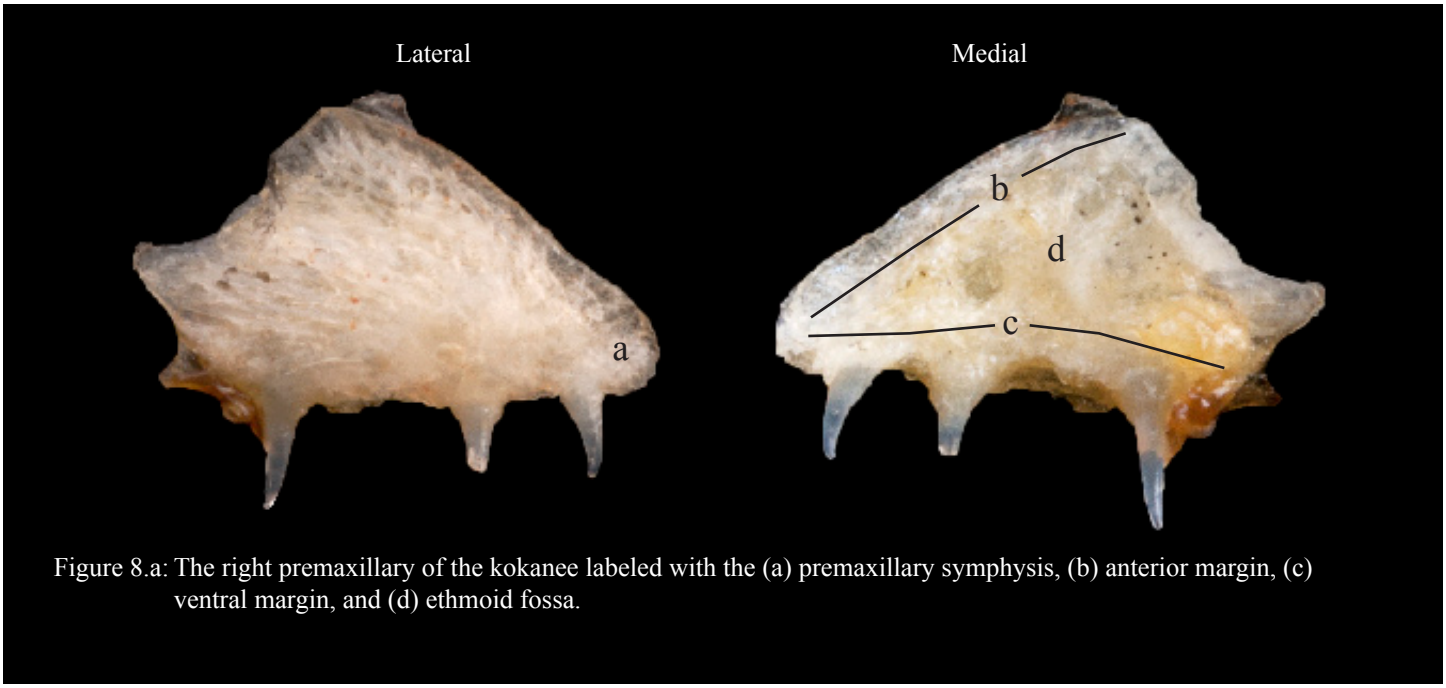

Figure 8.a: The right premaxillary of the kokanee labeled with the (a) premaxillary symphysis, (b) anterior margin, (c) ventral margin, and (d) ethmoid fossa.

8.b There are two heavily ossified ridges that begin at the premaxillary symphysis (a) and progress back, one along the anterior margin (b) the other along the ventral margin (c). The dental palate maintains a strong lateral curve and the ethmoid fossa (c) maintains a deep bowl shaped depression. The posterior margin does not have a prominent spur…**Chinook**

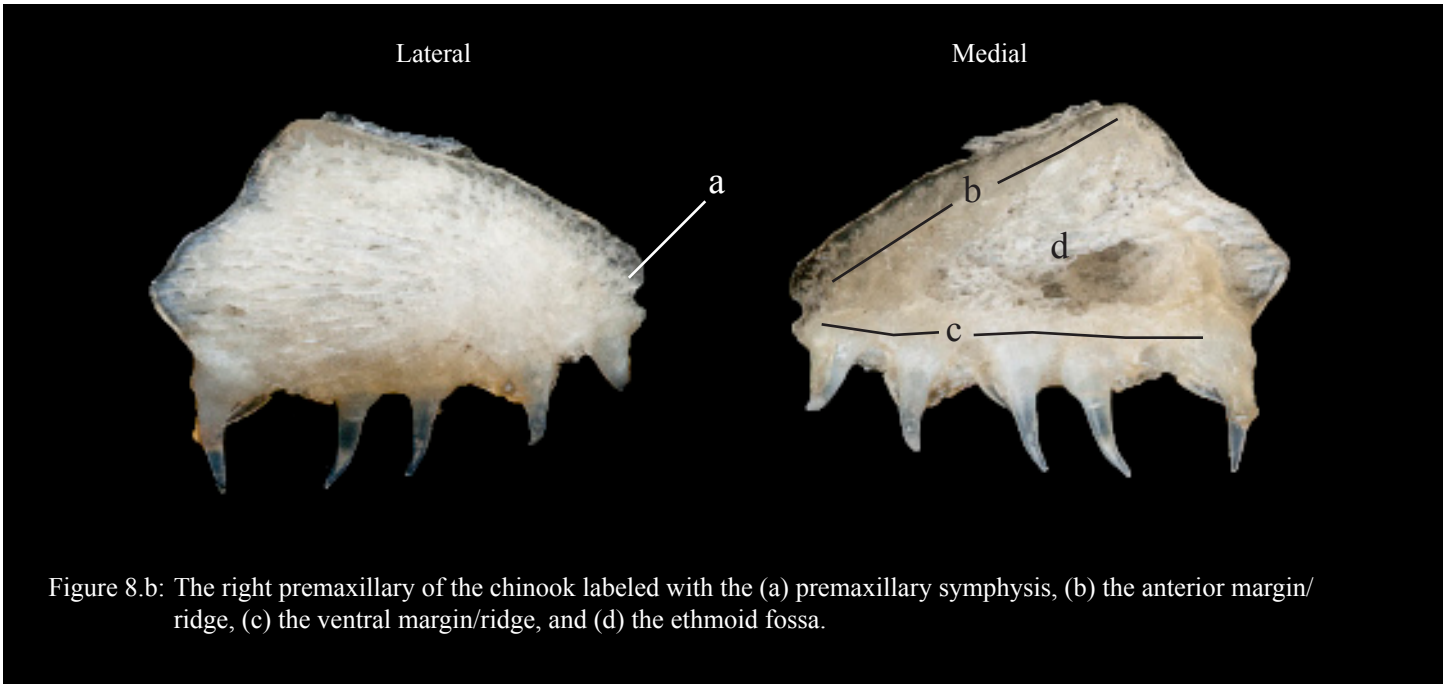

Figure 8.b: The right premaxillary of the chinook labeled with the (a) premaxillary symphysis, (b) the anterior margin/ridge, (c) the ventral margin/ridge, and (d) the ethmoid fossa.

1.a The maxillary body is short and wide. There are no teeth present along the ventrally curved dental palate (a). The maxillary head and neck project in a ventral-medially angled cylindrical bony structure (b) with the neck maintaining a small osseous nodule (c) and smooth palatine plate. The posterior portion of the maxillary has a ridge visible on both lateral and medial aspects (d). This ridge slopes to a dorsal-posterior point (e)… **mountain whitefish**

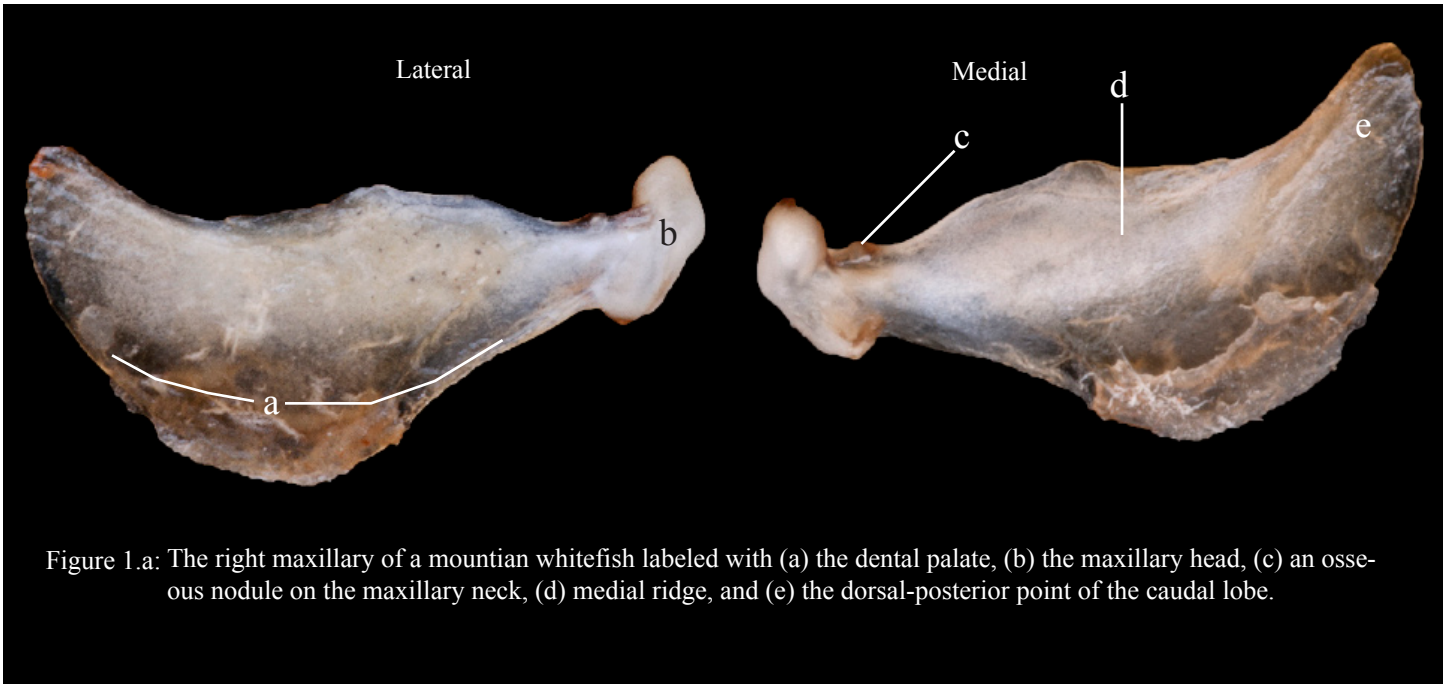

Figure 1.a: The right maxillary of a mountian whitefish labeled with (a) the dental palate, (b) the maxillary head, (c) an osseous nodule on the maxillary neck, (d) medial ridge, and (e) the dorsal-posterior point of the caudal lobe.

1.b The maxillary is not short and wide but rather is long and slender. There is a single row of homodont caniform teeth present on the relatively flat dental plate (a)…**go to 2**

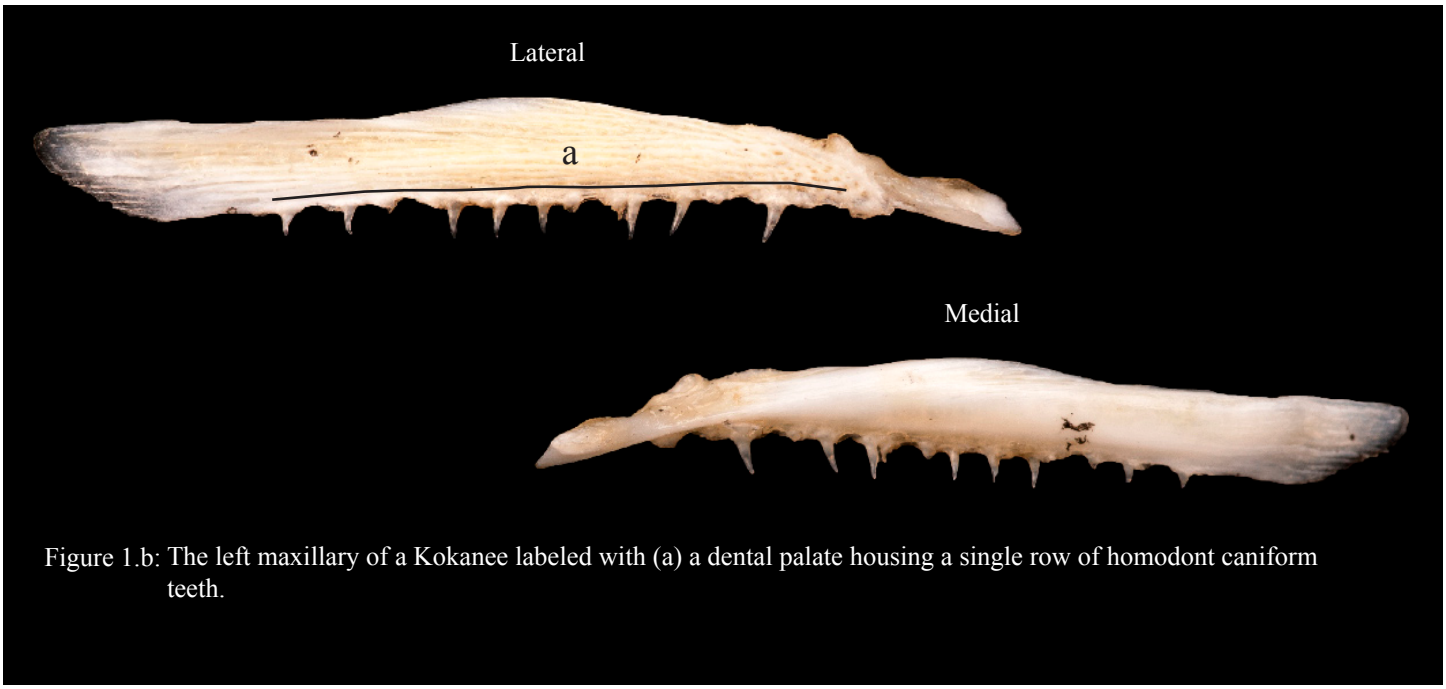

Figure 1.b: The left maxillary of a Kokanee labeled with (a) a dental palate housing a single row of homodont caniform teeth.

2.a The maxillary head (a) projects away from the maxillary body as a wide clubbed shaped structure with a at least one prominent ridge (b) and depression (c) on its lateral side… **go to 3**

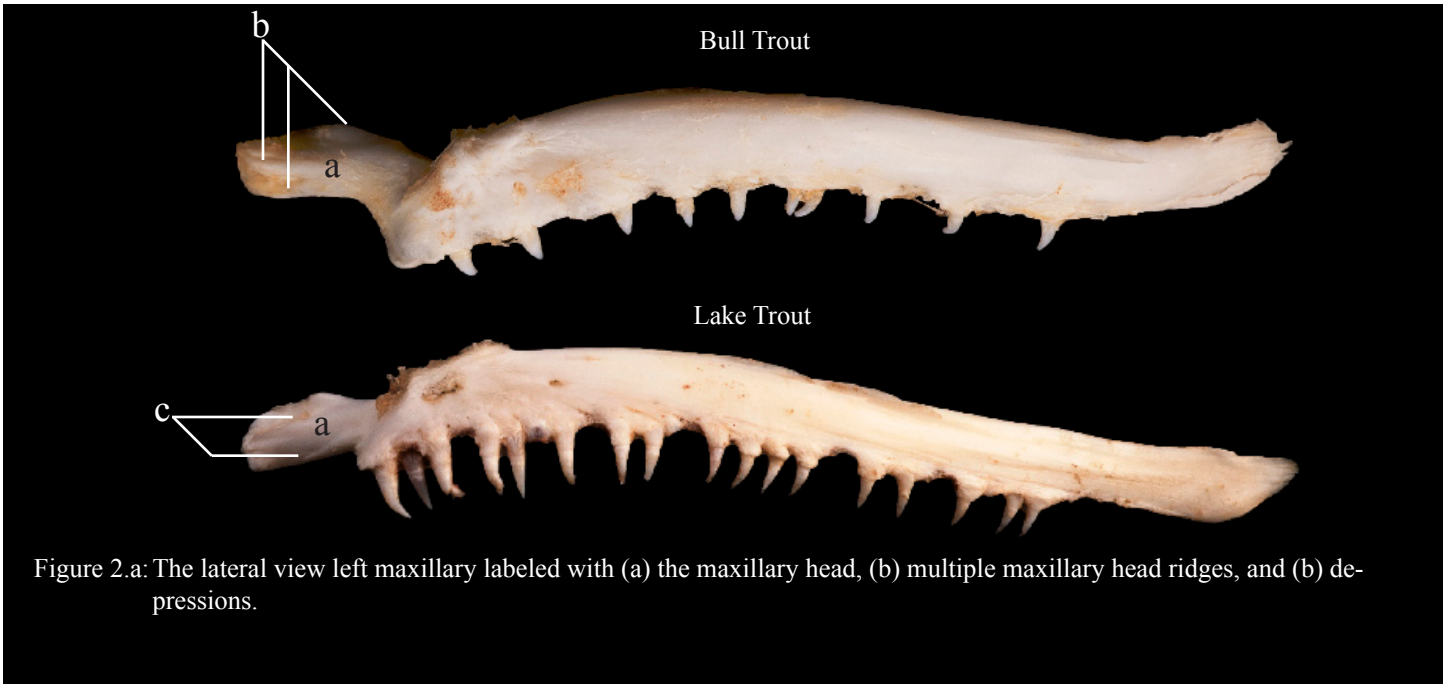

Figure 2.a: The lateral view left maxillary labeled with (a) the maxillary head, (b) multiple maxillary head ridges, and (b) depressions.

2.b The maxillary head (a) projects away from the maxillary body in a more cylindrical shaped structure. There is no visible ridging on the either smooth or shallow bowel shaped maxillary head... **go to 6**

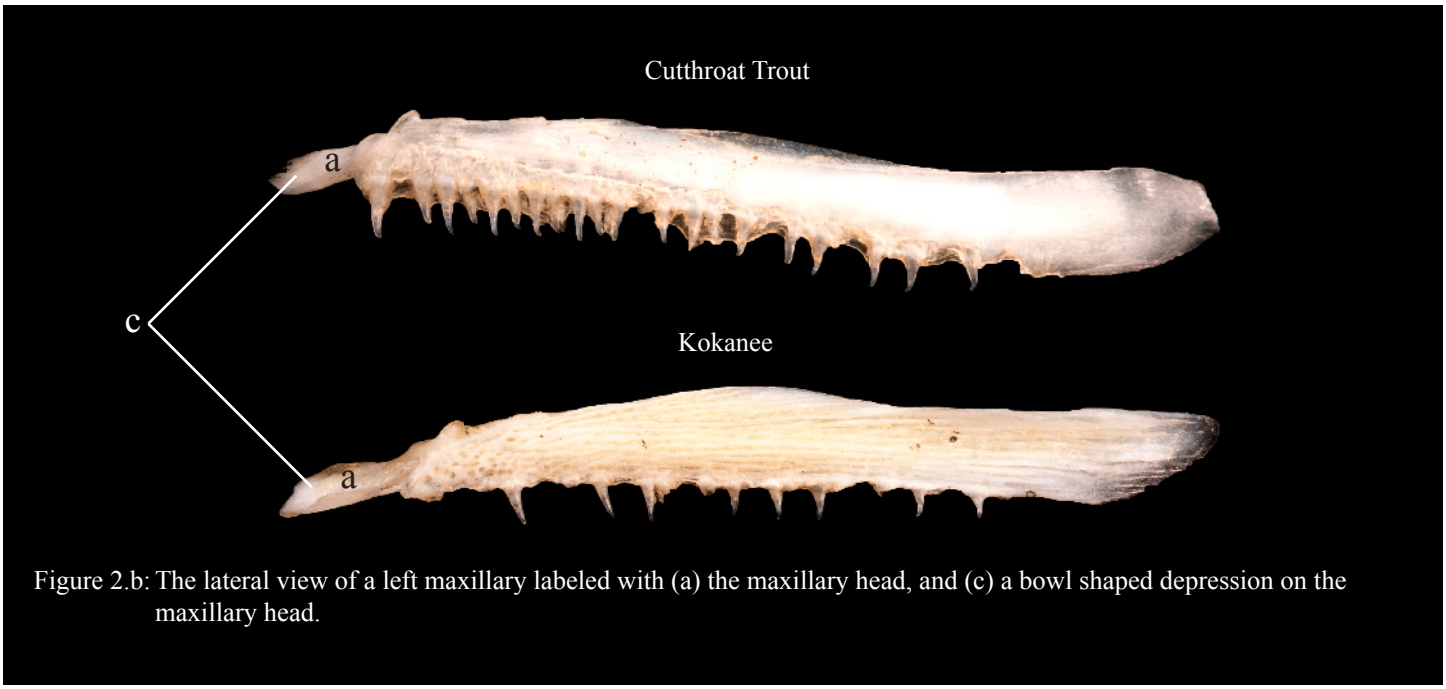

Figure 2.b: The lateral view of a left maxillary labeled with (a) the maxillary head, and (c) a bowl shaped depression on the maxillary head.

3.a There is a single prominent ridge (a) that runs the length of the mid-lateral maxillary head. Superior to this ridge is a deep depression (b). Posterior to the palatine fossa (c) the palatine sulcus (d) cuts a shallow crease into the anterior portion of the dorsal ridge (e). A subtle and rounded medial ridge (f) originates from near the anterior tip of the maxillary head (g)... **brown trout**

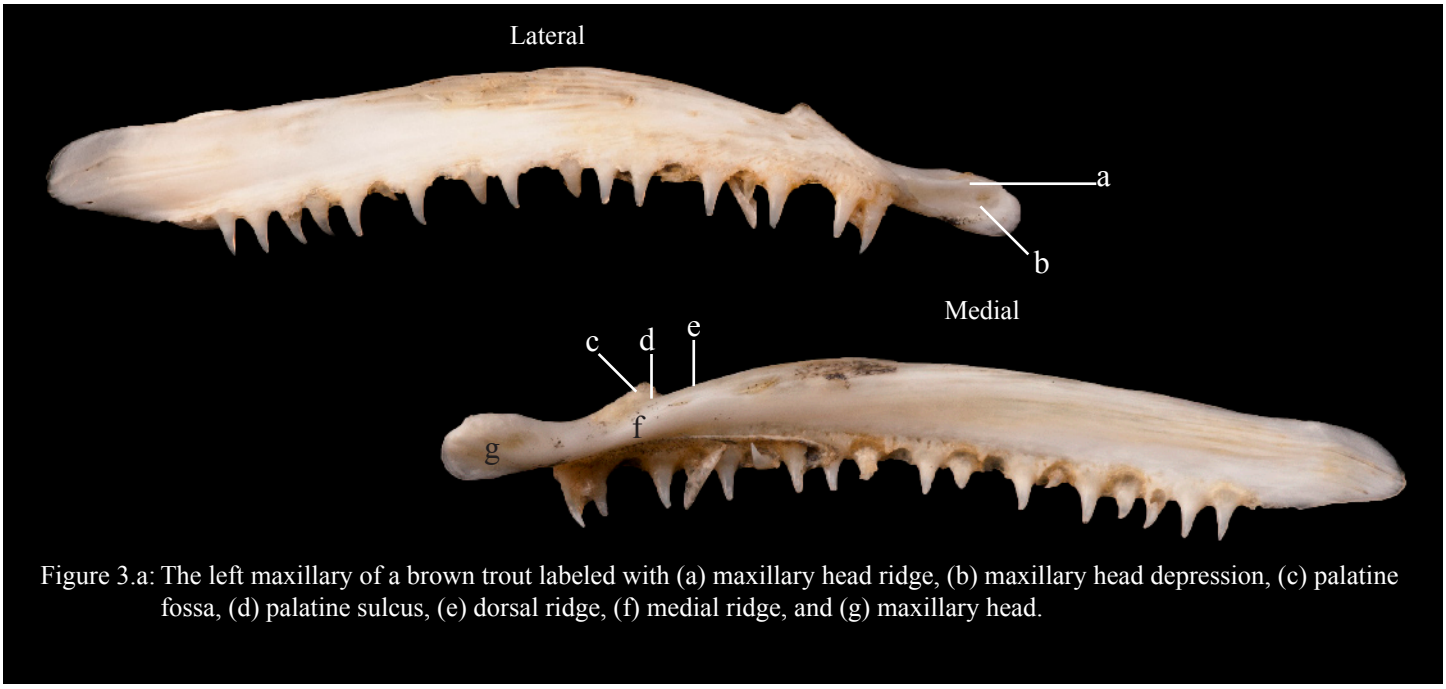

Figure 3.a: The left maxillary of a brown trout labeled with (a) maxillary head ridge, (b) maxillary head depression, (c) palatine fossa, (d) palatine sulcus, (e) dorsal ridge, (f) medial ridge, and (g) maxillary head.

3.b One single prominent ridge is not as apparent. Rather, three ridges are present on the lateral aspect of the maxillary head (a) with bowl shaped depressions between ridges… **go to 4**

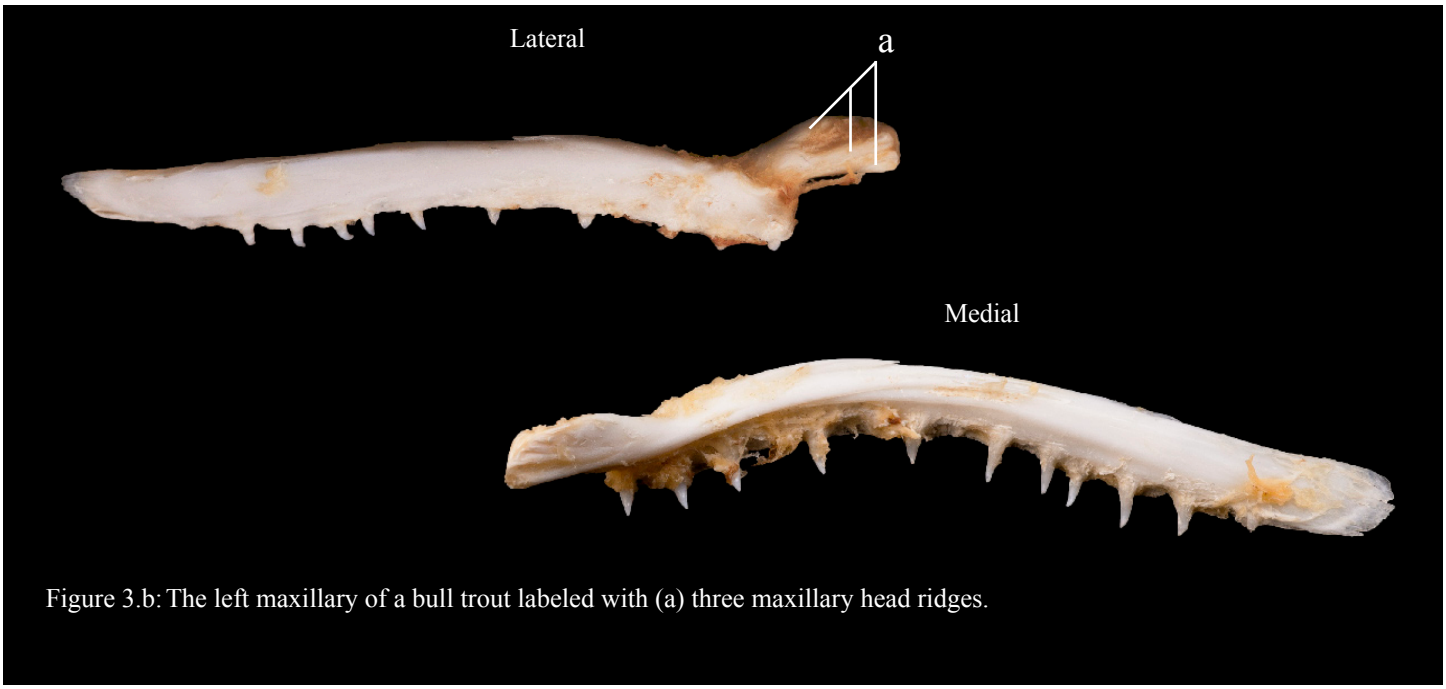

Figure 3.b: The left maxillary of a bull trout labeled with (a) three maxillary head ridges.

4.a There is a deep crease where the maxillary neck meets the maxillary body (a). A rounded edge (b) of the maxillary body (c) and palatine palate (d) projection anterior of this deep crease. The lateral side of the maxillary head is bifurcated by a prominent middle ridge (e). This ridge is bordered by a deep depression (superior, f) and a thinner sulcus (inferior, g). The medial ridge (h) originates on about the same plane as the ventral margin of the maxillary head and runs halfway down the maxillary body… **bull trout**

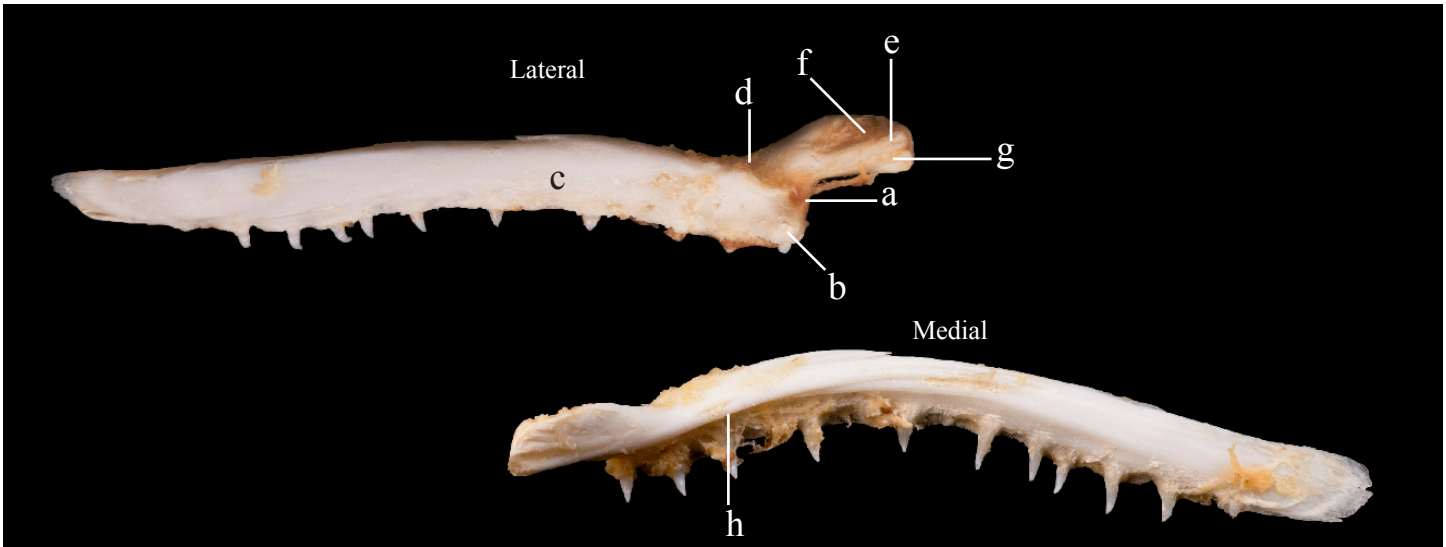

Figure 4.a: The left maxillary of a bull trout labeled with (a) deep crease, (b) maxillary body, (c) palatine plate, (d) anterior rounded edge of maxillary body, (e) prominent middle maxillary head ridge, (f) deep maxillary head depression, (g) thin maxillary head sulcus, and (h) medial ridge.

4.b There is not a deep crease (a) where the maxillary head meets the maxillary body (c). The maxillary bodies anterior most edge projects into a anterio-ventral point (d). The lateral side of the maxillary head is not dominated by one particular ridge… **go to 5**

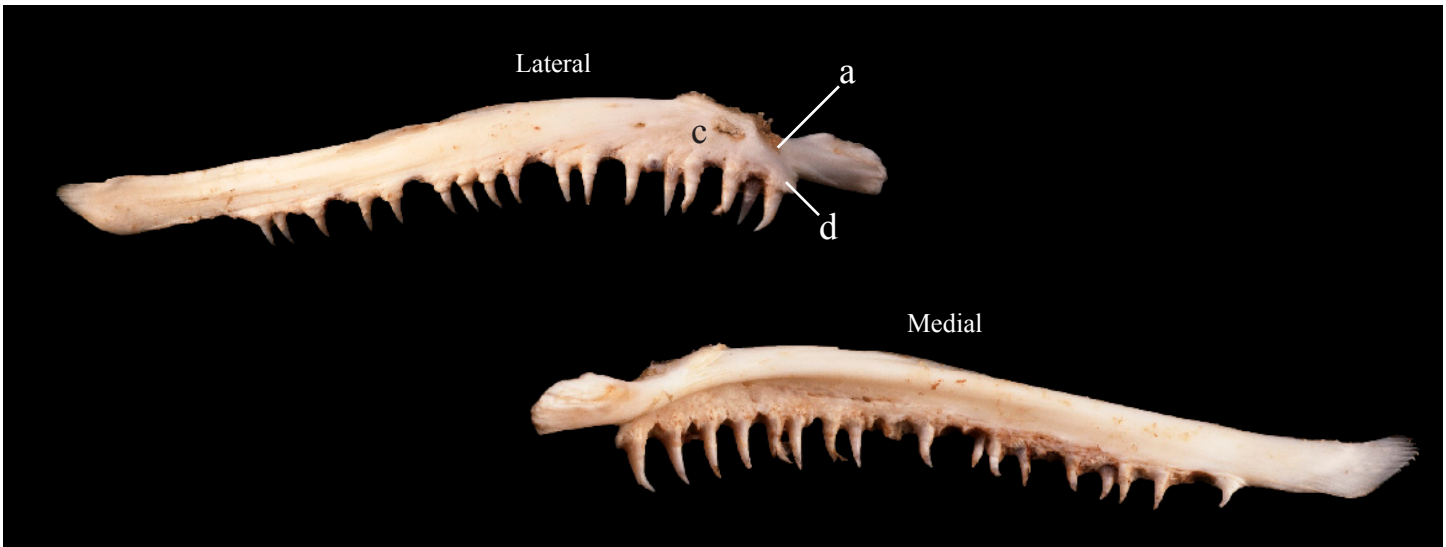

Figure 4.b: The left maxillary of a lake trout labeled with (a) area where the maxillary neck and body meet, (b) maxillary bodies anterio-ventral point, and (c) maxillary body.

5.a Two short ridges (a) run across the palatine plate. These ridges are not separated by the dorsal ridge, rather the second shallow sulci cuts through the dorsal ridge (b). The medial ridge (c) sits high on the maxillary body and maintains a rounded edge along its entire length. The dorsal margin is notched just before the posterior margin of the caudal lobe (d)… **lake trout**

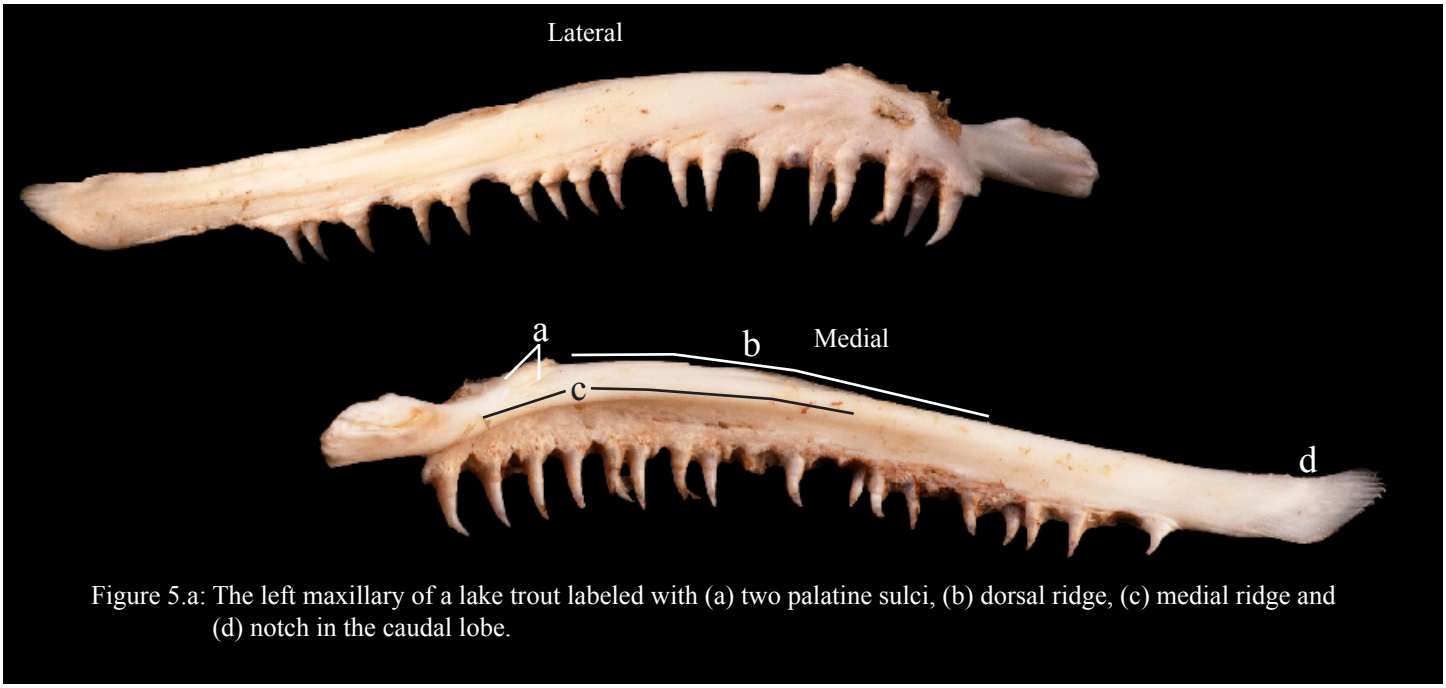

Figure 5.a: The left maxillary of a lake trout labeled with (a) two palatine sulci, (b) dorsal ridge, (c) medial ridge and (d) notch in the caudal lobe.

5.b One short (a) and one long (e) ridge run across the palatine plate and dorsal-medial face of the maxillary body. These ridges are separated by the dorsal ridge (b). The medial ridge (c) maintains a sharp edge as it leaves the maxillary neck and cuts down the first third of the maxillary body. The dorsal margin of the caudal lobe is not notched… **brook trout**

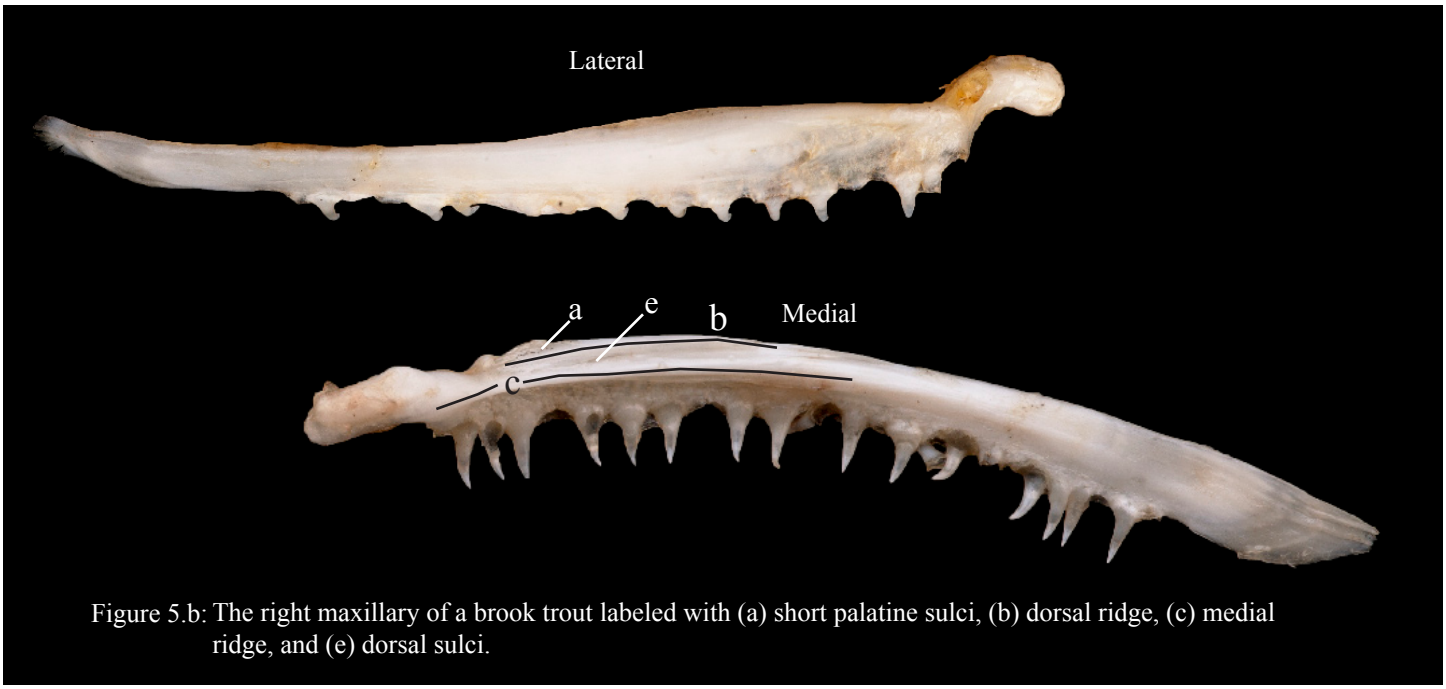

Figure 5.b: The right maxillary of a brook trout labeled with (a) short palatine sulci, (b) dorsal ridge, (c) medial ridge, and (e) dorsal sulci.

6.a The maxillary body (a) is heavily striated and pockmarked on its lateral surface... **go to 7**

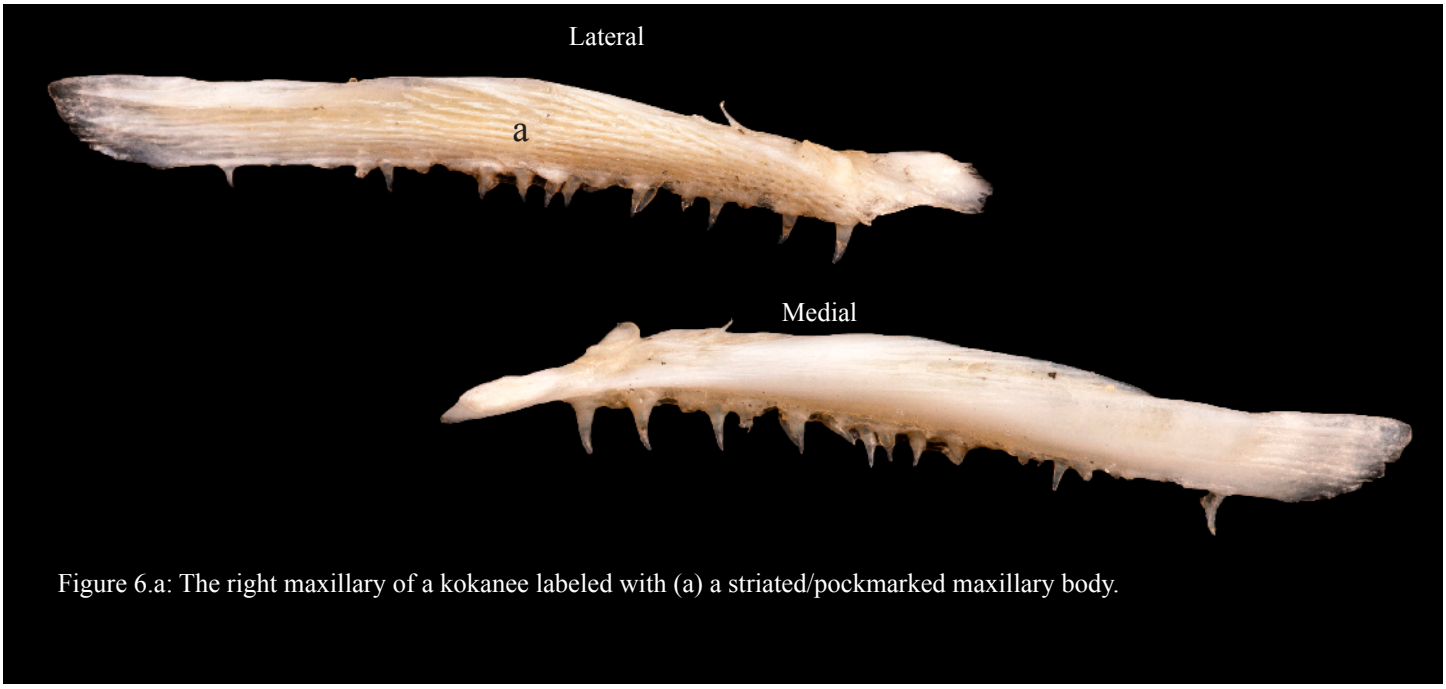

Figure 6.a: The right maxillary of a kokanee labeled with (a) a striated/pockmarked maxillary body.

6.b The lateral surface of the maxillary body (a) may contain a few subtle striations along its anterior portions but the middle and posterior sections of are smooth... **go to 8**

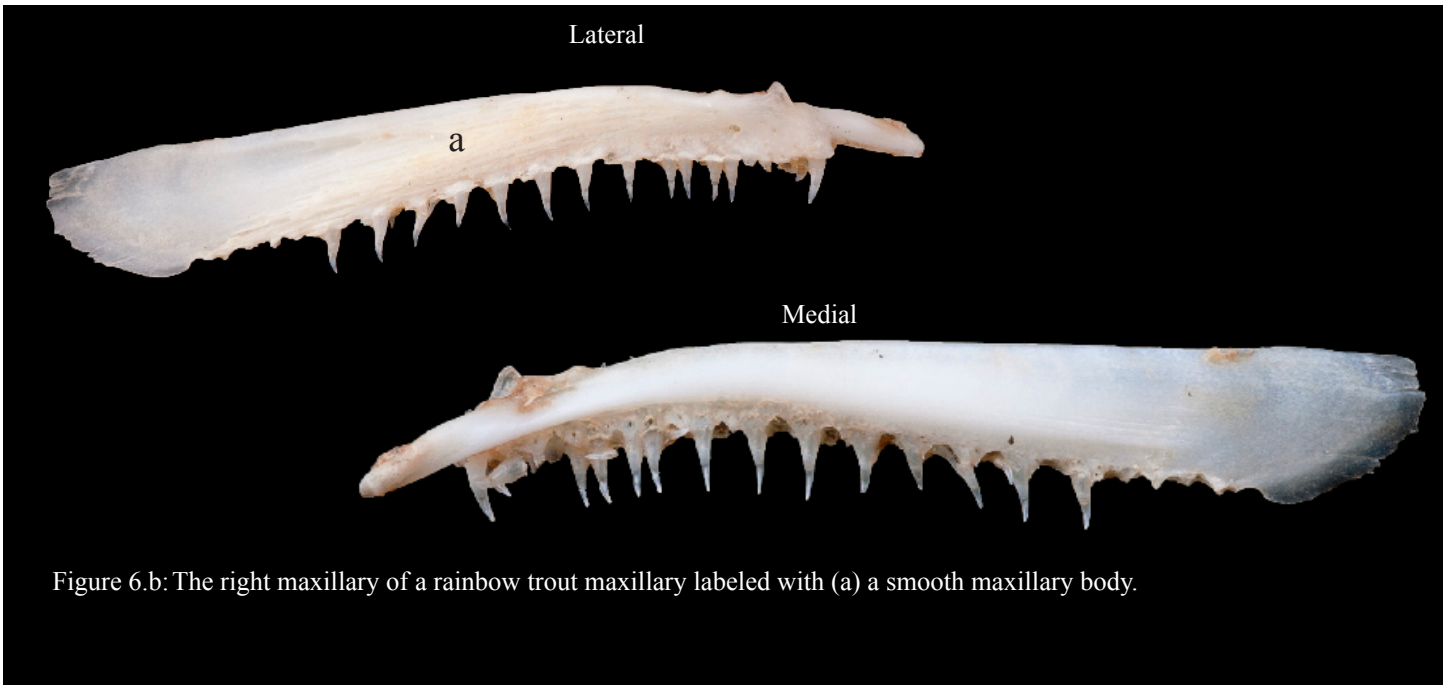

Figure 6.b: The right maxillary of a rainbow trout maxillary labeled with (a) a smooth maxillary body.

7.a The body of the maxillary has a dorso-ventral curvature causing the caudal lobe (a) to angle ventrally and the medial ridge (b) to maintain a position near the dorsal margin. The maxillary head and neck (c) are thin in comparison to the maxillary body. The dorsal ridge progresses superiorly and anteriorly over the palatine plate, as a large rounded structure (d)… **Chinook**

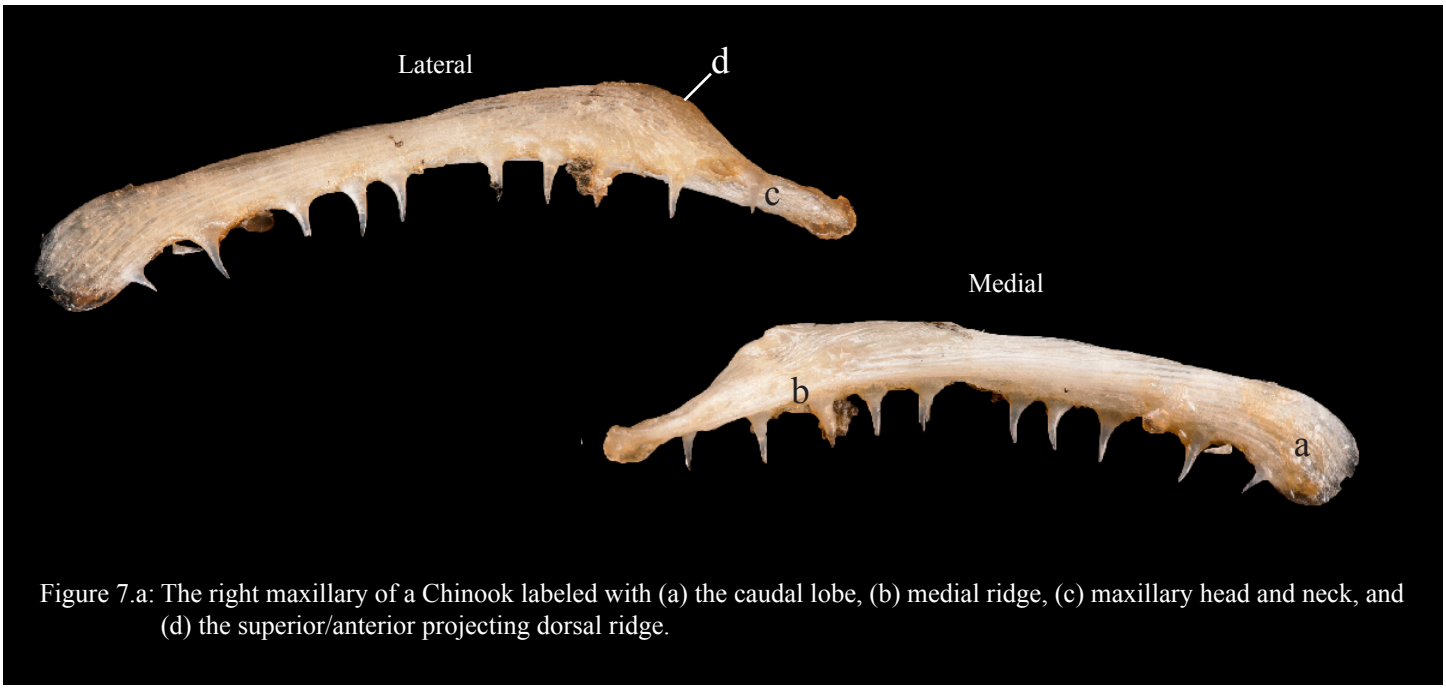

Figure 7.a: The right maxillary of a Chinook labeled with (a) the caudal lobe, (b) medial ridge, (c) maxillary head and neck, and (d) the superior/anterior projecting dorsal ridge.

7.a The body of the maxillary does not have a strong dorso-ventral curvature. The maxillary head and neck (c) maintain a flat lateral face with a shallow bowl shaped depression (e). Rather than a large and anterior projection of the dorsal ridge, the palatine fossa (f) is located on the anterior/dorsal most portion of the maxillary body, and is un-obscured by any other structure … **kokanee**

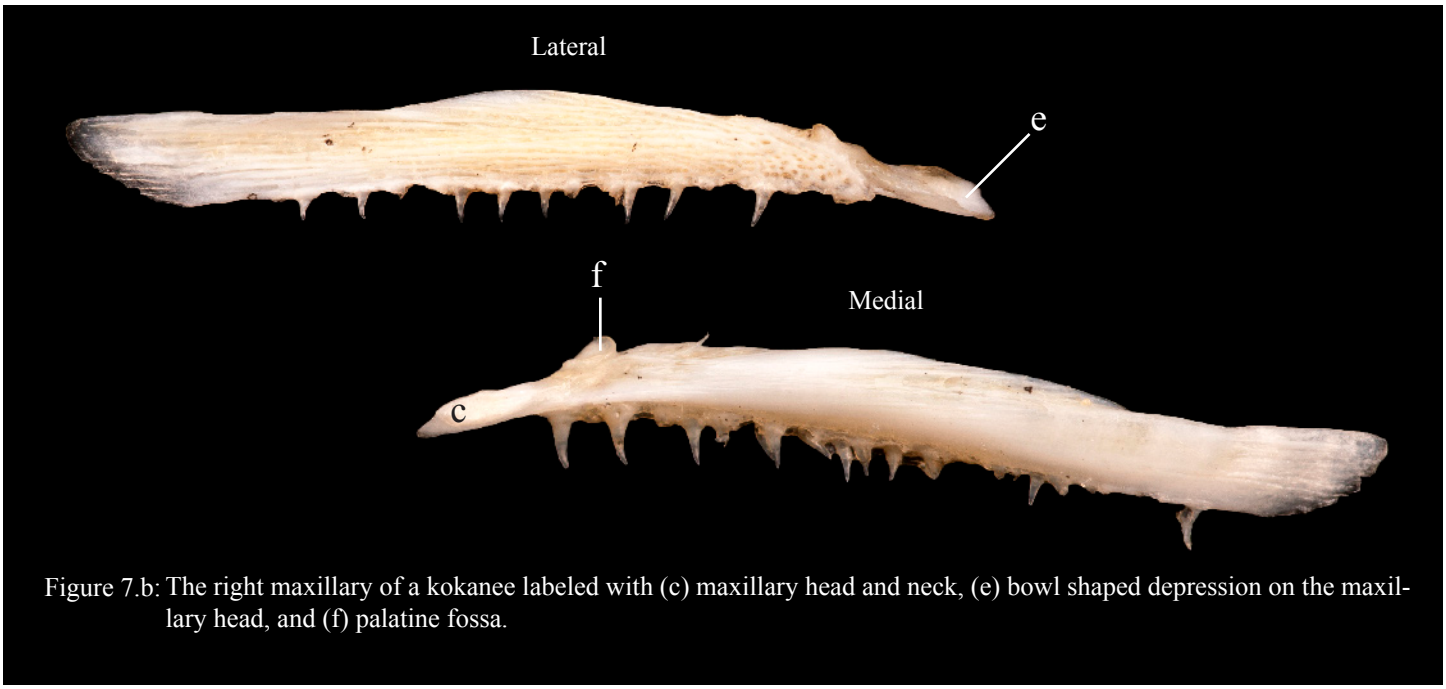

Figure 7.b: The right maxillary of a kokanee labeled with (c) maxillary head and neck, (e) bowl shaped depression on the maxillary head, and (f) palatine fossa.

8.a The maxillary head and neck (a) are flattened on their lateral surface and rounded on their medial surface. There is a single shallow depression (b) on the lateral maxillary head. There is not a shallow crease where the lateral maxillary body and neck meet. The medial ridge (c) originates from the back of the maxillary neck. The maxillary body (d) and caudal lobe (e) maintain a generally even width through the caudal lobe… **cutthroat trout**

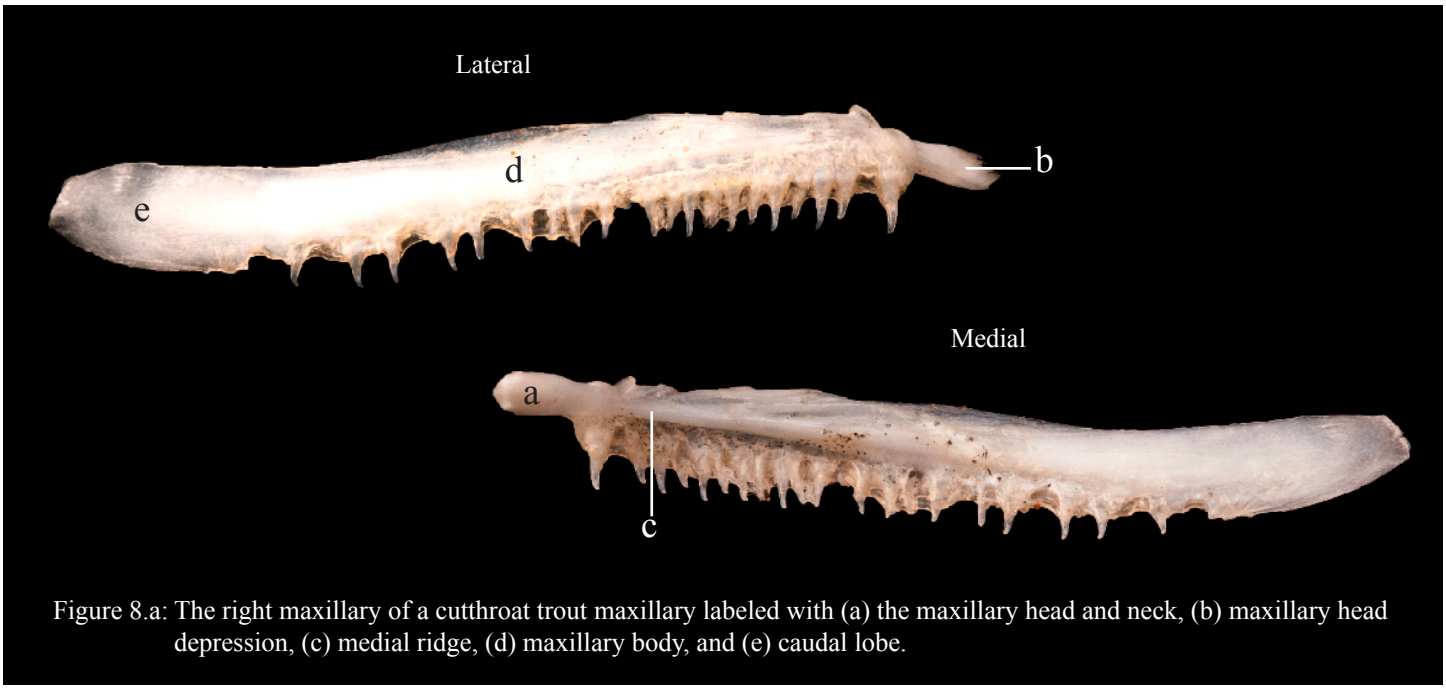

Figure 8.a: The right maxillary of a cutthroat trout maxillary labeled with (a) the maxillary head and neck, (b) maxillary head depression, (c) medial ridge, (d) maxillary body, and (e) caudal lobe.

8.b The maxillary head and neck (a) have a slightly more flattened lateral face but maintain an overall slender cylindrical appearance. There is a very shallow crease (f) where the lateral maxillary body and neck meet. The medial ridge (c) originates near the anterior tip of the maxillary head, and creates a thin line that progresses from the head onto the first half of the body. The maxillary body (d) caudal lobe (e) widen greatly towards the posterior margin... **rainbow trout**

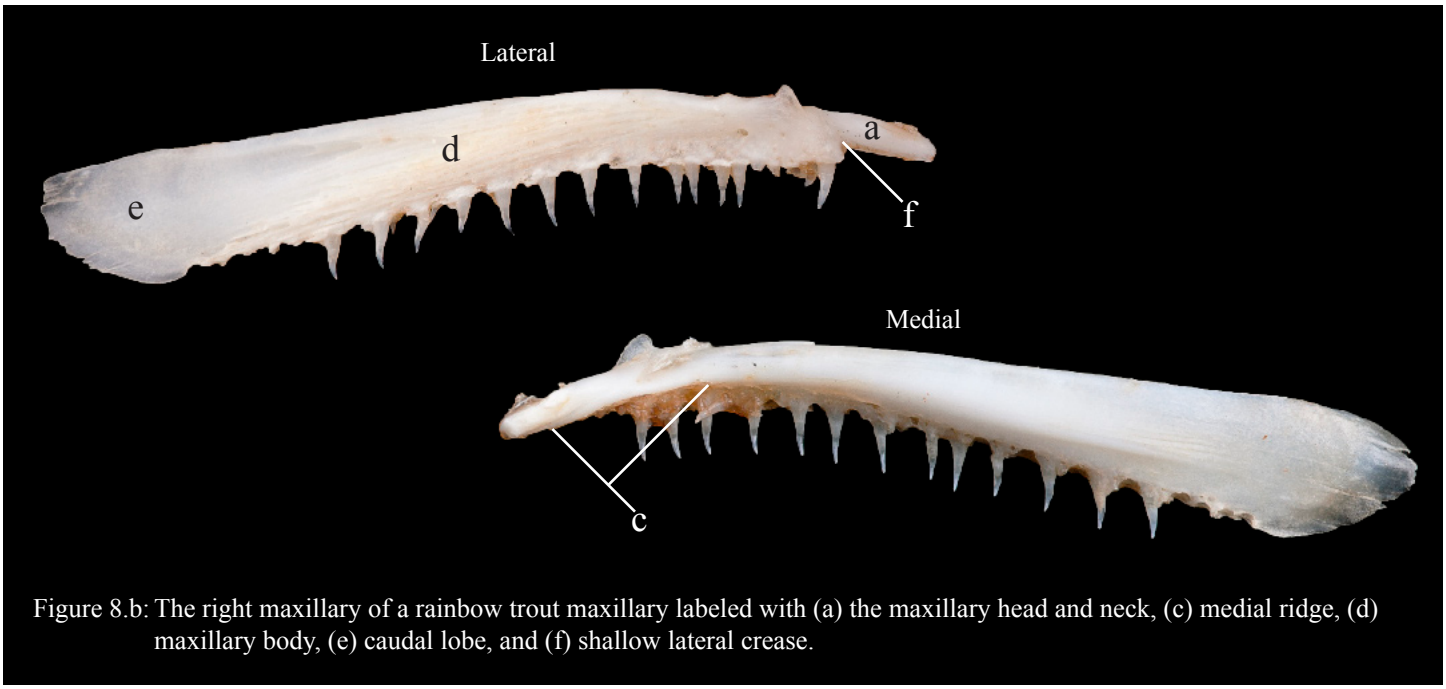

Figure 8.b: The right maxillary of a rainbow trout maxillary labeled with (a) the maxillary head and neck, (c) medial ridge, (d) maxillary body, (e) caudal lobe, and (f) shallow lateral crease.

1.a The dentary body (a) is reduced with a short and thin dental plate (b). There are no teeth or alveoli present. The coronoid process (c) and ventral limb (d) are large and separated by a wide meckelian notch (e)… **mountain whitefish**

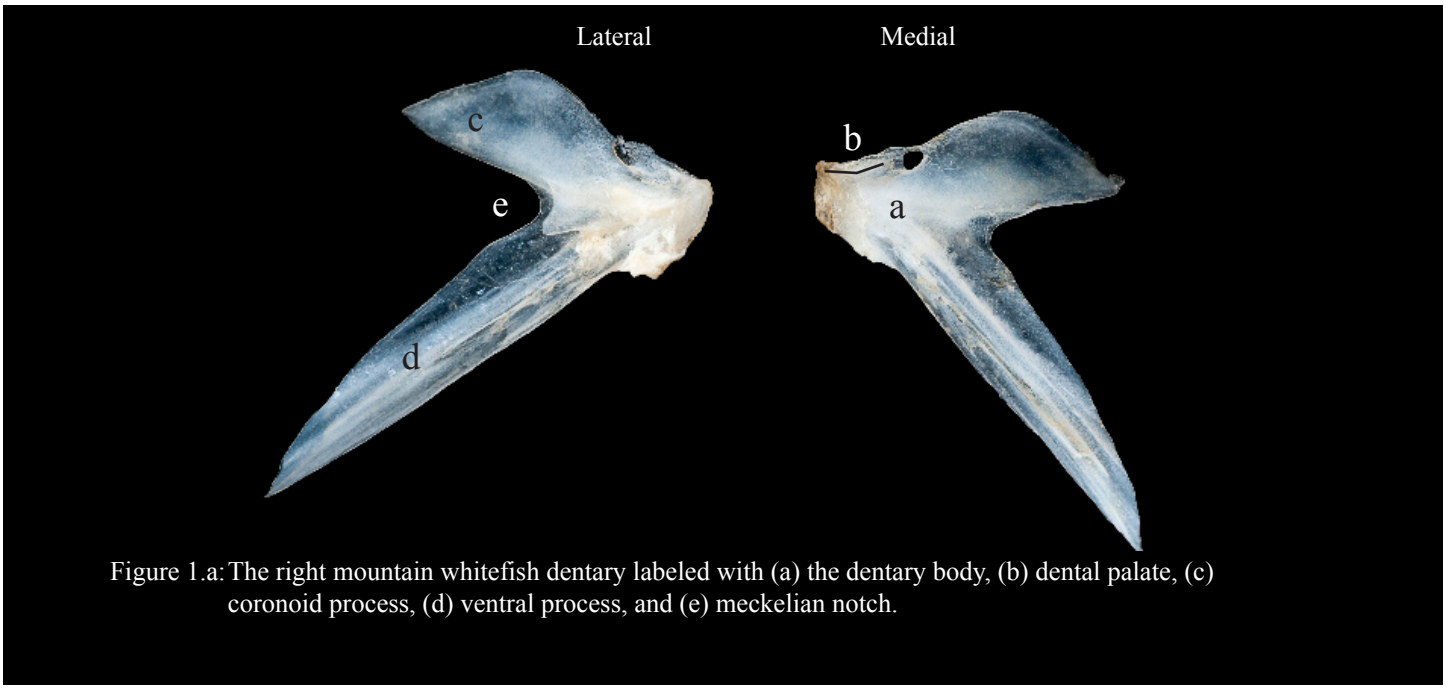

Figure 1.a: The right mountain whitefish dentary labeled with (a) the dentary body, (b) dental palate, (c) coronoid process, (d) ventral process, and (e) meckelian notch.

1.b The dentary body (a) and dental palate (b) are long. There is a single row of caniform homodont teeth or alveoli. The coronoid (c) and ventral (d) process are diminutive and are separated by a narrow meckelian notch (e)… **go to 2**

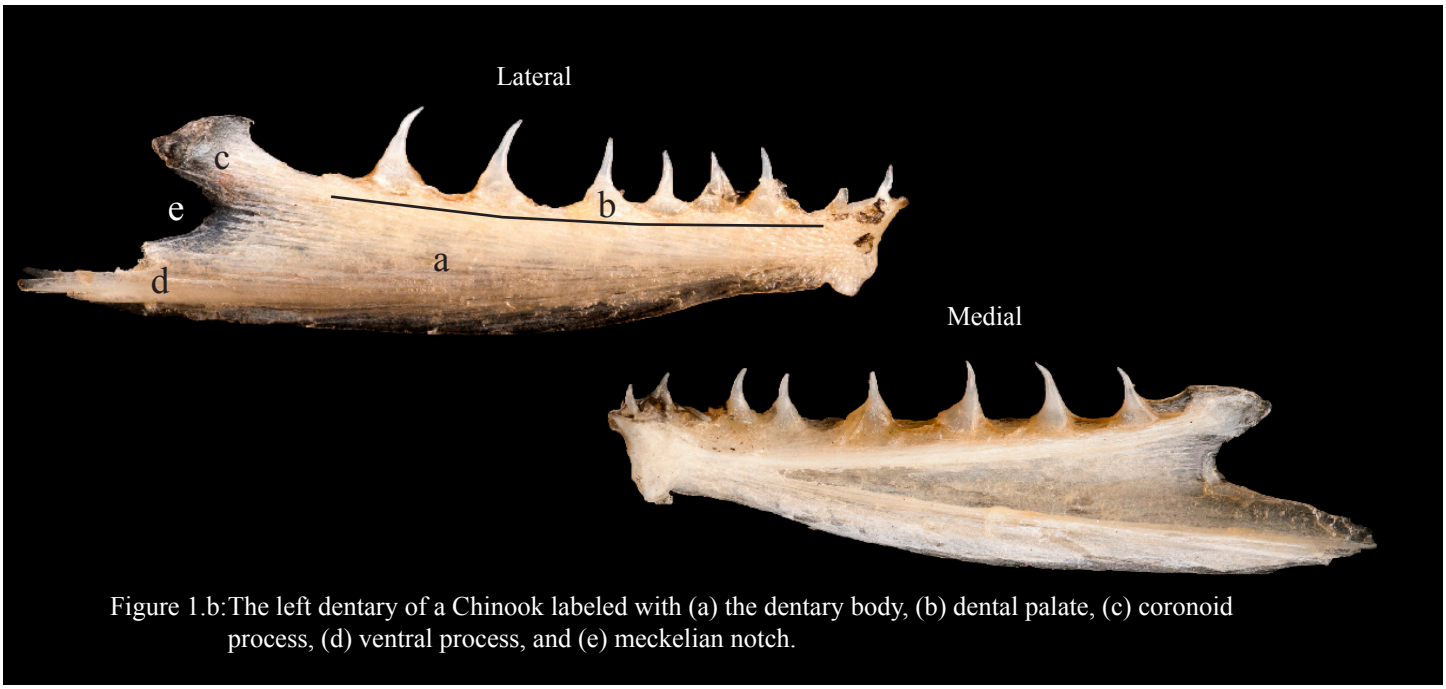

Figure 1.b: The left dentary of a Chinook labeled with (a) the dentary body, (b) dental palate, (c) coronoid process, (d) ventral process, and (e) meckelian notch.

2.a The ventral limb (a) and coronoid process (b) are evenly sized. The meckelian notch (c) has a relatively wide angle that originates near the midpoint between the coronoid process and ventral limb. The lingual palate (d) extends far back. The sublingual fossa (e) is positioned far ventral-posteriorly… **go to 3**

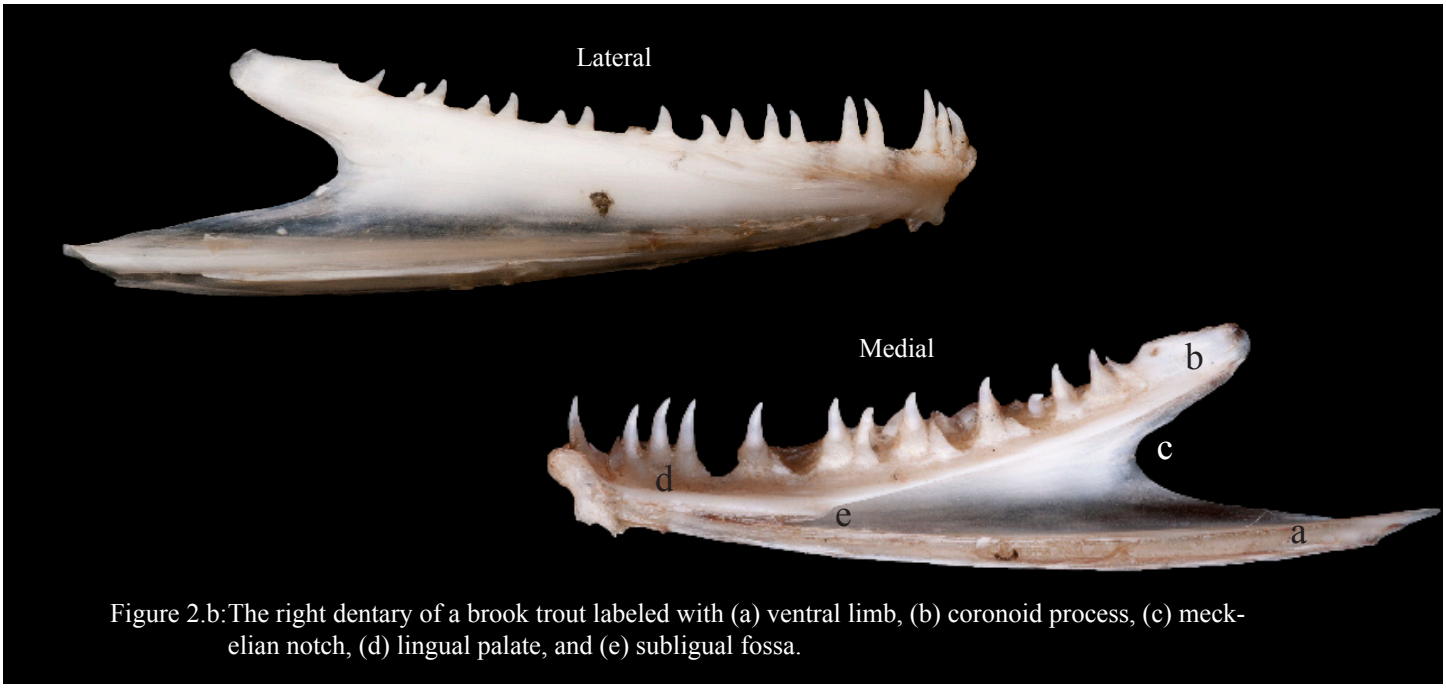

Figure 2.b: The right dentary of a brook trout labeled with (a) ventral limb, (b) coronoid process, (c) meckelian notch, (d) lingual palate, and (e) subligual fossa.

2.b The ventral limb (a) is the dominate feature and the coronoid process (b) is diminutive. The meckelian notch (c) is narrow and sits high just below the coronoid process. The lingual palate (d) does not extend far back… **go to 6**

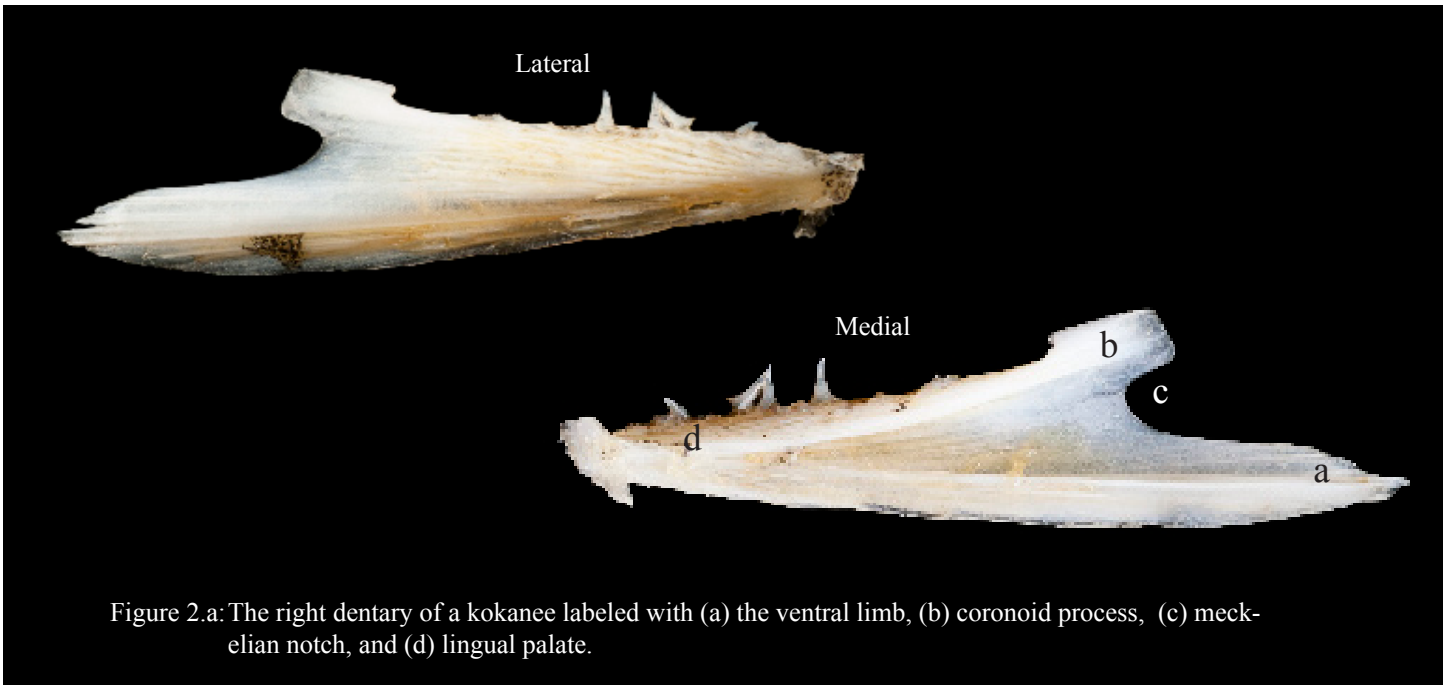

Figure 2.a: The right dentary of a kokanee labeled with (a) the ventral limb, (b) coronoid process, (c) meckelian notch, and (d) lingual palate.

3.a The dental plate (a) extend over the lateral side of the dentary body creating a small ridge (b) and post mandibular crease (c). A single row of five to six sensory pores (d) is present along the ventral-lateral margin. Each pore is located at the end of a long canal that branches of the main sensory canal. The ventral self (e) and ventral ridge (f) extend in a straight line that originates from the sublingual fossa (g) … **brown trout**

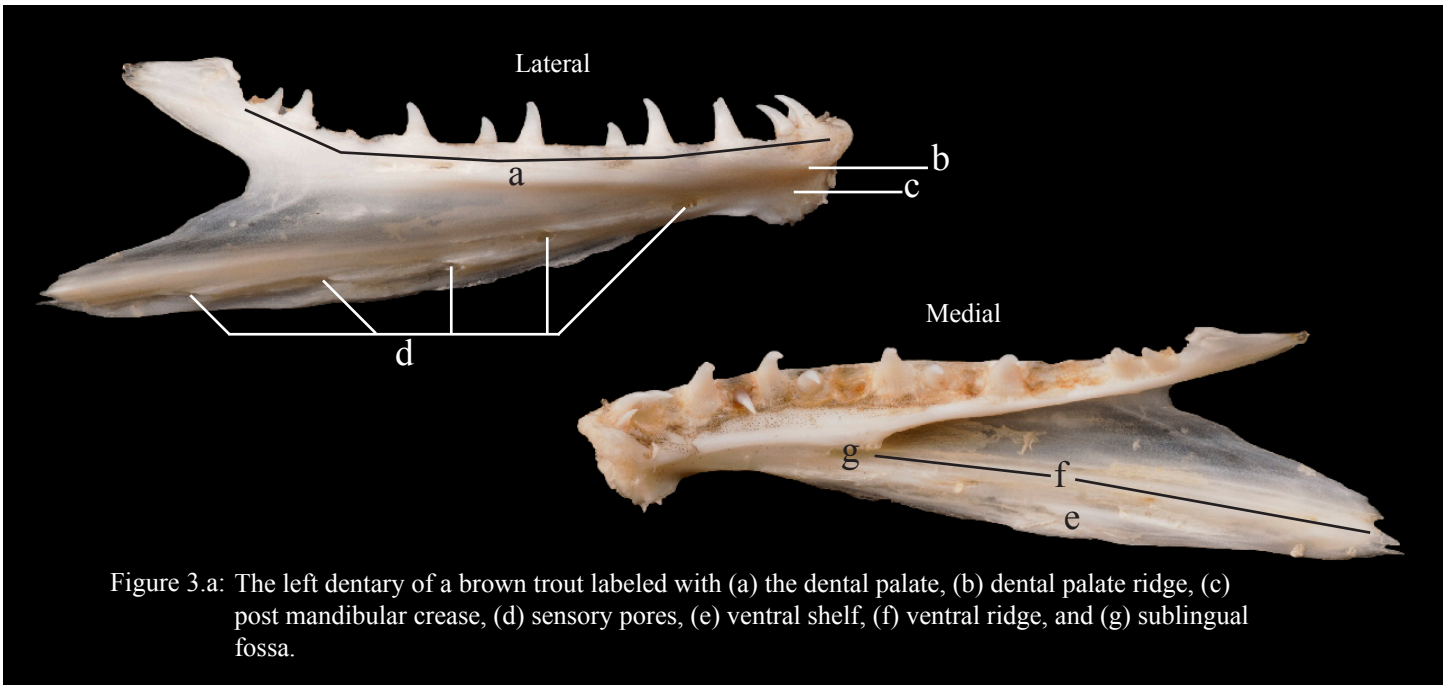

Figure 3.a: The left dentary of a brown trout labeled with (a) the dental palate, (b) dental palate ridge, (c) post mandibular crease, (d) sensory pores, (e) ventral shelf, (f) ventral ridge, and (g) sublingual fossa.

3.b The dental palate (a) does not extend over the lateral side of the dentary body and there is no post-mandibular crease or ridge. The mandibular symphysis (b) and lateral wall connect to each other in a more or less smooth and continuous osseous sheet. Generally two rows of sensory pores are present along the ventral lateral margin... **go to 4**

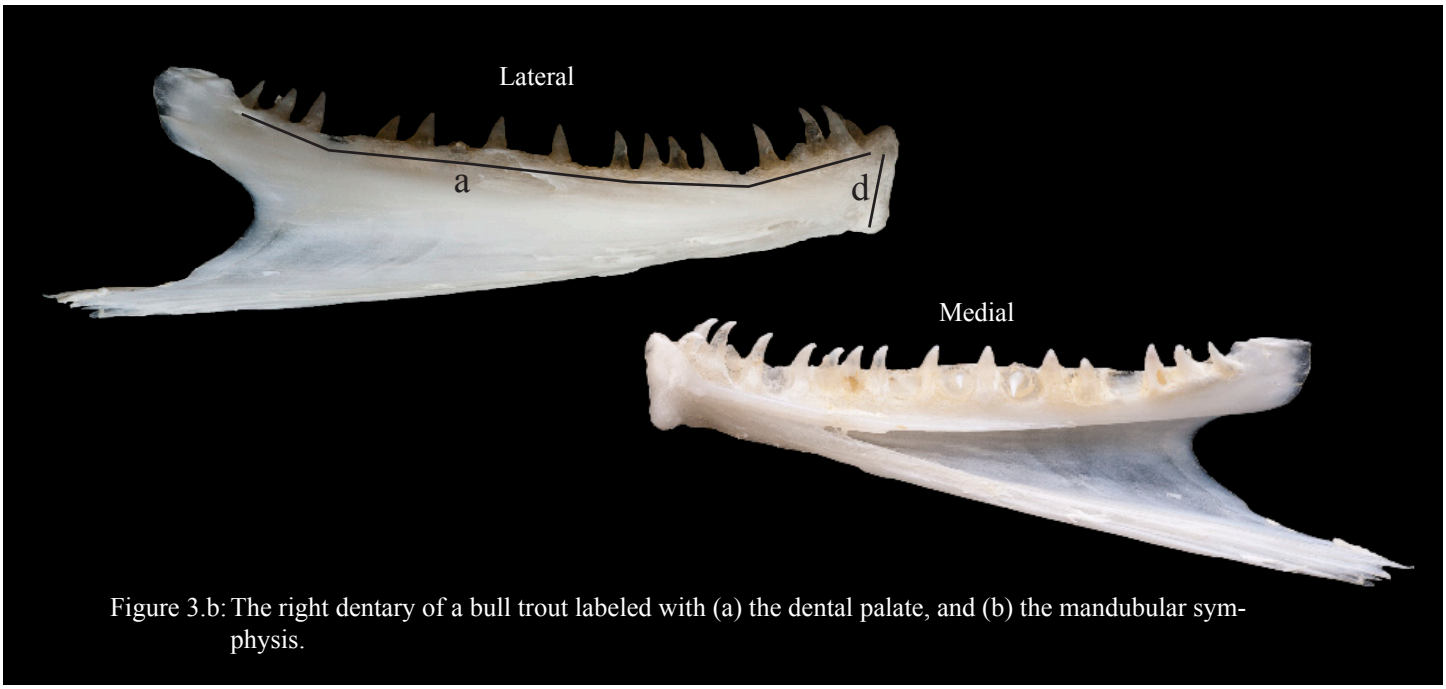

Figure 3.b: The right dentary of a bull trout labeled with (a) the dental palate, and (b) the mandubular symphysis.

Appendix A III: The dichotomous key for the dentary

4.a The ventral margin of the dentary is gently curved. A major row of five to six sensory pores (a) is present along the ventral margin. If a second, minor row of sensory pores is present there are between two and four pores (b) located superior to the major sensory pores. A narrow ventral shelf (c) widens slightly as it progresses towards the ventral tip. The ventral ridge (d) maintains a thin sharp edge… **brook trout**

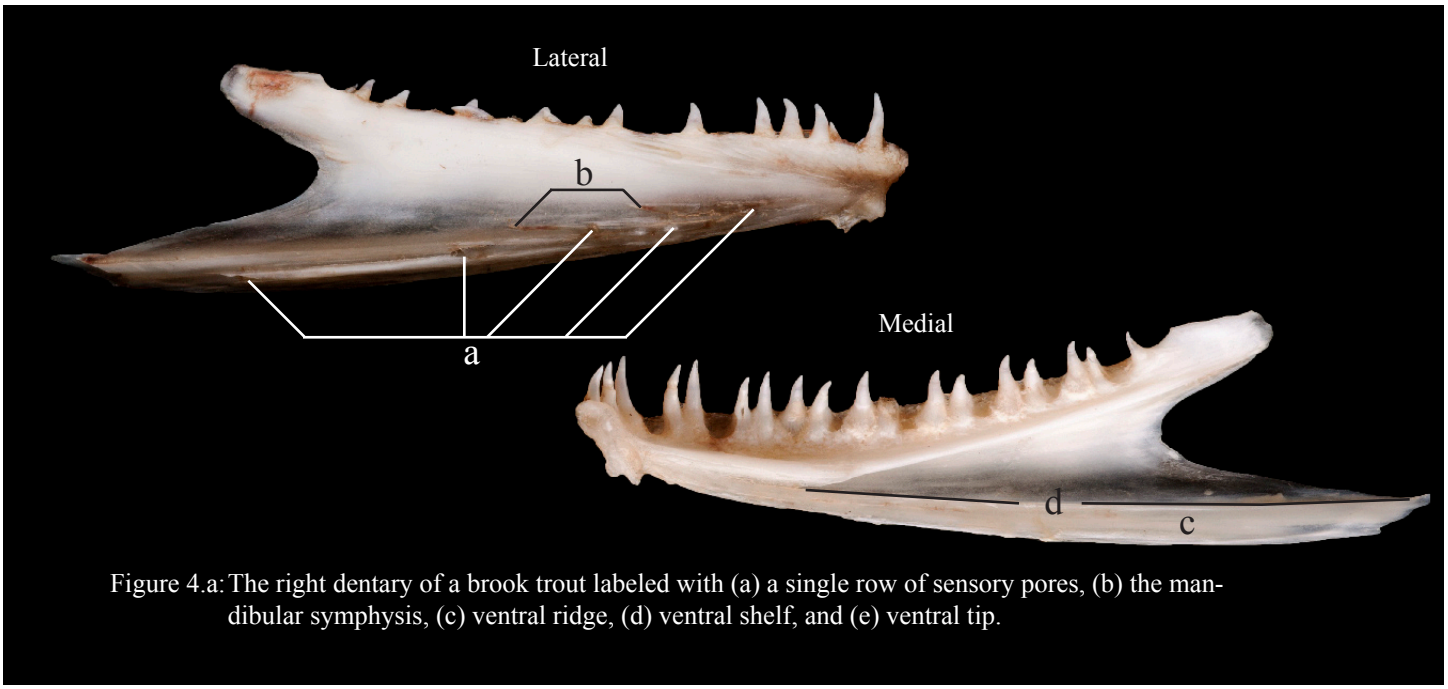

Figure 4.a: The right dentary of a brook trout labeled with (a) a single row of sensory pores, (b) the mandibular symphysis, (c) ventral ridge, (d) ventral shelf, and (e) ventral tip.

4.b The ventral margin of the dentary maintains a more or less strait line. Two sets of sensory pores (a, b) are present near the ventral-lateral margin of the dentary. Among these two sets of pores, the major set varies between four and seven, and the minor set varies between two and six. A very thin ventral shelf is present and maintains about the same thickness down the length of the ventral margin… **go to 5**

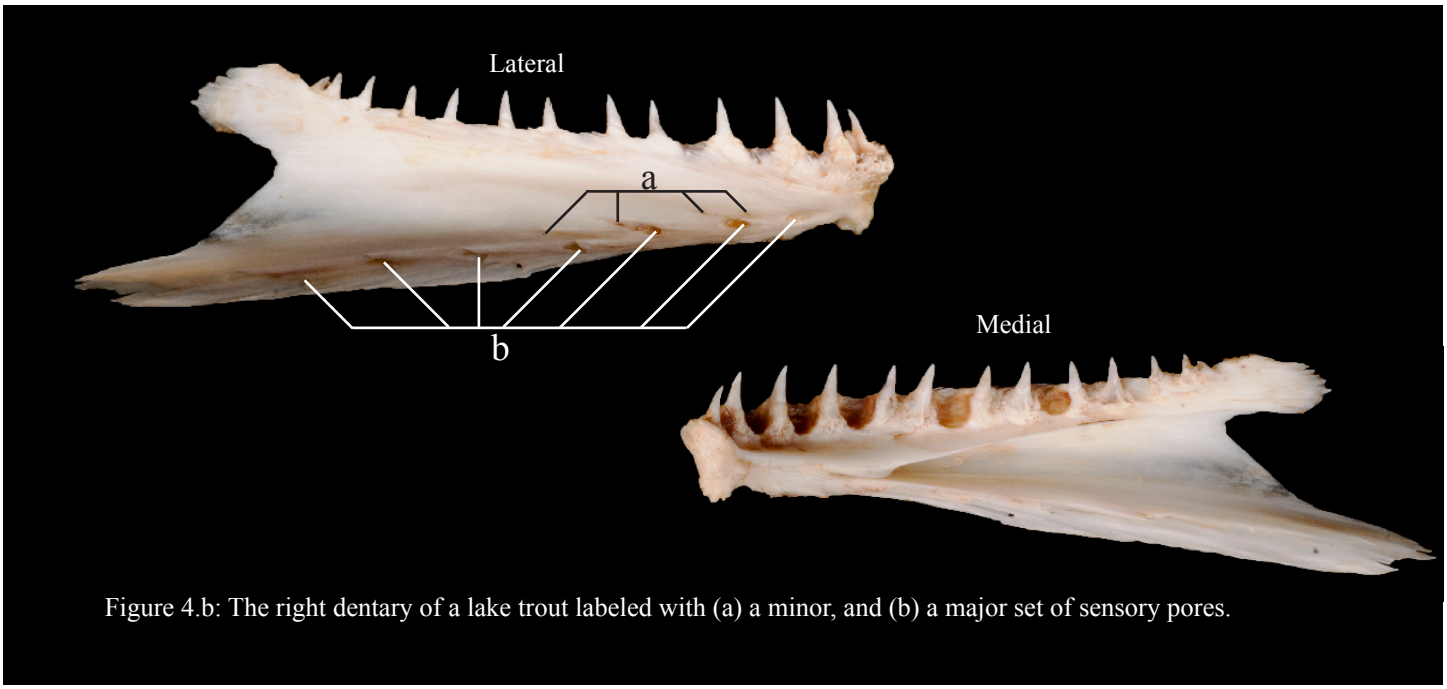

Figure 4.b: The right dentary of a lake trout labeled with (a) a minor, and (b) a major set of sensory pores.

5.a There is a major set of six to seven deep sensory pores (a). This is mirrored superiorly by a minor set of three to six sensory pores (b). The mandibular joint (c) juts down into a distinct point. The ventral limb has a prominent medial curvature. The ventral ridge (d) has a rounded edge… **lake trout**

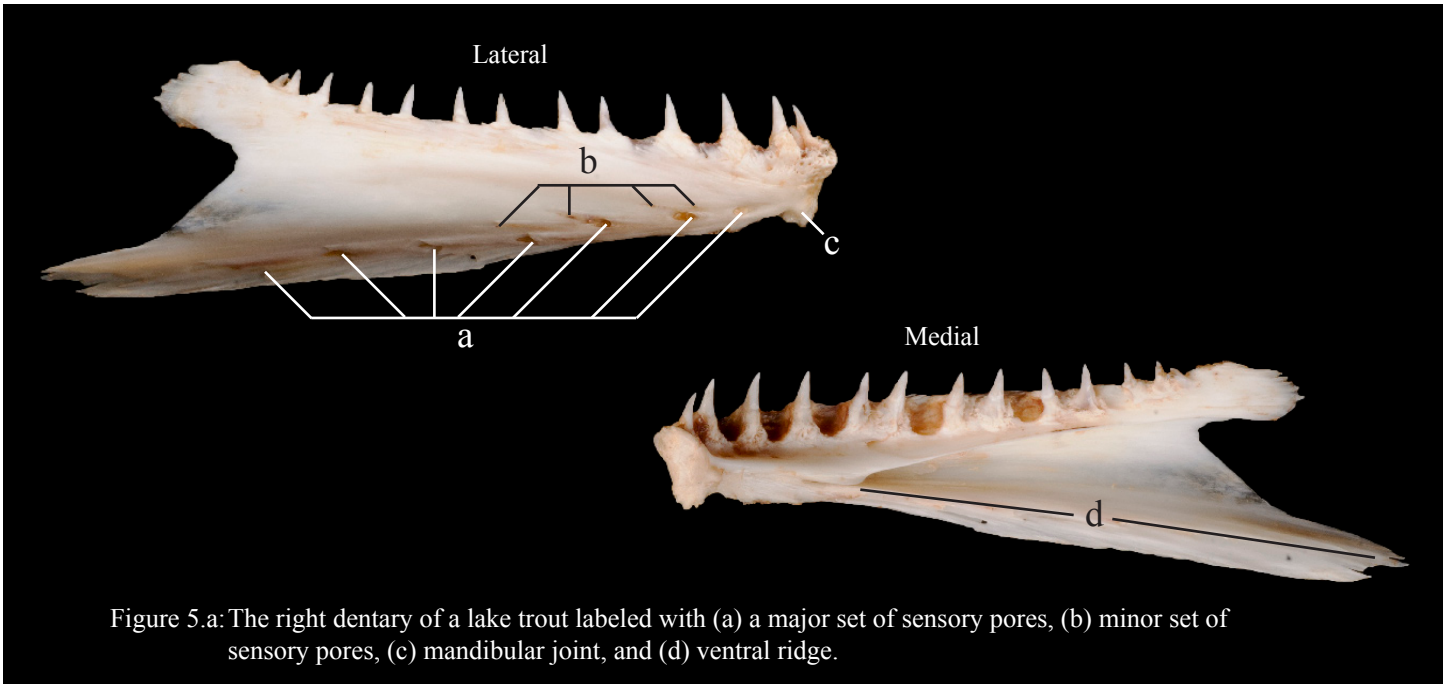

Figure 5.a: The right dentary of a lake trout labeled with (a) a major set of sensory pores, (b) minor set of sensory pores, (c) mandibular joint, and (d) ventral ridge.

5.b There is a major set of four to six sensory pores (a) located directly along the ventral margin. Two to four minor sensory pores are located superior major sensory pores. Occasionally the first minor pore may be inferior to the first major pore. The mandibular joint (c) does not jut down into a distinct point. The ventral limb has only a slight medial curve. The ventral ridge (d) has a prominent pointed edge… **bull trout**

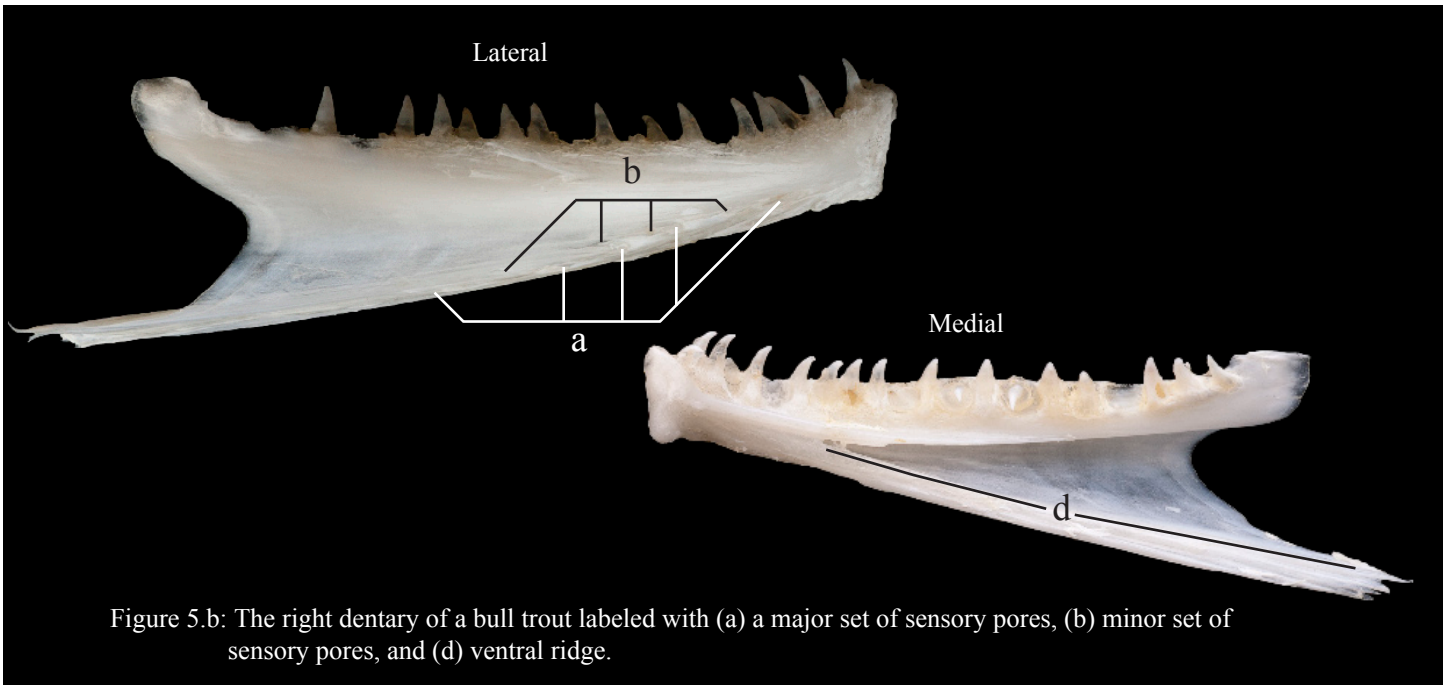

Figure 5.b: The right dentary of a bull trout labeled with (a) a major set of sensory pores, (b) minor set of sensory pores, and (d) ventral ridge.

6.a The entire lateral surface of the dentary is heavily striated and pockmarked... **go to 7**

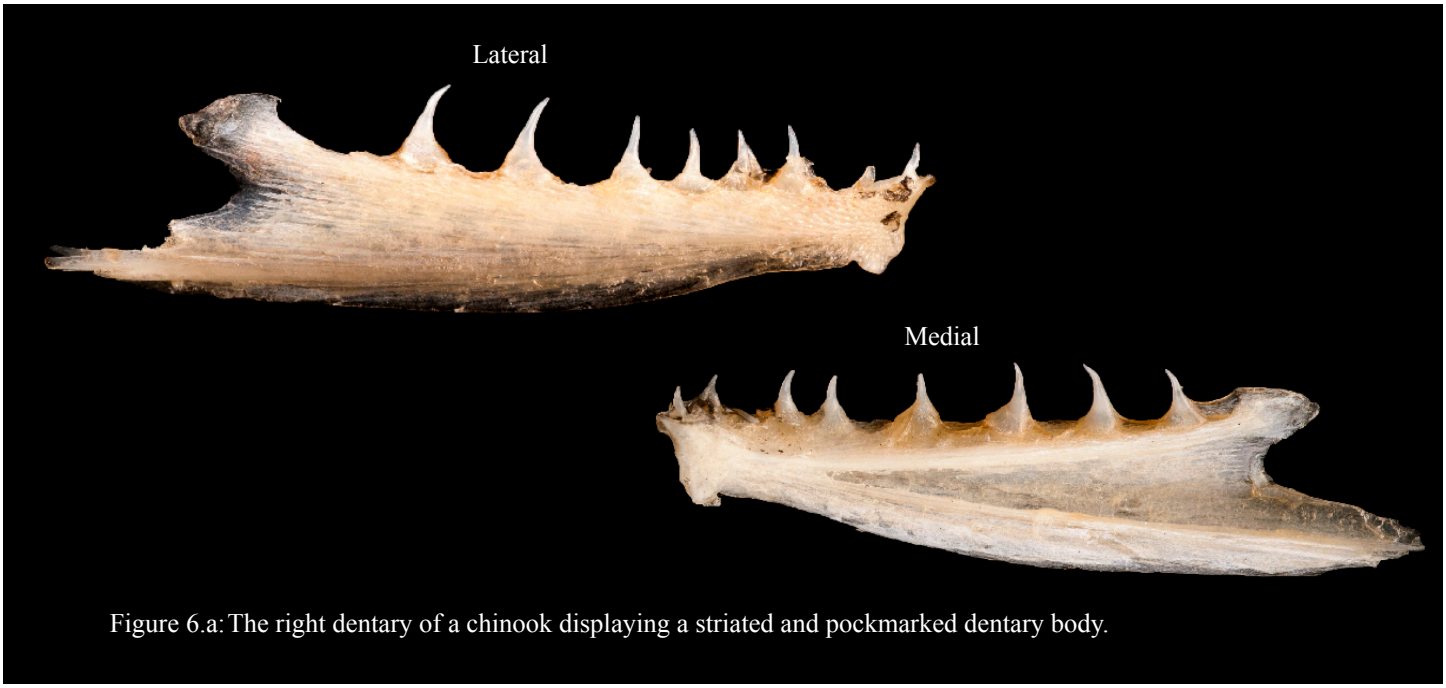

Figure 6.a: The right dentary of a chinook displaying a striated and pockmarked dentary body.

6.b There may be a few minor striations near the mandibular symphysis but the remainder of the lateral wall is smooth... **go to 8**

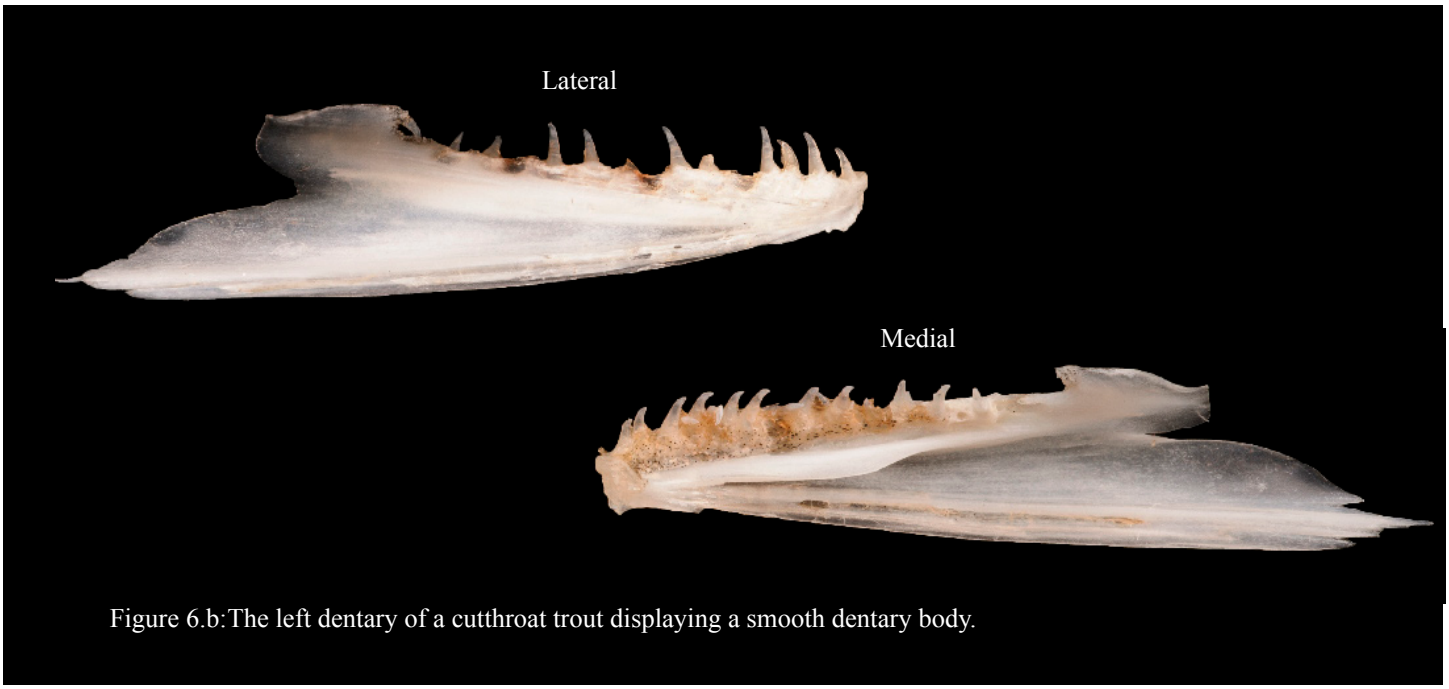

Figure 6.b: The left dentary of a cutthroat trout displaying a smooth dentary body.

7.a A wide ventral limb (a) juts far posterior of the coronoid process (b) and meckelian notch (c). The ventral limb bulges laterally creating a long deep depression along the superior side of the ventral ridge (d). A major set of four well defined major sensory pores (e) is visible near the ventral-lateral margin. A second set of three to five minor sensory pores (f) is located superior to the major pores. These minor pores can be found entrenched in a small grove (g) on the ventral limb… **kokanee**

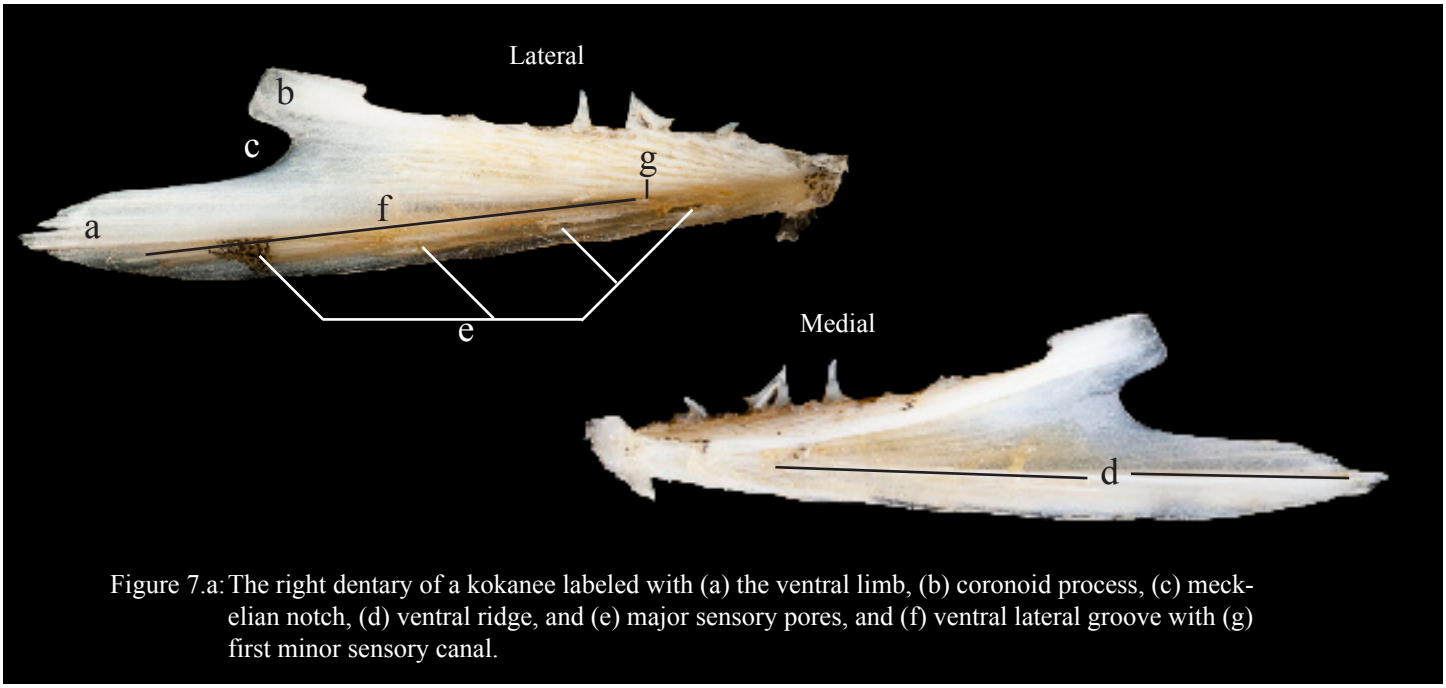

Figure 7.a: The right dentary of a kokanee labeled with (a) the ventral limb, (b) coronoid process, (c) meckelian notch, (d) ventral ridge, and (e) major sensory pores, and (f) ventral lateral groove with (g) first minor sensory canal.

7.b The ventral limb (a) does not jut far posterior of the coronoid process (b) and meckelian notch (c). There is no lateral bulging of the ventral limb. A single row of four to six sensory pores (e) is located near the ventral lateral margin… **Chinook**

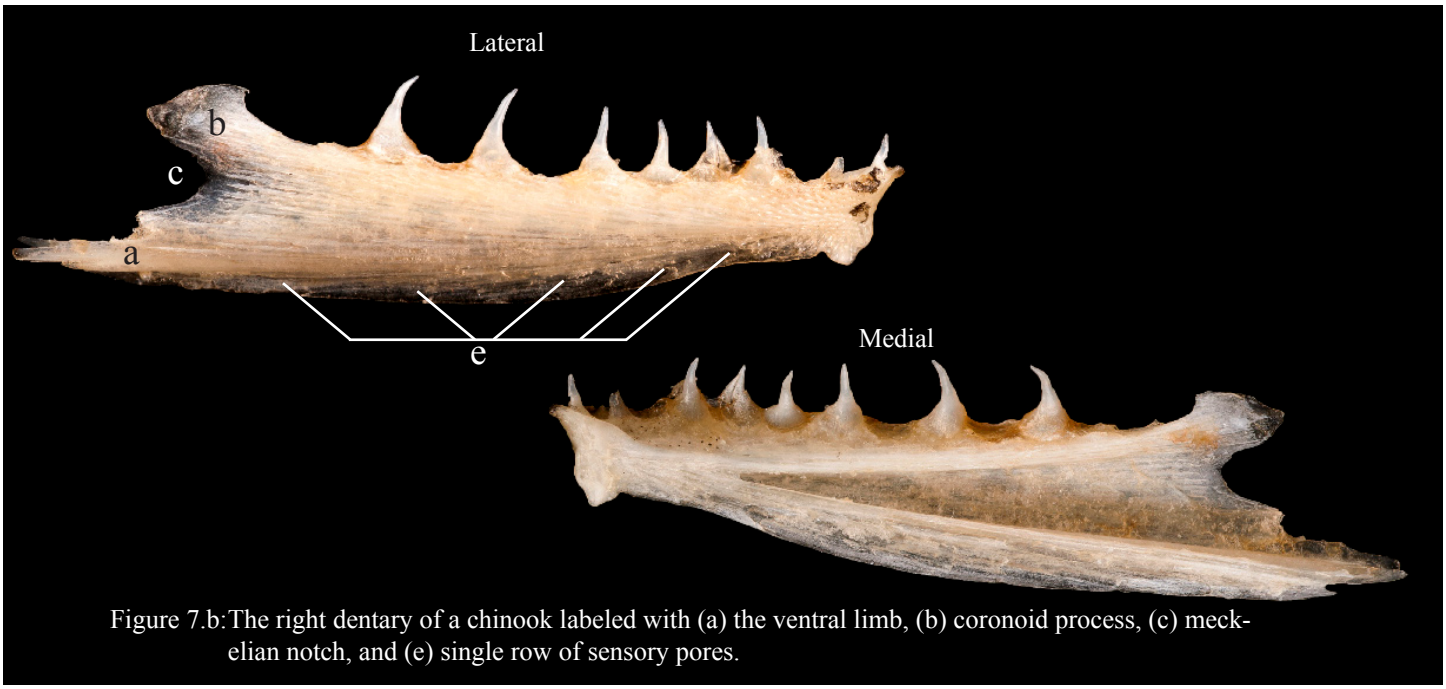

Figure 7.b: The right dentary of a chinook labeled with (a) the ventral limb, (b) coronoid process, (c) meckelian notch, and (e) single row of sensory pores.

8.a The ventral limb (a) is very wide and extends away from the mandibular symphysis in a strong ventral angle. Four to Five well defined major sensory pores (b) and two to four minor sensory pores (c) are visible on the lateral side of the ventral limb superior to the wide ventral shelf (d). The coronoid process is relatively small. A wide ventral shelf is present inferior to the ventral ridge (e)… **rainbow trout**

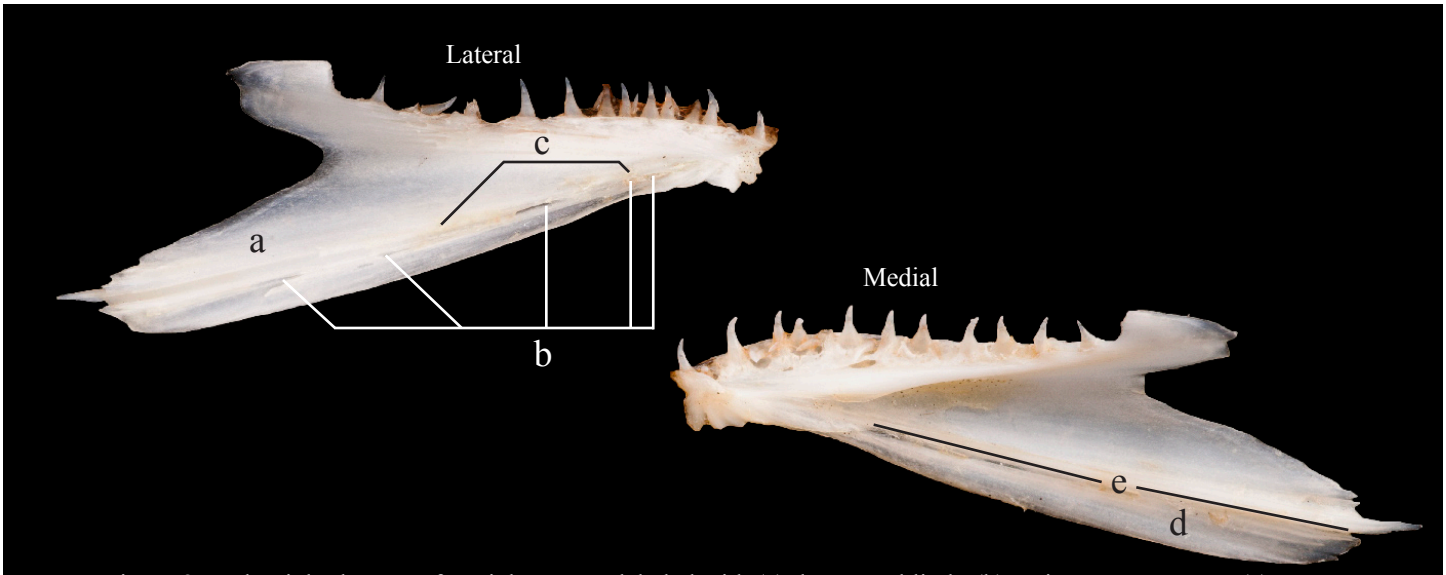

Figure 8.a: The right dentary of a rainbow trout labeled with (a) the ventral limb, (b) major sensory pores, (c) minor sensory pores, (d) ventral shelf, and (e) ventral ridge.

8.b The ventral limb (a) extends straight back. Five to six major sensory pores (b) and three to four minor sensory pores are located just along the ventral-lateral margin. A thin ventral shelf (d) runs along the ventral limb… **cutthroat trout**

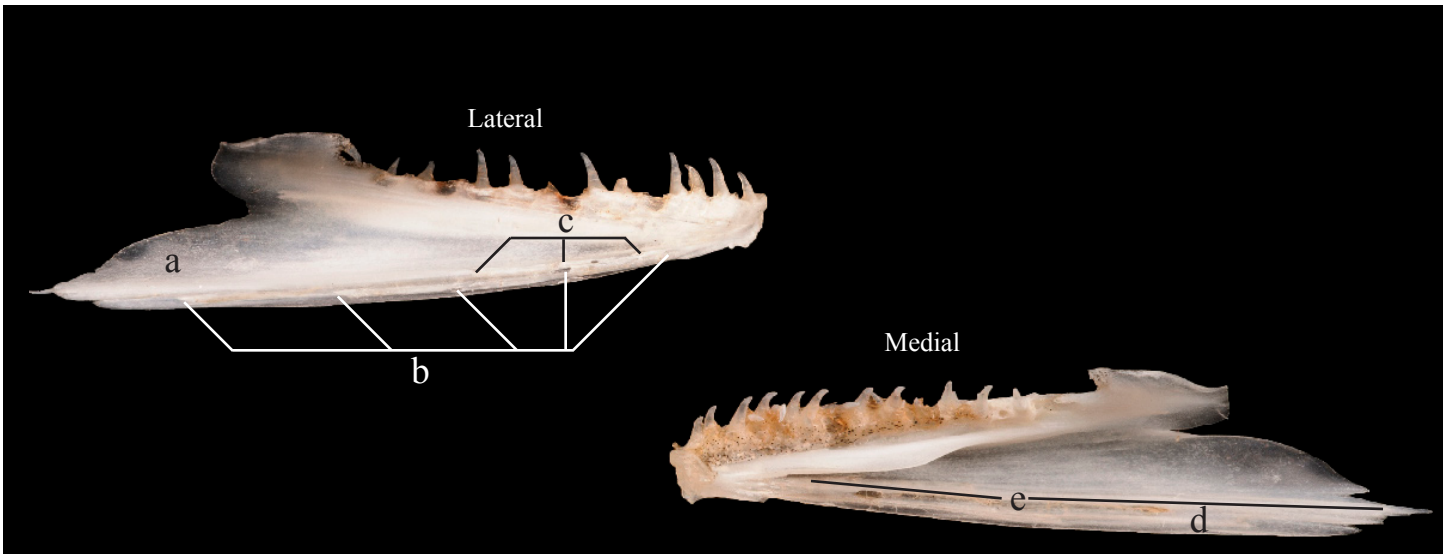

Figure 8.b:The right dentary of a cutthroat trout labeled with (a) the ventral limb, (b) major sensory pores, (c) minor sensory pores, (d) ventral shelf, and (e) ventral ridge.

1.a The dorso-posterior lobe (d) is large and has a more squared posterior margin. There is a small notch (e) inferior to the lateral prominence. The horizontal limb (f) is wide and connects to the vertical limb equal to or superior to where the dorso-posterior lobe ends… **mountain whitefish**

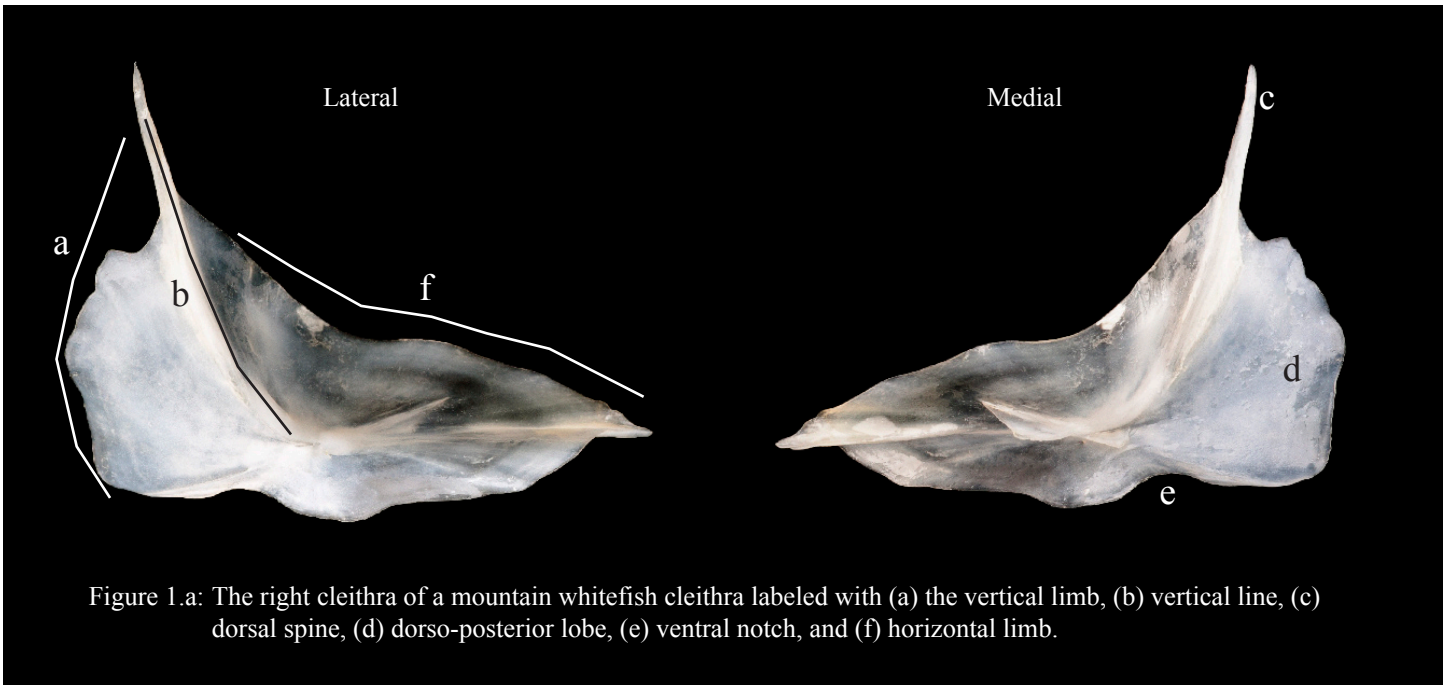

Figure 1.a: The right cleithra of a mountain whitefish cleithra labeled with (a) the vertical limb, (b) vertical line, (c) dorsal spine, (d) dorso-posterior lobe, (e) ventral notch, and (f) horizontal limb.

1.b The dorso-posterior lobe (d) is reduced in comparison to 1.a and has a more rounded posterior margin. A small notch (e) may or may not be present inferior to the lateral prominence. The horizontal limb (f) is not as wide and connects to the vertical limb (a) interior of where the dorso-posterior lobe ends… **go to 2**

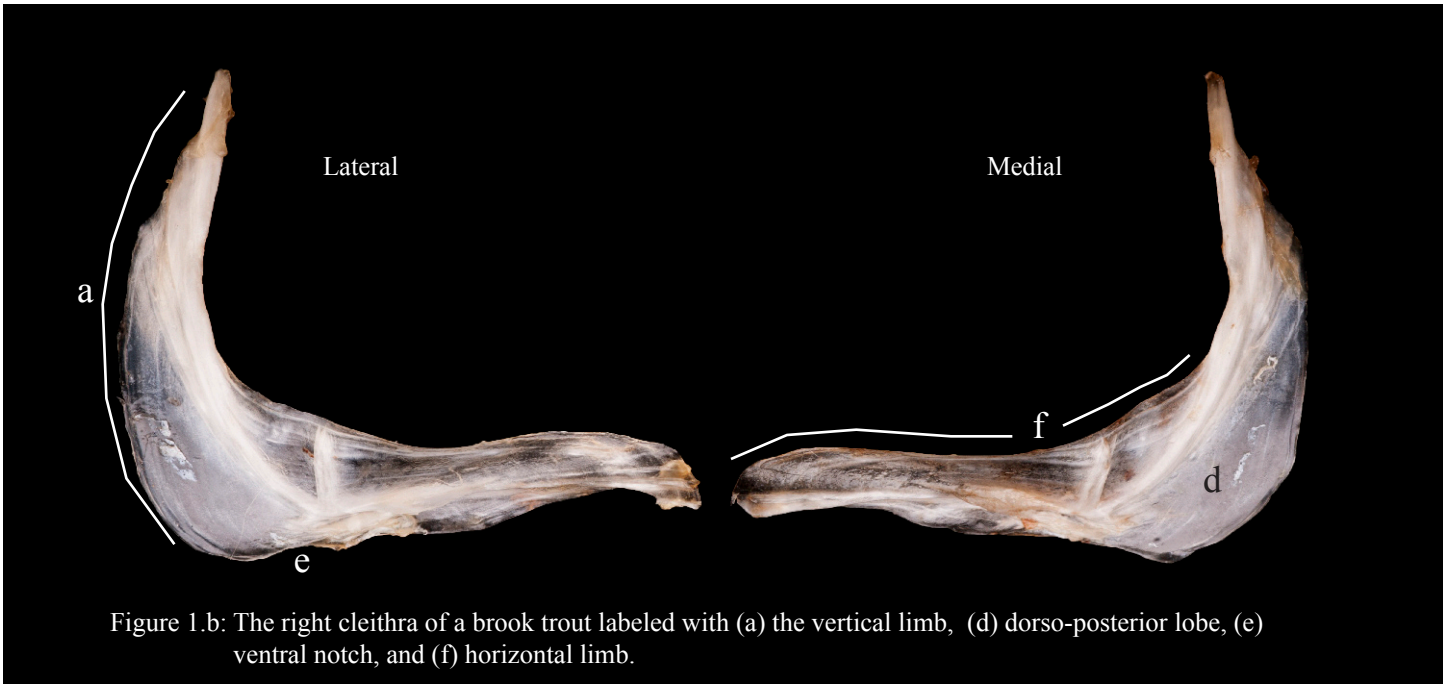

Figure 1.b: The right cleithra of a brook trout labeled with (a) the vertical limb, (d) dorso-posterior lobe, (e) ventral notch, and (f) horizontal limb.

2.a The horizontal limb (a) has a strong lateral curve. The lateral prominence is large and bulbous (b). A deeply cut horizontal sulcus (c) projects to a downward curved ventral tip (d). The dorsal lobe (e) follows the downward turned angle of the ventral tip and over hangs the anterior margin of the ventral lobe (f)… **brown trout**

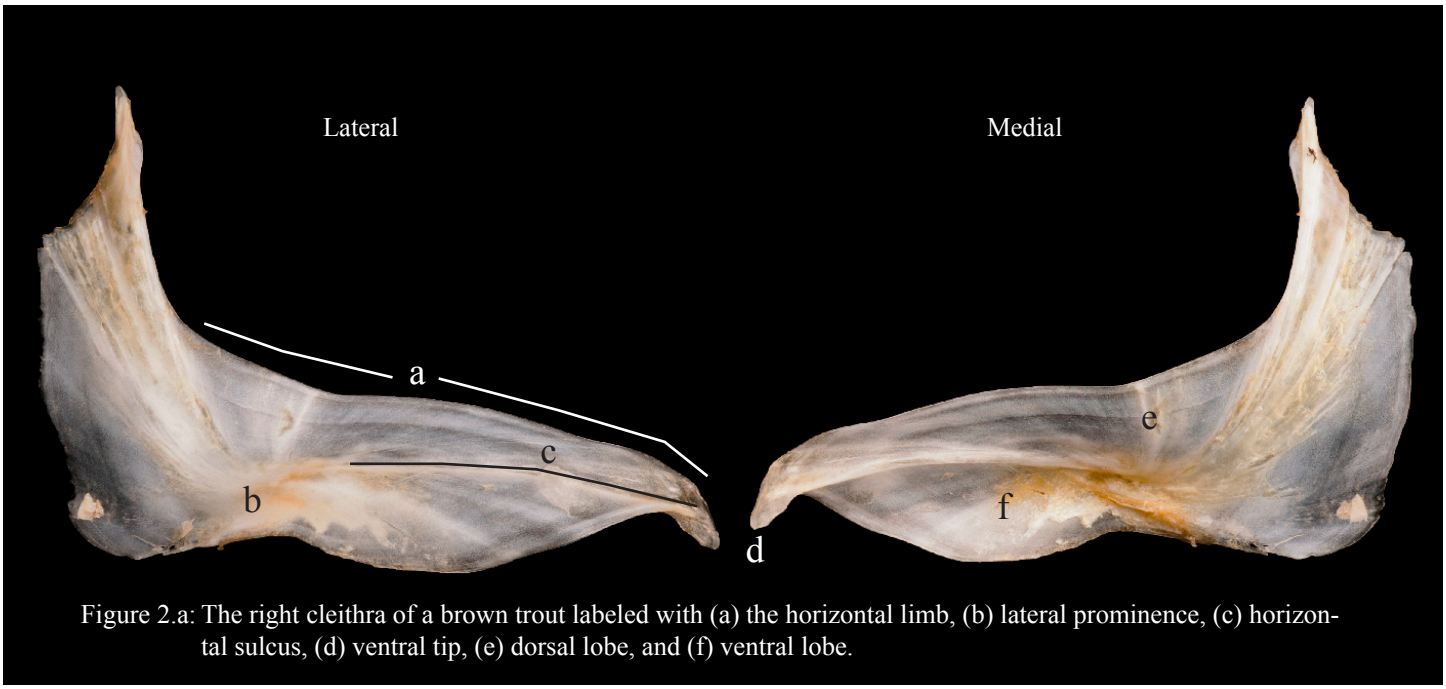

Figure 2.a: The right cleithra of a brown trout labeled with (a) the horizontal limb, (b) lateral prominence, (c) horizontal sulcus, (d) ventral tip, (e) dorsal lobe, and (f) ventral lobe.

2.b The horizontal limb (a) has a slight lateral curvature. The lateral prominence (b) is present but more subdued. The ventral tip (d) is either slightly down turned or projects straight out from the lateral prominence... **go to 3**

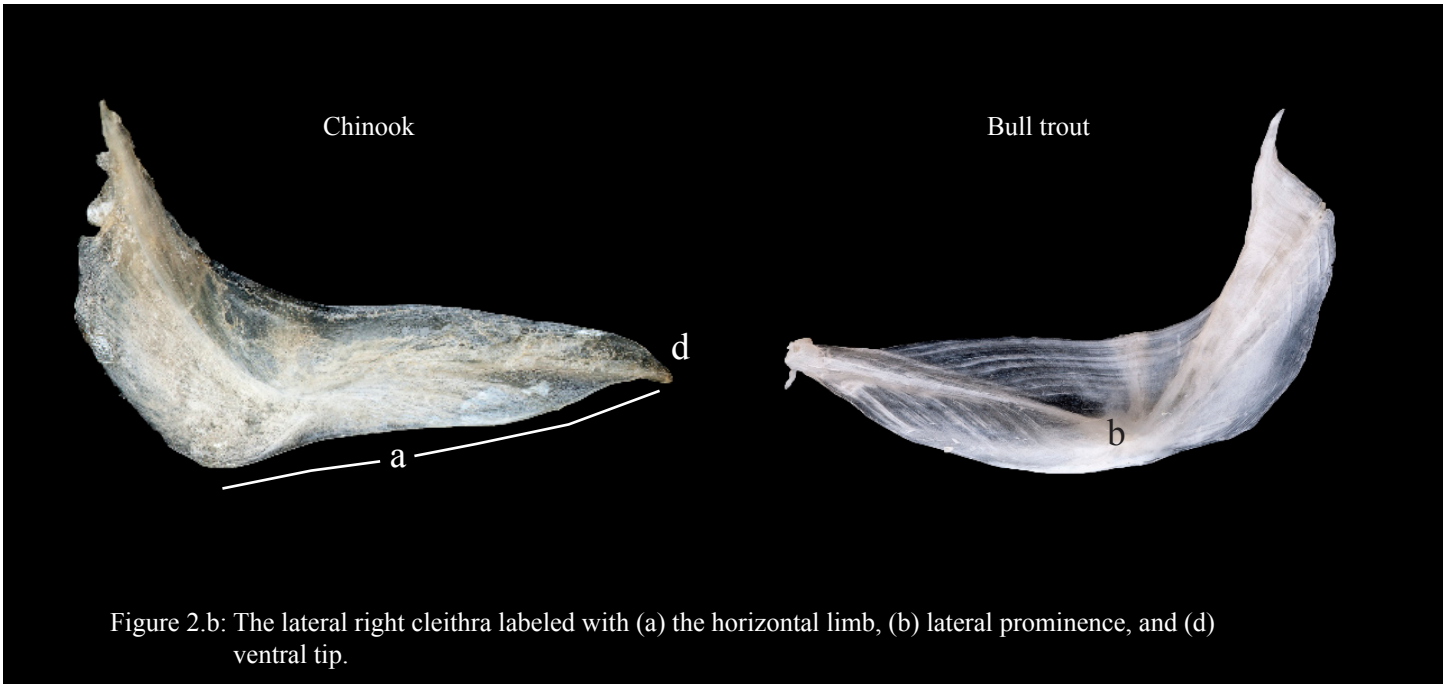

Figure 2.b: The lateral right cleithra labeled with (a) the horizontal limb, (b) lateral prominence, and (d) ventral tip.

3.a As the vertical line (a) transitions to the dorsal spine (b), it projects forward giving the vertical line a more curved appearance. The medial process (c) is relatively small and generally does not progress to the dorso-anterior margin... **go to 4**

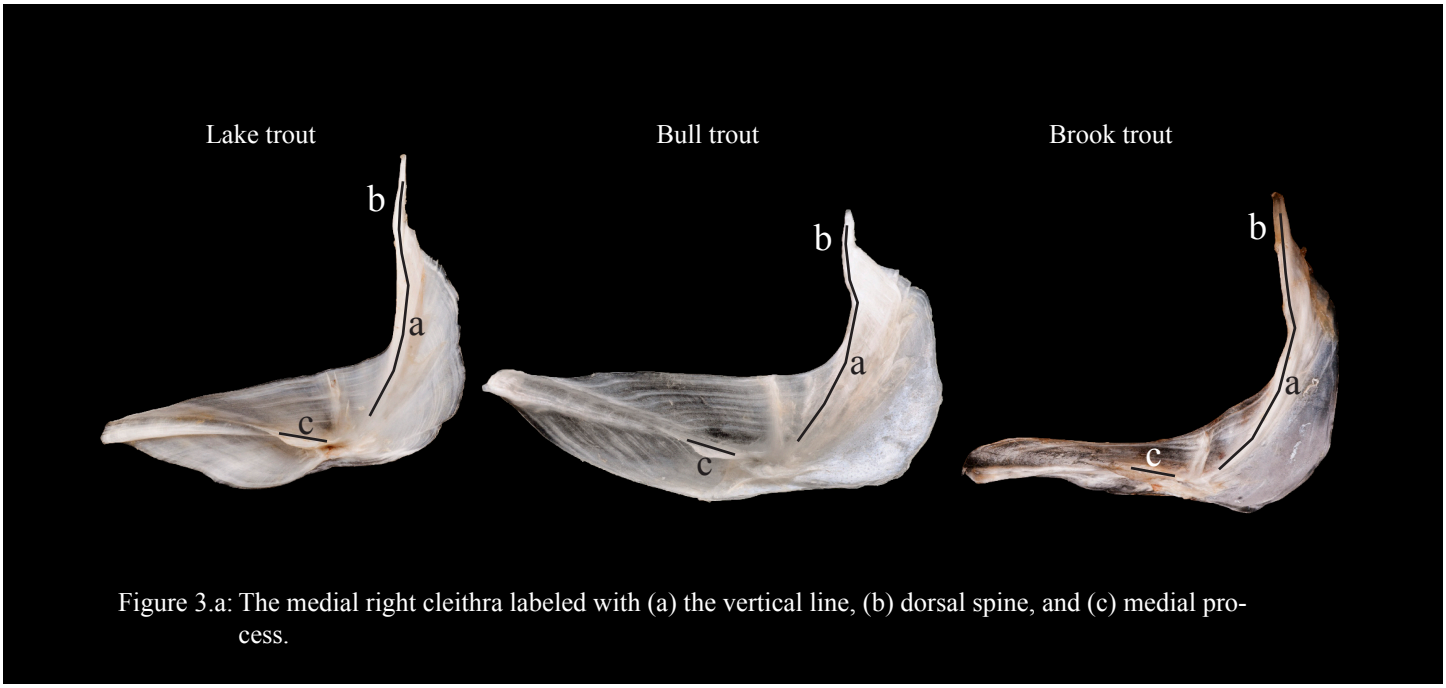

Figure 3.a: The medial right cleithra labeled with (a) the vertical line, (b) dorsal spine, and (c) medial process.

3.b The vertical line (a) generally maintains one continuous and straight anterior margin that transitions smoothly into the dorsal spine. The medial prominence is long and often progresses out from the medial side of the lateral prominence to the dorso-anterior margin of the horizontal limb... **go to 6**

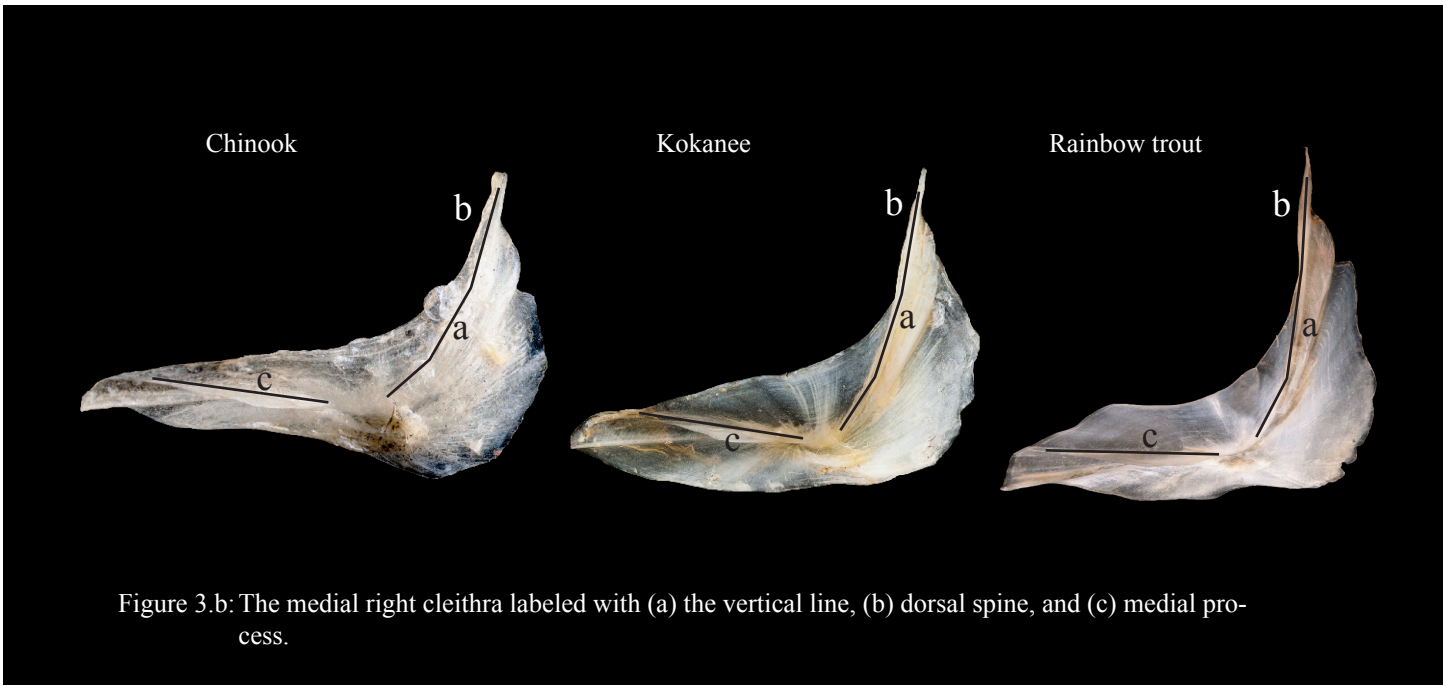

Figure 3.b: The medial right cleithra labeled with (a) the vertical line, (b) dorsal spine, and (c) medial process.

4.a The dorso-posterior lobe (a) is wide with a rounded posterior margin. The dorsal (b) and ventral lobe (c) are wide and separated by a horizontal line (d) and sulcus (e) that extend at an upturned angle. The ventral tip is squared (f)… **bull trout**

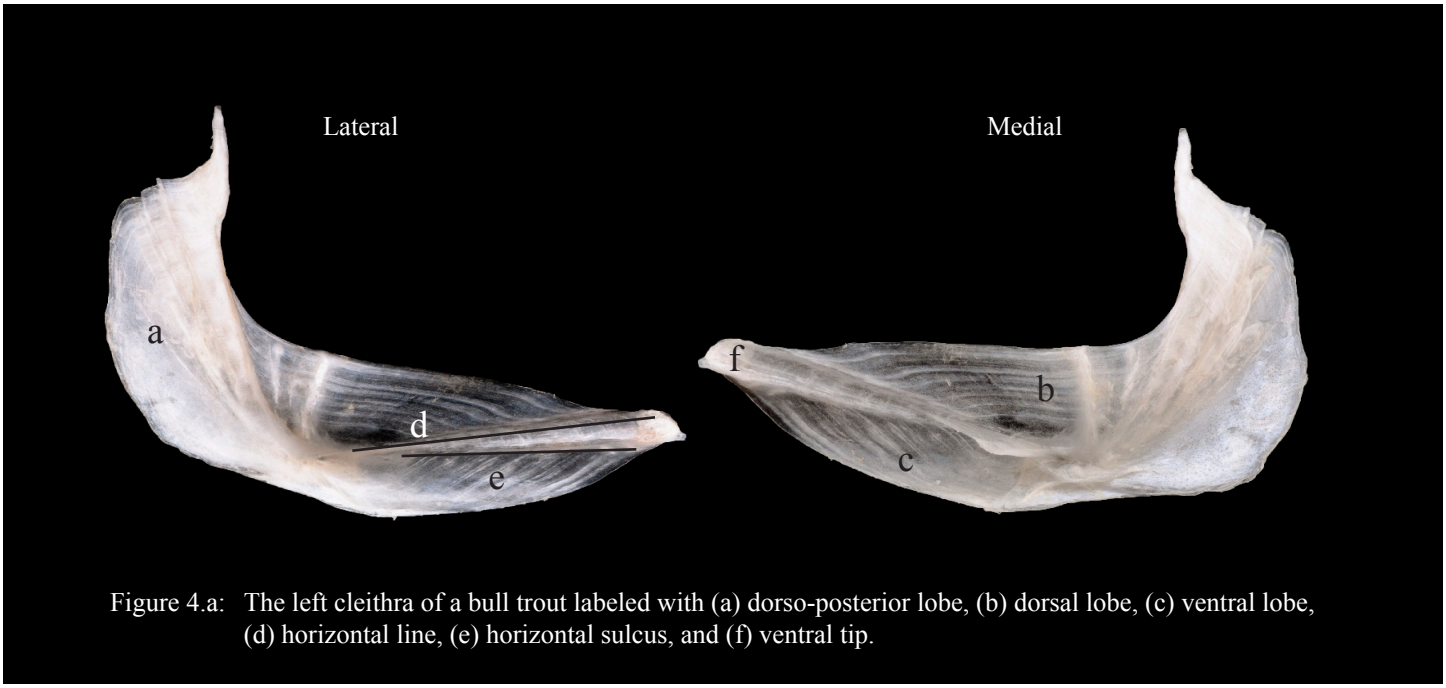

Figure 4.a: The left cleithra of a bull trout labeled with (a) dorso-posterior lobe, (b) dorsal lobe, (c) ventral lobe, (d) horizontal line, (e) horizontal sulcus, and (f) ventral tip.

4.b The dorso-posterior lobe (a) remains relatively thin. The horizontal line (d) has a slight down turned curvature and ends at a ventral tip (f) that points anterio-ventral to the remainder of the cleithra… **go to 5**

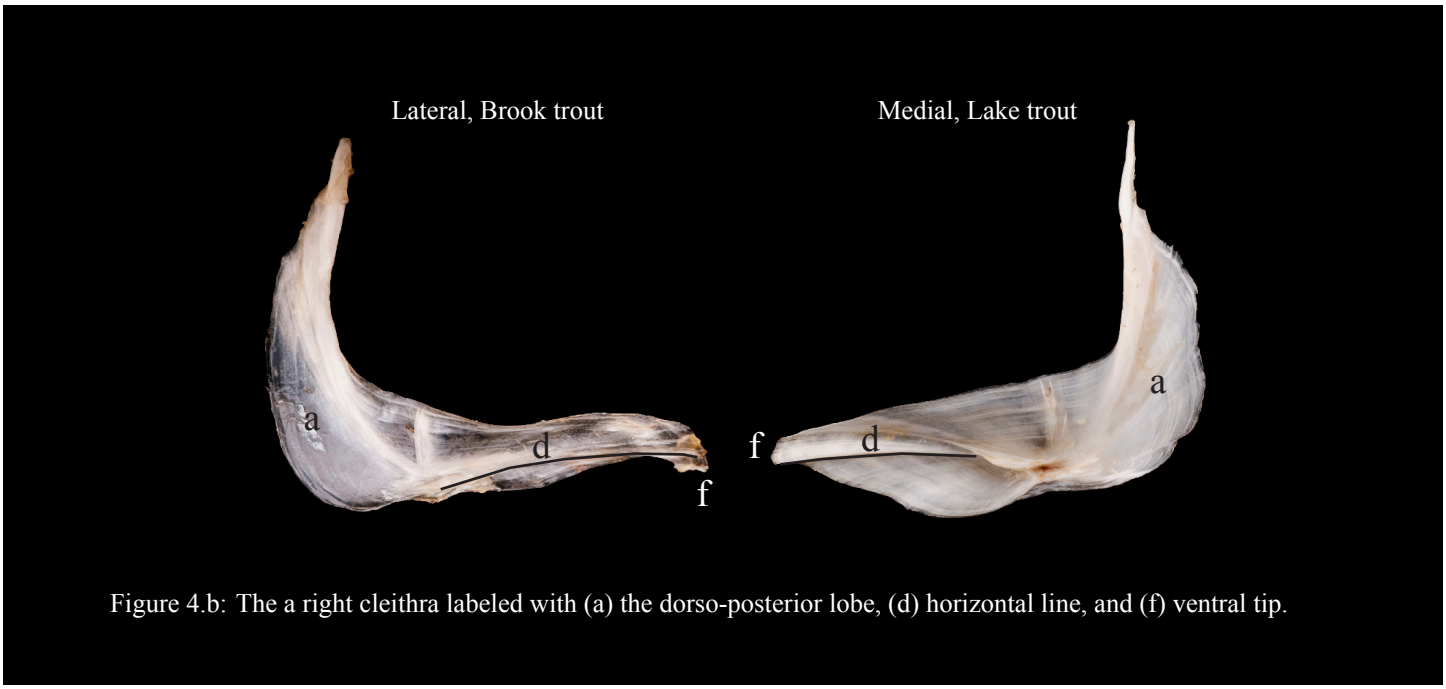

Figure 4.b: The a right cleithra labeled with (a) the dorso-posterior lobe, (d) horizontal line, and (f) ventral tip.

5.a The ventral (a) and dorsal (b) lobes of the horizontal limb are thin. The horizontal limb has a slight lateral curve and ends at a rounded ventral tip (c). The entire vertical limb (d) makes a gentle posterior bow that scoops laterally as it approaches the lateral prominence (e). The dorso-posterior lobe (f) is thin… **brook trout**

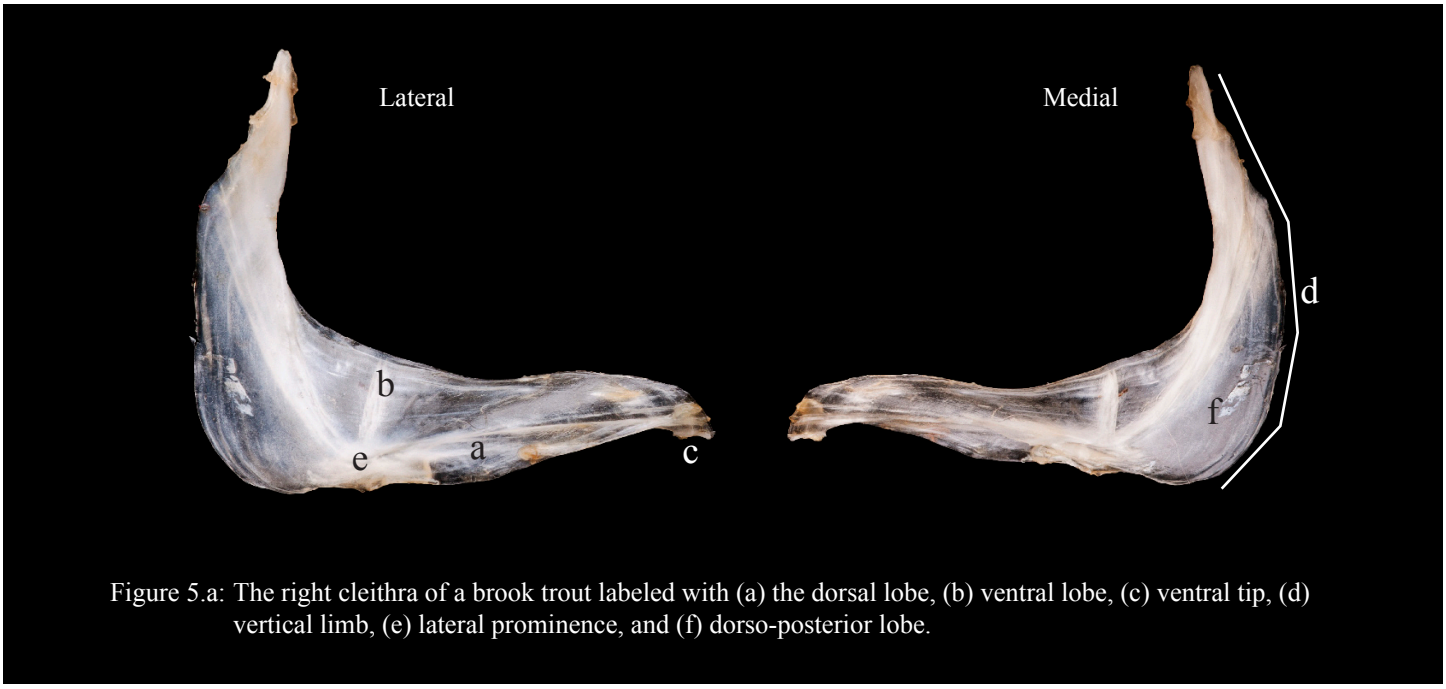

Figure 5.a: The right cleithra of a brook trout labeled with (a) the dorsal lobe, (b) ventral lobe, (c) ventral tip, (d) vertical limb, (e) lateral prominence, and (f) dorso-posterior lobe.

5.b On the horizontal limb, the ventral lobe (a) is noticeably wider then the dorsal lobe (b). The horizontal limb (f) is greatly curved laterally and ends at a pointed ventral tip (c). A prominent and long dorsal spine (g) projects upward away from the dorso-posterior lobe… **lake trout**

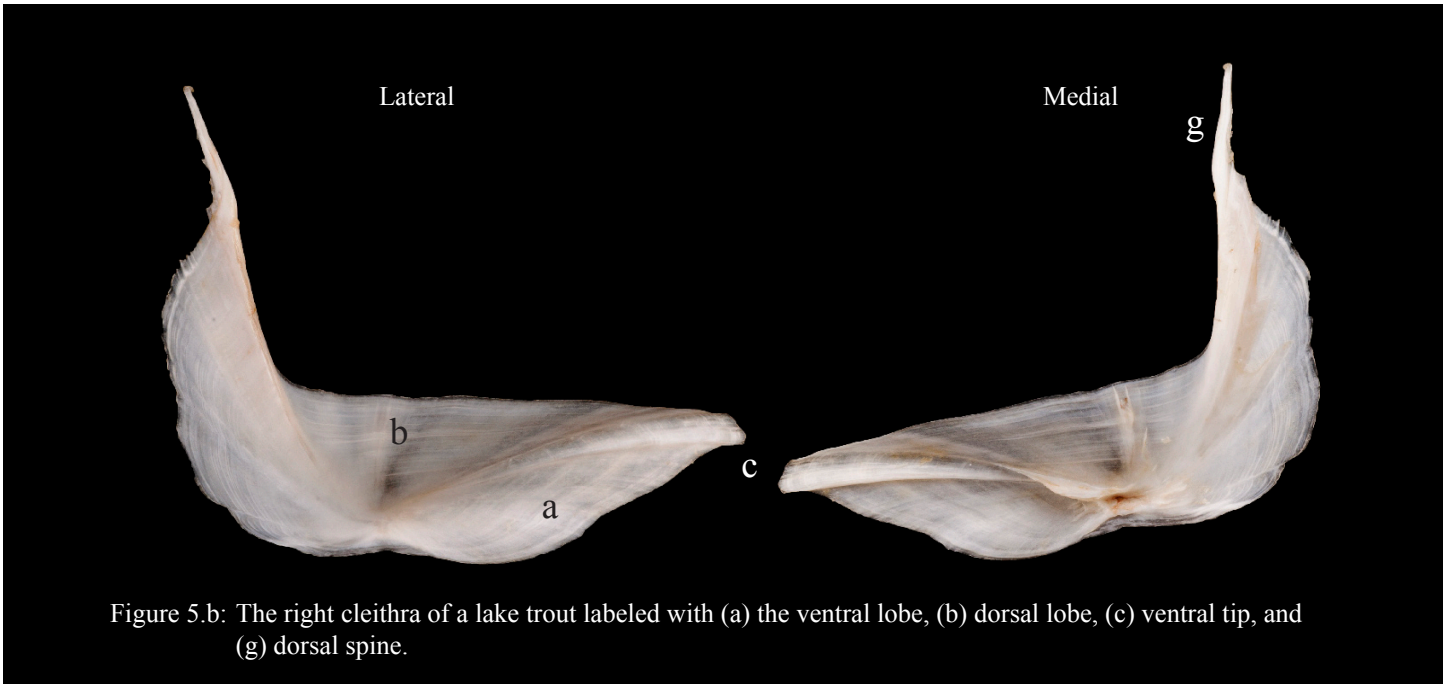

Figure 5.b: The right cleithra of a lake trout labeled with (a) the ventral lobe, (b) dorsal lobe, (c) ventral tip, and (g) dorsal spine.

6.a The majority of the dorso-posterior lobe's (a) medial side maintains numerous striations that progress back from the lateral prominence and vertical line towards the posterior margin... **go to 7**

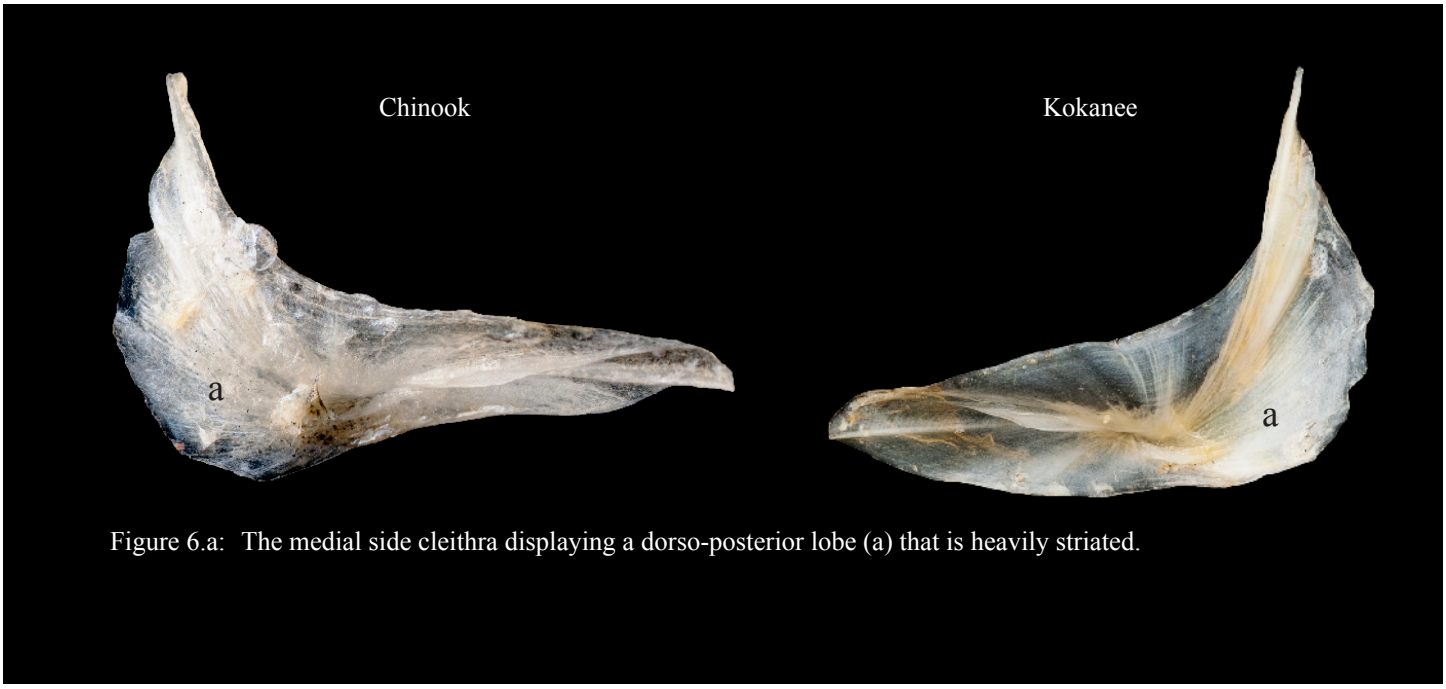

Figure 6.a: The medial side cleithra displaying a dorso-posterior lobe (a) that is heavily striated.

6.b Apart from a few striations near the vertical line (b) the medial side of the dorso-posterior lobe (a) is relatively smooth in most individuals. If striations on the dorso-posterior lobe are found projecting back from the medial side of the lateral prominence they are relatively minor, only occupying the area of the dorso-posterior lobe directly posterior to the lateral prominence... **go to 8**

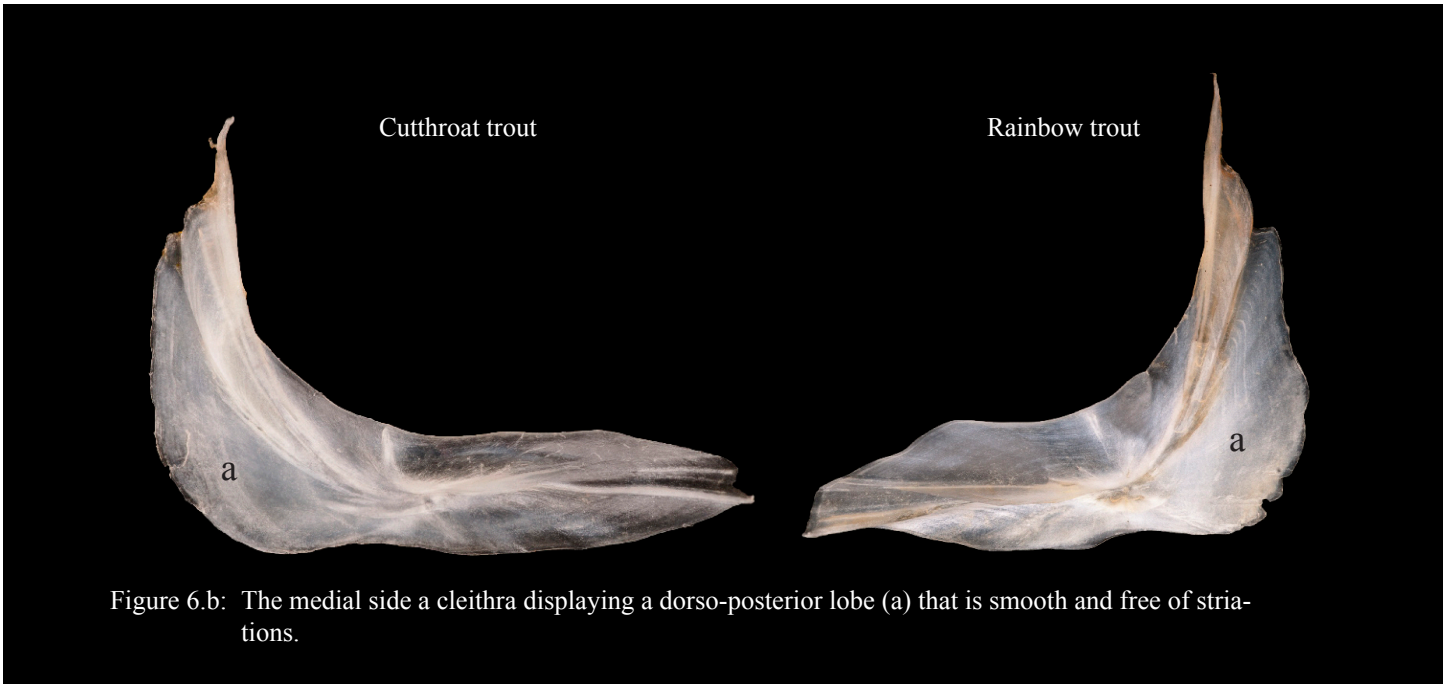

Figure 6.b: The medial side a cleithra displaying a dorso-posterior lobe (a) that is smooth and free of striations.

7.a The horizontal line (a) and horizontal sulcus (b) mirror each other in a gentle downward slope towards a pointed ventral tip (c). The ventral margin of the dorso-posterior lobe (d) and ventral lobe (e) have a slight lateral curve. The ventral lobe ends short of the ventral tip and dorsal lobe (f)… **Chinook**

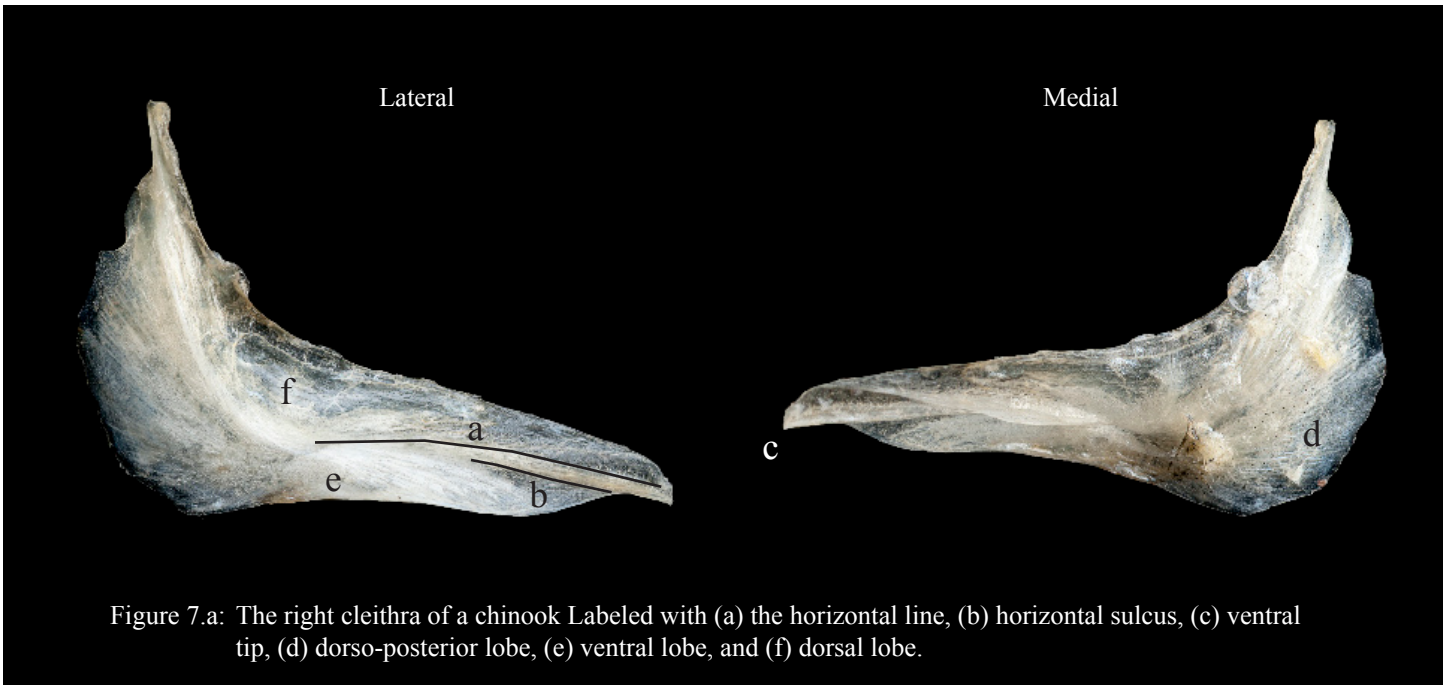

Figure 7.a: The right cleithra of a chinook Labeled with (a) the horizontal line, (b) horizontal sulcus, (c) ventral tip, (d) dorso-posterior lobe, (e) ventral lobe, and (f) dorsal lobe.

7.b The horizontal line (a) and sulcus (b) deviate from each other as they project strait towards the anterior margin. The wide ventral lobe (e) gently wraps into a cylindrical structure and that extends all the way to the ventral tip (c). The dorsal lobe (f) creates a triangular shape that fuses midway up the vertical line (g)… **kokanee**

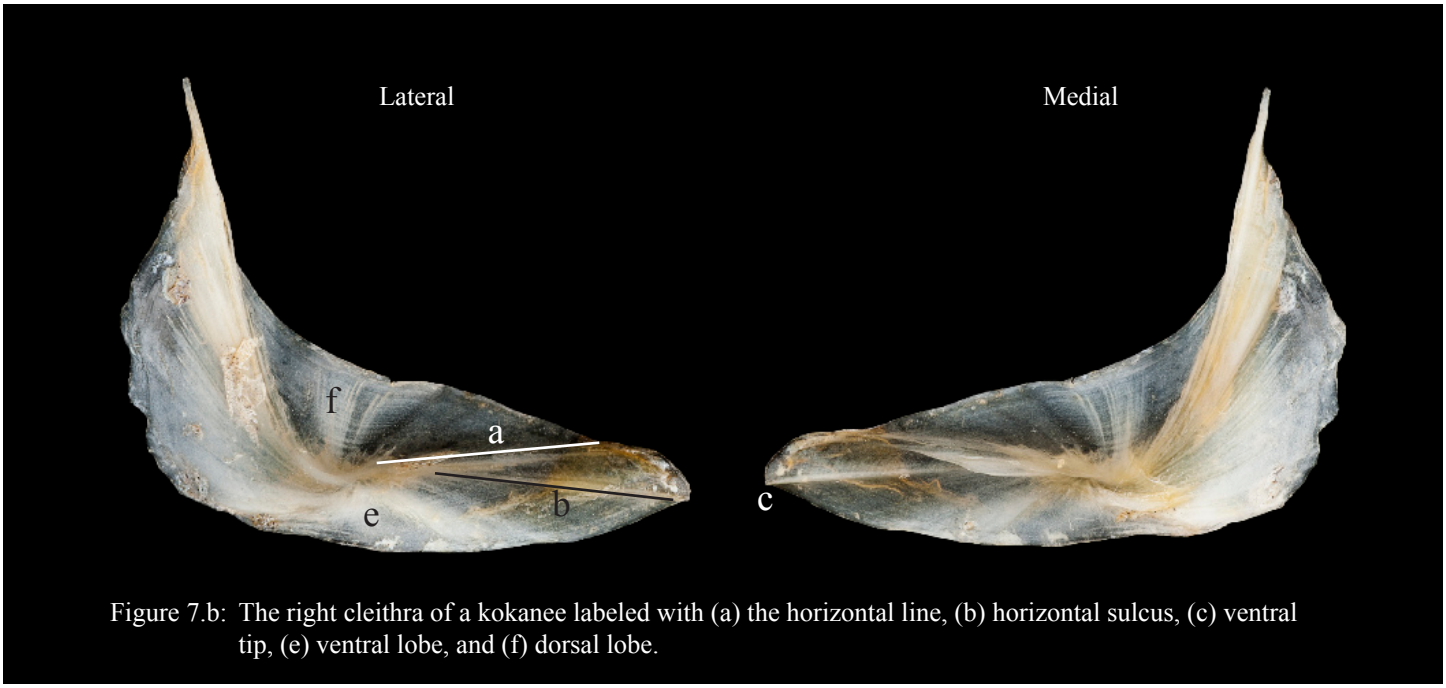

Figure 7.b: The right cleithra of a kokanee labeled with (a) the horizontal line, (b) horizontal sulcus, (c) ventral tip, (e) ventral lobe, and (f) dorsal lobe.

8.a The vertical line (a) extends straight up from the lateral prominence (b). The horizontal limb (c) and vertical limb (d) maintain similar lengths. The horizontal line (e) projects straight out from the lateral prominence. The horizontal sulcus (f) has a slight ventral curve as it projects to the ventral tip (g)… **rainbow trout**

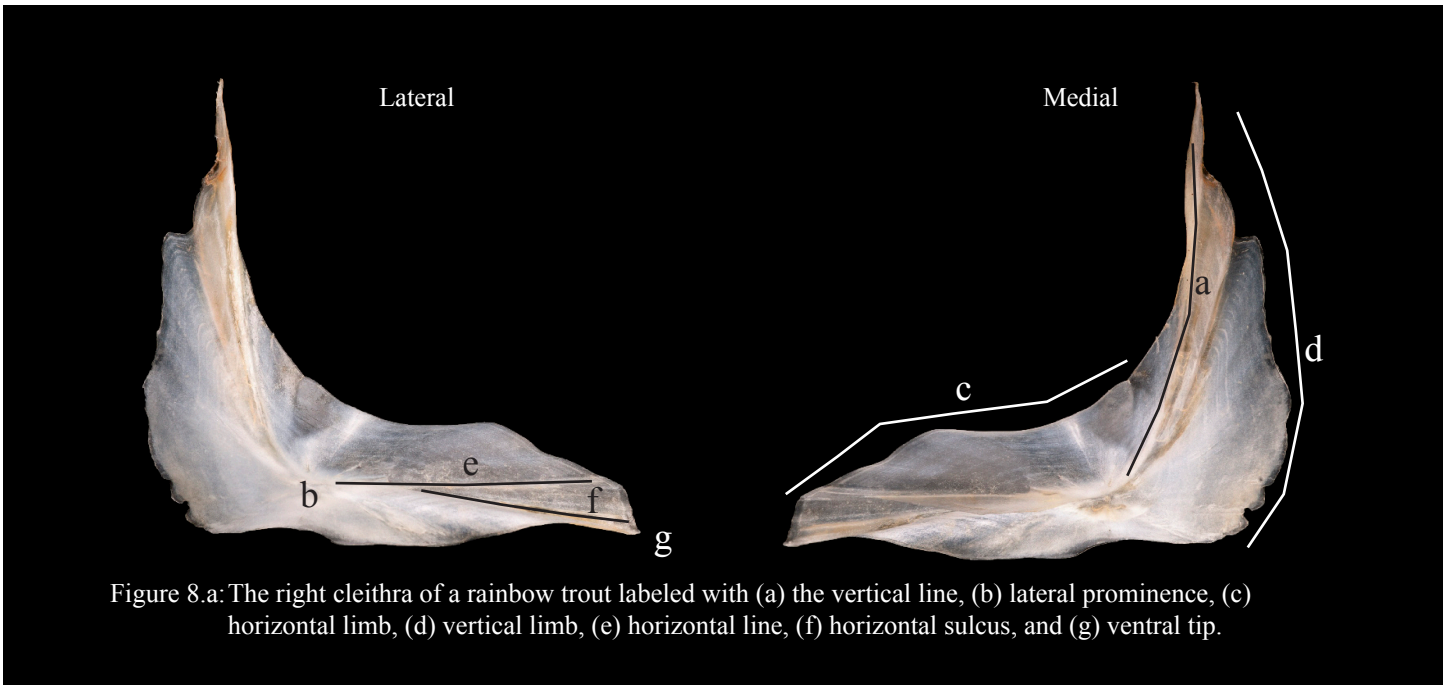

Figure 8.a: The right cleithra of a rainbow trout labeled with (a) the vertical line, (b) lateral prominence, (c) horizontal limb, (d) vertical limb, (e) horizontal line, (f) horizontal sulcus, and (g) ventral tip.

8.b The vertical line (a) extends up for the lateral prominence in a posterior angle. The horizontal limb (c) appears longer then the vertical limb (d). Both the horizontal line (g) and sulcus (h) maintain a slight ventral curvature as they project from the lateral prominence (b) to the ventral tip (j)… **cutthroat trout**

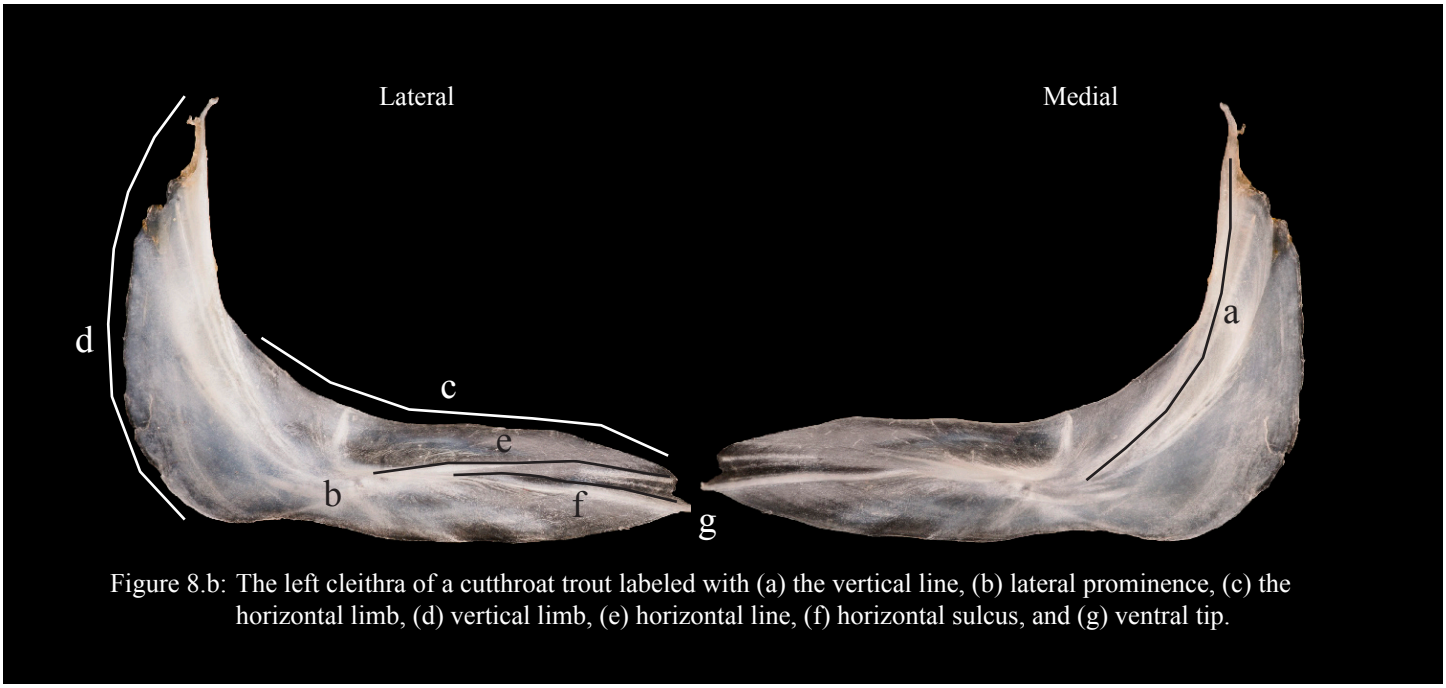

Figure 8.b: The left cleithra of a cutthroat trout labeled with (a) the vertical line, (b) lateral prominence, (c) the horizontal limb, (d) vertical limb, (e) horizontal line, (f) horizontal sulcus, and (g) ventral tip.

1.a The preopercle has an L shaped appearance. The horizontal limb (a) projects far forward into a pointed retroarticular joint (b). The quadrate ridge (c) projects all the way to the furthest anterio-ventral point of the retroarticular joint… **mountain whitefish**

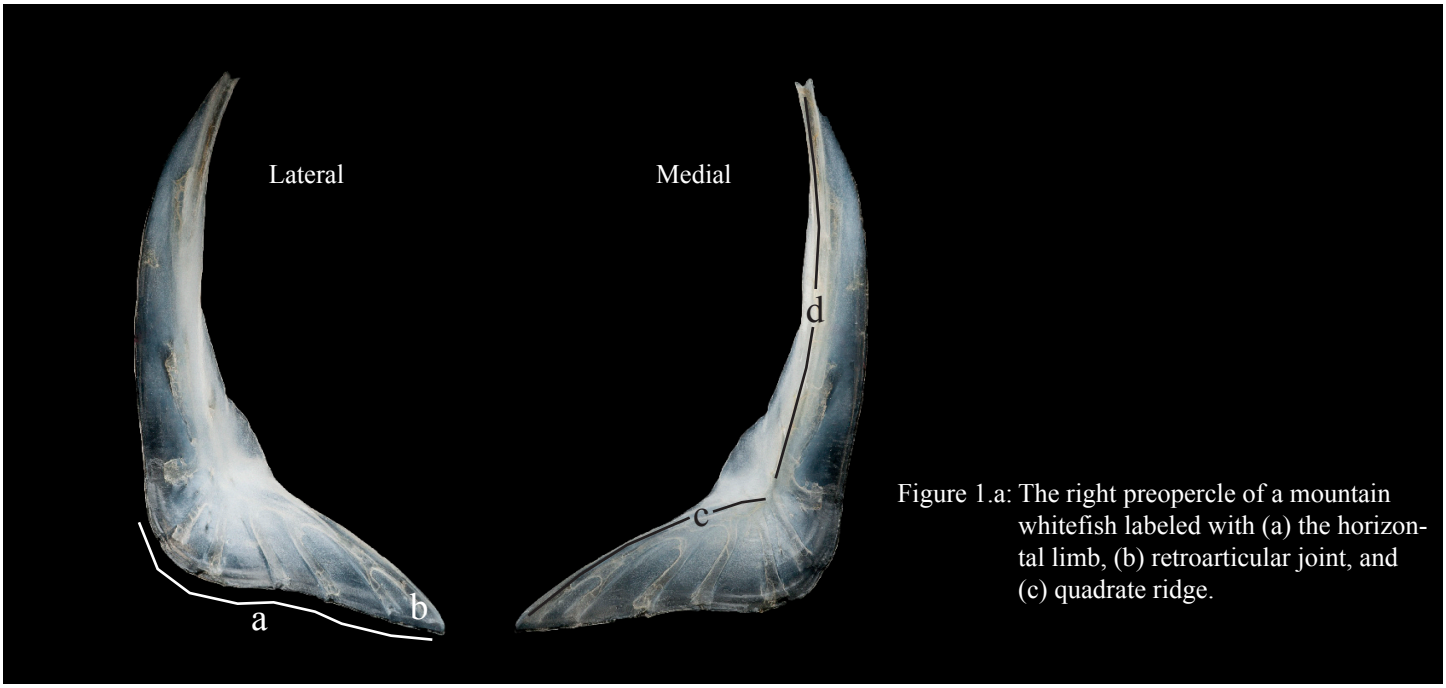

Figure 1.a: The right preopercle of a mountain whitefish labeled with (a) the horizontal limb, (b) retroarticular joint, and (c) quadrate ridge.

1.b The preopercle has more of a crescent shaped appearance. The horizontal limb (a) is short and ends in a round, blunted or minimally pointed retroarticular joint (b). The quadrate ridge (c) may progress to the furthest anterior margin of the horizontal limb yet the osseous membrane of the posterior wing extends further ventrally of where the quadrate ridge ends… **go to 2**

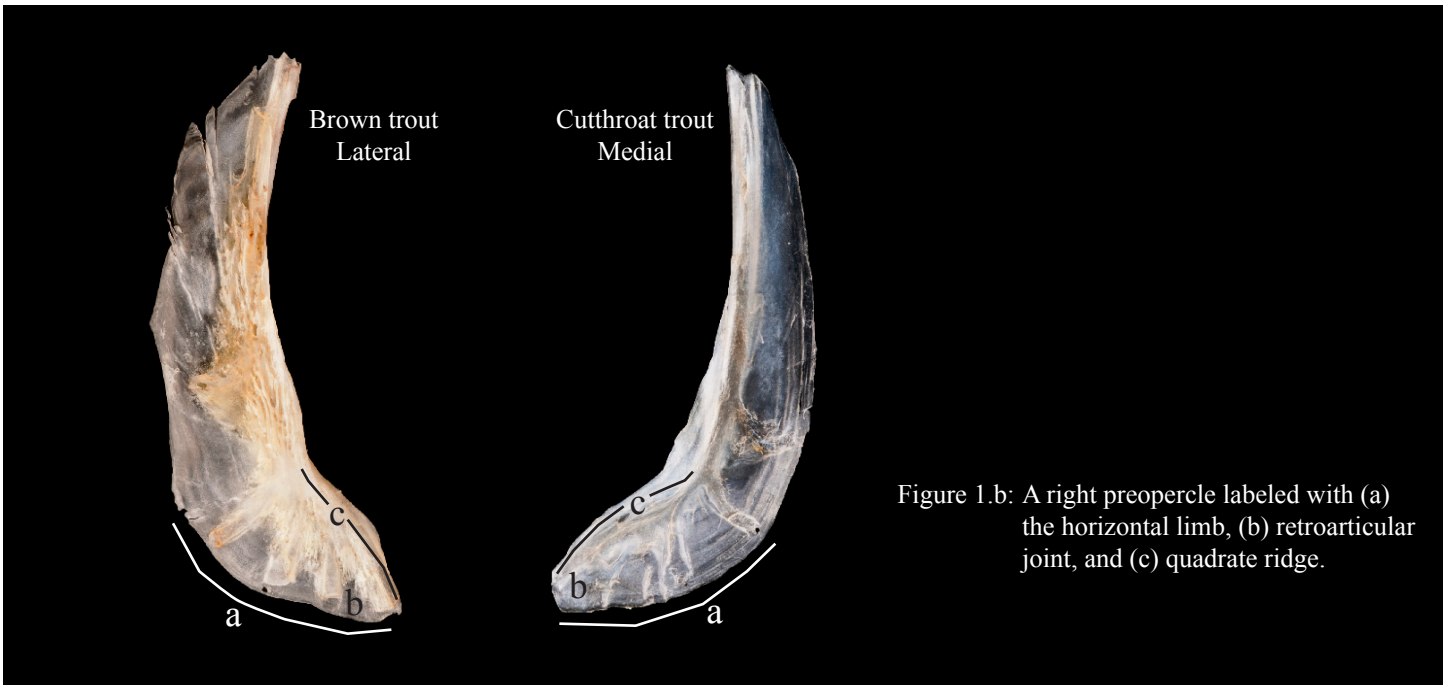

Figure 1.b: A right preopercle labeled with (a) the horizontal limb, (b) retroarticular joint, and (c) quadrate ridge.

2.a The hypomandibular ridge (a) leaves the quadrate ridge in a slight medial bow. The dorsal tip (b) points laterally. Four ventrally protruding sensory pores and canals (c) are present... **go to 3**

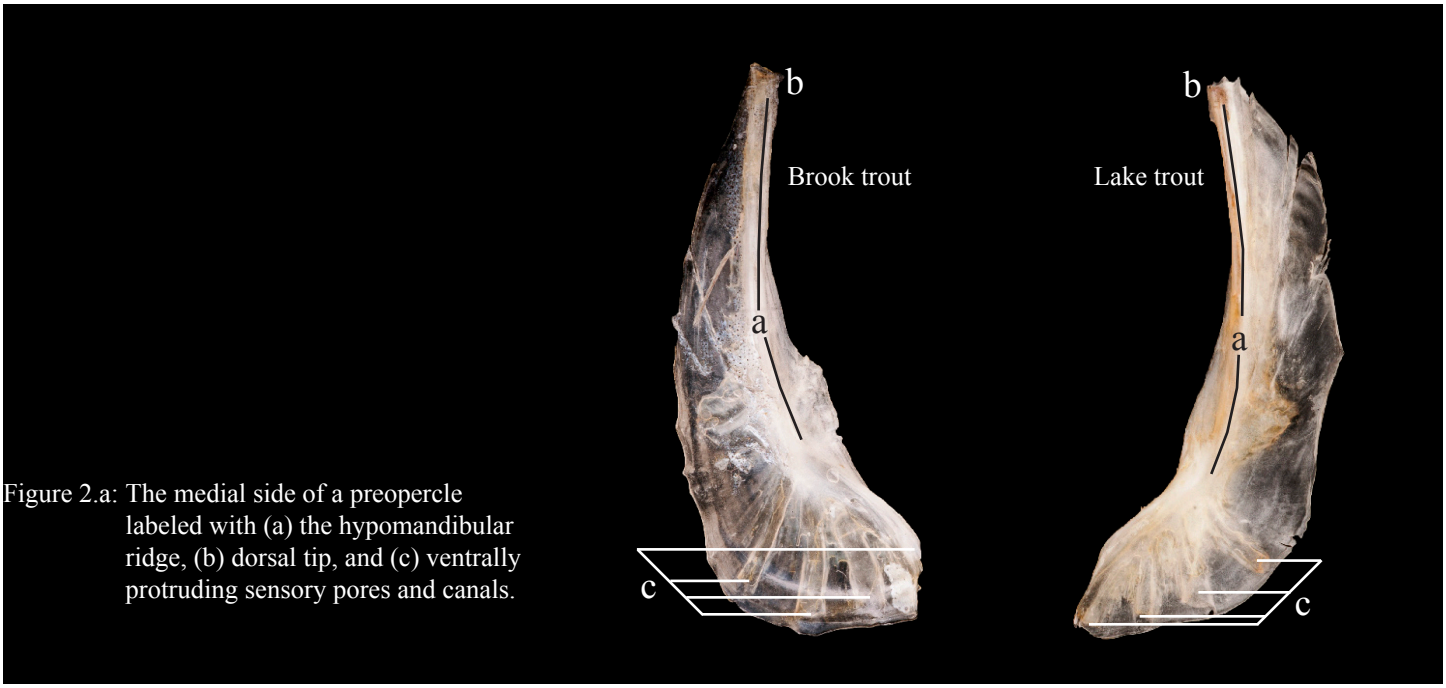

Figure 2.a: The medial side of a preopercle labeled with (a) the hypomandibular ridge, (b) dorsal tip, and (c) ventrally protruding sensory pores and canals.

2.b The hypomandibular ridge (a) leaves the quadrate ridge with a slight lateral, or no bowing at all. The dorsal tip (b) points directly dorsally or slightly medial. Five to six ventrally projecting sensory pores and canals (c) are present... **go to 6**

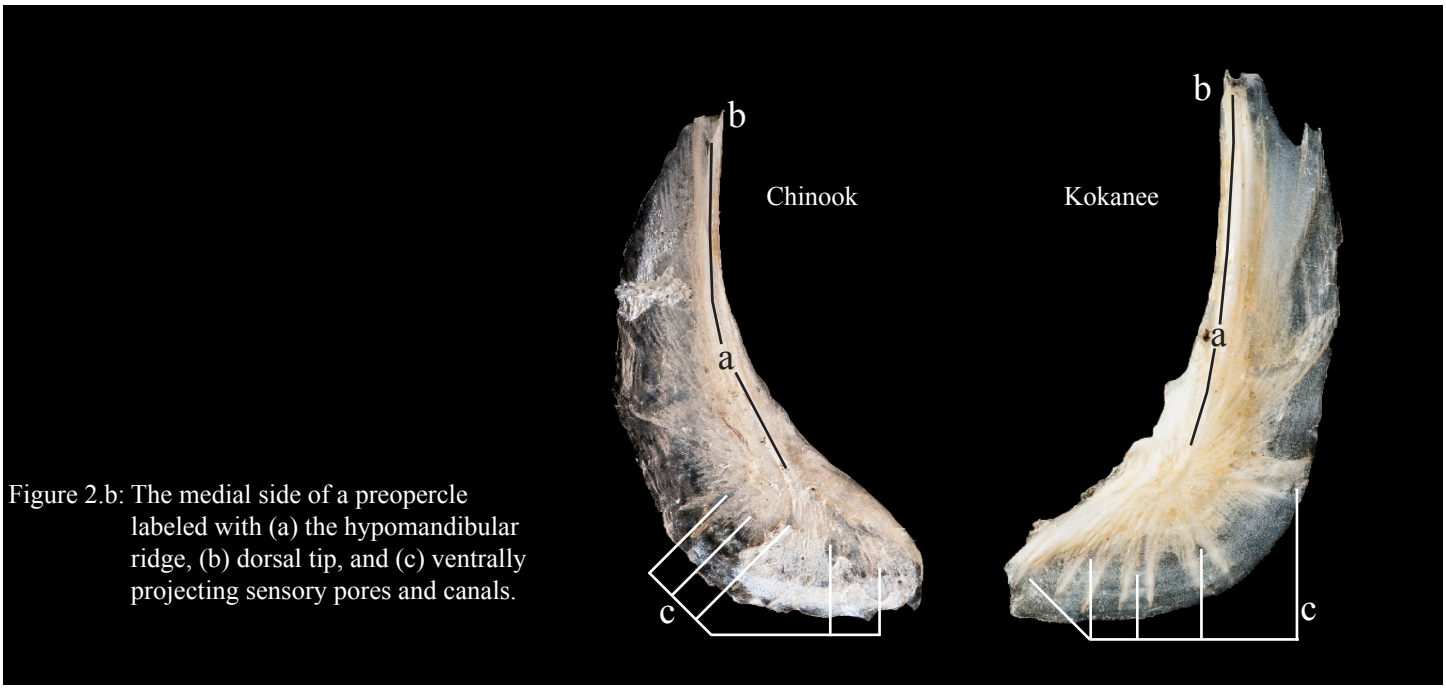

Figure 2.b: The medial side of a preopercle labeled with (a) the hypomandibular ridge, (b) dorsal tip, and (c) ventrally projecting sensory pores and canals.

3.a The horizontal limb (a) is very short and sits low on the preopercular body. There is a cluster of at least five sensory pore openings (b), each on the end of a small sensory canal that extends dorsally along the lateral side of the hyopmandibular ridge (c). Four ventrally extending sensory canals and pores (d) extend off the lateral side of the quadrate ridge (e) … **brown trout**

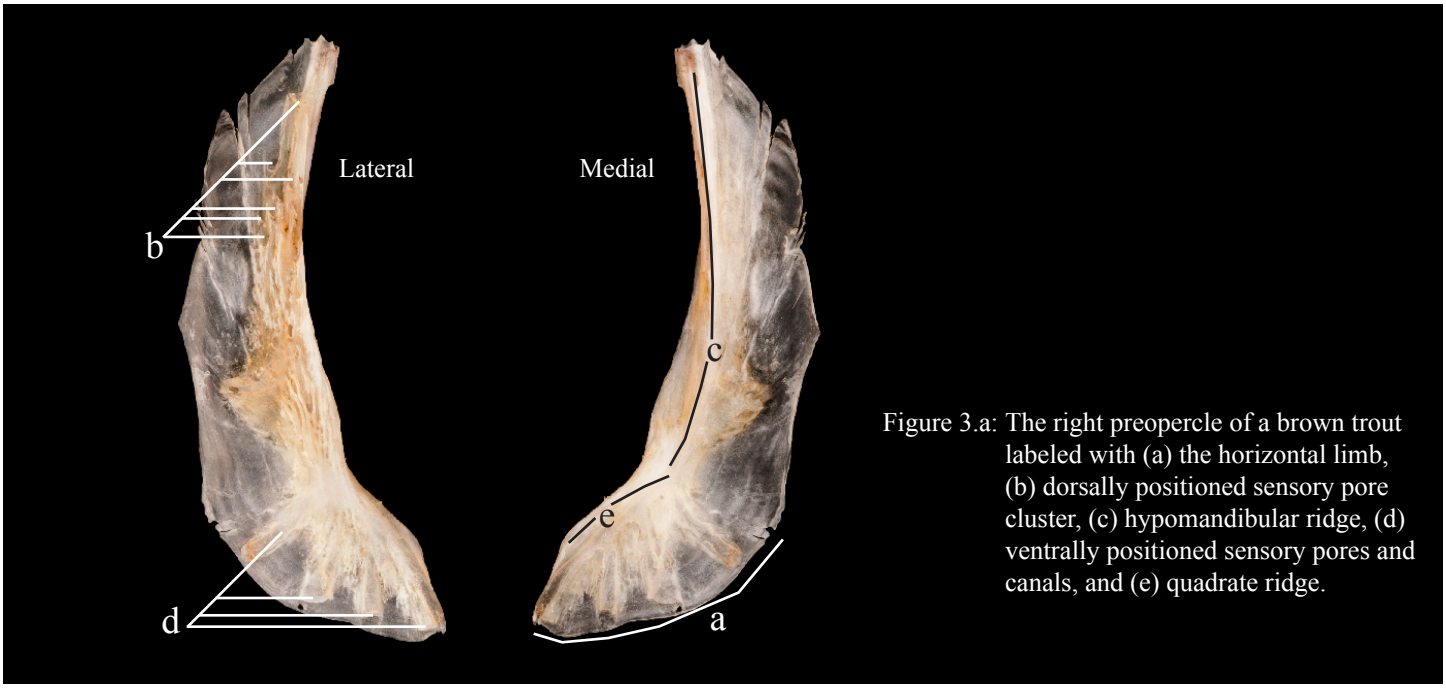

Figure 3.a: The right preopercle of a brown trout labeled with (a) the horizontal limb, (b) dorsally positioned sensory pore cluster, (c) hypomandibular ridge, (d) ventrally positioned sensory pores and canals, and (e) quadrate ridge.

3.b The horizontal limb (a) is longer than seen above and sits higher up on the preopercular body. There is no clustering of the dorsally protruding sensory pores. Four sensory pores and canals (d) extend ventrally from the quadrate ridge (e) and a single sensory pore and canal (f) extend either dorso-posteriorly or dorsally away from the hypomandibular ridge (c)... **go to 4**

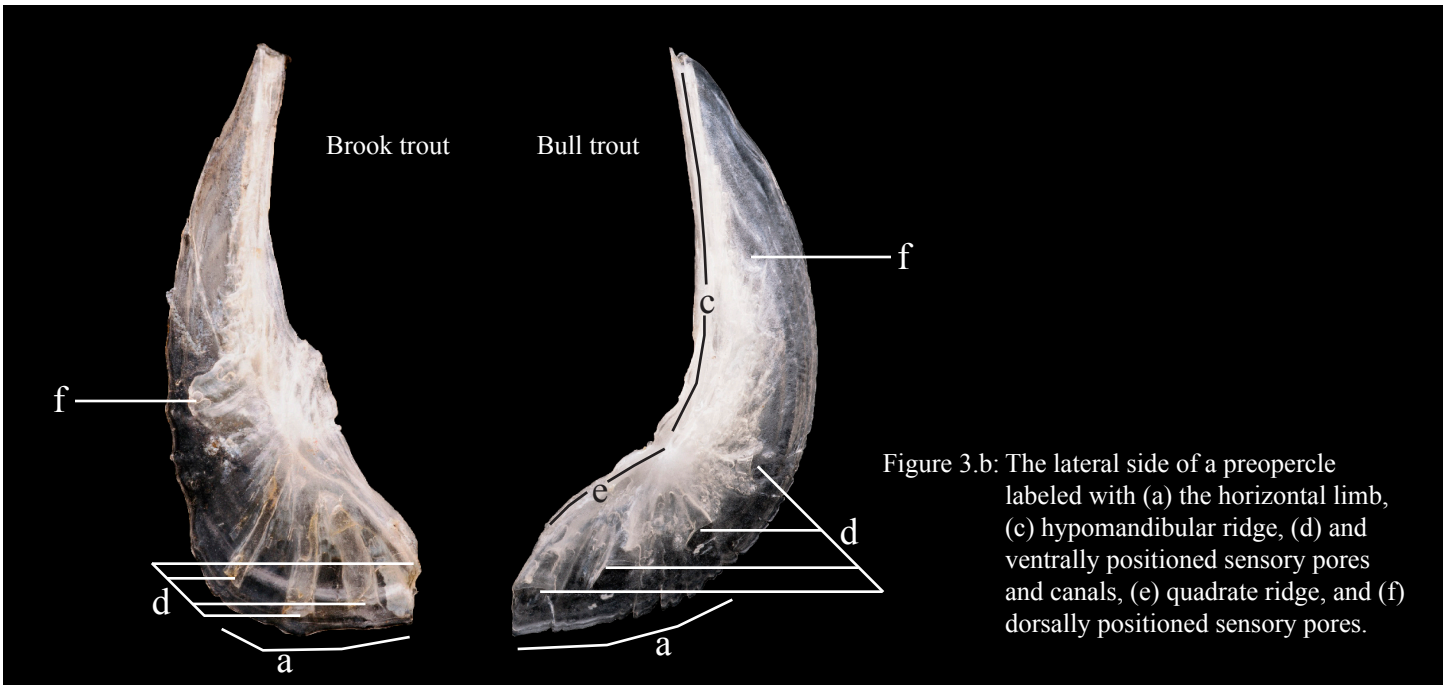

Figure 3.b: The lateral side of a preopercle labeled with (a) the horizontal limb, (c) hypomandibular ridge, (d) and ventrally positioned sensory pores and canals, (e) quadrate ridge, and (f) dorsally positioned sensory pores.

4.a The posterior wing (a) narrows considerably as it progresses up the vertical limb. One dorsally projecting (b) and four ventrally projecting (c) sensory pores are present. These pores may be located on the end of a very short sensory canal or directly adjacent to the hypomandibular (d) or quadrate ridge (e). The major sensory canal that runs through the hypomandibular ridge deviates posteriorly from this ridge and opens (f) up inferior to the dorsal tip… **lake trout**

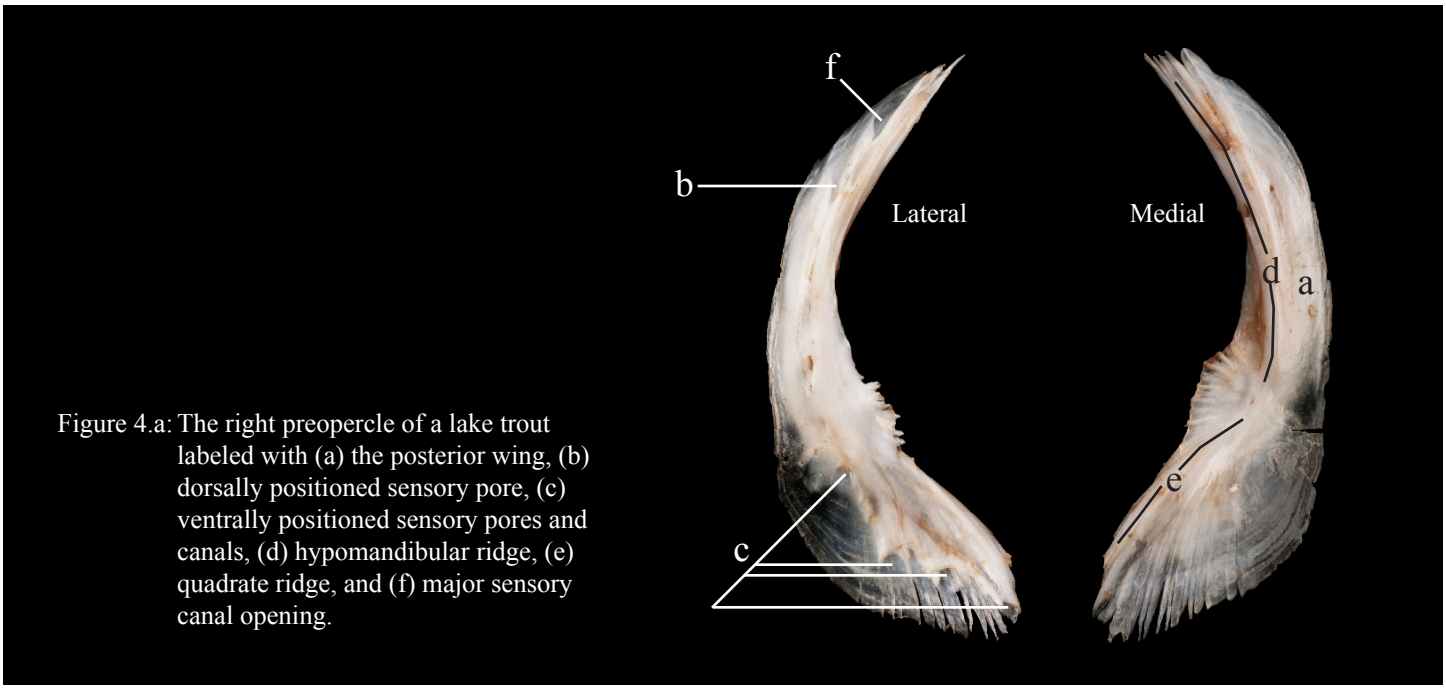

Figure 4.a: The right preopercle of a lake trout labeled with (a) the posterior wing, (b) dorsally positioned sensory pore, (c) ventrally positioned sensory pores and canals, (d) hypomandibular ridge, (e) quadrate ridge, and (f) major sensory canal opening.

4.b The posterior wing (a) remains wide as it progresses up the vertical limb. One dorsally projecting (b) and four ventrally (c) projecting sensory pores are present. Each of these pores is located at the end of a long sensory canal. The major sensory canal that runs through the hypomandibular ridge opens (f) up right at or just below the dorsal tip... **go to 5**

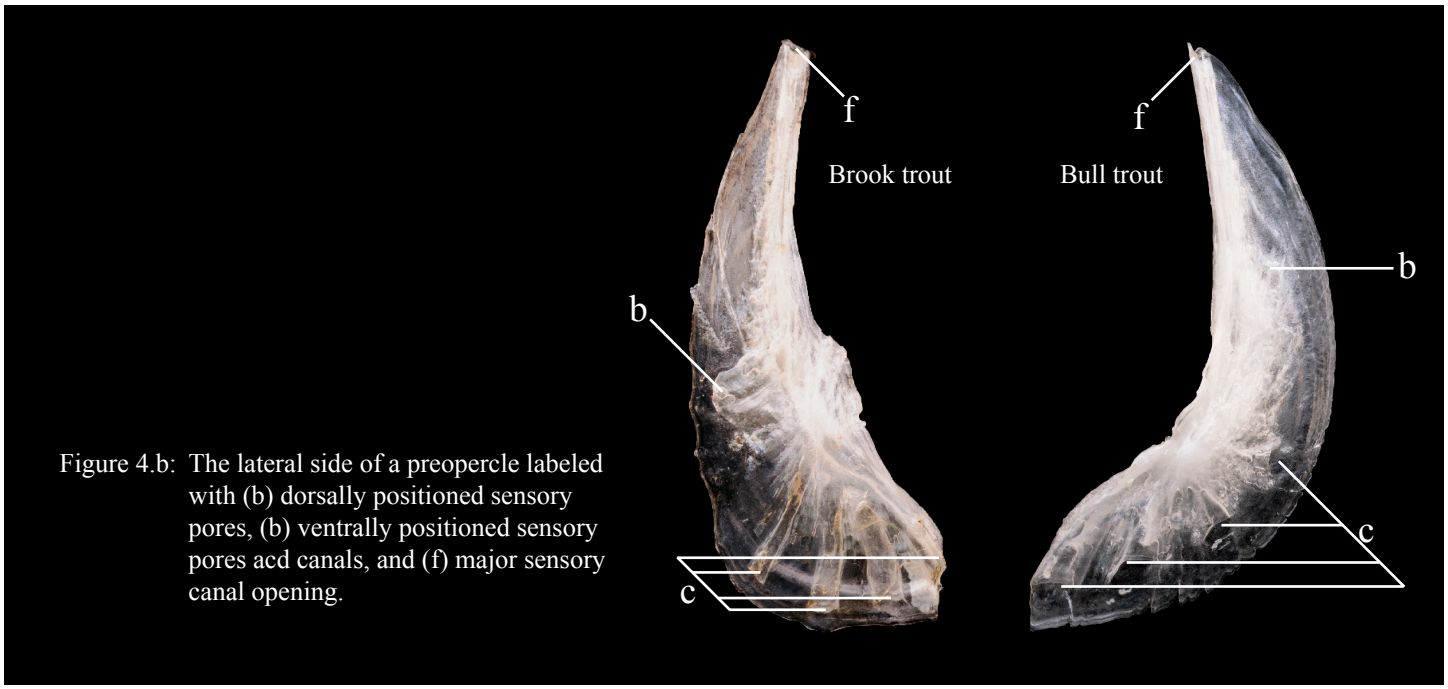

Figure 4.b: The lateral side of a preopercle labeled with (b) dorsally positioned sensory pores, (b) ventrally positioned sensory pores acd canals, and (f) major sensory canal opening.

5.a A single dorso-posterior projecting sensory pore (a) and canal is located low on the posterior wing. Four ventrally projecting sensory pores and canals (b) are positioned right next to each other. The horizontal limb (c) is short and has a blunted anterior end… **brook trout**

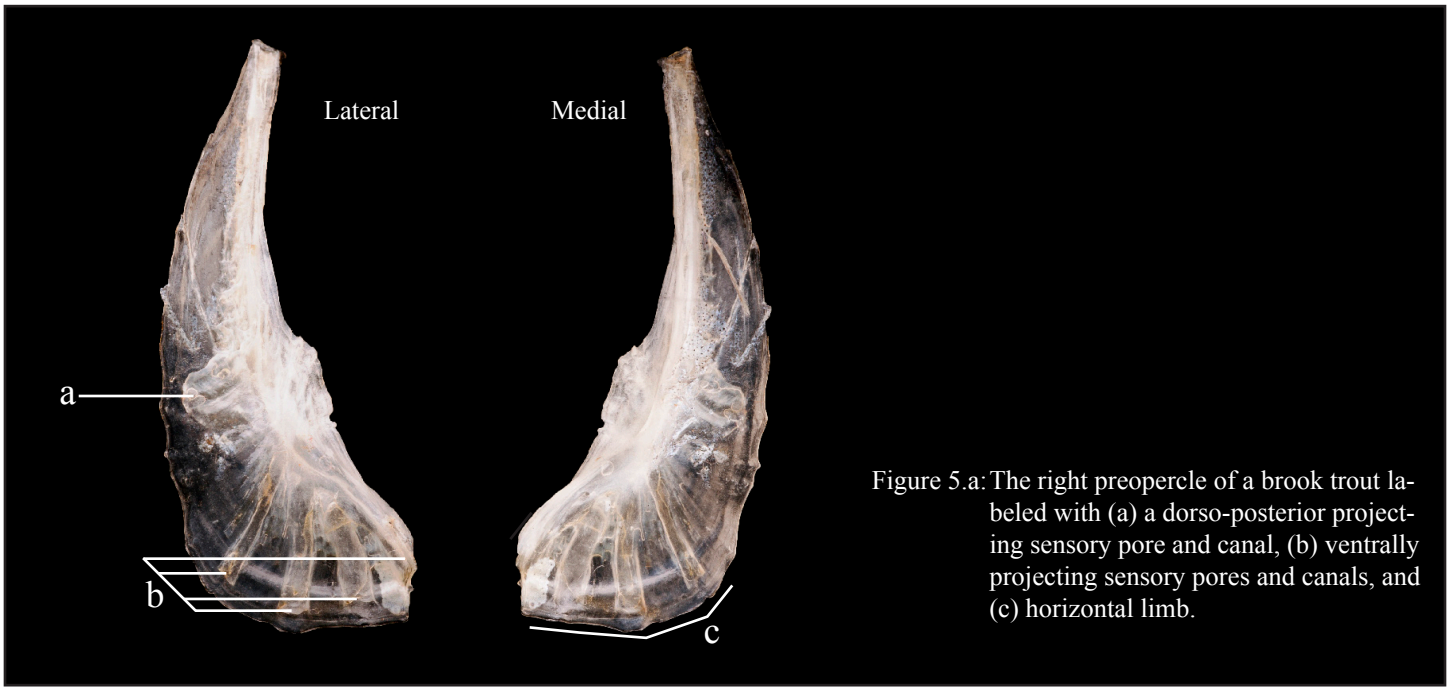

Figure 5.a: The right preopercle of a brook trout labeled with (a) a dorso-posterior projecting sensory pore and canal, (b) ventrally projecting sensory pores and canals, and (c) horizontal limb.

5.b A single dorsally projecting sensory pore and canal (a) is located high on the posterior wing. Four large ventrally projecting sensory canals (b) fan out from the quadrate ridge. The horizontal limb (c) is elongated… **bull trout**

Figure 5.b: The left preopercle of a bull trout preopercle labeled with (a) a dorso-posterior projecting sensory pore and canal, (b) ventrally projecting sensory pores and canals, and (c) horizontal limb.

6.a The posterior wing (a) remains slender and the horizontal limb (b) projects anteriorly at a slightly ventral angle into a gently rounded retroarticular joint (c). The lateral side of the posterior wing is smooth with the exception of a small area just posterior to the hypomandibular ridge (d) on some larger specimens... **go to 7**

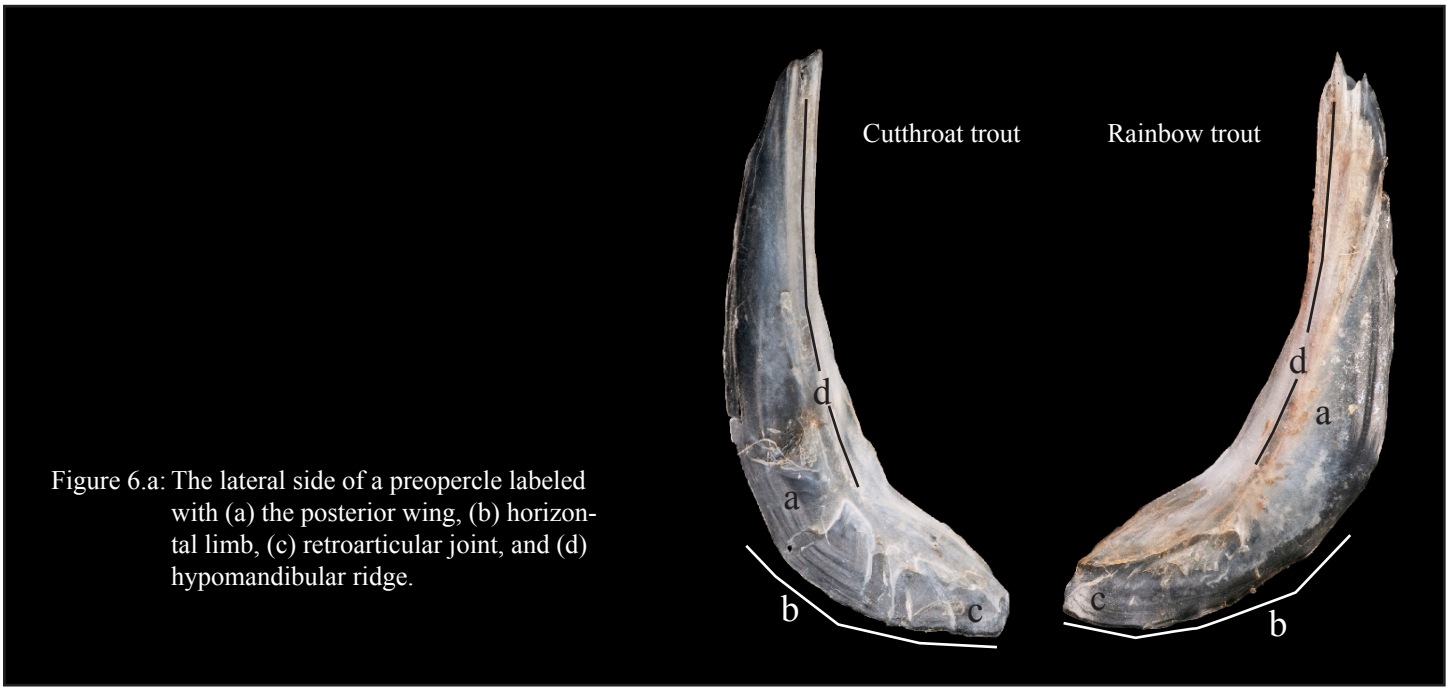

Figure 6.a: The lateral side of a preopercle labeled with (a) the posterior wing, (b) horizontal limb, (c) retroarticular joint, and (d) hypomandibular ridge.

6.b The posterior wing (a) remains wide and the horizontal limb (b) is short and blunted. The lateral side of the posterior wing has numerous striations and deep cut sensory pores and canals... **go to 8**

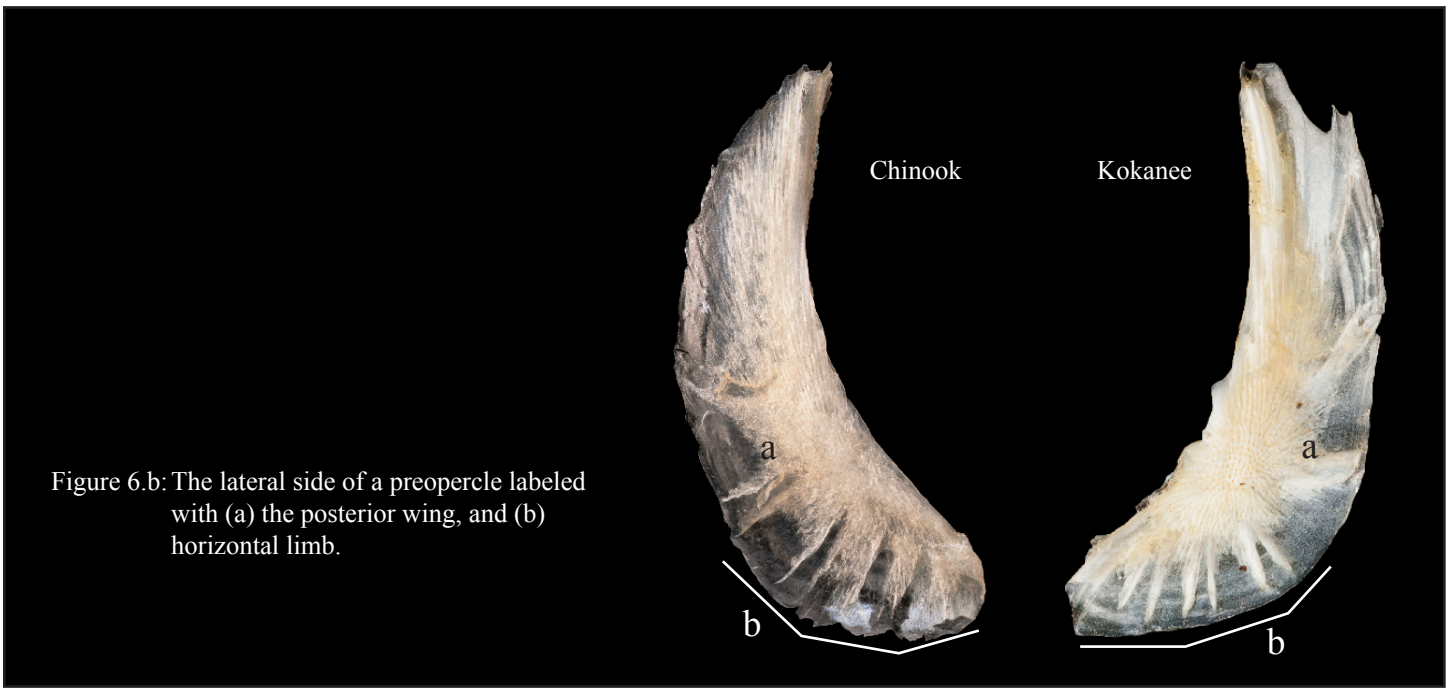

Figure 6.b: The lateral side of a preopercle labeled with (a) the posterior wing, and (b) horizontal limb.

7.a There are numerous clustered sensory pores (a), stacked nearly on top of each other, located along the posterior side of the hypomandibular ridge (b). A second set of clustered sensory pores and canals (c) is located inferior to the quadrate ridge (d)... **rainbow trout**

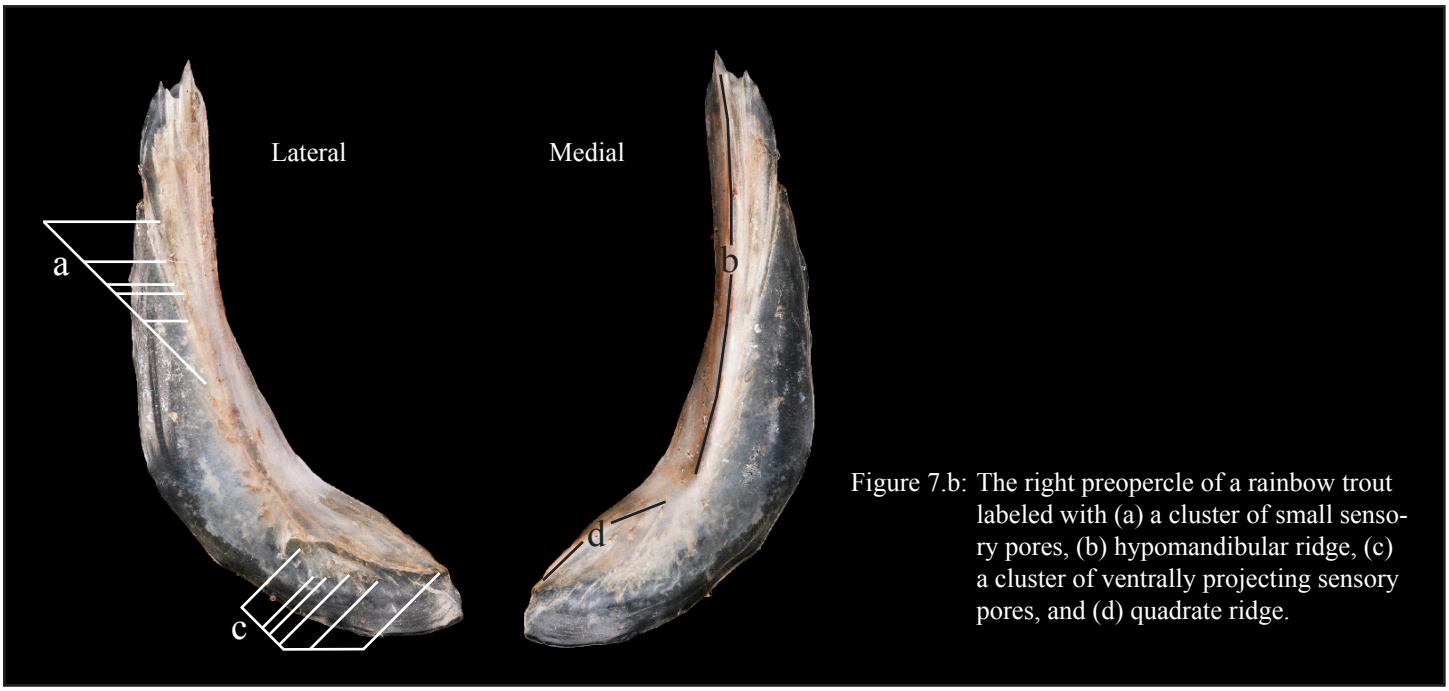

Figure 7.b: The right preopercle of a rainbow trout labeled with (a) a cluster of small sensory pores, (b) hypomandibular ridge, (c) a cluster of ventrally projecting sensory pores, and (d) quadrate ridge.

7.b There are a numerous non-clustered sensory pores (a) are located across the lateral side of the posterior wing. A second larger set of at least four ventrally descending sensory pores and canals (c) are located inferior to the quadrate ridge (d)... **cutthroat trout**

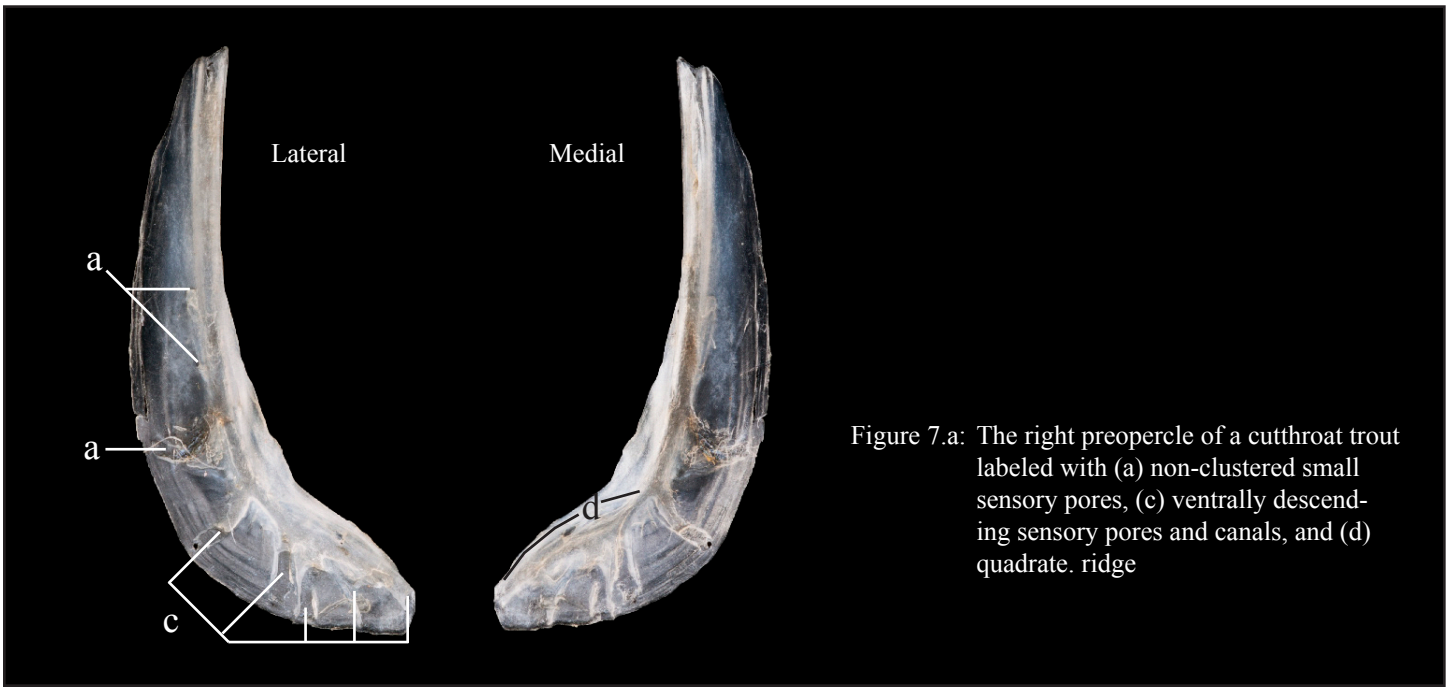

Figure 7.a: The right preopercle of a cutthroat trout labeled with (a) non-clustered small sensory pores, (c) ventrally descending sensory pores and canals, and (d) quadrate. ridge

8.a One or two long dorsally protruding spines (a) extend upward from the hypomandibular ridge (b) past the posterior margin. This leaves a single notch (c) along the dorsal portion of the preopercle. There are at least two dorsally projecting sensory pores and canals (d). Four to five ventrally descending sensory pores and canals (e) are located on the lower portion of the posterior wing… **kokanee**

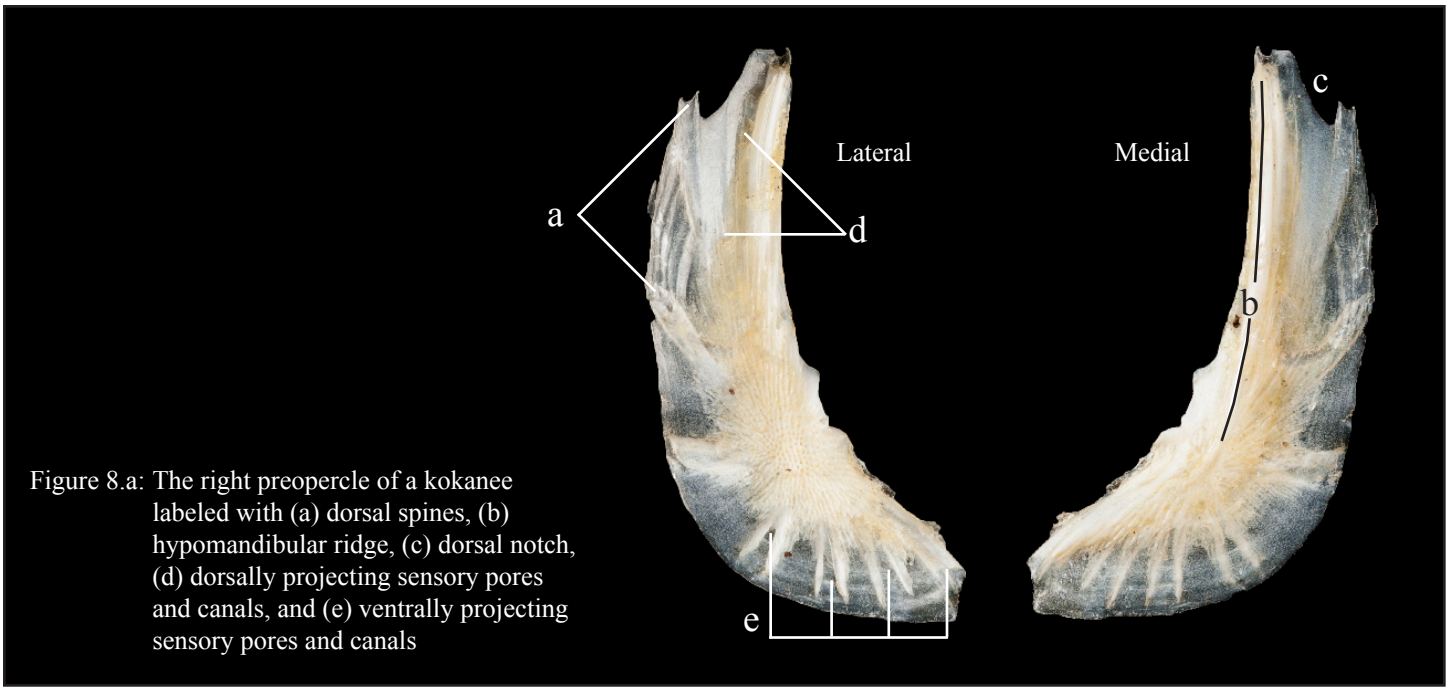

Figure 8.a: The right preopercle of a kokanee labeled with (a) dorsal spines, (b) hypomandibular ridge, (c) dorsal notch, (d) dorsally projecting sensory pores and canals, and (e) ventrally projecting sensory pores and canals

8.b There are no dorsally protruding spines that extend out past the posterior margin. There is no notch in the dorsal portion of the preopercle. Instead the entire preopercle has a gentle curvature giving it a definitive crescent shape. There are no dorsally projecting sensory pores or canals. Five to six ventrally/posteriorly projecting sensory pores and canals (e) are located on the lower portion of the posterior wing… **Chinook**

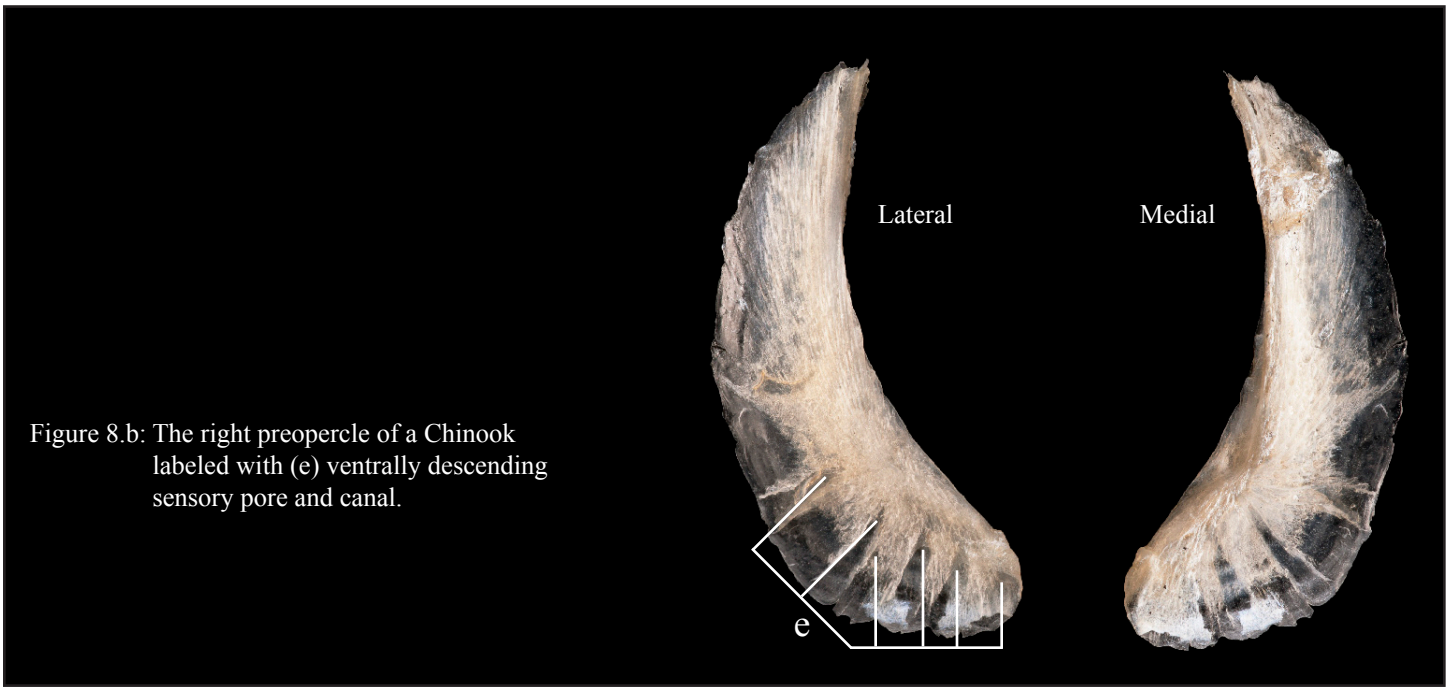

Figure 8.b: The right preopercle of a Chinook labeled with (e) ventrally descending sensory pore and canal.

1.a The dorsal lobe is large with a broadly curved dorsal margin (a) that sweeps back to a shallow posterior notch (b). The dorsal ridge (c) extends far back to near the posterior margins. The anterior ventral (d) tip is pointed… **mountain whitefish**

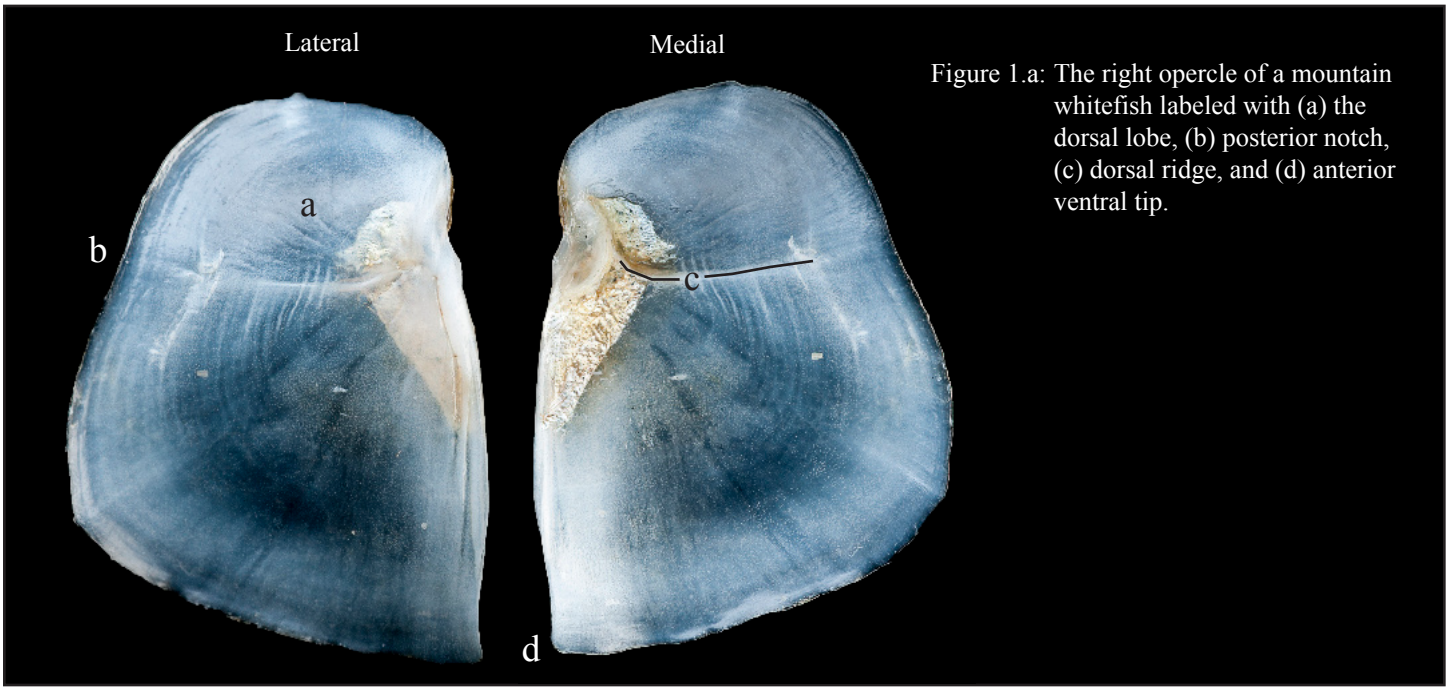

Figure 1.a: The right opercle of a mountain whitefish labeled with (a) the dorsal lobe, (b) posterior notch, (c) dorsal ridge, and (d) anterior ventral tip.

1.b The dorsal lobe (a) is relatively small and extends upward to a dorsal margin that is only slightly superior to the articular fossa (e). The dorsal ridge (c) is much shorter and ends much nearer to the articular fossa then the posterior margin. The anterior ventral tip (d) is more rounded... **go to 2**

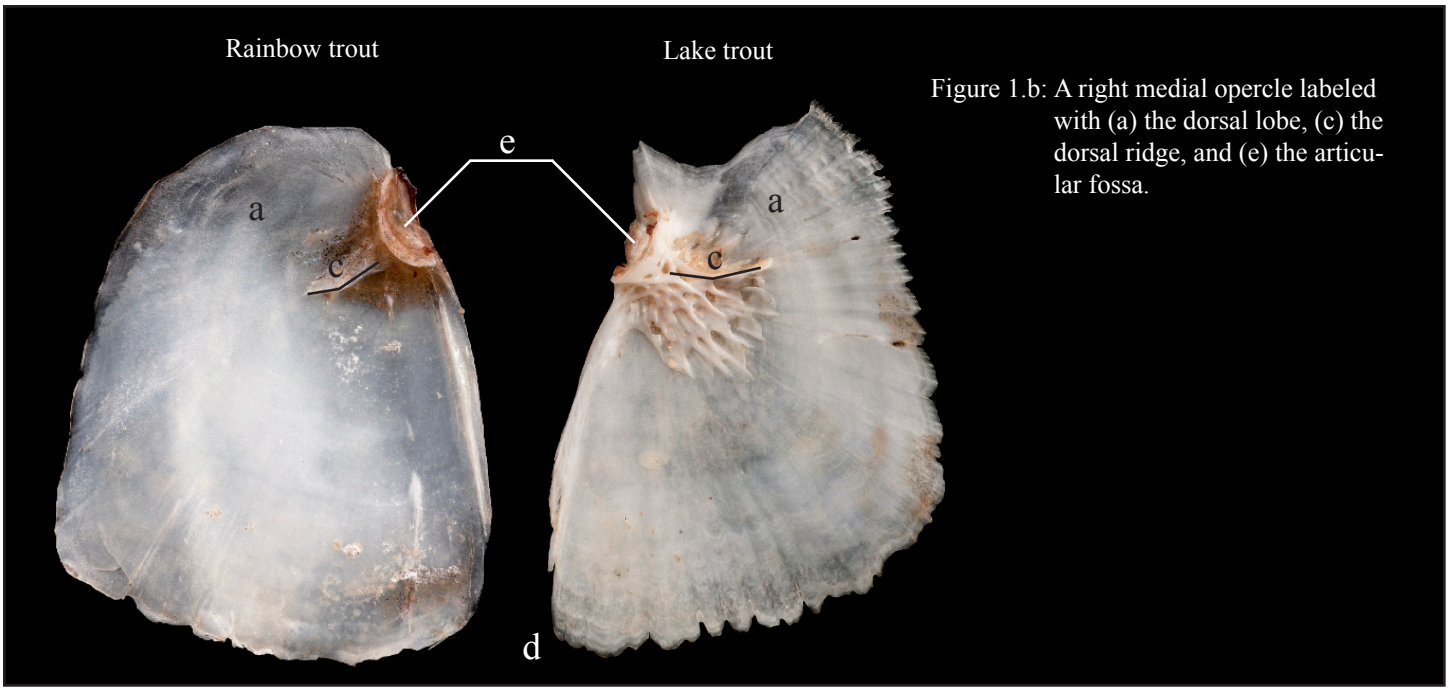

Figure 1.b: A right medial opercle labeled with (a) the dorsal lobe, (c) the dorsal ridge, and (e) the articular fossa.

2.a The anterior margin of the ventral lobe (a) scoops out from the articular fossa (b) to a far anterior position… **brown trout**

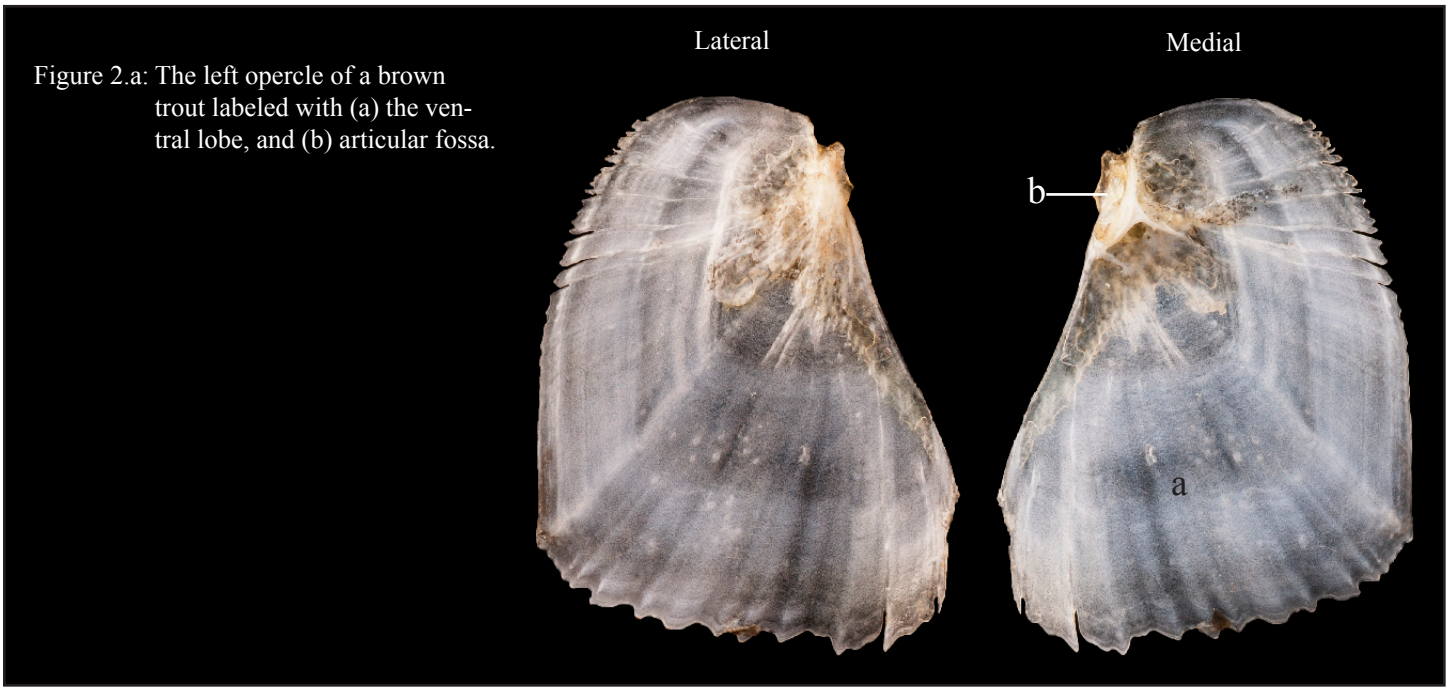

Figure 2.a: The left opercle of a brown trout labeled with (a) the ventral lobe, and (b) articular fossa.

2.b The anterior margin of the ventral lobe (a) does not scoop forward but rather is gently curved or flat... **go to 3**

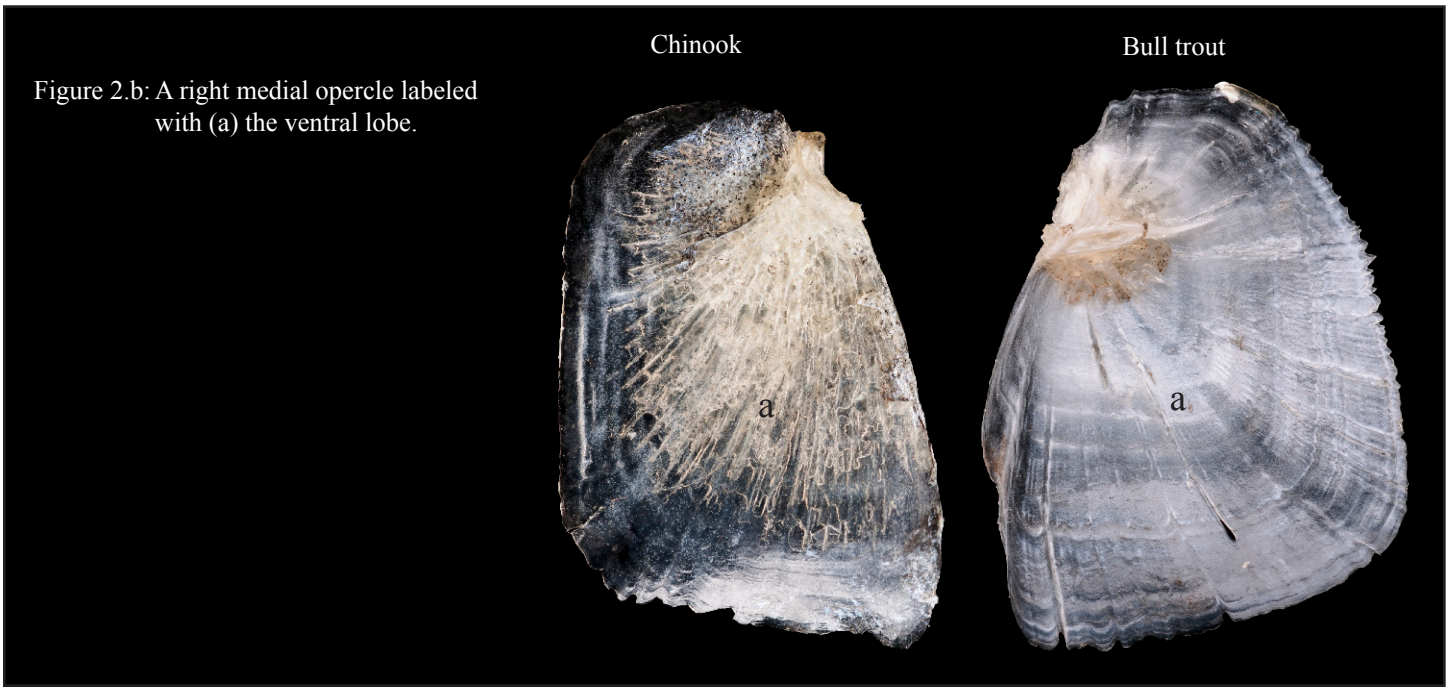

Figure 2.b: A right medial opercle labeled with (a) the ventral lobe.

3.a The anterior margin of the ventral lobe (a) has a noticeable forward curvature from the articular fossa (b) to the ventral tip (c)... **go to 4**

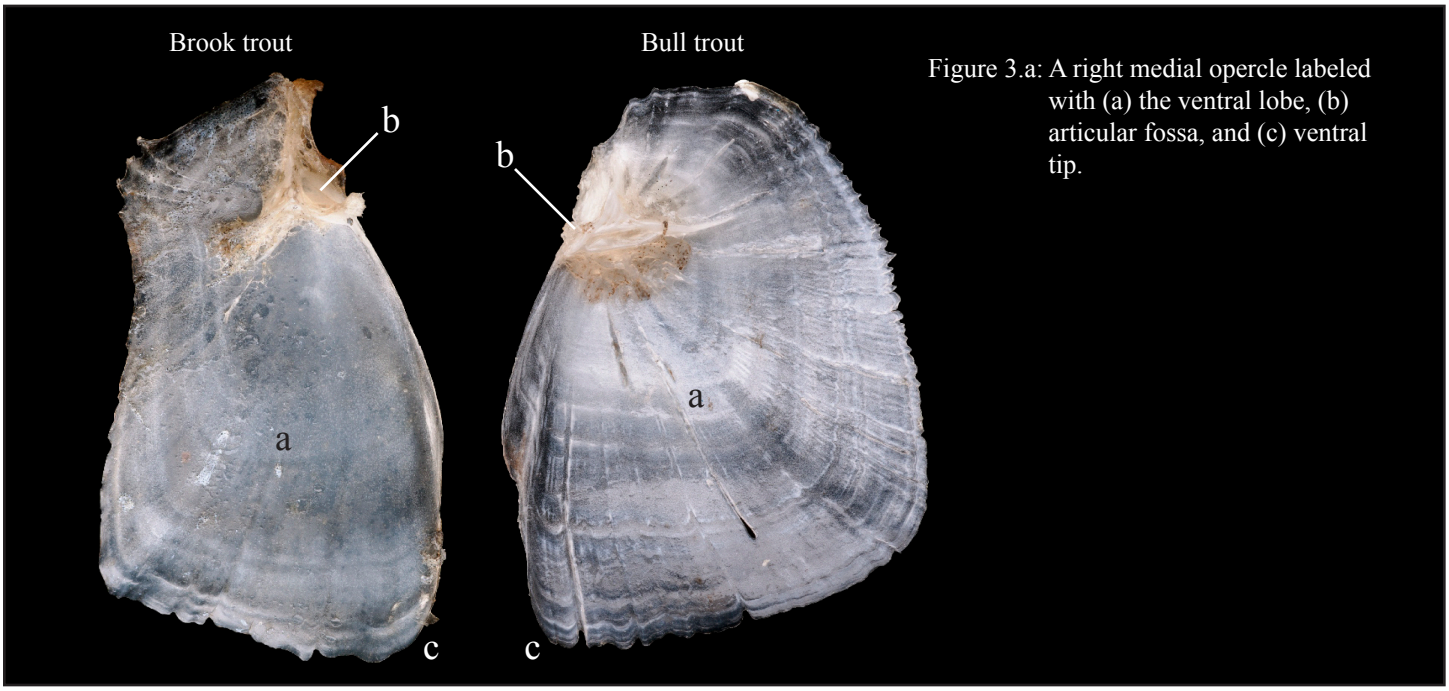

Figure 3.a: A right medial opercle labeled with (a) the ventral lobe, (b) articular fossa, and (c) ventral tip.

3.b The anterior margin of the ventral lobe (a) may have a slight forward curvature but generally appears to be flat. The posterior margin of the opercle also remains relatively flat... **go to 6**

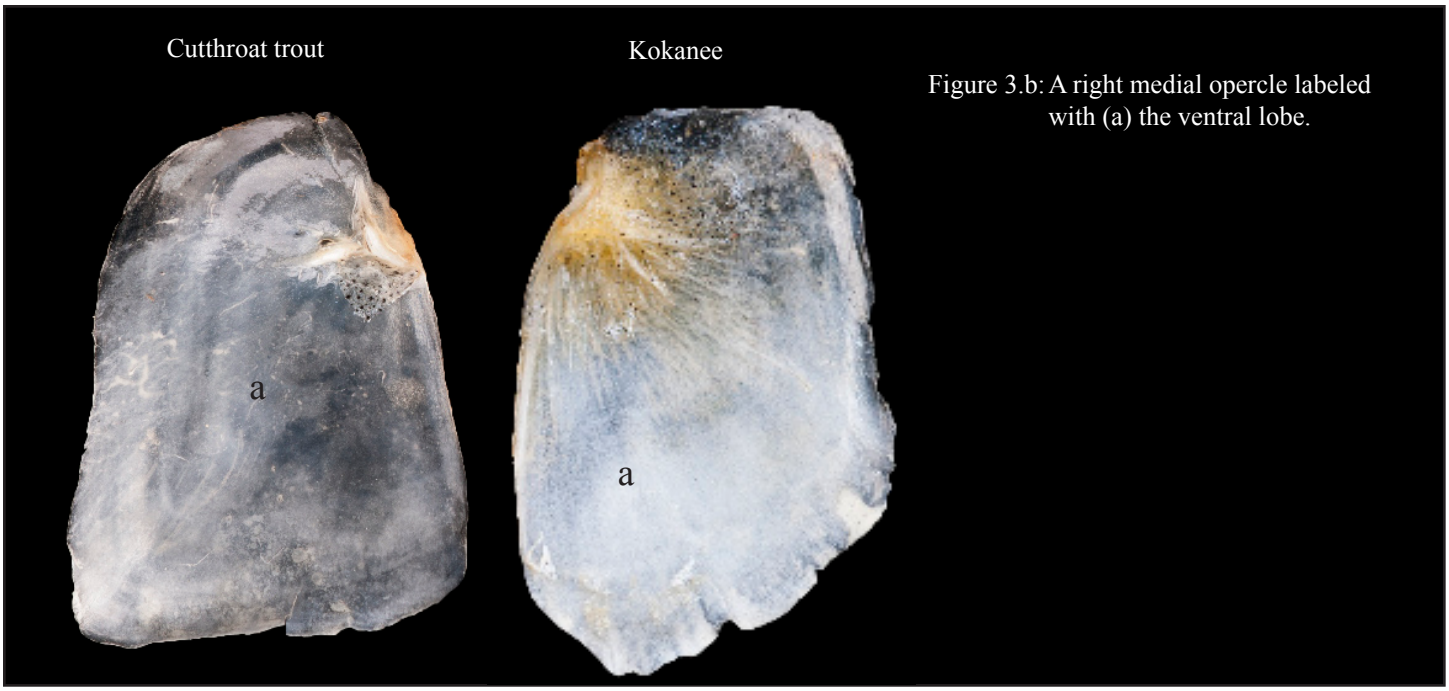

Figure 3.b: A right medial opercle labeled with (a) the ventral lobe.

4.a The dorsal lobe maintains a deep notch (a) along its dorsal margin. The vertical ridge (b) projects out of the anterior portion of this notch... **lake trout**

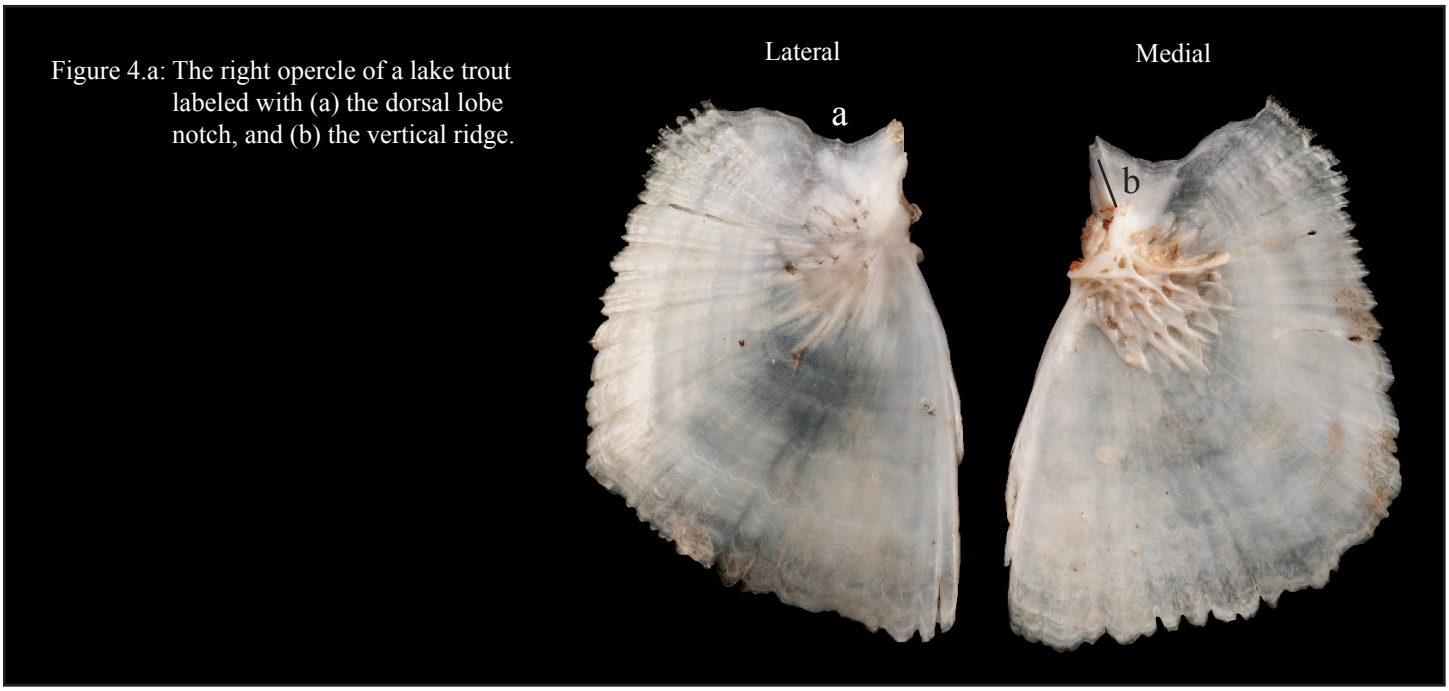

Figure 4.a: The right opercle of a lake trout labeled with (a) the dorsal lobe notch, and (b) the vertical ridge.

4.b The dorsal lobe (c) is not notched and the vertical ridge (b) is maintained within the dorsal margin... **go to 5**

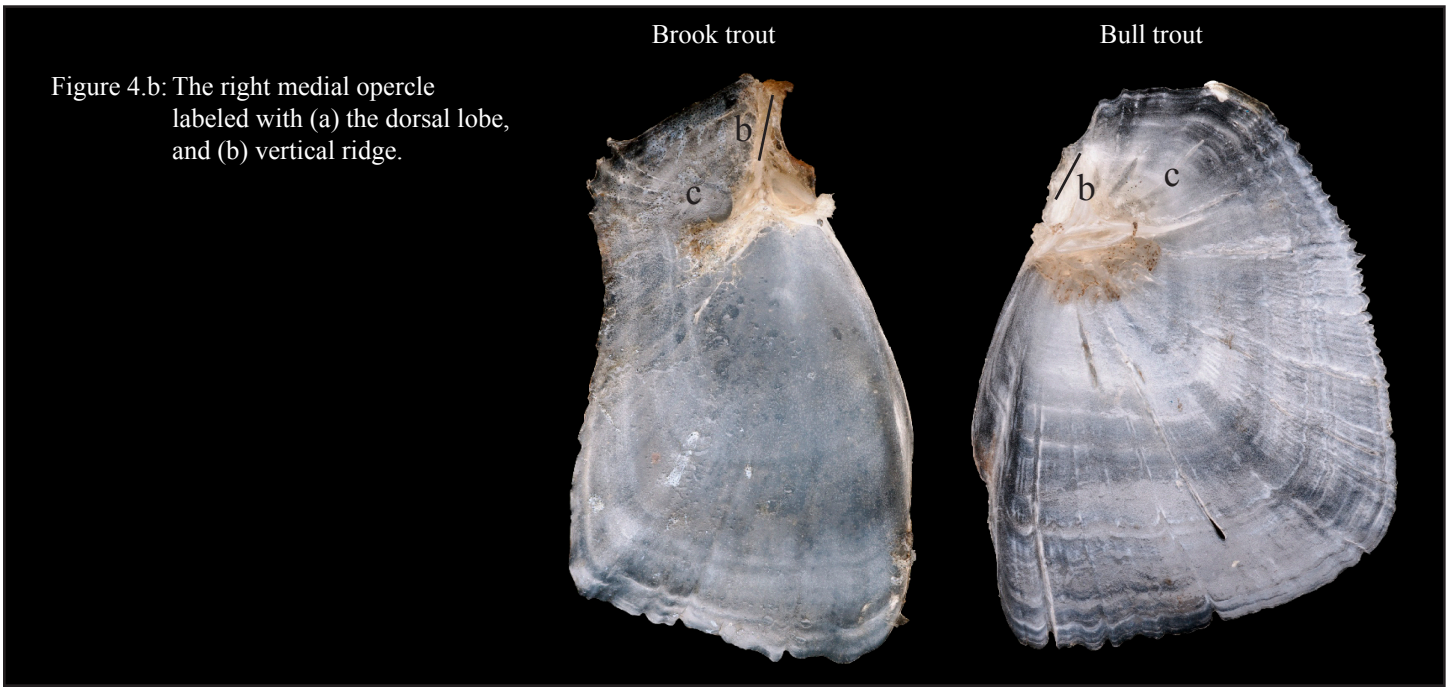

Figure 4.b: The right medial opercle labeled with (a) the dorsal lobe, and (b) vertical ridge.

5.a The dorsal margin is flat and has a ventrally descending angle. The posterior notch (a) is broad and gentle curved inward. The articular fossa (b) and dorsal ridge (c) are heavily ossified and stout in appearance. There are a number of vertically fanning striations (d) on the posterior portion of the dorsal lobe… **brook trout**

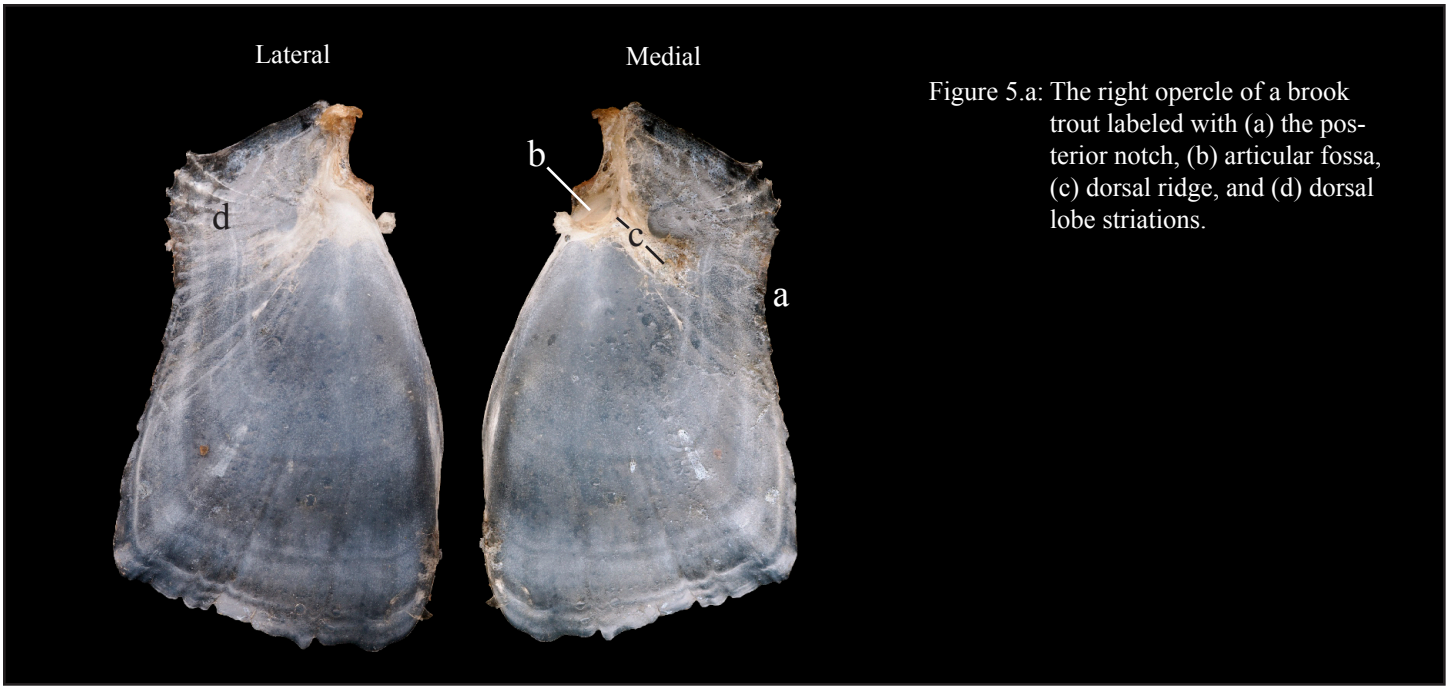

Figure 5.a: The right opercle of a brook trout labeled with (a) the posterior notch, (b) articular fossa, (c) dorsal ridge, and (d) dorsal lobe striations.

5.b The dorsal margin is curved. If there is a posterior notch it is slight. Instead, the posterior margin is gently curved. The articular fossa (b), and dorsal ridge (c) are not nearly as stout in appearance. There are no vertically fanning striations on the posterior portion of the dorsal lobe. There is a large cutaway (e) to the anterior portion of the ventral lobe… **bull trout**

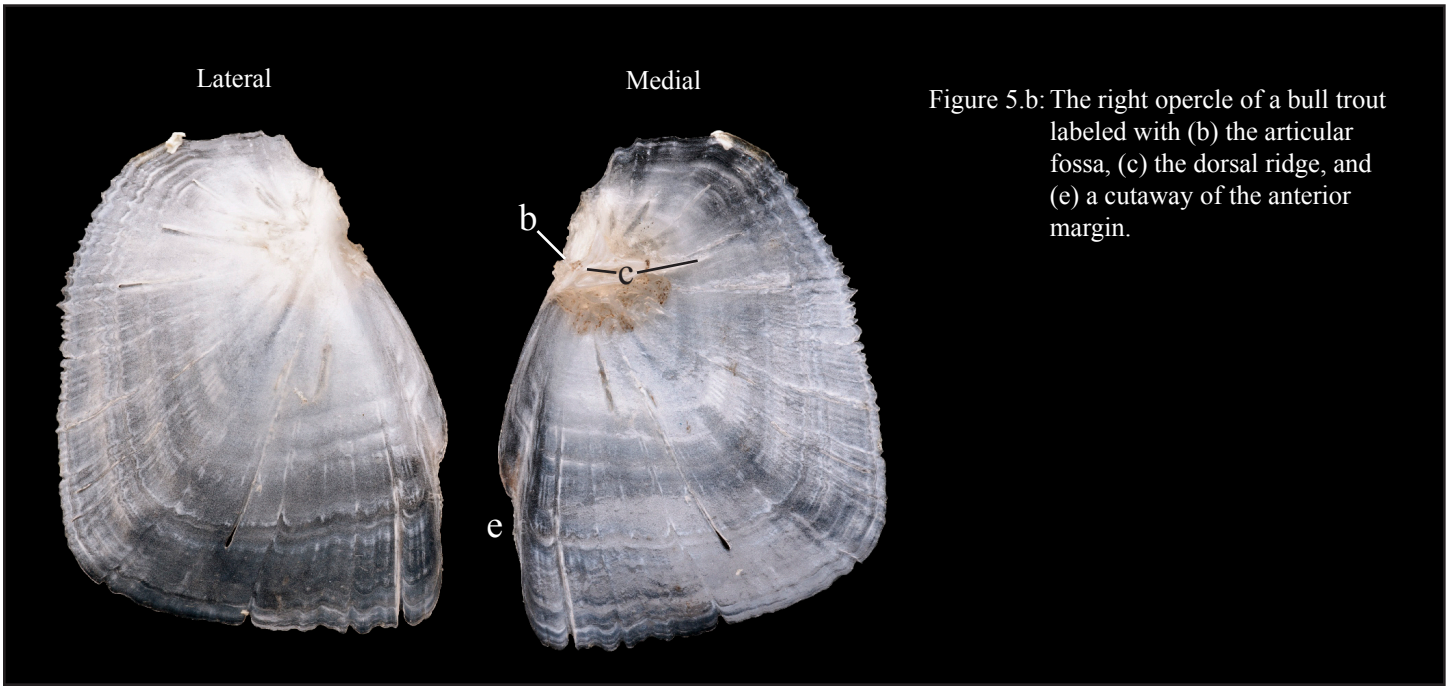

Figure 5.b: The right opercle of a bull trout labeled with (b) the articular fossa, (c) the dorsal ridge, and (e) a cutaway of the anterior margin.

6.a The lateral and medial surface of the opercular body maintain numerous striations that originate from or near the articular fossa and progress back towards the posterior and ventral margins... **go to 7**

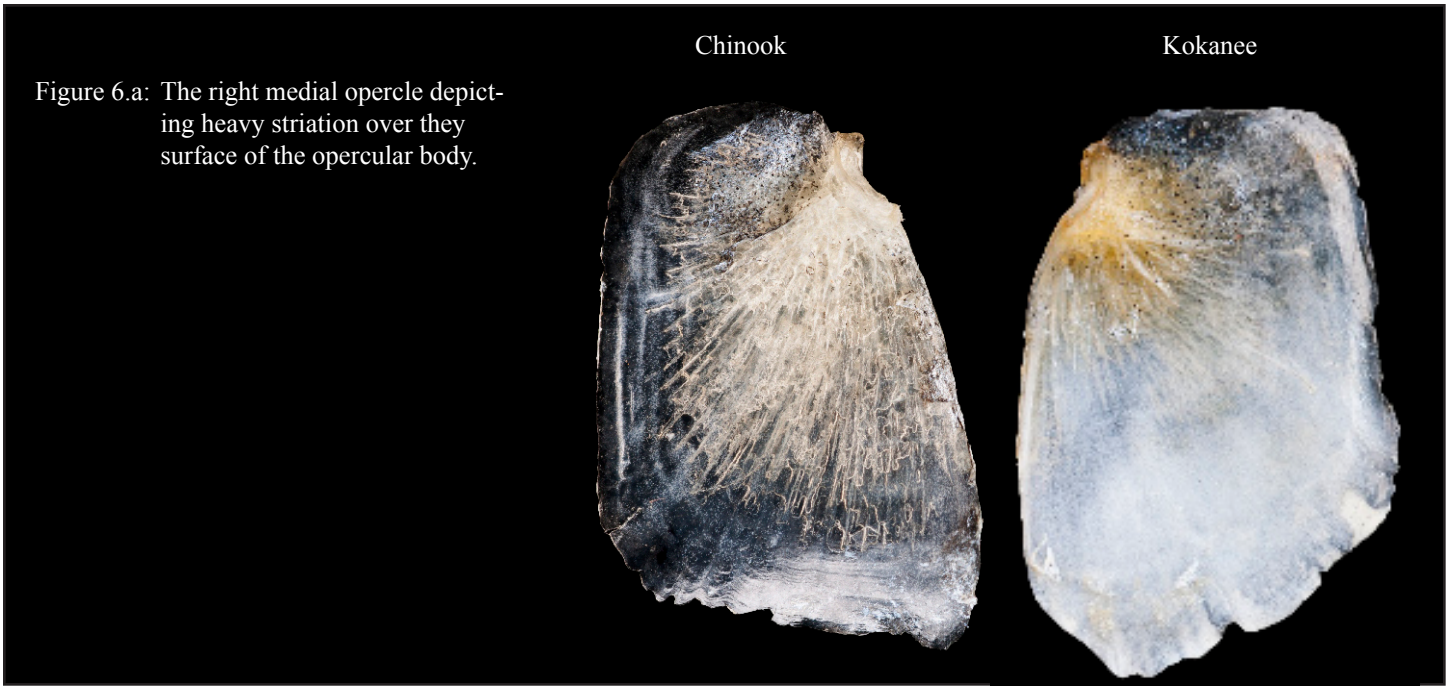

Figure 6.a: The right medial opercle depicting heavy striation over they surface of the opercular body.

6.b The lateral and medial surfaces of the opercular body remains relatively smooth with only a slight amount of striation being present near the lateral side of the articular fossa... **go to 8**

Figure 6.b: The right medial opercle depicting a smooth opercular body.

7.a The dorsal and posterior margins are flat and meet each other at an almost squared angle (a). There is an abrupt curve to the anterior margin, just inferior to the articular fossa (b). A well defined anterior ridge (c) runs from the articular fossa to where the anterior margin tapers back … **kokanee**

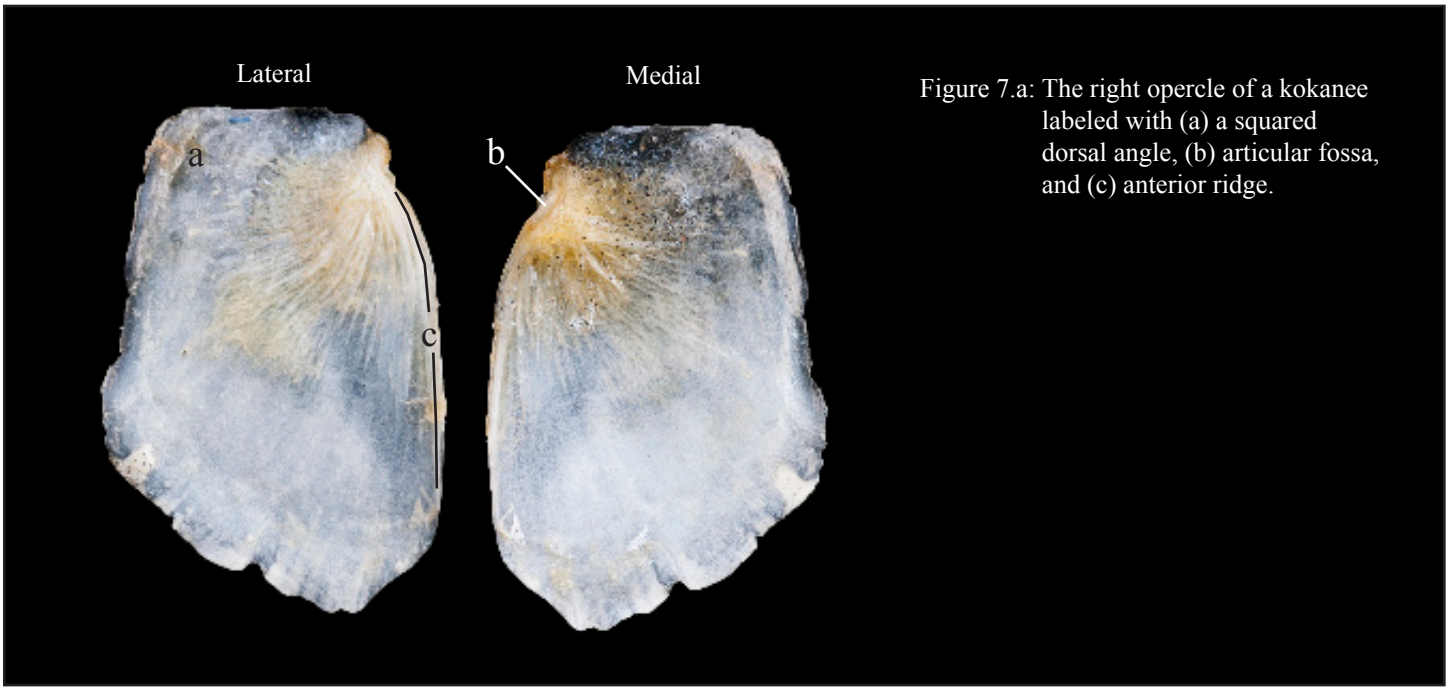

Figure 7.a: The right opercle of a kokanee labeled with (a) a squared dorsal angle, (b) articular fossa, and (c) anterior ridge.

7.b The posterior margin is flat but the dorsal margin is more curved. The anterior margin is not abruptly curved inferior to the articular fossa (b). The anterior ridge (b) is greatly reduced and obscured by the numerous striations down both sides of the opercular body… **Chinook**

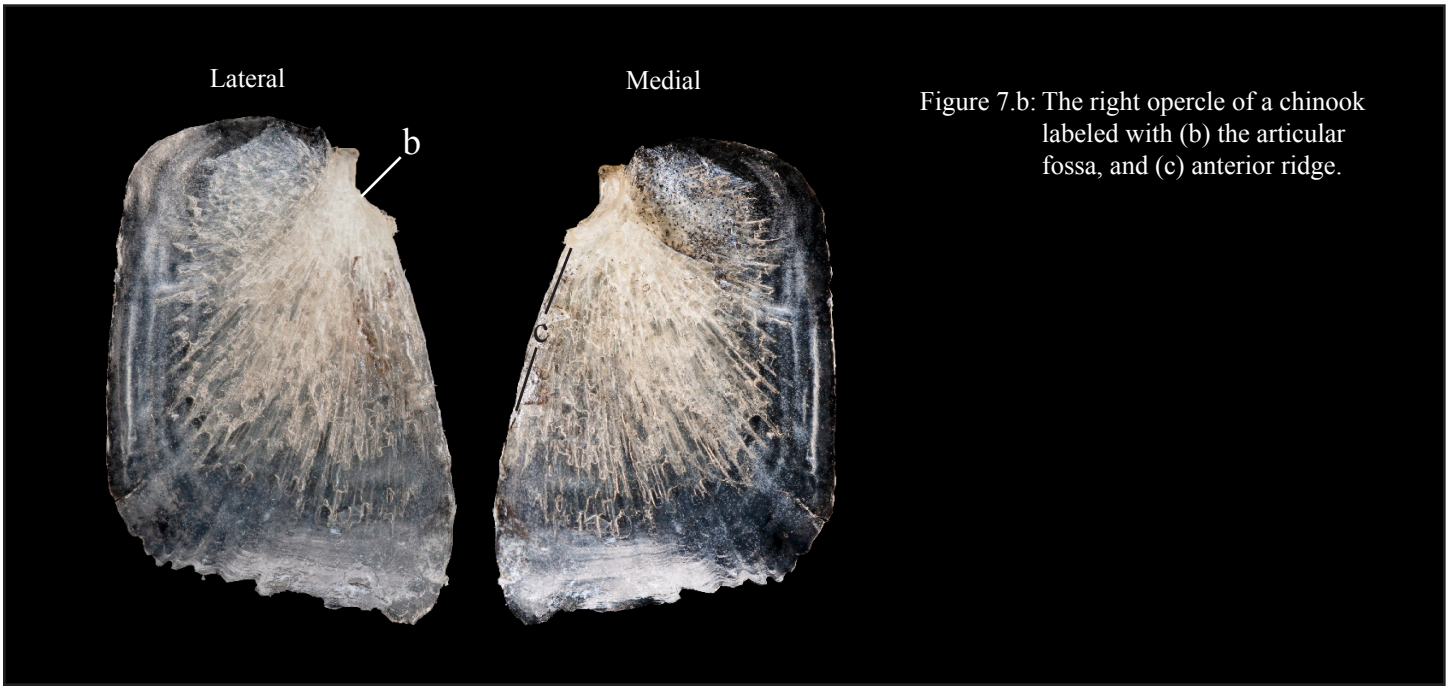

Figure 7.b: The right opercle of a chinook labeled with (b) the articular fossa, and (c) anterior ridge.

8.a The anterior margin maintains a relatively flat face that extends from the ventral to dorsal tips of the opercle. There is no tapering at the ventral portion of the anterior margin. The dorsal lobe (a) is relatively large and appears to sweep back from its flat anterior margins. The articular fossa (b) is not near the dorsal margin… **cutthroat trout**

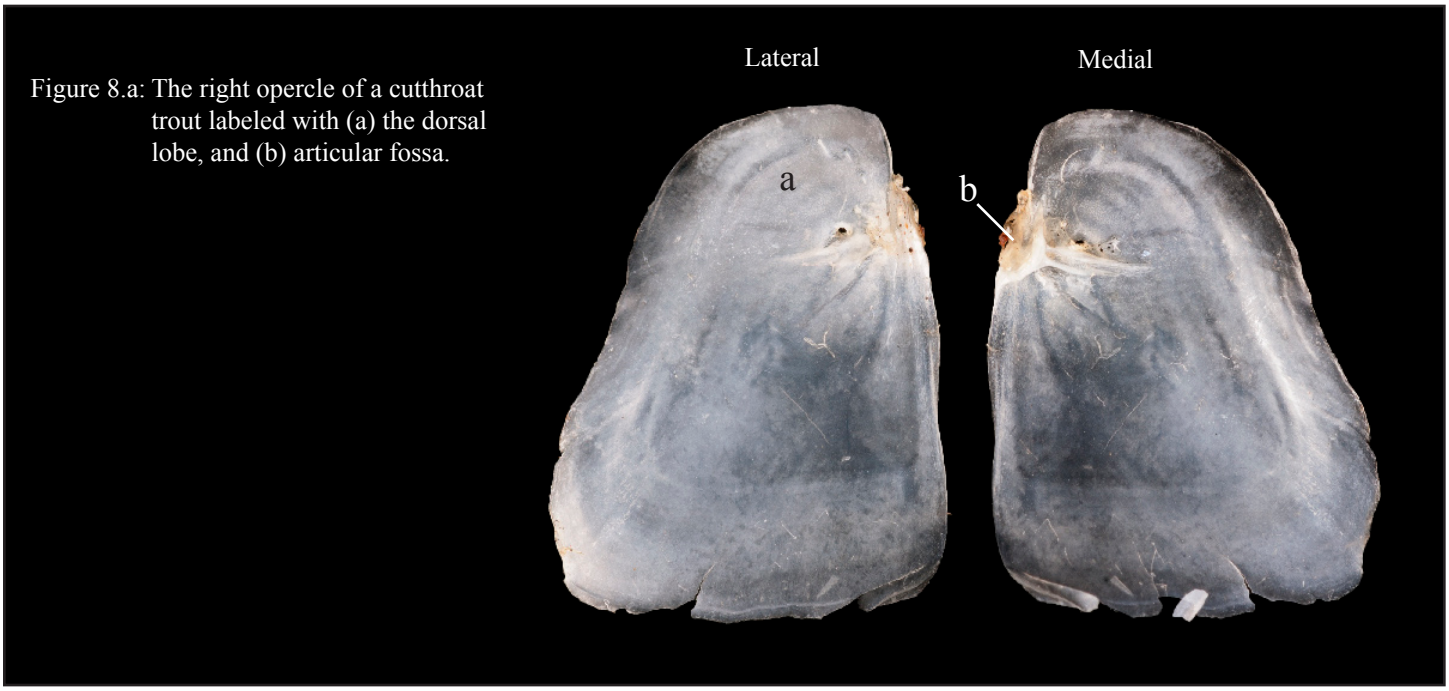

Figure 8.a: The right opercle of a cutthroat trout labeled with (a) the dorsal lobe, and (b) articular fossa.

8.b The anterior margin gently curved back near the articular fossa (b). The ventral portion of the anterior margin tappers back. The dorsal lobe (a) remains small and the articular fossa is near the dorsal margin… **rainbow trout**

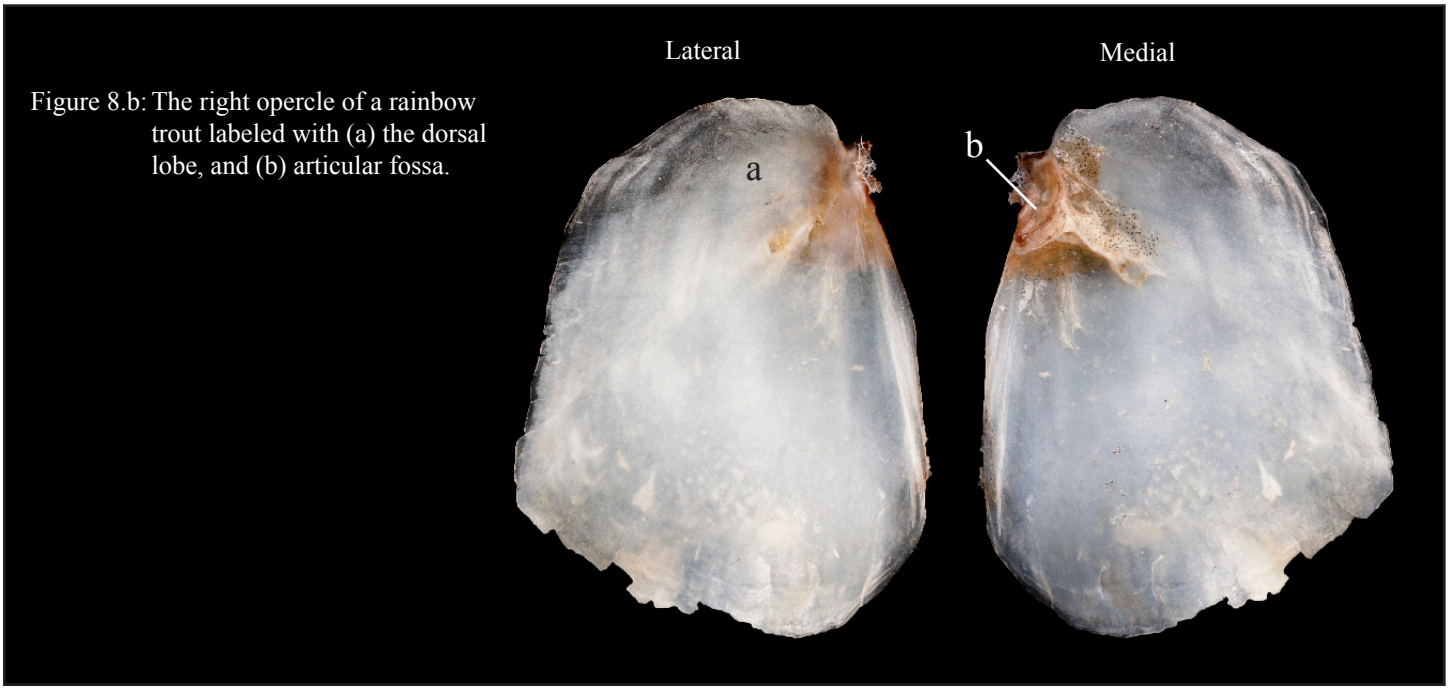

Figure 8.b: The right opercle of a rainbow trout labeled with (a) the dorsal lobe, and (b) articular fossa.

Appendix B: Regression Equations and Graphs

Appendix BI-IX contains a complete compendium of the most significant regression equation for back calculating fish total length from each bone and a graphical depiction of the most significant regression equations for each fish and bone as presented throughout the results section. In Appendix B, all graphs and equations will be presented for each fish as organized in Table 1. It should be noted that as described in the methods section of this document, regression equations have been constructed using the natural log of each bones measurements to meet the statistical assumptions of normality. However, to provide readers with an accurate representation of the actual data gathered in this study two graphs have been prepared for each regression analysis. The first of these graphs has been prepared using the raw data gathered from each bone. This second graph has been constructed using natural log transformed data. As sample populations of brown trout were too small (n=3) to accurately generate regression equations for bone length to total length back calculations brown trout have not been included in Appendix B. All measurements used for constructing associated regression equations and graphs can be found in Figure 3 on page 9.

Appendix B-I: Regression Equations and Graphs for the Cutthroat Trout

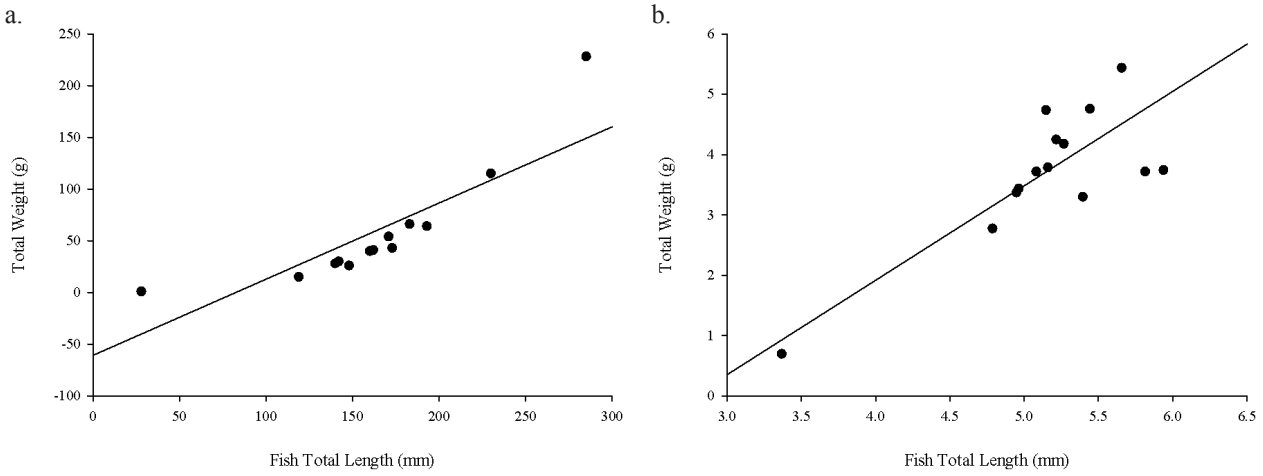

Figure B-I-1: Raw (a) and natural log transformed (b) total lengths (mm) and weights (g) of cutthroat trout used in this study with over laid regression line. Equations used to generate regressions presented in Table B-I 1 were constructed using the natural log transformed data points.

Table B-I-1: Total length (mm) to weight (g) regression equations for cutthroat trout with associated *p* value, R^2, and sample population used (n).

Species	TL Range (mm)	Wt Range (g)	Regression Equation	Regression *p* Value	r^2	n
Cutthroat Trout	28-285	1.0-228.0	-82.846+(0.857*TL)	<0.001	0.757	13

Table B-I-2: Total bone length (mm) to total fish length (g) regression equations for cutthroat trout with associated *p* value, R^2, sample population used (n) and associated figure number.

Bone	Bone Length Range (mm)	Regression Equations	*p* Value	r^2	Adjusted r^2	n	Figure Number
Premaxillary	0.205-0.700	2.51*(Premaxillary A) + 4.351	<0.001	0.985	0.971	7	B-I-2
Maxillary	1.075-2.860	1.375*(Maxillary A) + 3.883	<0.001	0.880	0.867	11	B-I-3
Dentary	0.815-1.535	1.711*(Dentary A) + 3.776	<0.001	0.867	0.850	10	B-I-4
Cleithra	1.085-1.660	1.309 * (Cleithra A) + 3.837	<0.001	0.633	0.581	9	B-I-5
Preopercle	0.855-1.940	1.871 * (Preopercle A) +3.638	<0.001	0.937	0.928	9	B-I-6
Opercle	0.850-1.185	2.401 * (Opercle D) +3.502	<0.001	0.779	0.735	7	B-I-7
Vertebra	A:0.14-0.32 B:0.105-0.28	3.085 * (Vertebra A) + 2.163 * (Vertebra B) + 4.208	<0.001	0.956	0.948	14	B-I-8

a.

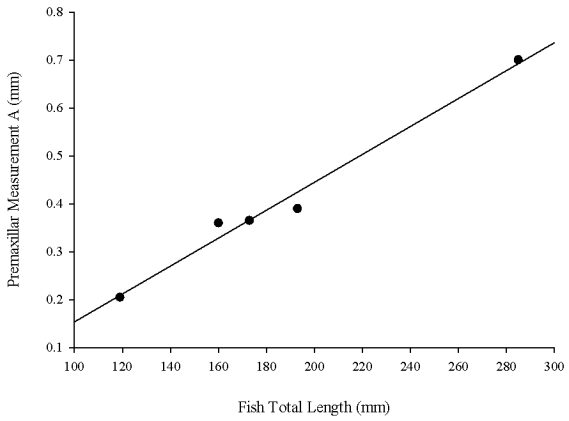

b.

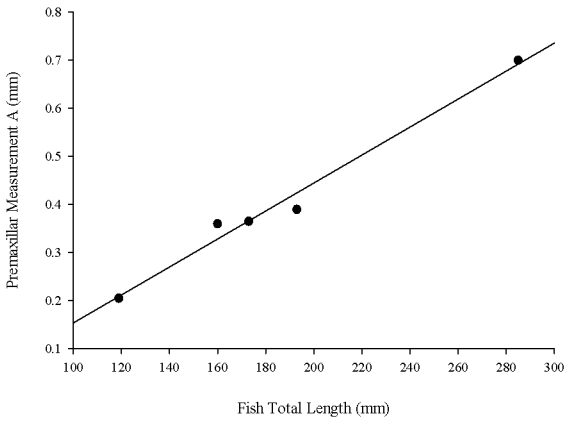

Figure B-I-2: Raw (a) and natural log transformed (b) measurements taken from the cutthroat trout premaxillary A (mm) and TL (mm) with over laid regression line. Equations used to generate regressions presented in Table B-I-2 were constructed using the natural log transformed data set.

a.

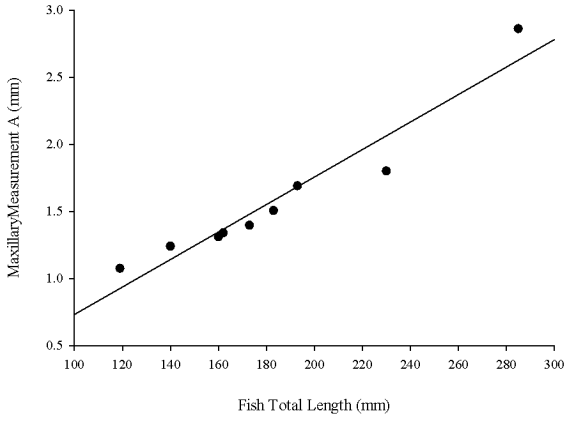

b.

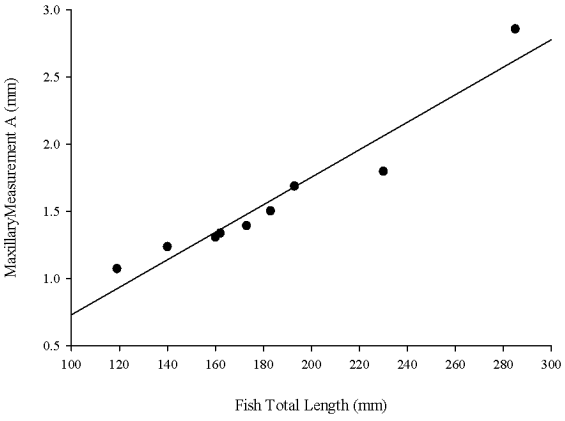

Figure B-I-3: Raw (a) and natural log transformed (b) measurements taken from the cutthroat trout maxillary A (mm) and TL (mm) with over laid regression line. Equations used to generate regressions presented in Table B-I-2 were constructed using the natural log transformed data set.

a.

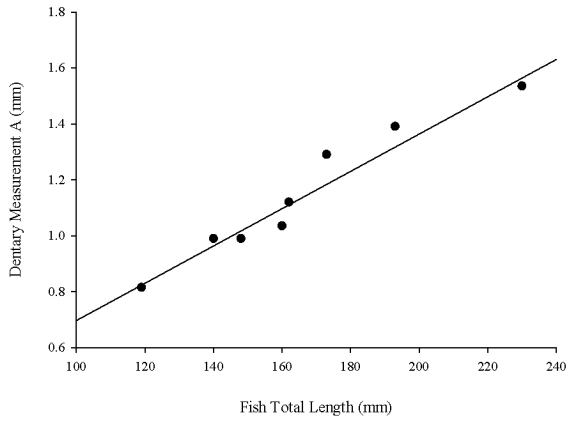

b.

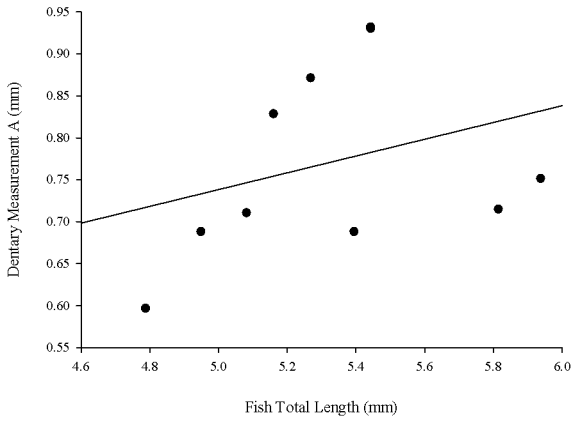

Figure B-I-4: Raw (a) and natural log transformed (b) measurements taken from the cutthroat trout dentary A (mm) and TL (mm) with over laid regression line. Equations used to generate regressions presented in Table B-I-2 were constructed using the natural log transformed data set.

a.

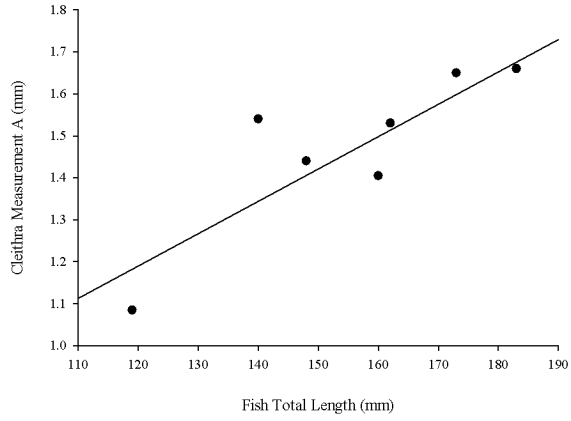

b.

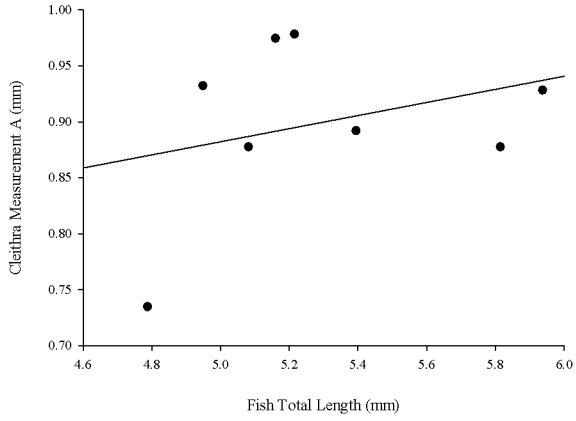

Figure B-I-5: Raw (a) and natural log transformed (b) measurements taken from the cutthroat trout cleithra A (mm) and TL (mm) with over laid regression line. Equations used to generate regressions presented in Table B-I-2 were constructed using the natural log transformed data set.

a.

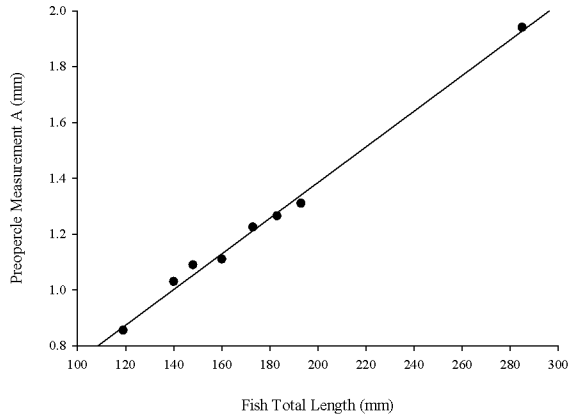

b.

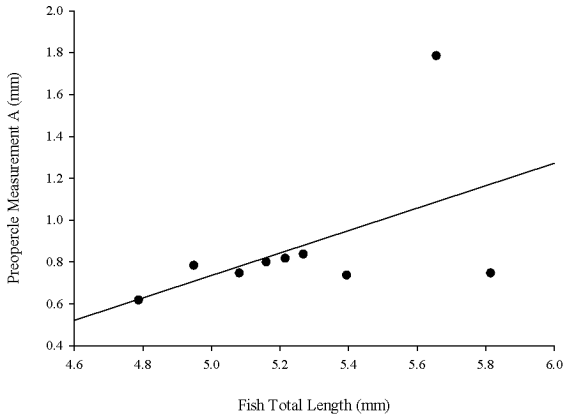

Figure B-I-6: Raw (a) and natural log transformed (b) measurements taken from the cutthroat trout preopercle A (mm) and TL (mm) with over laid regression line. Equations used to generate regressions presented in Table B-I-2 were constructed using the natural log transformed data set.

a.

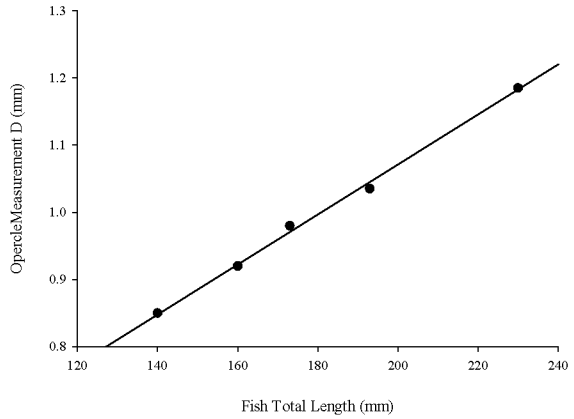

b.

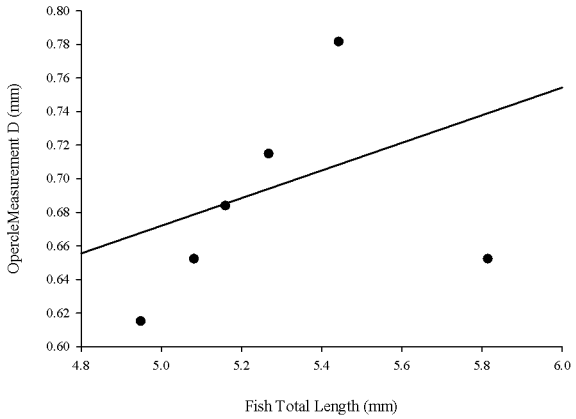

Figure B-I-7: Raw (a) and natural log transformed (b) measurements taken from the cutthroat trout opercle d (mm) and TL (mm) with over laid regression line. Equations used to generate regressions presented in Table B-I-2 were constructed using the natural log transformed data set.

a.

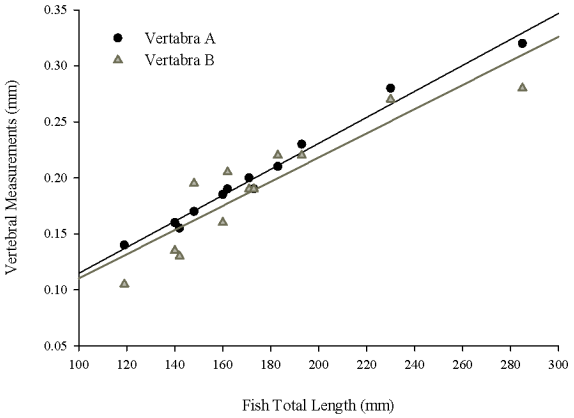

b.

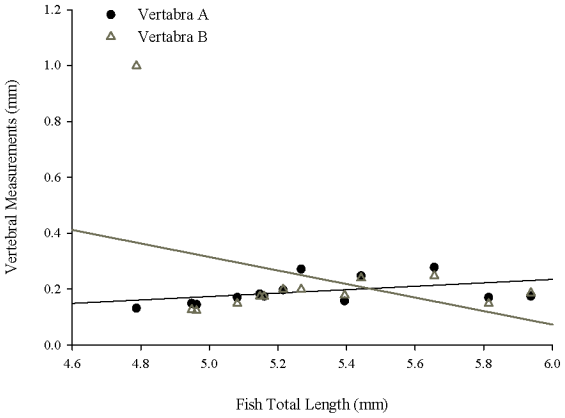

Figure B-I-8: Raw (a) and natural log transformed (b) measurements taken from the cutthroat trout vertebra A & B (mm) and TL (mm) with over laid regression line. Equations used to generate regressions presented in Table B-I-2 were constructed using the natural log transformed data set.

Appendix B-II: Regression Equations and Graphs for the Rainbow Trout

a.

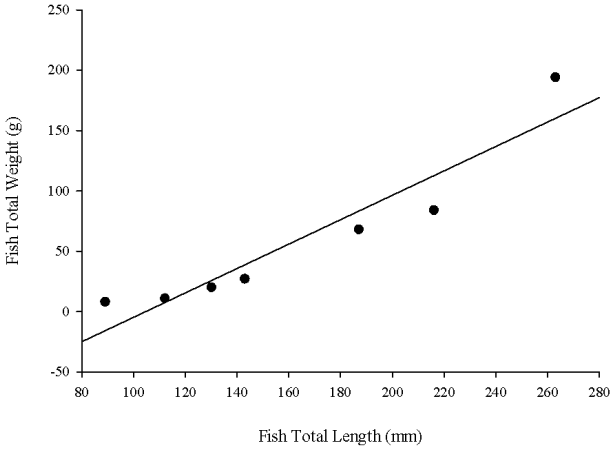

b.

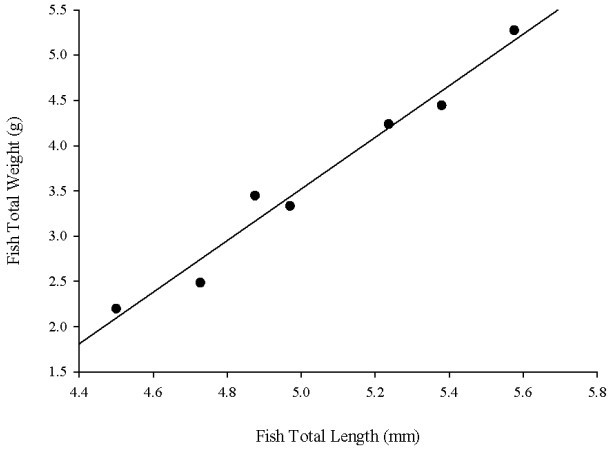

Figure B-II-1: Raw (a) and natural log transformed (b) total lengths (mm) and weights (g) of rainbow trout used in this study with over laid regression line. Equations used to generate regressions presented in Table B-II 1 were constructed using the natural log transformed data points.

Table B-II-1: Total length (mm) to weight (g) regression equations for rainbow trout with associated p value, R^2, and sample populatoin used (n).

Species	TL Range (mm)	Wt Range (g)	Regression Equasion	Regression *p* Value	r^2	n
Rainbow Trout	89-263	8.0-194.0	-105.696 + (1.01*TL)	<0.001	0.888	7

Table B-II-2: Total bone length (mm) to total fish length (g) regression equations for rainbow trout with associated p value, R^2, sample population used (n) and associated figure number.

Bone	Bone Length Range (mm)	Regression Equations	p Value	r^2	Adjusted r^2	n	Figure Number
Premaxillary	0.235-0.375	2.611*(Premaxillary C) + 4.469	<0.001	0.941	0.929	7	B-II-2
Maxillary	0.730-2.115	2.611*(Maxillary A) + 4.469	<0.001	0.941	0.929	7	B-II-3
Dentary	0.490-1.030	2.023*(Dentary C) +3.752	<0.001	0.977	0.974	9	B-II-4
Cleithra	0.985-1.620	1.475*(Cleithra A) + 3.632	<0.001	0.886	0.870	9	B-II-5
Preopercle	0.440-1.100	1.679*(Preopercle C) + 4.32 4	<0.001	0.943	0.936	10	B-II-6
Opercle	0.620-0.905	1.704*(Opercle B) + 4.105	<0.001	0.953	0.945	8	B-II-7
Vertebra	0.090-0.310	4.912*(vertebra B) + 4.307	<0.001	0.893	0.880	10	B-II-8

a.

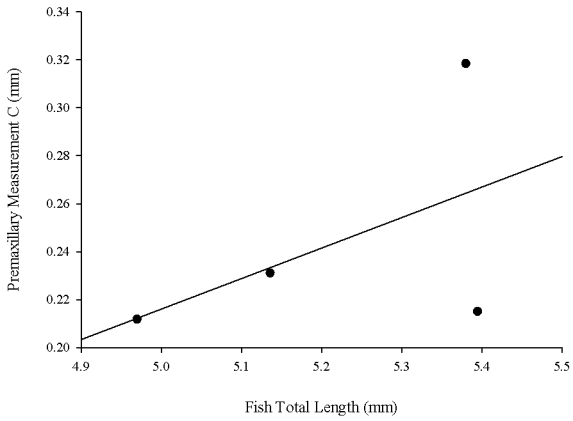

b.

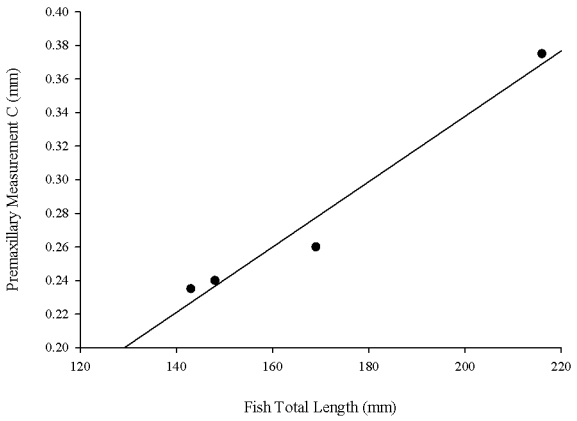

Figure B-II-2: Raw (a) and natural log transformed (b) measurements taken from the rainbow trout premaxillary C (mm) and TL (mm) with over laid regression line. Equations used to generate regressions presented in Table B-I-2 were constructed using the natural log transformed data set.

a.

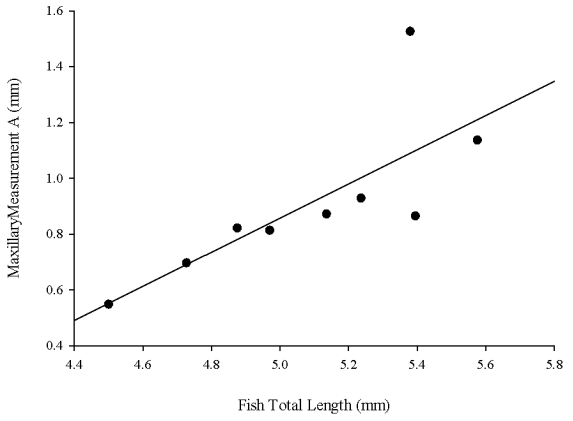

b.

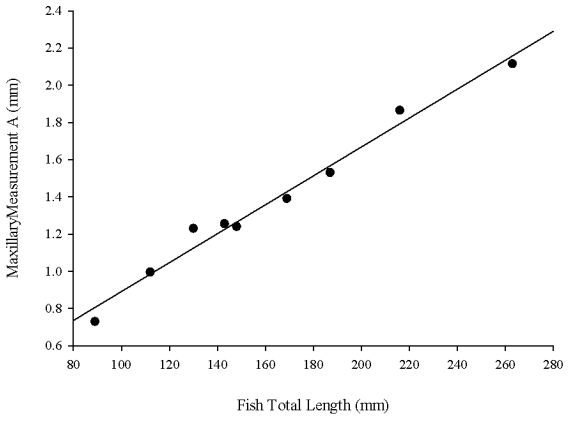

Figure B-II-3: Raw (a) and natural log transformed (b) measurements taken from the rainbow trout maxillary A (mm) and TL (mm) with over laid regression line. Equations used to generate regressions presented in Table B-I-2 were constructed using the natural log transformed data set.

a.

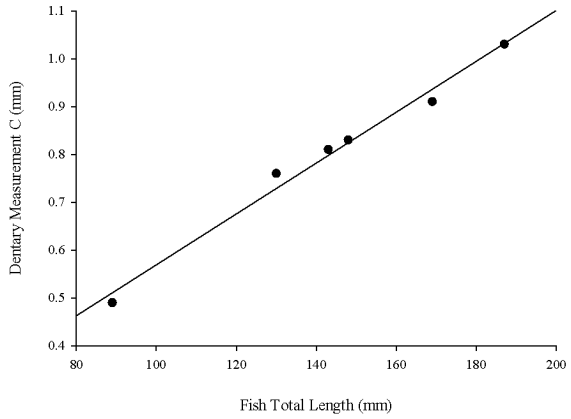

b.

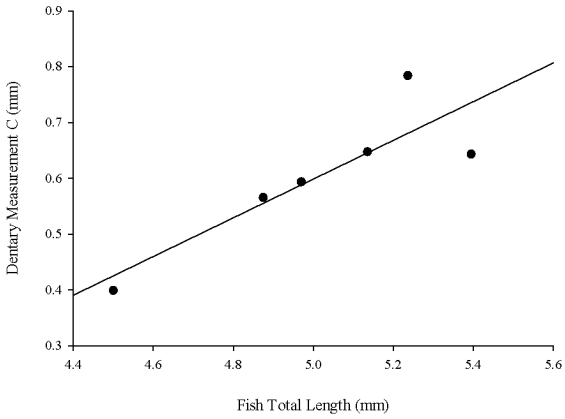

Figure B-II-2: Raw (a) and natural log transformed (b) measurements taken from the rainbow trout dentary C (mm) and TL (mm) with over laid regression line. Equations used to generate regressions presented in Table B-I-2 were constructed using the natural log transformed data set.

a.

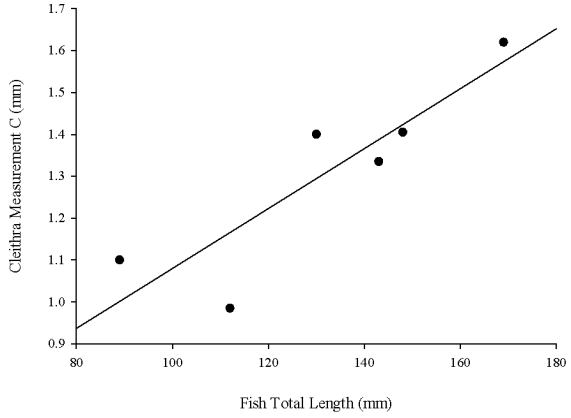

b.

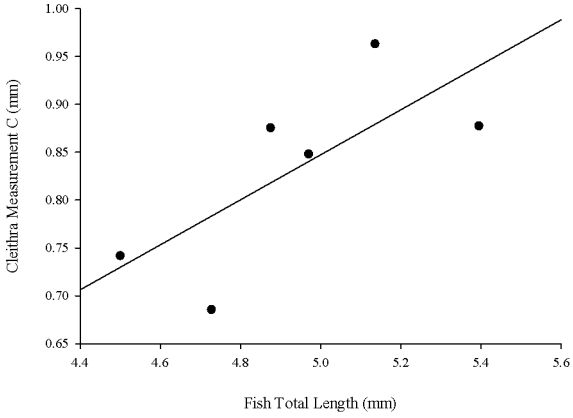

Figure B-II-3: Raw (a) and natural log transformed (b) measurements taken from the rainbow trout cleithra C (mm) and TL (mm) with over laid regression line. Equations used to generate regressions presented in Table B-I-2 were constructed using the natural log transformed data set.

a.

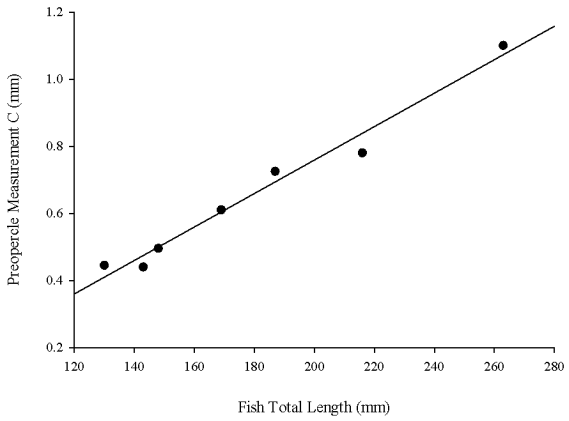

b.

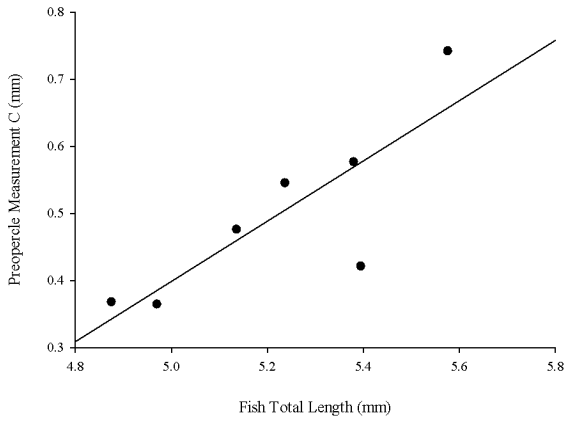

Figure B-II-2: Raw (a) and natural log transformed (b) measurements taken from the rainbow trout preopercle C (mm) and TL (mm) with over laid regression line. Equations used to generate regressions presented in Table B-I-2 were constructed using the natural log transformed data set.

a.

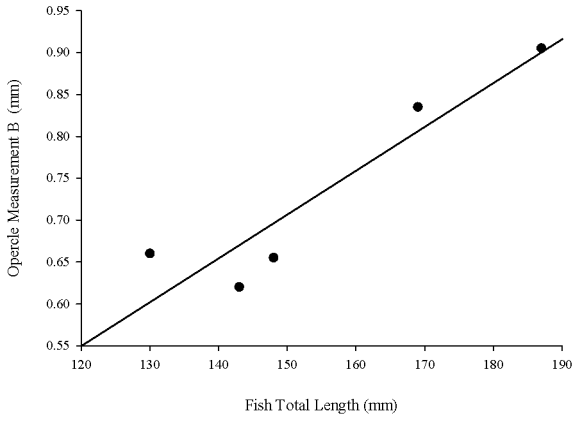

b.

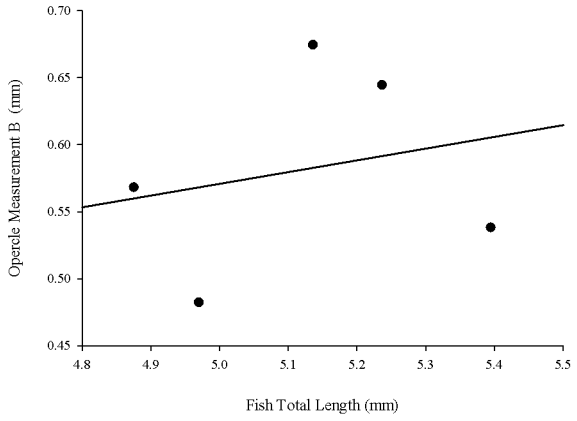

Figure B-II-3: Raw (a) and natural log transformed (b) measurements taken from the rainbow trout opercle B (mm) and TL (mm) with over laid regression line. Equations used to generate regressions presented in Table B-I-2 were constructed using the natural log transformed data set.

a.

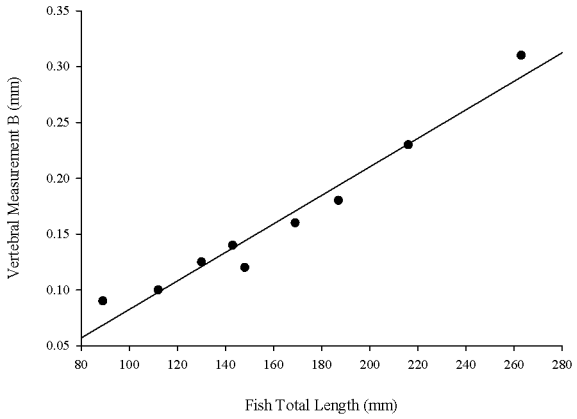

b.

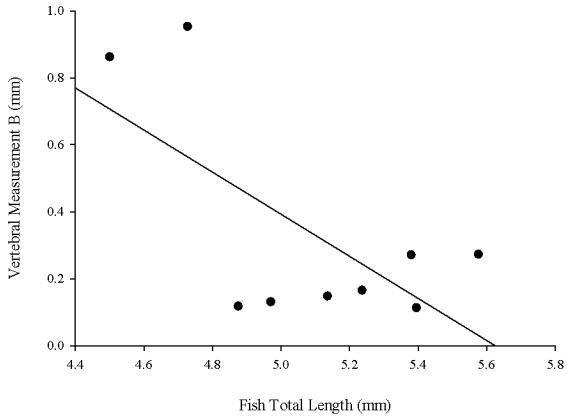

Figure B-II-2: Raw (a) and natural log transformed (b) measurements taken from the rainbow trout vertebra B (mm) and TL (mm) with over laid regression line. Equations used to generate regressions presented in Table B-I-2 were constructed using the natural log transformed data set.

Appendix B-III: Regression Equations and Graphs for Kokanee

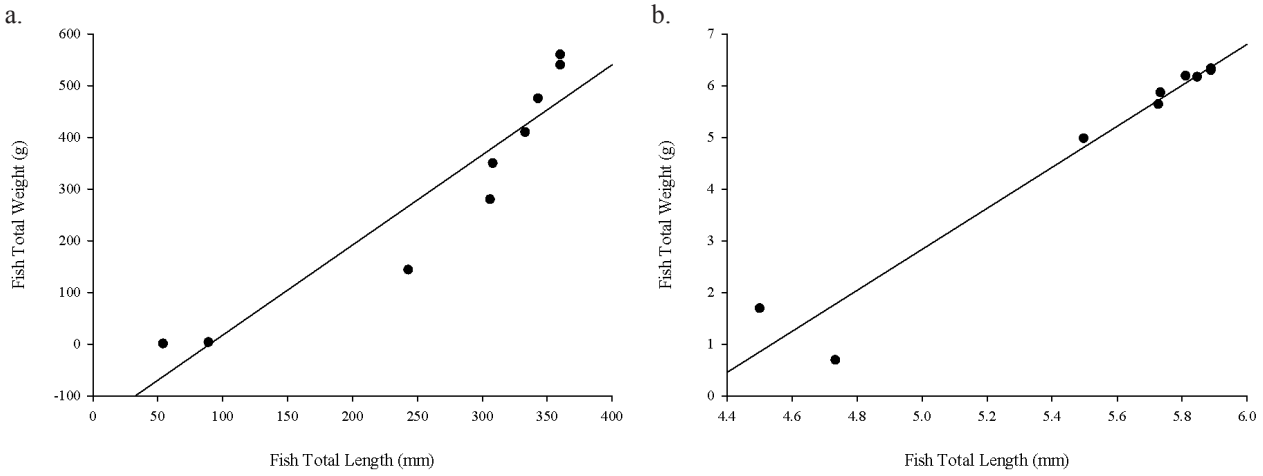

Figure B-III-1: Raw (a) and natural log transformed (b) total lengths (mm) and weights (g) of Kokanee used in this study with over laid regression line. Equations used to generate regressions presented in Table B-III 1 were constructed using the natural log transformed data points.

Table B-III-1: Total length (mm) to weight (g) regression equations for Kokanee with associated p value, R^2, and sample population used (n).

Species	TL Range (mm)	Wt Range (g)	Regression Equation	Regression *p* Value	r^2	n
Kokanee	54-360	1.0-560.0	-156.445 + (1.741*TL)	<0.001	0.883	9

Table B-III-2: Total bone length (mm) to total fish length (g) regression equations for Kokanee with associated p value, R^2, sample populatoin used (n) and associated figure number.

Bone	Bone Length Range (mm)	Regression Equations	p Value	r^2	Adjusted r^2	n	Figure Number
Dentary	0.060-1.730	2.015*(Dentary E)+4.148	<0.001	0.902	0.886	8	B-III-2
Cleithra	2.180-4.100	1.162*(Cleithra A)+4.024	<0.001	0.934	0.925	9	B-III-3
Opercle	1.305-2.380	1.22*(Opercle A)+4.33	<0.001	0.935	0.919	6	B-III-4
Vertebra	0.090-0.385	7.20*(Vertebra A)+3.74	0.001	0.844	0.817	8	B-III-5

a.

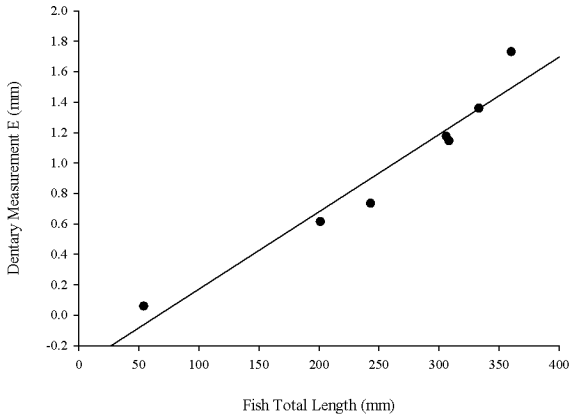

b.

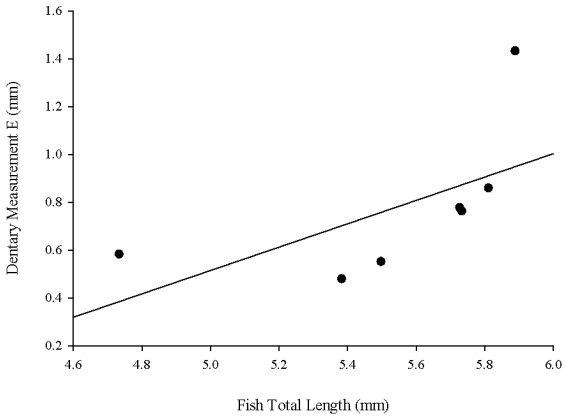

Figure B-III-2: Raw (a) and natural log transformed (b) measurements taken from the Kokanee dentary E (mm) and TL (mm) with over laid regression line. Equations used to generate regressions presented in Table B-III-2 were constructed using the natural log transformed data set.

a.

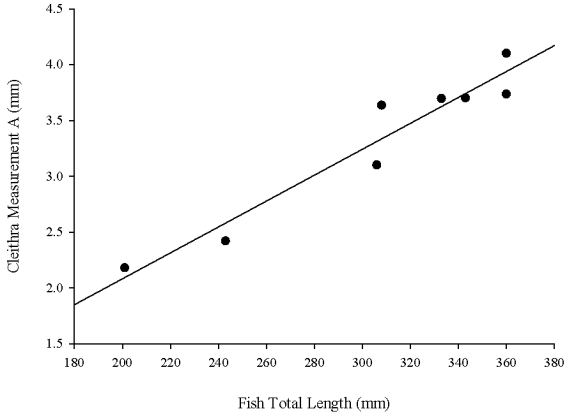

b.

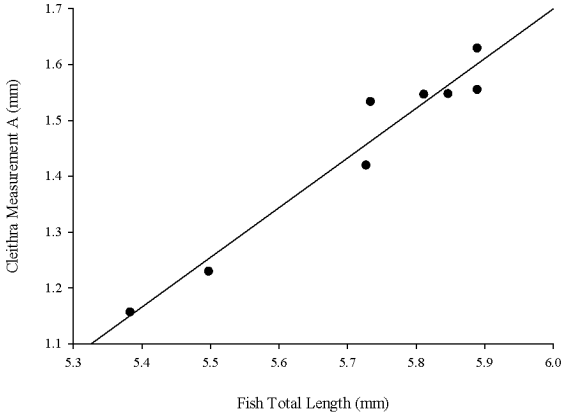

Figure B-III-3: Raw (a) and natural log transformed (b) measurements taken from the Kokanee cleithra A (mm) and TL (mm) with over laid regression line. Equations used to generate regressions presented in Table B-III-2 were constructed using the natural log transformed data set.

a.

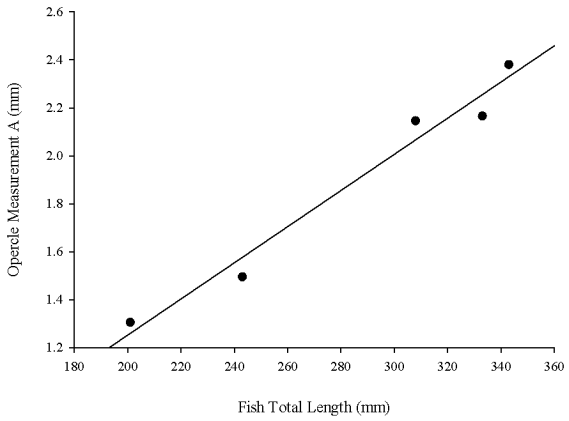

b.

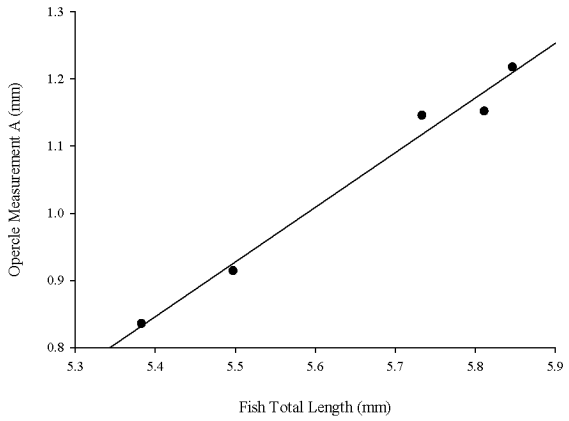

Figure B-III-4: Raw (a) and natural log transformed (b) measurements taken from the Kokanee opercle A (mm) and TL (mm) with over laid regression line. Equations used to generate regressions presented in Table B-III-2 were constructed using the natural log transformed data set.

a.

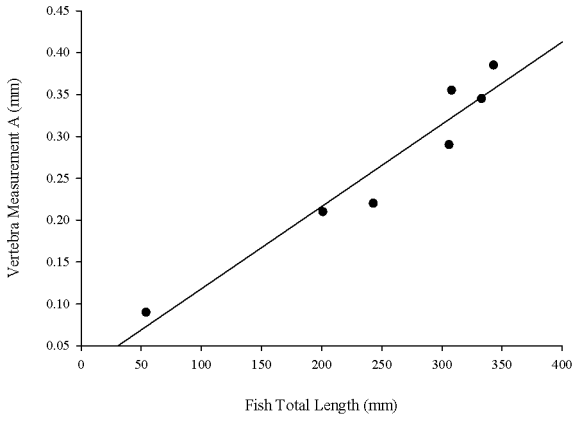

b.

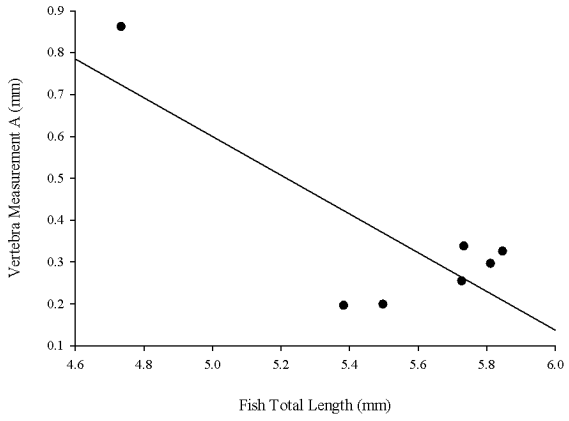

Figure B-III-5: Raw (a) and natural log transformed (b) measurements taken from the Kokanee vertebra A (mm) and TL (mm) with over laid regression line. Equations used to generate regressions presented in Table B-III-2 were constructed using the natural log transformed data set.

Appendix B-IV: Regression Equations and Graphs for Chinook

a.

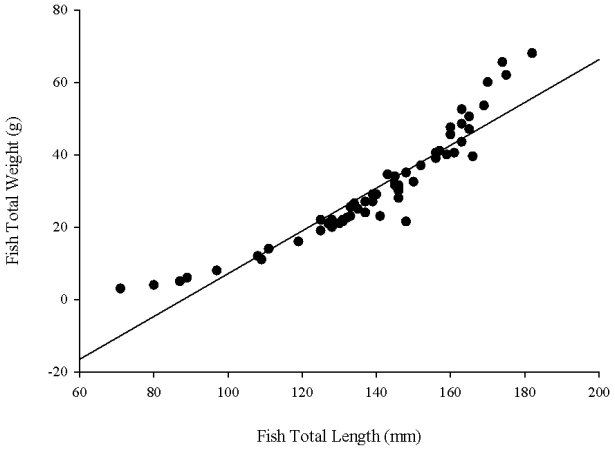

b.

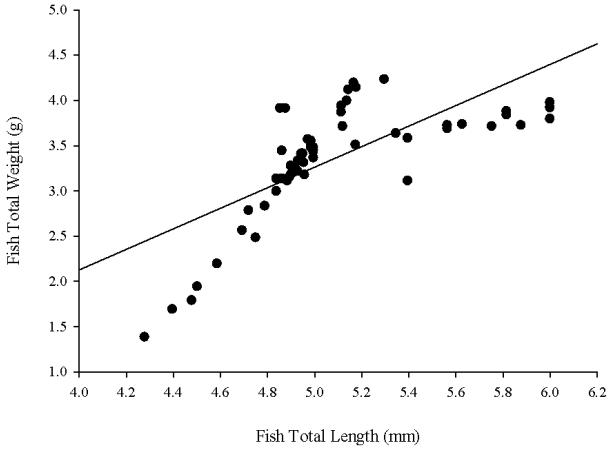

Figure B-IV-1: Raw (a) and natural log transformed (b) total lengths (mm) and weights (g) of Chinook used in this study with over laid regression line. Equations used to generate regressions presented in Table B-IV-1 were constructed using the natural log transformed data points.

Table B-IV-1: Total length (mm) to weight (g) regression equations for Chinook with associated p value, R^2, and sample populatoin used (n).

Species	TL Range (mm)	Wt Range (g)	Regression Equasion	Regression p Value	r^2	n
Chinook	71-182	3.0-68.0	-51.924 + (0.591*TL)	<0.001	0.877	62

Table B-IV-2: Total bone length (mm) to total fish length (g) regression equations for Chinook with associated p value, R^2, sample populatoin used (n) and associated figure number.

Bone	Bone Length Range (mm)	Regression Equations	p Value	r^2	Adjusted r^2	n	Figure Number
Premaxillary	0.190-0.525	2.188*(Premaxillary A)+4.282	<0.001	0.803	0.799	54	B-IV-2
Maxillary	0.660-1.750	1.48*(Maxillary A) + 3.673	<0.001	0.908	0.906	58	B-IV-3
Dentary	0.670-1.810	1.351*(Dentary B)+3.654	<0.001	0.925	0.924	62	B-IV-4
Cleithra	A:0.905-2.11 C:0.42-0.108	1.02*(Cleithra A)+0.418*(Cleithra C)+3.683	<0.001	0.928	0.926	57	B-IV-5
Preopercle	0.635-1.605	1.55*(Preopercle A)+3.71	<0.001	0.933	0.931	60	B-IV-6
Opercle	B:0.325-0.92 D:0.535-1.39	0.81*(Opercle B)+0.89*(Opercle D)+3.90	<0.001	0.929	0.927	57	B-IV-7
Pharyngeal Arch	A:0.55-0.88 C:0.05-0.255	1.60*(Pharyngeal Arch A)+0.43*(Pharyngeal C)+4.10	<0.001	0.778	0.768	48	B-IV-8
Vertebra	A:0.09-0.22 B:0.07-0.22	2.24*(Vertebra A)+4.03*(Vertebra B)+4.05	<0.001	0.690	0.679	59	B-IV-9

a.

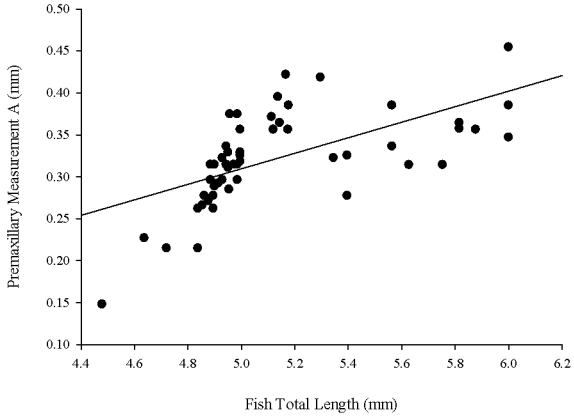

b.

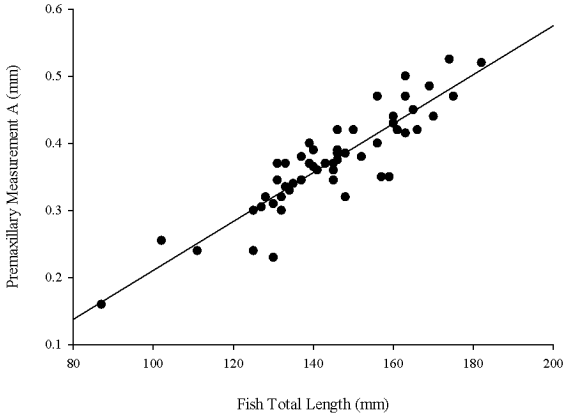

Figure B-IV-2: Raw (a) and natural log transformed (b) measurements taken from the Chinook premaxillary A (mm) and TL (mm) with over laid regression line. Equations used to generate regressions presented in Table B-IV-2 were constructed using the natural log transformed data set.

a.

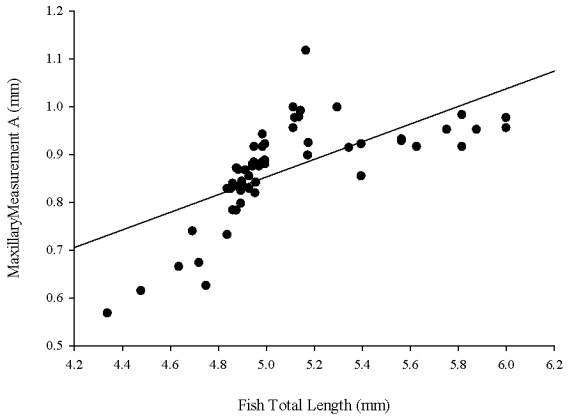

b.

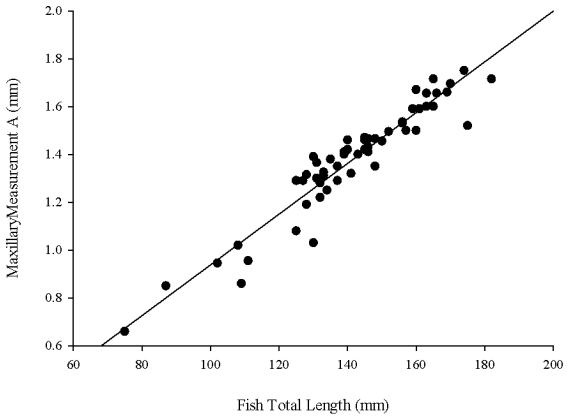

Figure B-IV-3: Raw (a) and natural log transformed (b) measurements taken from the Chinook maxillary A (mm) and TL (mm) with over laid regression line. Equations used to generate regressions presented in Table B-IV-2 were constructed using the natural log transformed data set.

a.

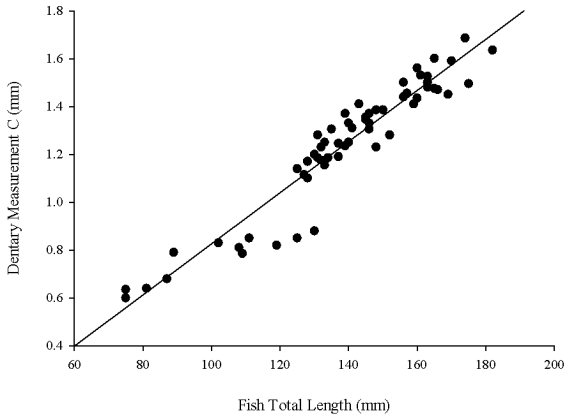

b.

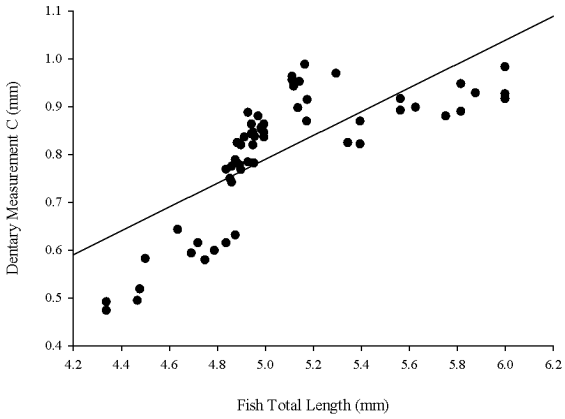

Figure B-IV-4: Raw (a) and natural log transformed (b) measurements taken from the Chinook dentary C (mm) and TL (mm) with over laid regression line. Equations used to generate regressions presented in Table B-IV-2 were constructed using the natural log transformed data set.

a.

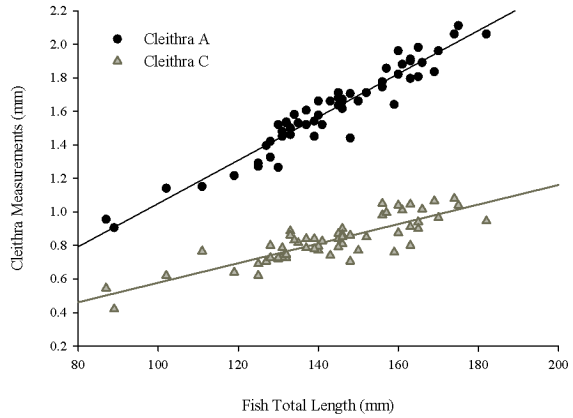

b.

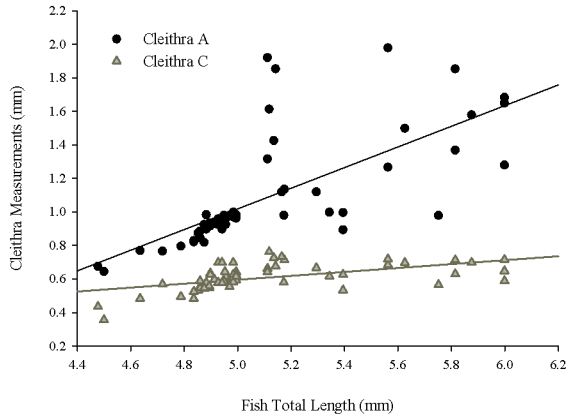

Figure B-IV-5: Raw (a) and natural log transformed (b) measurements taken from the Chinook cleithra A & C (mm) and TL (mm) with over laid regression line. Equations used to generate regressions presented in Table B-IV-2 were constructed using the natural log transformed data set.

a.

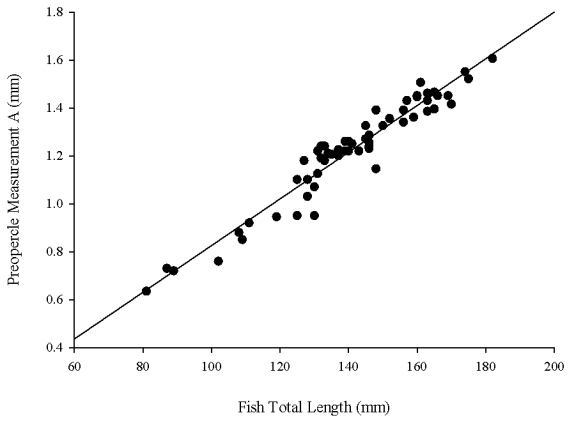

b.

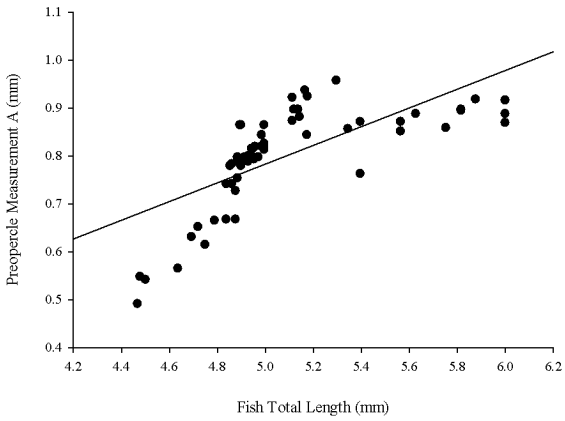

Figure B-IV-6: Raw (a) and natural log transformed (b) measurements taken from the Chinook Preopercle A (mm) and TL (mm) with over laid regression line. Equations used to generate regressions presented in Table B-IV-2 were constructed using the natural log transformed data set.

a.

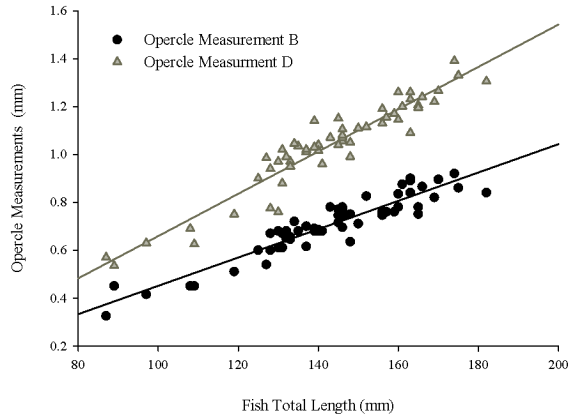

b.

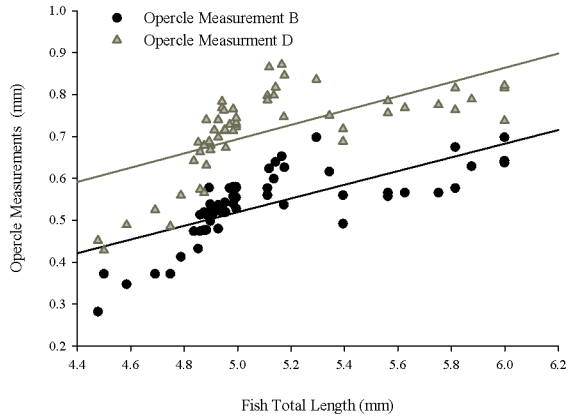

Figure B-IV-7: Raw (a) and natural log transformed (b) measurements taken from the Chinook opercle B & D (mm) and TL (mm) with over laid regression line. Equations used to generate regressions presented in Table B-IV-2 were constructed using the natural log transformed data set.

a.

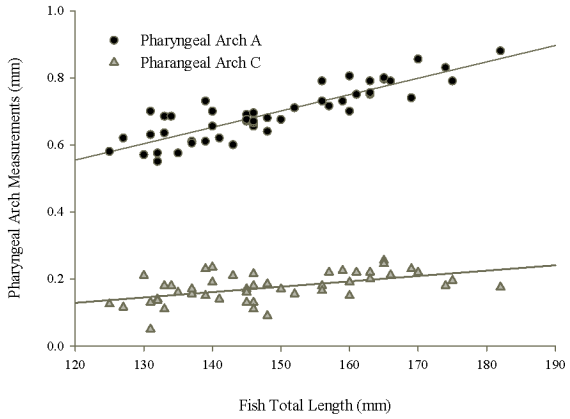

b.

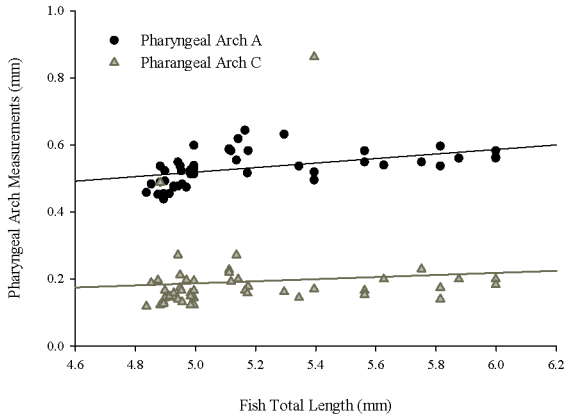

Figure B-IV-8: Raw (a) and natural log transformed (b) measurements taken from the Chinook pharyngeal arch A & C (mm) and TL (mm) with over laid regression line. Equations used to generate regressions presented in Table B-IV-2 were constructed using the natural log transformed data set.

a.

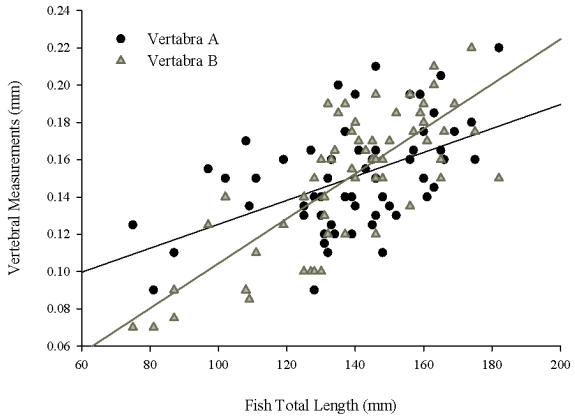

b.

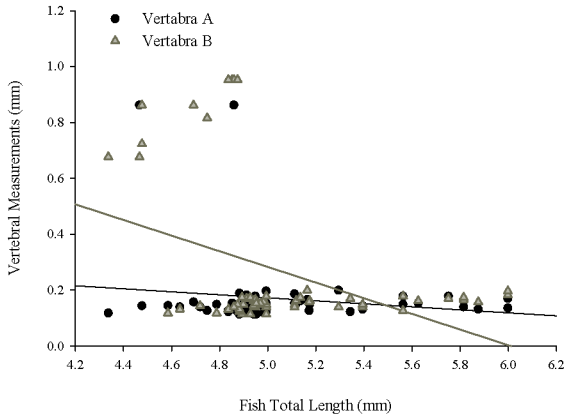

Figure B-IV-9: Raw (a) and natural log transformed (b) measurements taken from the Chinook vertebra A & B (mm) and TL (mm) with over laid regression line. Equations used to generate regressions presented in Table B-IV-2 were constructed using the natural log transformed data set.

Appendix B-V: Regression Equations and Graphs for Mountain Whitefish

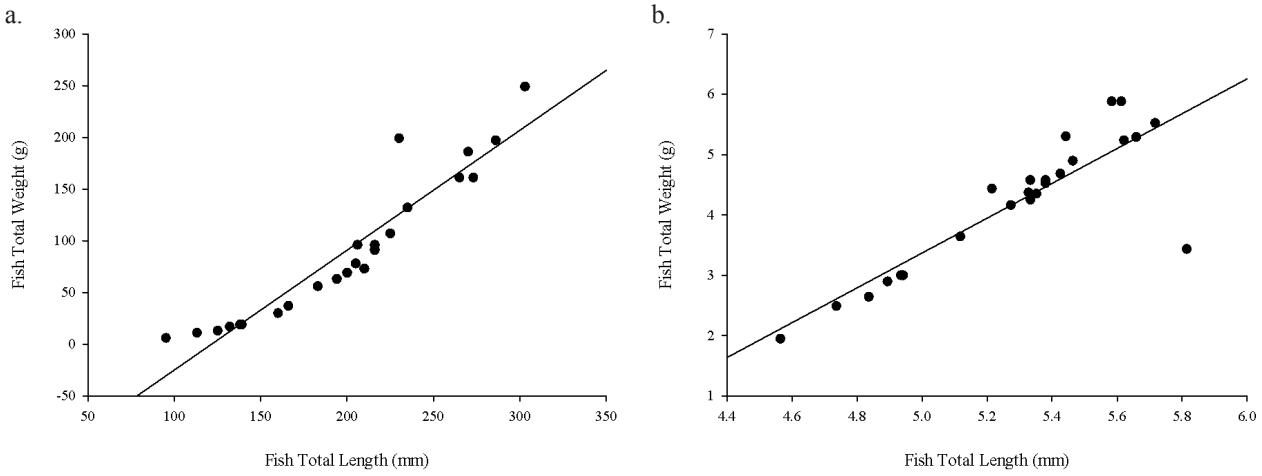

Figure B-V-1: Raw (a) and natural log transformed (b) total lengths (mm) and weights (g) of mountain whitefish used in this study with over laid regression line. Equations used to generate regressions presented in Table B-V-1 were constructed using the natural log transformed data points.

Table B-V-1: Total length (mm) to weight (g) regression equations for mountain whitefish with associated p value, R^2, and sample population used (n).

Species	TL Range (mm)	Wt Range (g)	Regression Equation	Regression p Value	r^2	n
Mountain Whitefish	95-303	6.0-249.0	-140.684+(1.158*TL)	<0.001	0.888	24

Table B-V-2: Total bone length (mm) to total fish length (g) regression equations for mountain whitefish with associated p value, R^2, sample population used (n) and associated figure number.

Bone	Bone Length Range (mm)	Regression Equations	p Value	r^2	Adjusted r^2	n	Figure Number
Premaxillary	B:0.8-0.235 C:0.13-0.355	2.071*(Premaxillary B)+2.59*(Premaxillary C) + 4.542	<0.001	0.840	0.814	15	B-V-2
Maxillary	0.405-1.120	2.259*(Maxillary A)+4.108	<0.001	0.842	0.834	20	B-V-3
Dentary	A:0.42-0.845 D:0.10-0.310	2.386*(Dentary A)+2.963*(Dentary D)+3.671	<0.001	0.880	0.862	16	B-V-4
Cleithra	1.100-2.700	1.636*(Cleithra A)+3.615	<0.001	0.979	0.978	19	B-V-5
Preopercle	0.870-2.395	1.57*(Preopercle A)+3.80	<0.001	0.960	0.958	22	B-V-6
Opercle	D:0.805-1.98 E:0.64-1.640	1.33*(Opercle D)+ -0.79*(Opercle E)+3.68	<0.001	0.880	0.862	16	B-V-7
Pharyngeal Arch	0.555-0.700	1.91*(Pharyngeal Arch A)+4.43	<0.001	0.601	0.557	11	B-V-8
Vertebra	0.120-0.355	5.44*(Vertebra A)+4.16	<0.001	0.889	0.883	22	B-V-9

a.

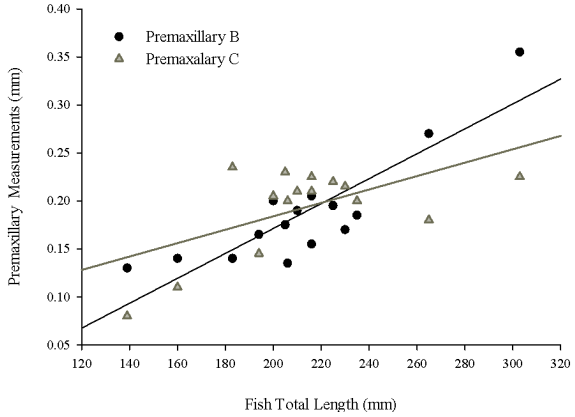

b.

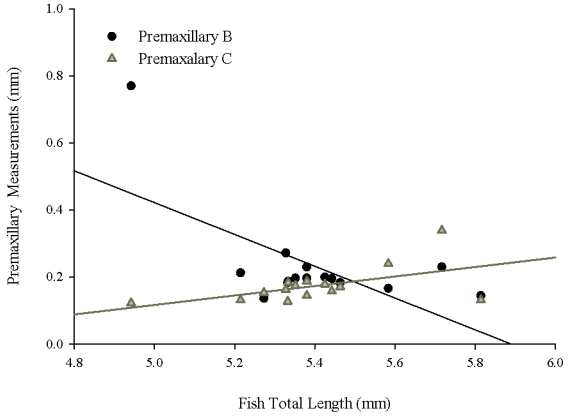

Figure B-V-2: Raw (a) and natural log transformed (b) measurements taken from the mountain whitefish premaxillary B & C (mm) and TL (mm) with over laid regression line. Equations used to generate regressions presented in Table B-V-2 were constructed using the natural log transformed data set.

a.

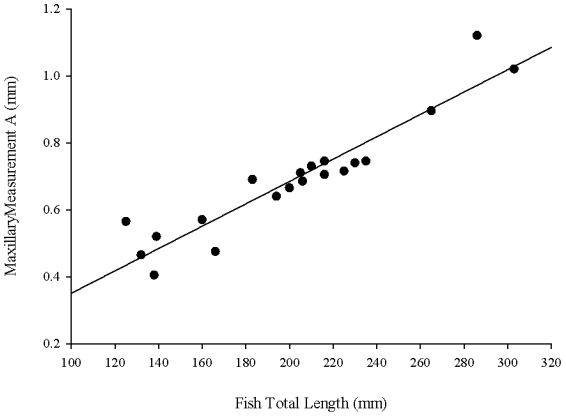

b.

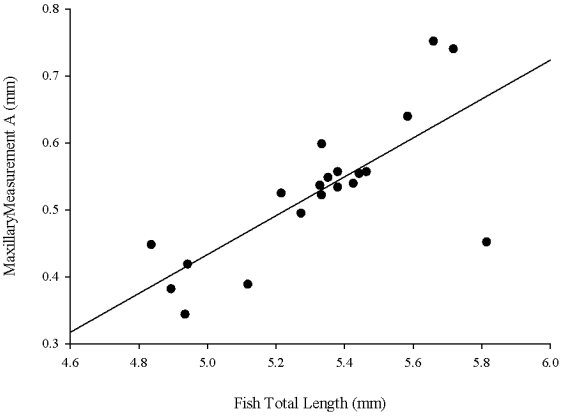

Figure B-V-3: Raw (a) and natural log transformed (b) measurements taken from the mountain whitefish maxillary A (mm) and TL (mm) with over laid regression line. Equations used to generate regressions presented in Table B-V-2 were constructed using the natural log transformed data set.

a.

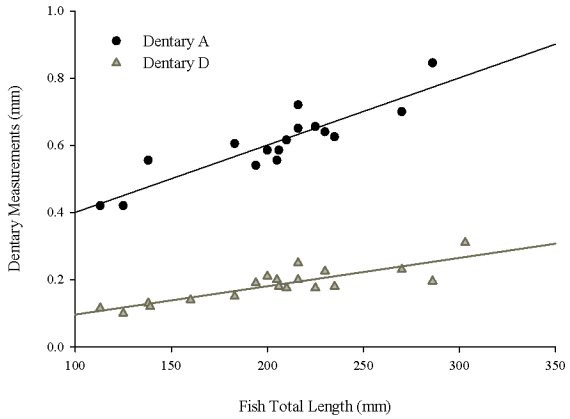

b.

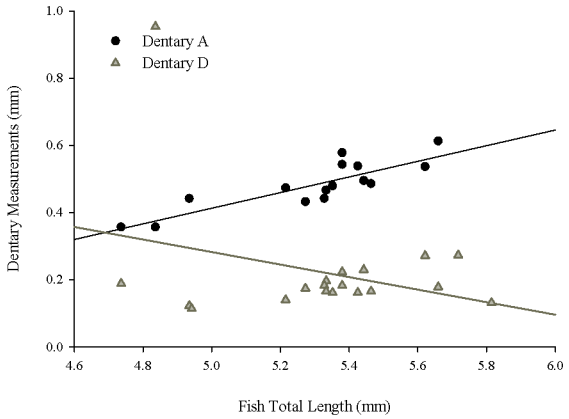

Figure B-V-4: Raw (a) and natural log transformed (b) measurements taken from the mountain whitefish dentary A & D (mm) and TL (mm) with over laid regression line. Equations used to generate regressions presented in Table B-V-2 were constructed using the natural log transformed data set.

a.

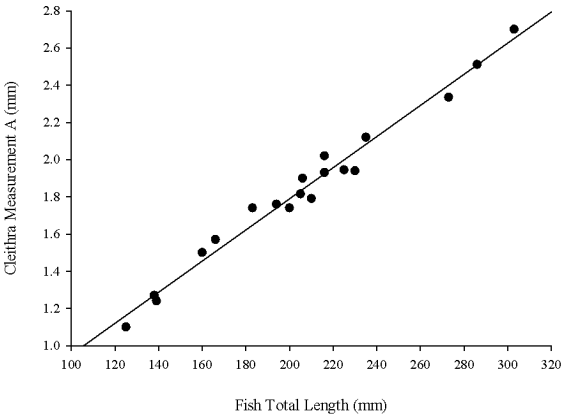

b.

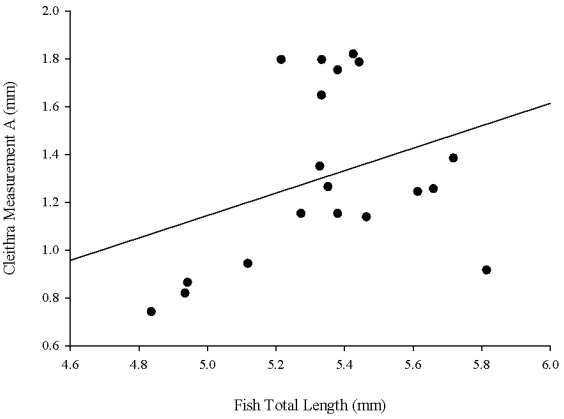

Figure B-V-5: Raw (a) and natural log transformed (b) measurements taken from the mountain whitefish cleithra A (mm) and TL (mm) with over laid regression line. Equations used to generate regressions presented in Table B-V-2 were constructed using the natural log transformed data set.

a.

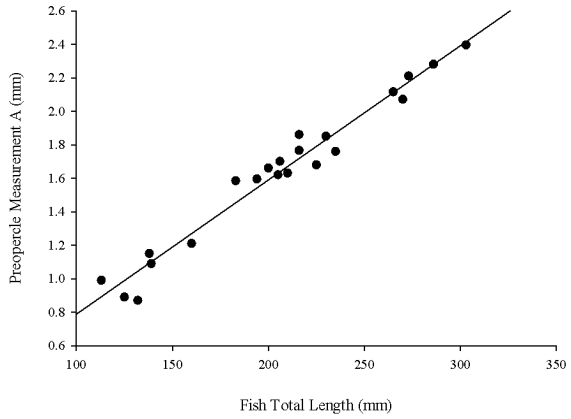

b.

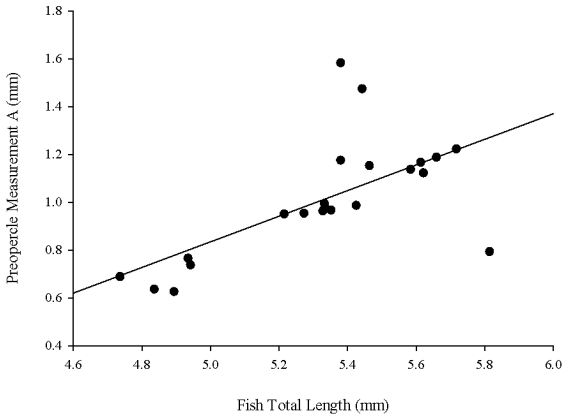

Figure B-V-6: Raw (a) and natural log transformed (b) measurements taken from the mountain whitefish preopercle A (mm) and TL (mm) with over laid regression line. Equations used to generate regressions presented in Table B-V-2 were constructed using the natural log transformed data set.

a.

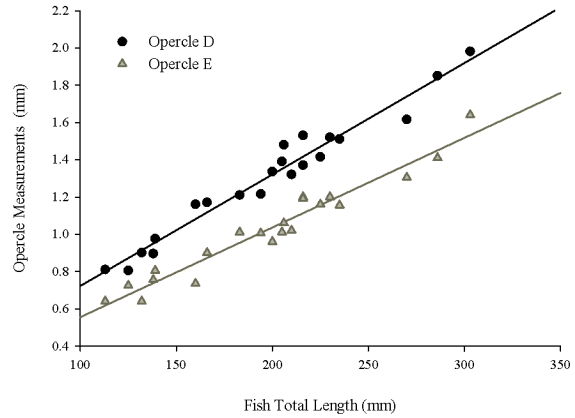

b.

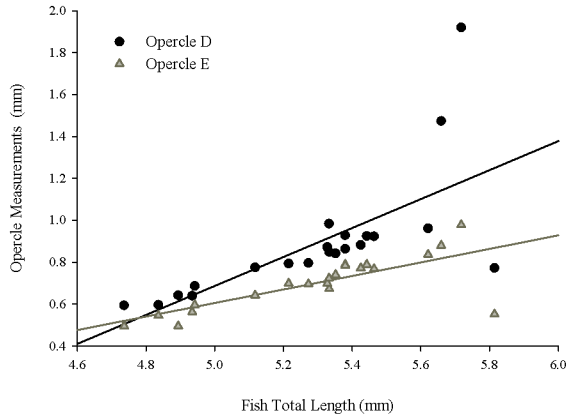

Figure B-V-7: Raw (a) and natural log transformed (b) measurements taken from the mountain whitefish opercle D & E (mm) and TL (mm) with over laid regression line. Equations used to generate regressions presented in Table B-V-2 were constructed using the natural log transformed data set.

a.

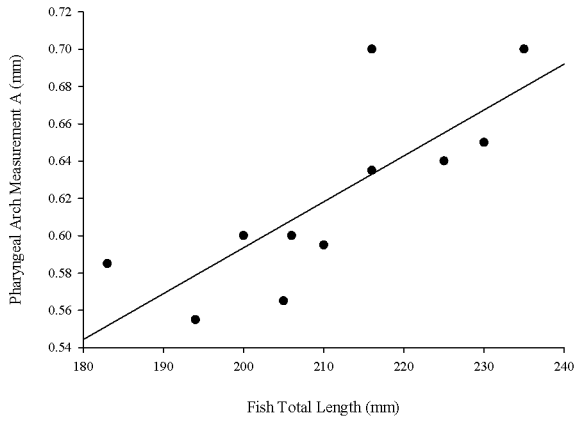

b.

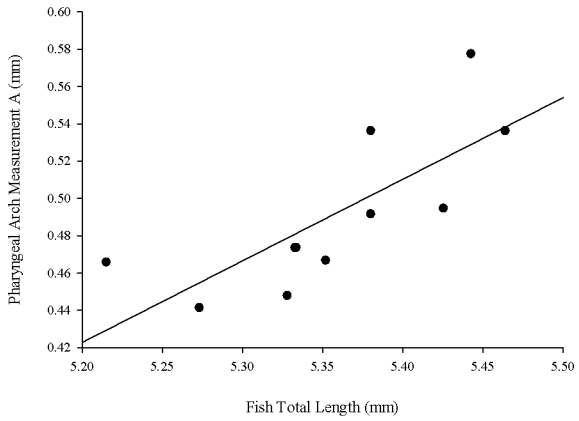

Figure B-V-8: Raw (a) and natural log transformed (b) measurements taken from the mountain whitefish pharyngeal arch A (mm) and TL (mm) with over laid regression line. Equations used to generate regressions presented in Table B-V-2 were constructed using the natural log transformed data set.

a.

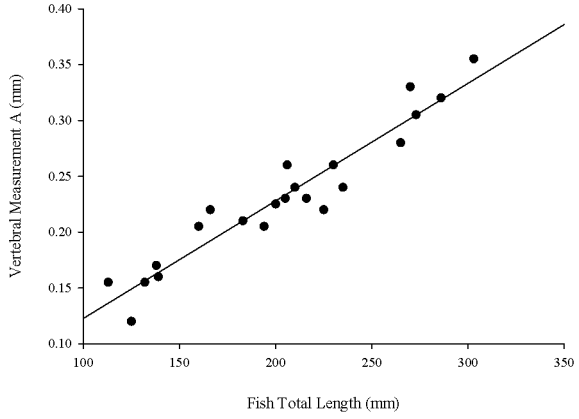

b.

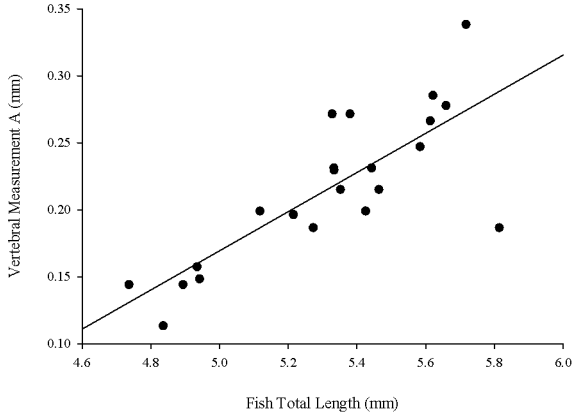

Figure B-V-9: Raw (a) and natural log transformed (b) measurements taken from the mountain whitefish vertebra A (mm) and TL (mm) with over laid regression line. Equations used to generate regressions presented in Table B-V-2 were constructed using the natural log transformed data set.

Appendix B-VI: Regression Equations and Graphs for Bull Trout

a.

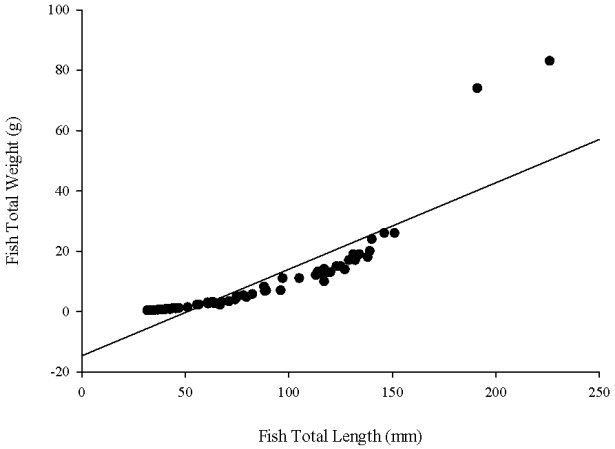

b.

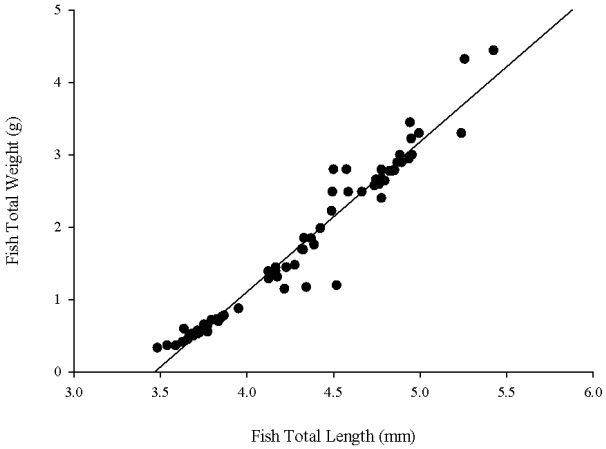

Figure B-VI-1: Raw (a) and natural log transformed (b) total lengths (mm) and weights (g) of bull trout used in this study with over laid regression line. Equations used to generate regressions presented in Table B-VI-1 were constructed using the natural log transformed data points.

Table B-VI-1: Total length (mm) to weight (g) regression equations for bull trout with associated p value, R^2, and sample population used (n).

Species	TL Range (mm)	Wt Range (g)	Regression Equation	Regression p Value	r^2	n
Bull trout	31.5-544	0.394-1426.5	-14.588+(0.286 * TL)	<0.001	0.747	68

Table B-VI-2: Total bone length (mm) to total fish length (g) regression equations for bull trout with associated p value, R^2, sample population used (n) and associated figure number.

Bone	Bone Length Range (mm)	Regression Equations	p Value	r^2	Adjusted r^2	n	Figure Number
Dentary	0.390-2.565	1.995*(Dentary B)+3.029	<0.001	0.877	0.875	66	B-VI-2
Cleithra	A:0.390-2.11 B:0.08-0.550	2.506*(Cleithra A)+ -1.19*(Cleithra B)+2.98	<0.001	0.948	0.946	62	B-VI-3
Preopercle	0.280-1.710	2.22*(Preopercle A)+3.17	<0.001	0.921	0.920	68	B-VI-4
Opercle	B:0.15-0.840 C:0.10-0.540 D:0.20-1.240	2.10*(Opercle B)+ -2.91*(Opercle C)+2.52*(Opercle D)+3.18	<0.001	0.943	0.940	68	B-VI-5
Pharyngeal Arch	A:0.15-1.100 B:0.05-0.610	3.27*(Pharyngeal Arch A)+ -1.23*(Pharyngeal Arch B)+3.22	<0.001	0.868	0.864	61	B-VI-6
Vertebra	0.030-0.499	5.66*(Vertebra B)+3.47	<0.001	0.661	0.654	50	B-VI-7

a.

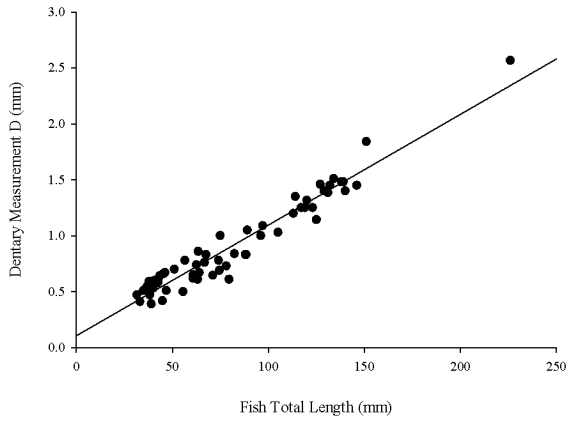

b.

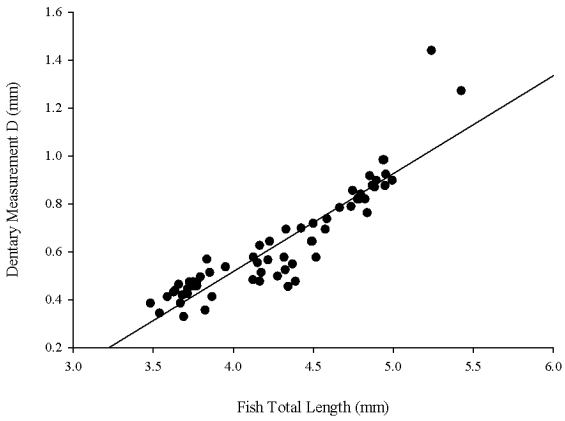

Figure B-VI-2: Raw (a) and natural log transformed (b) measurements taken from the bull trout dentary D (mm) and TL (mm) with over laid regression line. Equations used to generate regressions presented in Table B-VI-2 were constructed using the natural log transformed data set.

a.

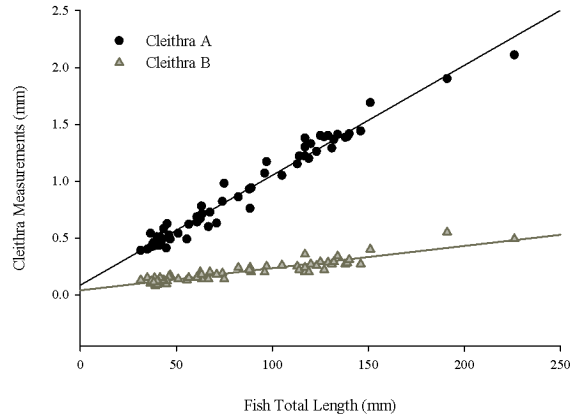

b.

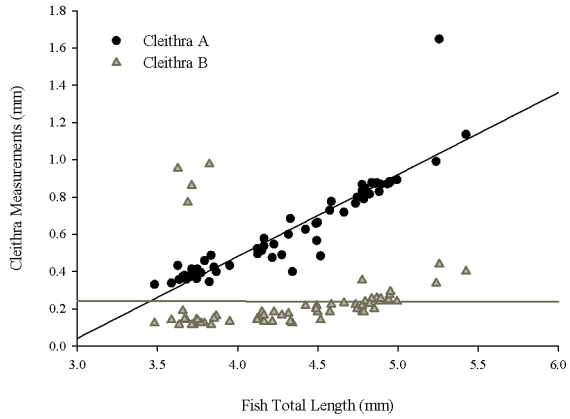

Figure B-VI-3: Raw (a) and natural log transformed (b) measurements taken from the bull trout cleithra A & B (mm) and TL (mm) with over laid regression line. Equations used to generate regressions presented in Table B-VI-2 were constructed using the natural log transformed data set.

a.

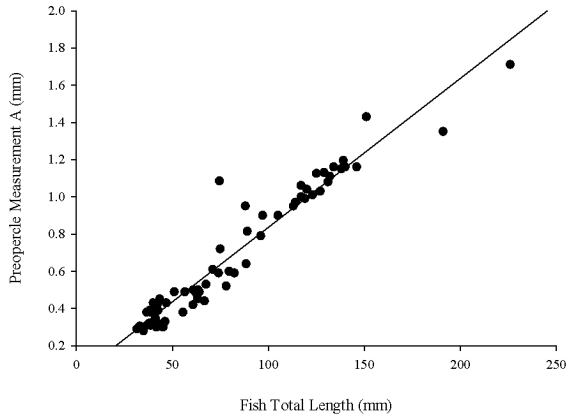

b.

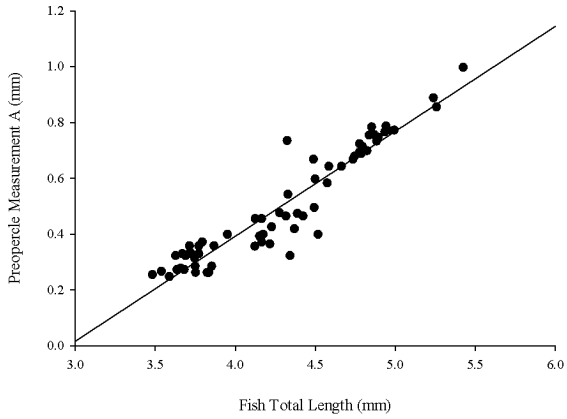

Figure B-VI-4: Raw (a) and natural log transformed (b) measurements taken from the bull trout preopercle A (mm) and TL (mm) with over laid regression line. Equations used to generate regressions presented in Table B-VI-2 were constructed using the natural log transformed data set.

a.

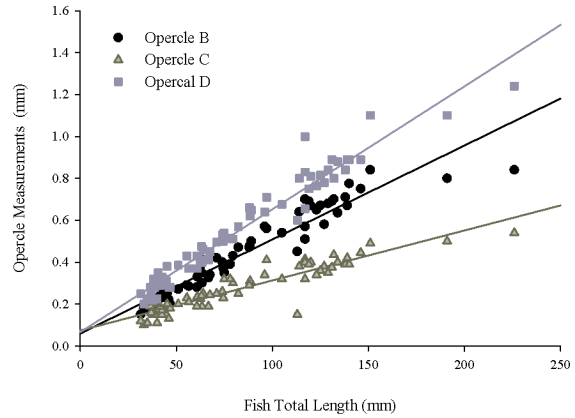

b.

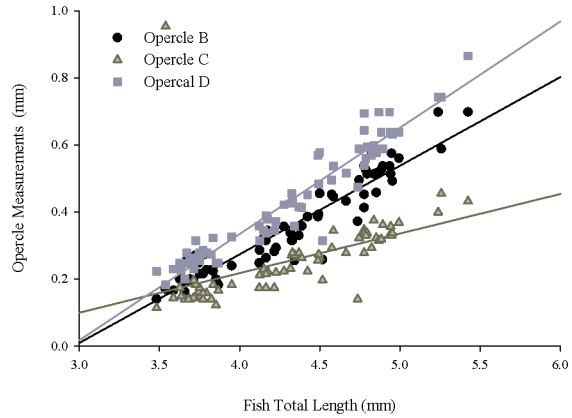

Figure B-VI-5: Raw (a) and natural log transformed (b) measurements taken from the bull trout opercle B, C & D (mm) and TL (mm) with over laid regression line. Equations used to generate regressions presented in Table B-VI-2 were constructed using the natural log transformed data set.

a.

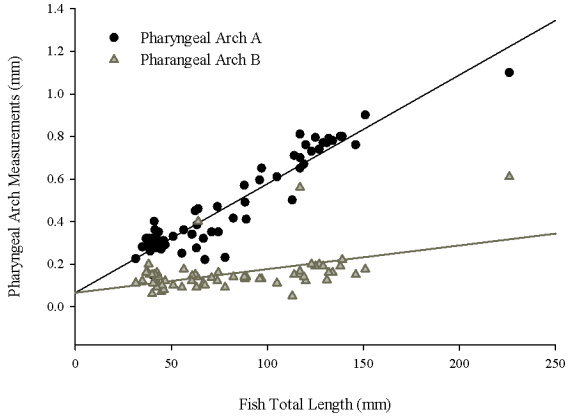

b.

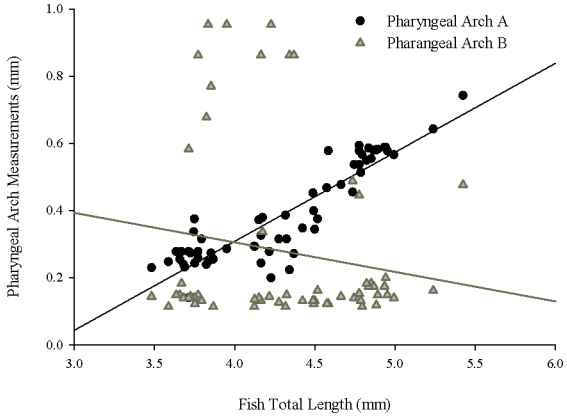

Figure B-VI-6: Raw (a) and natural log transformed (b) measurements taken from the bull trout pharyngeal arch A & B (mm) and TL (mm) with over laid regression line. Equations used to generate regressions presented in Table B-VI-2 were constructed using the natural log transformed data set.

a.

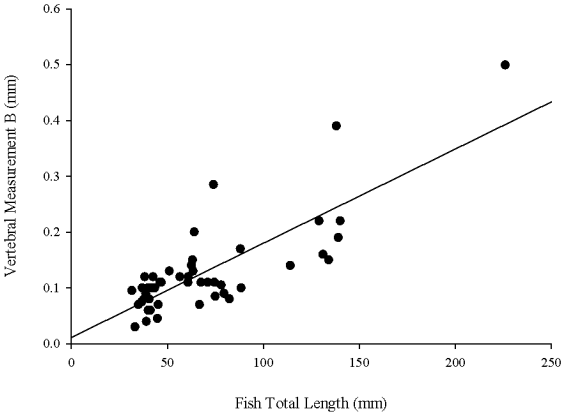

b.

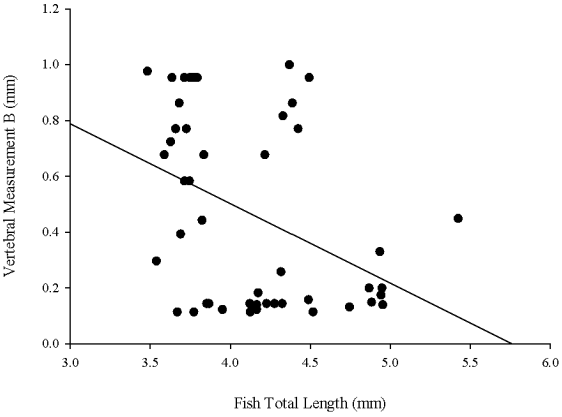

Figure B-VI-7: Raw (a) and natural log transformed (b) measurements taken from the bull trout vertebra B (mm) and TL (mm) with over laid regression line. Equations used to generate regressions presented in Table B-VI-2 were constructed using the natural log transformed data set.

a.

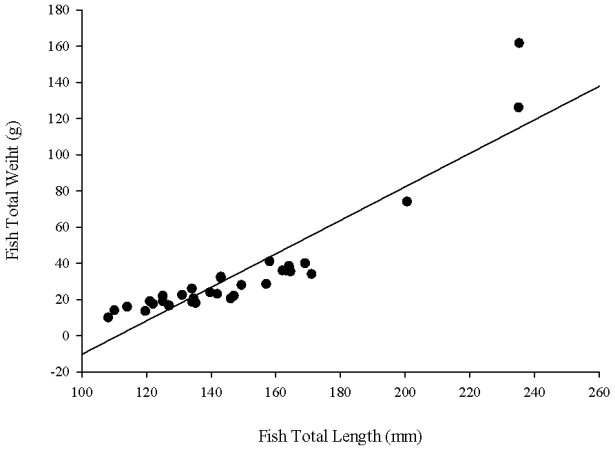

b.

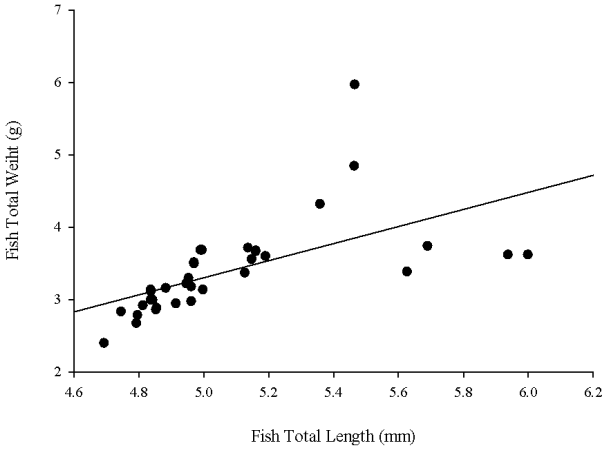

Figure B-VI-1: Raw (a) and natural log transformed (b) total lengths (mm) and weights (g) of bull trout used in this study with over laid regression line. Equations used to generate regressions presented in Table B-VI-1 were constructed using the natural log transformed data points.

Table B-VII-1: Total length (mm) to weight (g) regression equations for brook trout with associated p value, R^2, and sample population used (n).

Species	TL Range (mm)	Wt Range (g)	Regression Equation	Regression p Value	r^2	n
Brook Trout	108.1-235.2	10.0-161.5	-102.801+(0.925*TL)	<0.001	0.830	32

Table B-VII-2: Total bone length (mm) to total fish length (g) regression equations for brook trout with associated p value, R^2, sample population used (n) and associated figure number.

Bone	Bone Length Range (mm)	Regression Equations	p Value	r^2	Adjusted r^2	n	Figure Number
Premaxillary	0.240-0.400	2.672*(Premaxillary B)+4.22 5	<0.001	0.555	0.527	18	B-VII-2
Maxillary	0.163-2.710	20.416*(Maxillary A)+4.65	<0.001	0.396	0.372	27	B-VII-3
Dentary	C:0.75-1.850 E:0.355-1.08	1.077*(Dentary C)+0.711*(Dentary E)+3.885	<0.001	0.964	0.961	35	B-VII-4
Cleithra	1.080-2.770	1.461*(Cleithra A)+3.635	<0.001	0.913	0.911	35	B-VII-5
Preopercle	A:0.79-2.070 B:0.19-0.510	1.03*(Preopercle A)+1.06*(Preopercle B)+3.93	<0.001	0.870	0.862	35	B-VII-6
Opercle	D:0.60-1.600 E:0.60-1.410	0.90*(Opercle D)+0.95*(Opercle E)+3.81	<0.001	0.930	0.925	27	B-VII-7
Pharyngeal Arch	0.450-1.185	1.93*(Pharyngeal Arch A)+3.94	<0.001	0.888	0.884	32	B-VII-8
Vertebra	0.140-0.350	3.84*(Vertebra A)+4.32	<0.001	0.638	0.623	26	B-VII-9

a.

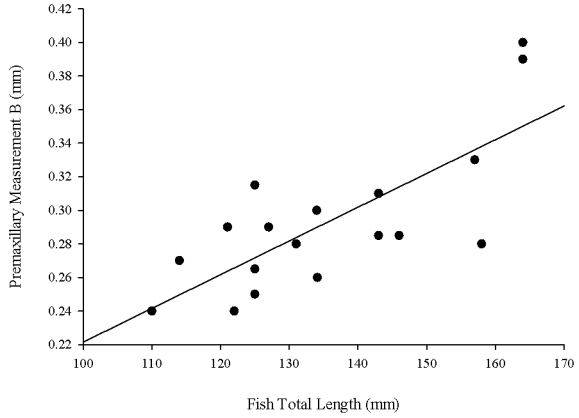

b.

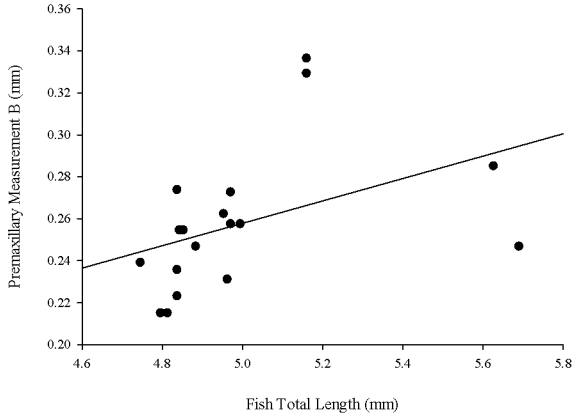

Figure B-VII-2: Raw (a) and natural log transformed (b) measurements taken from the brook trout premaxillary B (mm) and TL (mm) with over laid regression line. Equations used to generate regressions presented in Table B-VII-2 were constructed using the natural log transformed data set.

a.

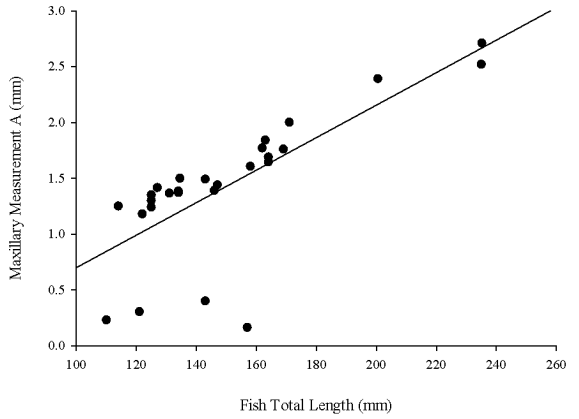

b.

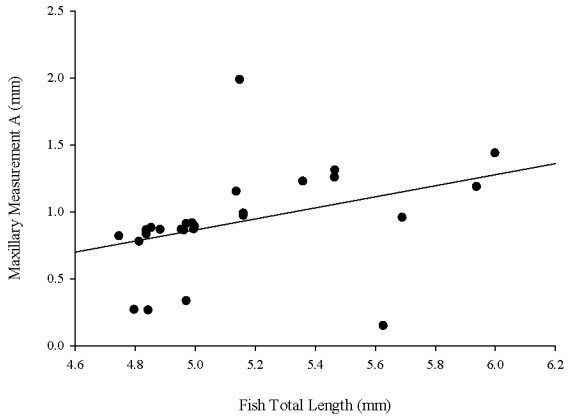

Figure B-VII-3: Raw (a) and natural log transformed (b) measurements taken from the brook trout maxillary A (mm) and TL (mm) with over laid regression line. Equations used to generate regressions presented in Table B-VII-2 were constructed using the natural log transformed data set.

a.

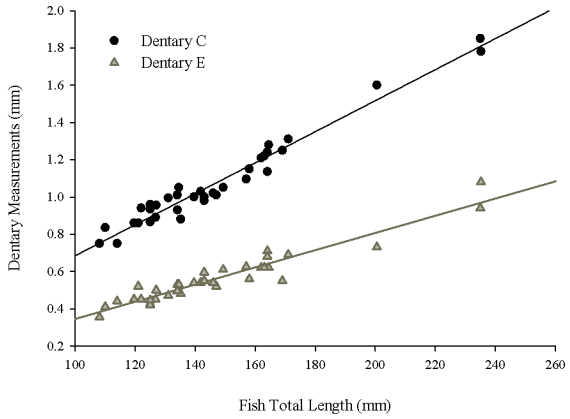

b.

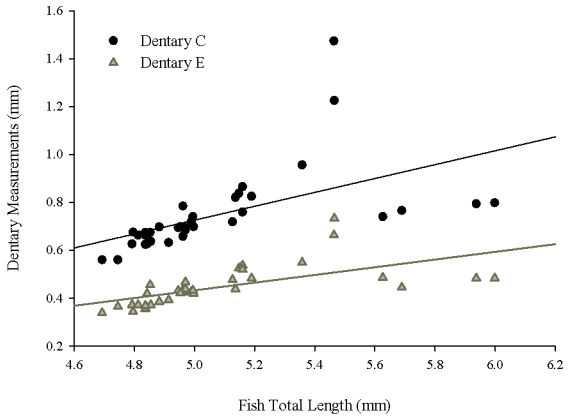

Figure B-VII-4: Raw (a) and natural log transformed (b) measurements taken from the brook trout dentary C & E (mm) and TL (mm) with over laid regression line. Equations used to generate regressions presented in Table B-VII-2 were constructed using the natural log transformed data set.

a.

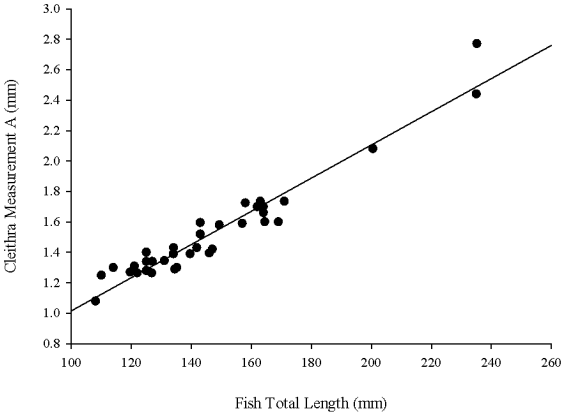

b.

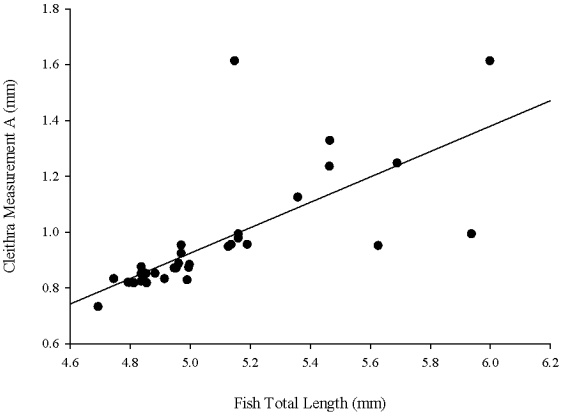

Figure B-VII-5: Raw (a) and natural log transformed (b) measurements taken from the brook trout cleithra A (mm) and TL (mm) with over laid regression line. Equations used to generate regressions presented in Table B-VII-2 were constructed using the natural log transformed data set.

a.

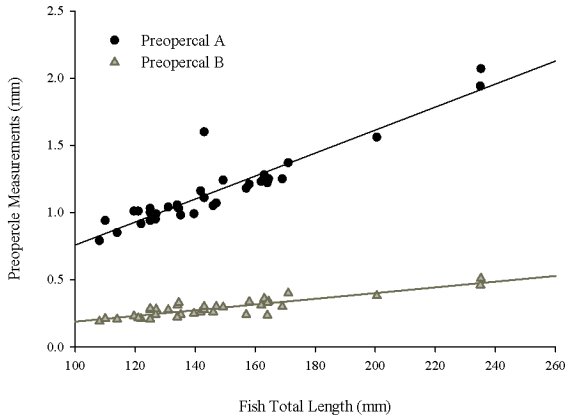

b.

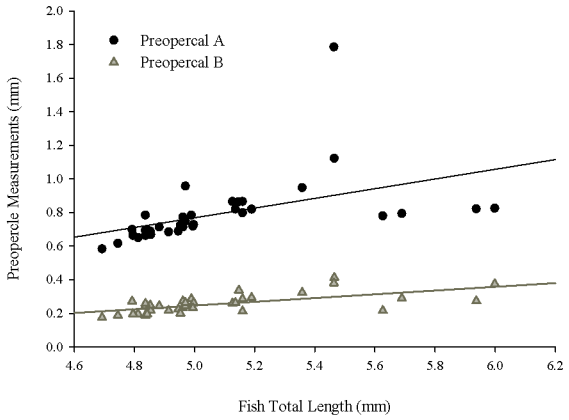

Figure B-VI-6: Raw (a) and natural log transformed (b) measurements taken from the brook trout preopercle A & B (mm) and TL (mm) with over laid regression line. Equations used to generate regressions presented in Table B-VII-2 were constructed using the natural log transformed data set.

a.

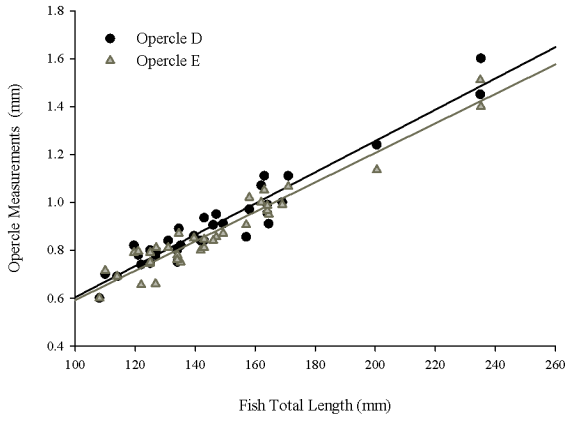

b.

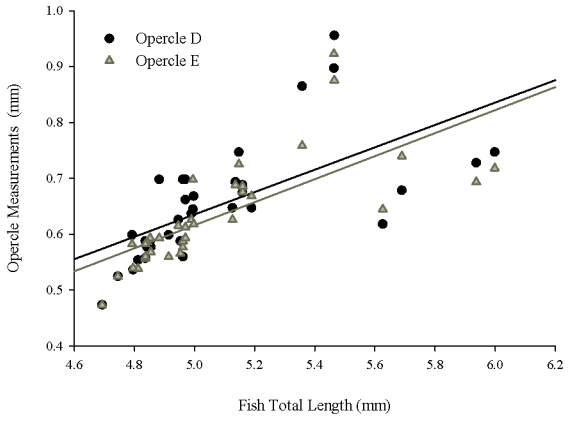

Figure B-VII-7: Raw (a) and natural log transformed (b) measurements taken from the brook trout opercle D & E (mm) and TL (mm) with over laid regression line. Equations used to generate regressions presented in Table B-VII-2 were constructed using the natural log transformed data set.

a.

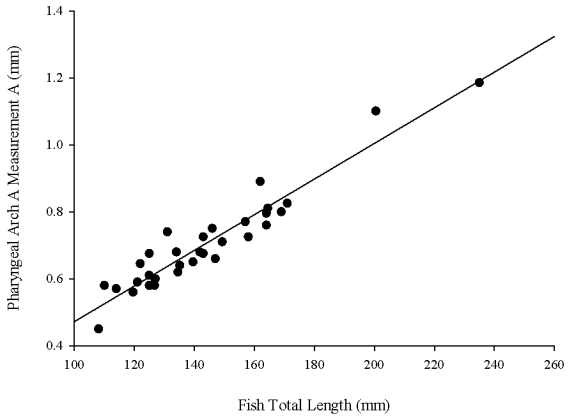

b.

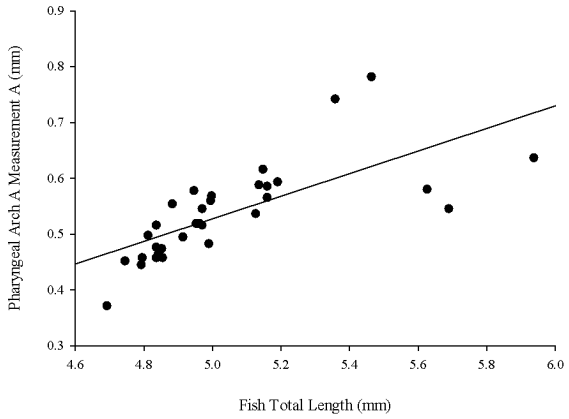

Figure B-VII-8: Raw (a) and natural log transformed (b) measurements taken from the brook trout pharyngeal arch A (mm) and TL (mm) with over laid regression line. Equations used to generate regressions presented in Table B-VII-2 were constructed using the natural log transformed data set.

a.

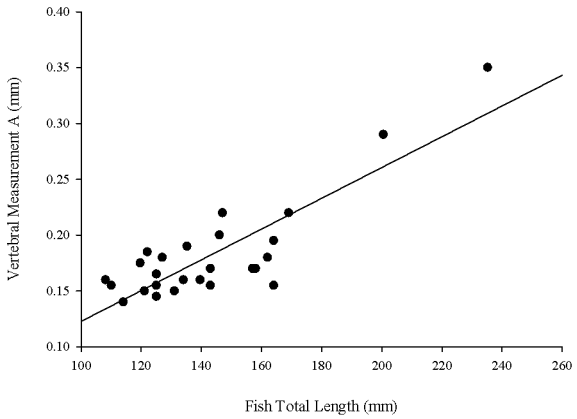

b.

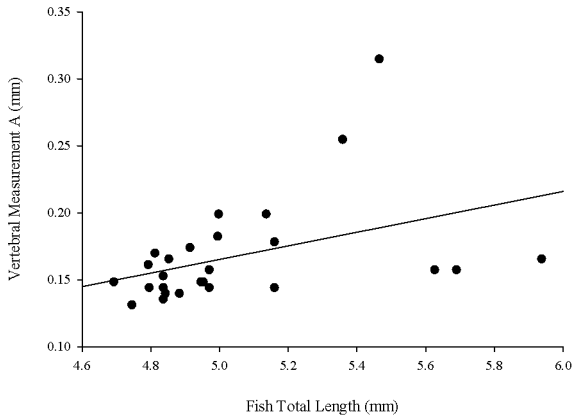

Figure B-VII-9: Raw (a) and natural log transformed (b) measurements taken from the brook trout vertebra A (mm) and TL (mm) with over laid regression line. Equations used to generate regressions presented in Table B-VII-2 were constructed using the natural log transformed data set.

Appendix B-VIII: Regression Equations and Graphs for the Lake Trout

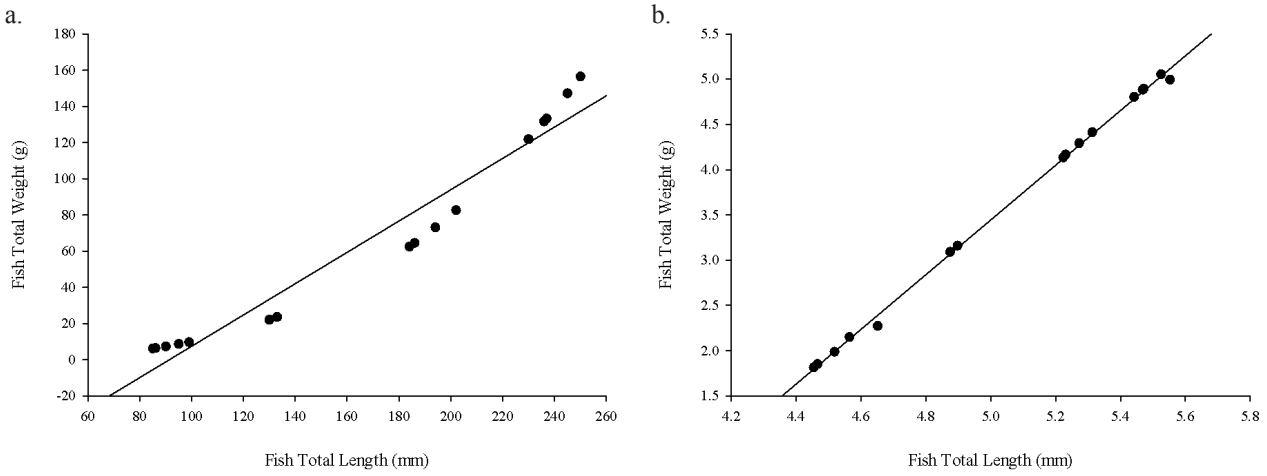

Figure B-VIII-1: Raw (a) and natural log transformed (b) total lengths (mm) and weights (g) of lake trout used in this study with over laid regression line. Equations used to generate regressions presented in Table B-VIII-1 were constructed using the natural log transformed data points.

Table B-VIII-1: Total length (mm) to weight (g) regression equations for lake trout with associated p value, R^2, and sample population used (n).

Species	TL Range (mm)	Wt Range (g)	Regression Equation	Regression p Value	r^2	n
Lake Trout	85-791	21.97-4949	-78.92+(0.864*TL)	<0.001	0.951	16

Table B-VIII-2: Total bone length (mm) to total fish length (g) regression equations for lake trout with associated p value, R^2, sample population used (n) and associated figure number.

Bone	Bone Length Range (mm)	Regression Equations	p Value	r^2	Adjusted r^2	n	Figure Number
Premaxillary	A:0.205-0.53 C:0.195-0.60	4.450*(Premaxillary A)+ -0.74*(Premaxillary C) + 3.962	<0.001	0.951	0.940	12	B-VIII-2
Maxillary	0.780-2.270	2.028*(Maxillary A) + 3.282	<0.001	0.709	0.689	17	B-VIII-3
Dentary	B:0.84-2.290 D:0.11-0.265	2.34*(Dentary B)+ -2.915*(Dentary D)+3.378	<0.001	0.987	0.985	14	B-VIII-4
Cleithra	A:0.88-2.320 C:0.63-1.685	3.17*(Cleithra A)+ -1.73*(Cleithra C)+3.13	<0.001	0.970	0.964	13	B-VIII-5
Preopercle	A:0.595-1.82 C:0.305-0.655	2.13*(Preopercle A)+ -0.79*(Preopercle C)+3.73	<0.001	0.981	0.978	14	B-VIII-6
Opercle	A:0.47-1.190 D:0.50-1.430 E:0.46-1.165	-4.88*(Opercle A)+5.05*(Opercle D)+1.72*(Opercle E)+3.69	<0.001	0.987	0.983	13	B-VIII-7
Vertebra	A:0.095-0.305 B:0.080-0.255	10.29*(Vertebra A)+ -5.26*(Vertebra B)+3.92	<0.001	0.959	0.951	13	B-VIII-8

a.

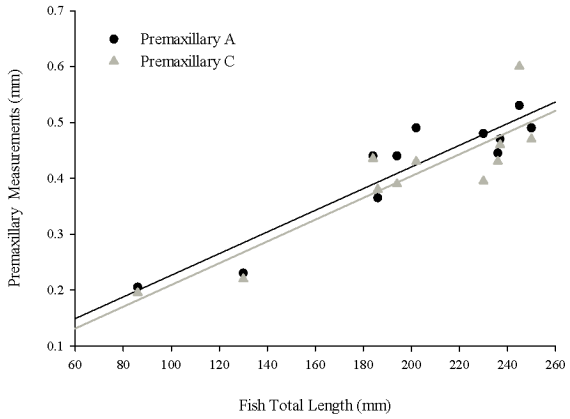

b.

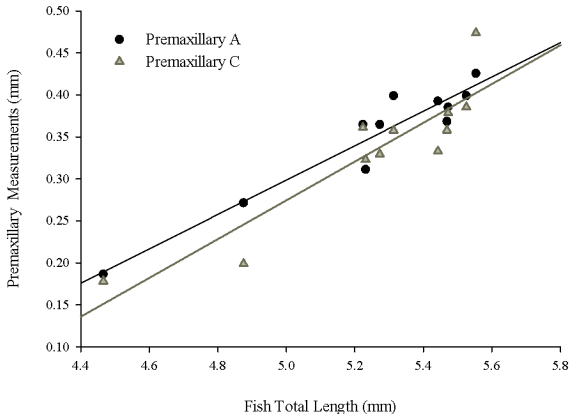

Figure B-VIII-2: Raw (a) and natural log transformed (b) measurements taken from the lake trout premaxillary A & C (mm) and TL (mm) with over laid regression line. Equations used to generate regressions presented in Table B-VIII-2 were constructed using the natural log transformed data set.

a.

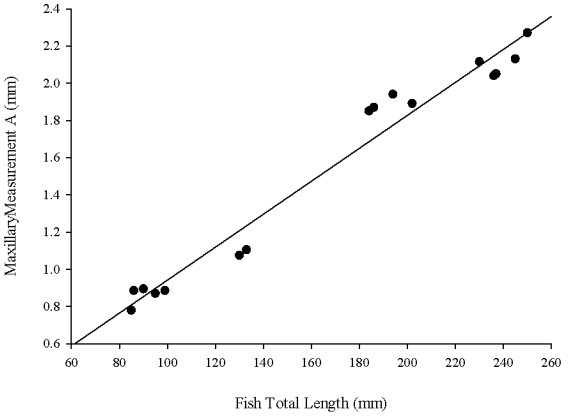

b.

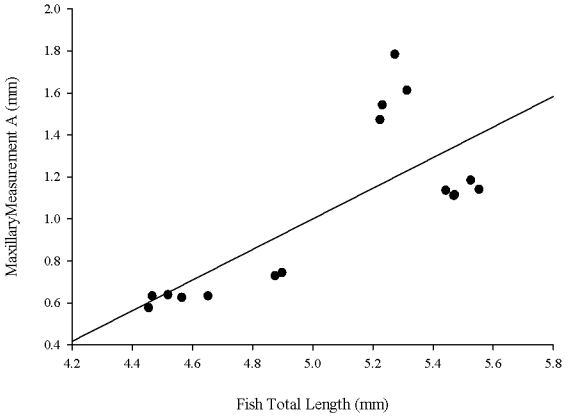

Figure B-VIII-3: Raw (a) and natural log transformed (b) measurements taken from the lake trout maxillary A (mm) and TL (mm) with over laid regression line. Equations used to generate regressions presented in Table B-VIII-2 were constructed using the natural log transformed data set.

a.

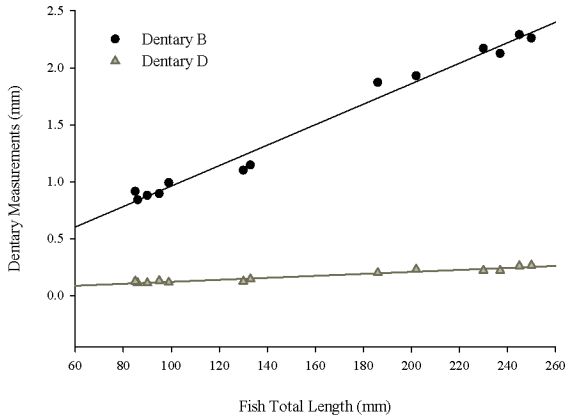

b.

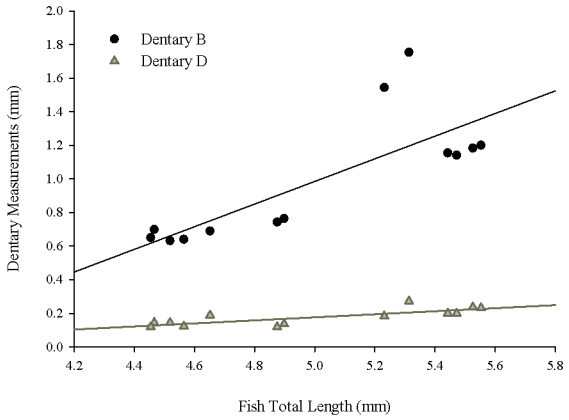

Figure B-VIII-4: Raw (a) and natural log transformed (b) measurements taken from the lake trout dentary B & D (mm) and TL (mm) with over laid regression line. Equations used to generate regressions presented in Table B-VIII-2 were constructed using the natural log transformed data set.

a.

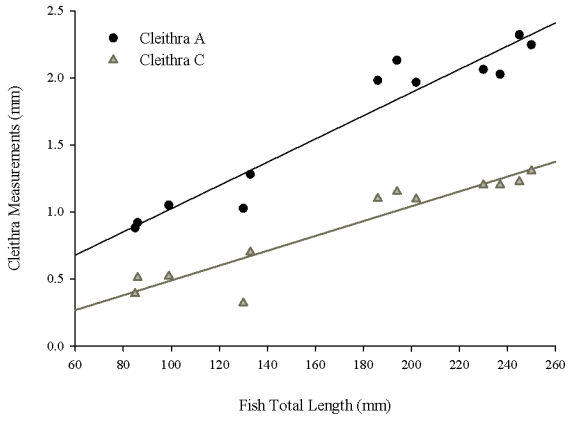

b.

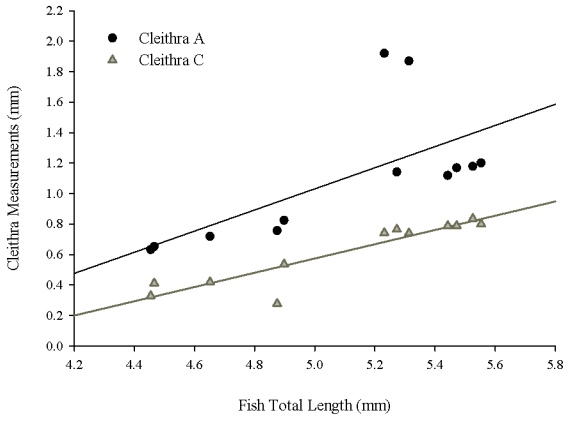

Figure B-VIII-5: Raw (a) and natural log transformed (b) measurements taken from the lake trout cleithra A & C (mm) and TL (mm) with over laid regression line. Equations used to generate regressions presented in Table B-VIII-2 were constructed using the natural log transformed data set.

a.

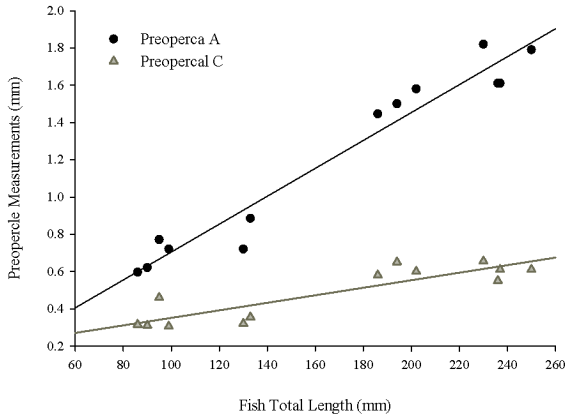

b.

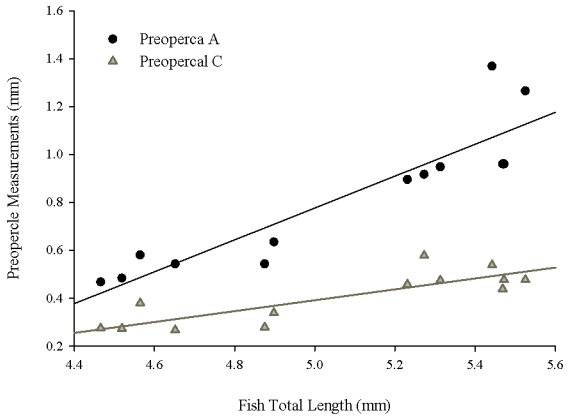

Figure B-VIII-6: Raw (a) and natural log transformed (b) measurements taken from the lake trout preopercle A & C (mm) and TL (mm) with over laid regression line. Equations used to generate regressions presented in Table B-VIII-2 were constructed using the natural log transformed data set.

a.

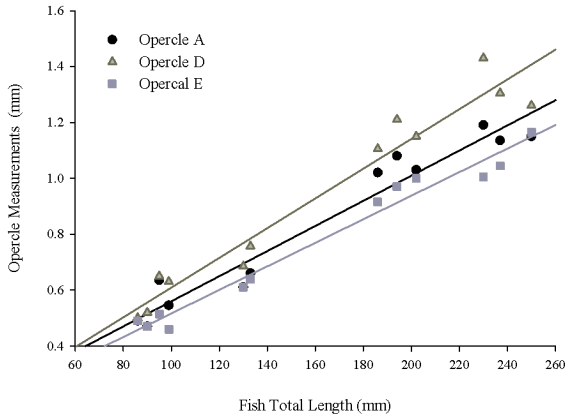

b.

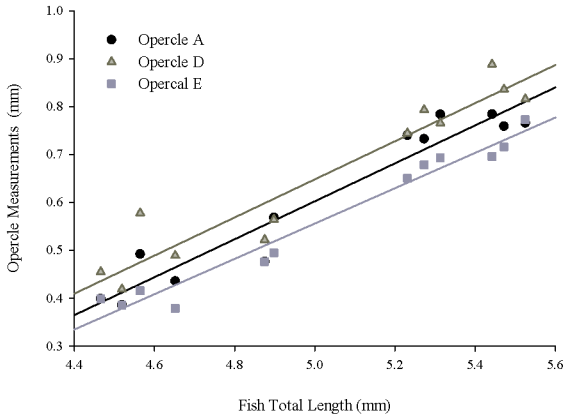

Figure B-VIII-7: Raw (a) and natural log transformed (b) measurements taken from the lake trout opercle A, D, & E (mm) and TL (mm) with over laid regression line. Equations used to generate regressions presented in Table B-VIII-2 were constructed using the natural log transformed data set.

a.

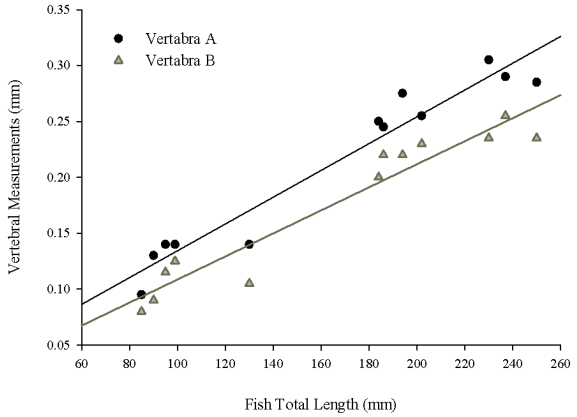

b.

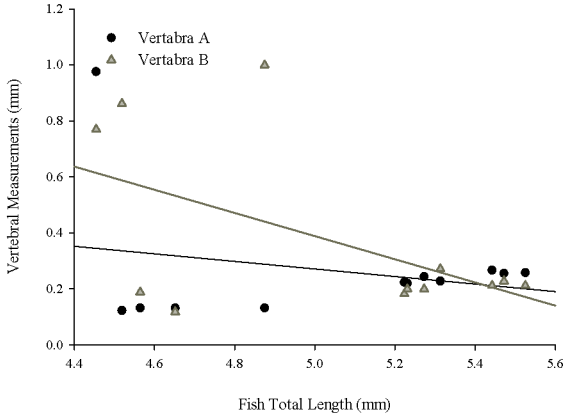

Figure B-VIII-8: Raw (a) and natural log transformed (b) measurements taken from the lake trout vertebra A & B (mm) and TL (mm) with over laid regression line. Equations used to generate regressions presented in Table B-VIII-2 were constructed using the natural log transformed data set.